



Provided by the author(s) and University of Galway in accordance with publisher policies. Please cite the published version when available.

Title	Cell Cycle-dependence of cisplatin-and carboplatin-induced dna damage
Author(s)	Villalan, Sangamitra
Publication Date	2011-09-30
Item record	http://hdl.handle.net/10379/2524

Downloaded 2024-03-13T09:17:33Z

Some rights reserved. For more information, please see the item record link above.





NUI Galway
OÉ Gaillimh

**CELL CYCLE-DEPENDENCE OF
CISPLATIN- AND CARBOPLATIN-
INDUCED DNA DAMAGE RESPONSES
IN HUMAN CELLS LACKING OR
EXPRESSING DNA POLYMERASE η**

A thesis presented to the National University of Ireland for the degree of
Doctor of Philosophy
by

Sangamitra Villalan, M.Sc.
Centre for Chromosome Biology
School of Natural Sciences
National University of Ireland, Galway

September 2011

Head of School: Dr. Heinz-Peter Nasheuer
Head of Biochemistry: Dr. Michael P. Carty
Research Supervisor: Dr. Michael P. Carty

Table of Contents

Acknowledgement

Abbreviations

Abstract

Chapter 1 – Introduction

1.1. Cancer	2
1.2. Characteristics of cancer cells	2
1.3. Sources of DNA damage	4
1.3.1. DNA damage by ultraviolet light (UV)	5
1.3.2. DNA damage by ionising radiation	6
1.3.3. DNA damage by chemical agents	7
1.4. DNA damage by chemotherapeutic drugs	7
1.4.1. Platinum-based chemotherapeutic drugs	7
1.4.2. Cisplatin-induced DNA damage	9
1.4.3 Carboplatin-induced DNA damage	13
1.4.4. Oxaliplatin-induced DNA damage	14
1.5. Platinum resistance	15
1.6. DNA Repair	15
1.6.1. Mismatch repair (MMR)	17
1.6.2. Nucleotide excision repair (NER)	17
1.6.2.1. Interstrand crosslink (ICL) repair	18
1.6.3. Double strand break production	20
1.6.3.1. Double strand break recognition	20
1.6.3.2. Homologous recombination repair	21
1.6.3.3. Non-homologous end-joining repair (NHEJ)	23

1.7. Translesion synthesis (TLS)	23
1.7.1. <i>DNA polymerase zeta (ζ)</i>	26
1.7.2. <i>DNA polymerase kappa (κ)</i>	27
1.7.3. <i>DNA polymerase iota (ι)</i>	27
1.7.4. <i>Rev I</i>	28
1.7.5. <i>DNA polymerase eta (η)</i>	29
1.7.6. <i>Role of DNA polymerase η in replication past platinum adducts</i>	30
1.7.7. <i>The polymerase switch</i>	31
1.8. The DNA damage responses (DDR)	33
1.8.1. <i>DNA damage sensor proteins</i>	34
1.8.1.1. γ H2AX	35
1.8.2. <i>Transducers: the PIK kinases</i>	36
1.8.2.1. Activation of phosphoinositide kinases (PIK Kinases)	36
1.8.2.2. Ataxia telangiectasia, mutated (ATM)	36
1.8.2.3. Ataxia telangiectasia and Rad-3-related (ATR)	37
1.8.2.4. DNA-dependent protein kinase (DNA-PK)	38
1.9. Replication protein A (RPA)	41
1.9.1. <i>Binding of RPA to ssDNA, protein-protein interactions and repair</i>	43
1.9.2. <i>Cell cycle-dependent RPA phosphorylation</i>	44
1.9.3. <i>Role of RPA in the DNA damage response</i>	44
1.10. DNA damage and cell cycle progression	46
1.10.1. <i>Role of cyclins in cell cycle regulation</i>	46
1.10.2. <i>Cell cycle synchronisation</i>	49
1.11. DNA damage-induced cell cycle checkpoints	51
1.11.1. <i>Checkpoint kinase 1 (Chk1)</i>	52

1.11.2. Checkpoint kinase 2 (Chk2)	52
1.11.3. The G1-phase checkpoint	53
1.11.4. DNA damage-induced S-phase checkpoints	54
1.11.5. G2- and M-phase checkpoints	55
1.12. Cell cycle effects of cisplatin	56
1.12.1 Effects of DNA damaging agents on cell cycle progression	56
1.12.2 Effects of cell cycle stage at the time of exposure on the response to DNA damaging agents	58
1.13. Research objectives	61
Chapter 2 - Materials and Methods	
2.1. Cell lines	63
2.2. Cell culture	63
2.3. Cryopreservation	63
2.4. Resuscitation	64
2.5. Cell synchronisation Mitotic arrest	64
2.6. Treatment with platinum-based drugs and inhibitors	65
2.7. XTT-Cell viability assay	65
2.8. Trypan blue assay	66
2.9. Preparation of cell extracts	66
2.10. Protein assay	67
2.11. Sodium dodecyl sulphate polyacrylamide gel electrophoresis (SDS-PAGE)	67
2.12. Western immunoblotting	68
2.13. Cell cycle analysis by flow cytometry	70
2.14. Immunofluorescence	72

Chapter 3 – Results

3.1. Pol η expression in XP30R0 and TR30-2 cells	75
3.2. Analysis of nocodazole toxicity	76
3.3. Cell synchronisation using nocodazole	77
3.3.1. <i>Effect of nocodazole treatment on subsequent cell cycle progression</i>	80
3.3.2. <i>Identification of G1- and S-phase cells, post-nocodazole treatment and release</i>	81
3.4. Cell cycle-dependence of cisplatin and carboplatin toxicity	82
3.5. <i>Characterisation of the effects of cisplatin and carboplatin on cell cycle progression and DNA damage responses in G1-phase cells</i>	87
3.5.1. <i>Effect of cisplatin and carboplatin on cell cycle progression in G1-phase cells lacking or expressing DNA pol η</i>	87
3.5.2. <i>BrdU incorporation after cisplatin and carboplatin treatment of G1-phase cells lacking or expressing DNA pol η</i>	92
3.5.3. <i>Expression of cyclin B and cyclin E after treatment of G1-phase XP30R0 and TR30-2 cells with cisplatin</i>	96
3.5.4. <i>Expression of cyclin B and cyclin E after treatment of G1-phase XP30R0 and TR30-2 cells with carboplatin</i>	98
3.6. Activation of DNA damage responses	100
3.6.1. <i>H2AX phosphorylation in cisplatin- and carboplatin-treated G1-phase XP30R0 cells</i>	100
3.6.1.1. Nuclear staining for γ H2AX in cisplatin- and carboplatin-treated G1-phase XP30R0 cells	101
3.6.2. <i>Phosphorylation of RPA2 on serine 4/serine 8 in cisplatin- and carboplatin-treated G1-phase XP30R0 and TR30-2 cells</i>	104
3.6.2.1. Nuclear RPA2 serine4/serine8 staining in cisplatin- and carboplatin-treated G1-phase XP30R0 cells	106
3.6.2.2. Effect of inhibition of PIK kinases or CDKs on cisplatin- and carboplatin-induced RPA2 hyperphosphorylation in G1-phase XP30R0 cells	110
3.6.3. <i>The timing of cisplatin- and carboplatin-induced Chk1 and RPA2 phosphorylation in XP30R0 cells treated in G1-phase</i>	112

3.7. Characterisation of the effects of cisplatin and carboplatin on cell cycle progression and DNA damage responses in S-phase cells	115
3.7.1. <i>Effect of cisplatin and carboplatin on cell cycle progression in S-phase cells lacking or expressing DNA pol η</i>	115
3.7.2. <i>Determination of BrdU incorporation in S-phase cells after cisplatin- and carboplatin-treatment in S-phase cells lacking or expressing DNA pol η</i>	120
3.7.3. <i>Expression of cyclin B and cyclin E after treatment of S-phase XP30R0 and TR30-2 cells with cisplatin</i>	124
3.7.4. <i>Expression of cyclin B and cyclin E after treatment of S-phase XP30R0 and TR30-2 cells with carboplatin</i>	126
3.8. Activation of DNA damage responses	128
3.8.1. <i>H2AX phosphorylation in cisplatin- and carboplatin-treated S-phase XP30R0 cells</i>	128
3.8.1.1. Nuclear staining for γ H2AX in cisplatin- and carboplatin-treated S-phase XP30R0 cells	129
3.8.2. <i>Phosphorylation of RPA2 on serine 4/serine 8 in cisplatin and carboplatin-treated S-phase XP30R0 and TR30-2 cells</i>	132
3.8.2.1. Nuclear RPA2 serine4/serine8 staining in cisplatin- and carboplatin-treated S-phase XP30R0	134
3.8.2.2. Effect of PIK kinase and CDK on cisplatin- and carboplatin-induced RPA2 hyperphosphorylation in S-phase XP30R0 cells	137
3.8.3. <i>The timing of cisplatin- and carboplatin-induced Chk1 and RPA2 phosphorylation in XP30R0 cells treated in S-phase</i>	139
3.9. Characterisation of the effects of cisplatin and carboplatin on cell cycle progression and DNA damage responses in M-phase cells	143
3.9.1. <i>Effect of cisplatin and carboplatin on cell cycle progression in M-phase cells lacking or expressing DNA pol η</i>	143
3.9.2. <i>Determination of BrdU incorporation after cisplatin and carboplatin treatment in M-phase cells lacking or expressing DNA pol η</i>	147
3.9.3. <i>Expression of cyclin B and cyclin E after treatment of M-phase XP30R0 and TR30-2 cells with cisplatin</i>	151
3.9.4. <i>Expression of cyclin B and cyclin E after treatment of M-phase XP30R0</i>	

<i>and TR30-2 cells with carboplatin</i>	153
3.10. Activation of DNA damage responses	155
3.10.1. <i>H2AX phosphorylation in cisplatin-and carboplatin-treated M-phase XP30R0 cells</i>	155
3.10.2. <i>Phosphorylation of RPA2 on serine 4/serine 8 in cisplatin and carboplatin-treated M-phase XP30R0 and TR30-2 cells</i>	156
3.10.2.1. Effect of PIK kinase and CDK inhibitors on cisplatin-and carboplatin-induced RPA2 hyperphosphorylation in M-phase XP30R0 cells	158
3.10.3. <i>The timing of cisplatin- and carboplatin-induced Chk1 and RPA2 phosphorylation in XP30R0 cells treated in M-phase</i>	159
3.11. Comparative analysis of cisplatin or carboplatin treatment in different cell cycle phases	163
3.11.1. <i>Cell viability following treatment in different phases</i>	163
3.11.2. <i>Analysis of cell cycle progression among cells treated in different phases</i>	163
3.11.3. <i>Analysis of key DNA damage responses in cells treated in different phases</i>	164
Chapter 4 – Discussion	167 - 178
Chapter 5 – Conclusions and future directions	180 - 182
Chapter 6 – Bibliography	184 - 231
Chapter 7 – Publications	

Acknowledgement

I would like to sincerely thank my research supervisor Dr. Michael P Carty for his supervision, advices, and guidance throughout my research. Above all and the most needed, he provided me unflinching encouragement and support in various ways. Looking back, I am surprised and at the same time very grateful for all I have received throughout these years. It has certainly shaped me as a person and has led me where I am now.

Special thanks to the DDR group – Severine, Elaine Aine, Kathleen, Ania and Sarah for sharing the glory and sadness of conferences deadlines and day-to-day research, creating a happy working environment.

Thank to the Drs. Pat Morgan and Gerry Morgan for their hospitality in hosting me during my initial days in Ireland and for the encouragement and support throughout my research life. Thank to my family, especially my dad who have encouraged me and believed in my abilities. A big thank you to my husband Gopi, without you it would have been certainly much harder to travel this path. Finally, I would like to thank everybody who was important to the successful realisation of thesis, as well as expressing my apology that I could not mention personally one by one.

Abbreviations

APS	Ammonium persulfate
AT	Ataxia telangiectasia
ATM	Ataxia telangiectasia-mutated
ATR	ATM and Rad3 related
ATRIP	ATR-interacting protein
BER	Base excision repair
BRCA1	Breast cancer type 1 susceptibility protein
BRCA2	Breast cancer type 2 susceptibility protein
BRCT	BRCA1 C-terminal
BrdU	Bromodeoxyuridine
BSA	Bovine serum albumin
CDK	Cyclin dependent kinase
Chk1	Chk1 protein kinase
Chk2	Chk2 protein kinase
CIN	Chromosomal instability
CPD	Cyclobutyl-Pyrimidine Dimer
DAPI	4',6-Diamidino-2-Phenylindole
DBD	DNA-Binding Domains
DDR	DNA damage response
DMSO	Dimethylsulfoxide
DNA	Deoxyribonucleic Acid
DNA-PK	DNA protein kinase
DNA-PK _{cs}	DNA protein kinase catalytic subunit
DSB	Double-strand break
dsDNA	Double stranded DNA
EDTA	Ethylene diamine tetraacetic acid
Erk	Extracellular signal-regulated protein kinase
FA	Fanconi anaemia
FANCD2	Fanconi Anaemia Protein D2
FATC	FAT C-terminal
FBS	Foetal bovine serum

FHA	Forkhead-associated
FITC	Fluorescein isothiocyanate
GIN	Genetic instability
HBSS	Hanks balanced salt solution
HJ	Holliday junction
HMBG1	High mobility group 1 protein
HR	Homologous recombination
hSSB	Human single-stranded DNA binding protein
ICL	DNA interstrand crosslink
IR	Ionizing radiation
MAPK	Mitogen-activated protein kinase
MDM1	Mediator of DNA damage checkpoint 1
MDM2	Murine double minute
MEF	Mouse embryonic fibroblast
MEM	Minimum essential medium eagle
MIN	Microsatellite instability
MMR	Mismatch repair
Mre11	Meiotic recombination 11
MRN	Mre11-Rad50-Nbs1 complex
mTOR	Mammalian target of rapamycin
Nbs1	Nijmegen breakage syndrome protein 1
NER	Nucleotide excision repair
NHEJ	Non-homologous end joining
NSCLC	Non-small cell lung cancer
OB-fold	Oligosaccharide-oligonucleotide binding fold
PAGE	Polyacrylamide gel electrophoresis
PARP-1	poly(ADP-ribose) polymerase -1
PBS	Phosphate-buffered saline
PCC	Premature chromatin condensation
PCNA	Proliferating cell nuclear antigen
PFA	Paraformaldehyde
PI	Propidium iodide
PIKK	Phosphoinositide 3-kinase-like kinase
PIP	PCNA-interacting protein

Plk1	Polo-like kinase-1
PMSF	Phenylmethanesulfonyl Fluoride
Pol β	DNA polymerase β (beta)
Pol δ	DNA polymerase δ (delta)
Pol ζ	DNA polymerase ζ (zeta)
Pol η	DNA polymerase η (eta)
PRKDC	Protein Kinase, DNA-activated, catalytic polypeptide
PVDF	Polyvinylidene fluoride
ROS	Reactive oxygen species
RPA1	Replication protein A, 70kDa subunit
RPA2	Replication protein A, 32kDa subunit
RPA3	Replication protein A, 14kDa subunit
SAPK/JNK	Stress-activated protein kinase/jun N-terminal kinase
SDS-PAGE	Sodium dodecyl sulphate-polyacrylamide gel electrophoresis
SMC1	Structural maintenance of chromosomes protein-1
SSB	Single strand break
ssDNA	Single stranded DNA
SV40	Simian virus 40
TBS-T	Tris buffered saline – Tween 20
TCR	Transcription coupled repair
TEMED	N,N,N,N'-Tetra-methyl-ethylenediamine
TLS	Translesion synthesis
Tween-20	Polyoxyethylene-Sorbitan Monolaurate
UBZ	Ubiquitin-binding domain
UV	Ultraviolet radiation
XP	Xeroderma pigmentosum
XPV	Xeroderma pigmentosum, variant
γ H2AX	H2AX pSer139

Abstract

Platinum-based chemotherapeutic drugs such as cisplatin and carboplatin induce intra- and interstrand crosslinks, resulting in replication arrest, and cell death. Translesion synthesis by DNA polymerase η , is one way in which human cells can tolerate platinum-induced adducts. Because these adduct block replication, the cell cycle stage at the time of drug exposure, and the DNA polymerases expressed could affect the outcome of exposure. The aim of this research was therefore to investigate the effects of cell cycle phase at the time of drug exposure on cell viability, cell cycle progression and activation of DNA damage responses in pol η -deficient (XP30R0) and pol η -expressing (TR30-2) human fibroblast cell lines. Using nocodazole arrest and release to generate populations of cells enriched in G1, S or M phases, it was found that XP30R0 cells in S-phase were more sensitive to drug treatment compared to cells that were in G1- and M-phase at the time of treatment. When G1 cells were treated with drug, cell arrest in S- and G2/M-phases was detected by flow cytometry. When S-phase XP30R0 cells were treated with cisplatin, a strong S-phase arrest was detected, however, when treated with carboplatin, arrest in S phase was less pronounced, and there was evidence for S-phase arrest in a second cell cycle. In TR30-2 cells, the extent of S-phase arrest was less than in XP30R0 cells, consistent with a role for pol η in replication of damaged DNA. In M-phase XP30R0 cells following treatment, cells were delayed entering S and by 24 hours post-treatment, strong S-phase arrest occurred. Using western blotting and immunofluorescence, it was found that DNA damage-induced phosphorylation of key PIK kinase substrates including H2AX, Chk1 and RPA2, was induced following drug treatment of XP30R0 cells in all cell cycle phases. Comparison of the timing of Chk1 ser317 and RPA2 ser4/ser8 phosphorylation demonstrated that activation of the Chk1 phosphorylation was an earlier event than RPA2 phosphorylation, independent of the cell cycle phase at the time of exposure. RPA2 phosphorylation was consistent with prolonged replication arrest in S-phase cells. Using small molecule inhibitors, roles for DNA-PK and CDK1/2 in damage-induced RPA2 phosphorylation were identified. The data provides an insight into the molecular events that determine the outcome of drug exposure in cells treated at different phases of the cell cycle, and may be relevant to

identification of pathways that can be targeted to improve the efficacy of these drugs in cancer therapy.

Chapter 1: Introduction

1.1. Cancer

Cancer is the second leading cause of death worldwide according to the International Union against Cancer, with 12 million cases of cancer diagnosed and 7 million deaths in 2008 (Jemal et al., 2008). It is estimated that approximately 25% of deaths in United States and in Ireland is due to cancer (Jemal et al., 2010; Jemal et al., 2008). The three most commonly diagnosed types of cancer in the US among women in 2010 were breast, lung, bronchus, and colorectum, accounting for 52% of estimated cancer cases in women (Edwards et al., 2010). Among men, cancers of the prostate, lung, bronchus, and colorectum account for 52% of all newly diagnosed cancers (Edwards et al., 2010). Despite recent developments in understanding cancer at a molecular level, broad-based therapies such as surgery, radiotherapy and chemotherapy still play a critical role in cancer treatment.

Cancer ultimately arises from alterations in an individual cell. A normal human cell in culture can divide between 40 and 60 times before it stops dividing (Hayflick and Moorhead, 1961). This is called the Hayflick limit (Hayflick and Moorhead, 1961). Occasionally cells become immortal and continue to multiply giving rise to abnormal cells that can form a mass of cells termed a tumour. Tumours can be benign or malignant. Benign tumours do not have the ability to metastasise (spread from one organ to other) and do not pose significant health risk and may be left untreated, or can be removed by surgery, depending on the nature of the tumour (Medeiros et al., 2009). On the other hand, malignant tumour cells invade adjacent tissues and organs (Nguyen et al., 2009). Cancer cells can also circulate through the body via the blood or lymphatic systems and lodge in distant organs, giving rise to secondary malignant tumours. This process is called metastasis, and, if left untreated, is often fatal (Nguyen et al., 2009).

1.2. Characteristics of cancer cells

It has been proposed that cancer cells all share a number of key characteristics that have been termed the six hallmarks of cancer (Hanahan and Weinberg, 2000). Normal cells acquire the six hallmarks in a multistep process and evolve into malignant cancer cells. The six hallmarks are self-sufficiency in growth signals, insensitivity to anti-growth signals, evasion of apoptosis, limitless replicative potential, sustained

angiogenesis and tissue invasion and metastasis (Hanahan and Weinberg, 2000). These characteristics are acquired in part by the development of genomic instability in cancer cells, which generates random mutations in key genes (Hanahan and Weinberg, 2000).

DNA damage from both endogenous and exogenous sources is a major source of genomic instability. It is estimated that about 10^5 lesions occur in the genome of a normal cell per day (Hoeijmakers, 2009). DNA repair is therefore essential to preserve the integrity of the genome (Hoeijmakers, 2009). The integrity of the genome in normal cells is maintained by the tumour suppressor genes (Rb, p53, APC) and oncogenes (Ras, Myc, Erk) (Berdasco and Esteller, 2010; Ciccia and Elledge, 2010; Negrini et al., 2010).

Chromosomal instability (CIN) is a major type and most common genomic instability in which abnormal chromosome structures and numbers are detected in cancer cells due to, for example, defects in the spindle assembly checkpoint (SAC) or in mitotic chromosome segregation (Negrini et al., 2010). Micro- and mini-satellite instability (MIN) is another form of genomic instability that is characterised by the expansion, contraction, deletion or point mutation of a number of oligonucleotide repeats present in micro- and mini-satellite sequences (Nikiforov et al., 1998).

Another mechanism for chromosome instability in cancer is due to the loss of telomeres (Blackburn, 1999). Telomeres are tandem arrays of short G-rich repetitive sequences (Riethman et al., 1989) added on to the ends of chromosomes by the enzyme telomerase (McEachern et al., 2000). During cell division, telomere length is maintained in germ cells by telomerase. However, somatic cells do not express telomerase to prevent telomere loss as they divide. As a result, in somatic cells the telomeres eventually shorten to initiate cell cycle arrest in G1-phase called replicative senescence (Harley et al., 1990). In contrast, many tumour cells constitutively express telomerase and continue to divide indefinitely (Jiang et al., 1999). Comparative genomic hybridization (CGH) analysis reveals gains and losses of gene copy number across the genome (Korkola and Gray, 2010). Specific aberrations, both amplifications and deletions at particular sites in the genome, are likely to harbour genes whose alteration favours tumour progression (Korkola and Gray, 2010). Thus, recurring genetic alterations may point to an important role of particular mutations in

tumour pathogenesis. Use of CGH has shown that the copy number alterations (CNAs) from telomere-deficient mice are similar to those observed in human cancers (Artandi and DePinho, 2010).

Faithful transmission of the genetic material to daughter cells is essential to maintain genome stability and for cell survival. Since DNA is prone to damage by various damaging agents a number of repair systems have evolved to correct DNA damage (Kerzendorfer and O'Driscoll, 2009). In mammalian cells there are four major repair pathways: nucleotide excision repair (NER), mismatch repair (MMR), base excision repair (BER) and double-strand break repair pathways (DSBR). Inherited mutations in various DNA repair genes can result in genomic instability, causing cancer-prone human syndromes (Friedberg, 2001; Herrick and Bensimon, 2009; Hoeijmakers, 2007; Kastan and Bartek, 2004). For example, defects in NER proteins results in one of the three photosensitive syndromes: xeroderma pigmentosum (XP) (Cleaver and Revet, 2008), Cockayne syndrome (CS) and trichothiodystrophy (TTD). Mismatch repair deficiency is linked predominantly to cancers of the colon, especially hereditary non-polyposis colon cancer (HNPCC), endometrium and ovary (Hewish et al., 2010). Ataxia-telangiectasia, Nijmegen breakage syndrome (NBS) and ataxia telangiectasia-like disorder (ATLD) are caused by defects in the genes *ATM*, *NBS*, *MRE11* respectively. These genes are involved in the DNA damage response particularly in double-strand break repair (Hewish et al., 2010).

1.3. Sources of DNA damage

DNA damage can arise from either endogenous or exogenous sources (Hoeijmakers, 2001b) (Figure 1.1). As noted above, DNA is under constant attack from various environmental agents and as a result of normal metabolic processes that occur in a cell. DNA damage mainly affects the structure of the DNA double helix by modifying individual bases.

(a) Endogenous damage occurs due to various metabolites produced as a by-product of biochemical reactions within the cell, such as reactive oxygen species (ROS) (Galaris and Evangelou, 2002). Despite the action of DNA repair systems, oxidatively modified DNA is abundant, in the range of 1-200 modified nucleosides per 10^5 intact nucleosides per cell (Nordberg and Arner, 2001). Oxidatively modified DNA leads to

base pair mutations, rearrangements, deletions and insertions (Hamada et al., 2001). Point mutations and deletions in proto-oncogenes or tumour suppressor genes contribute to tumour development (De Bont and van Larebeke, 2004). Aldehydes derived from lipid peroxidation form another threat to DNA by forming adducts such as etheno-, propano- and malondialdehyde-derived DNA bases (Epe, 2002). Several oestrogen metabolites can also cause DNA damage directly or indirectly, through redox cycling processes that generate reactive radical species (Yager and Liehr, 1996). Aqueous hydrolysis of the glycosidic bond results in the formation of mutagenic abasic sites in DNA (De Bont and van Larebeke, 2004). DNA bases are also susceptible to hydrolytic deamination (De Bont and van Larebeke, 2004).

(b) Exogenous damage to DNA occurs as a result of exposure to, for example, ultraviolet radiation (UV), ionising radiation (IR) and many chemical agents.

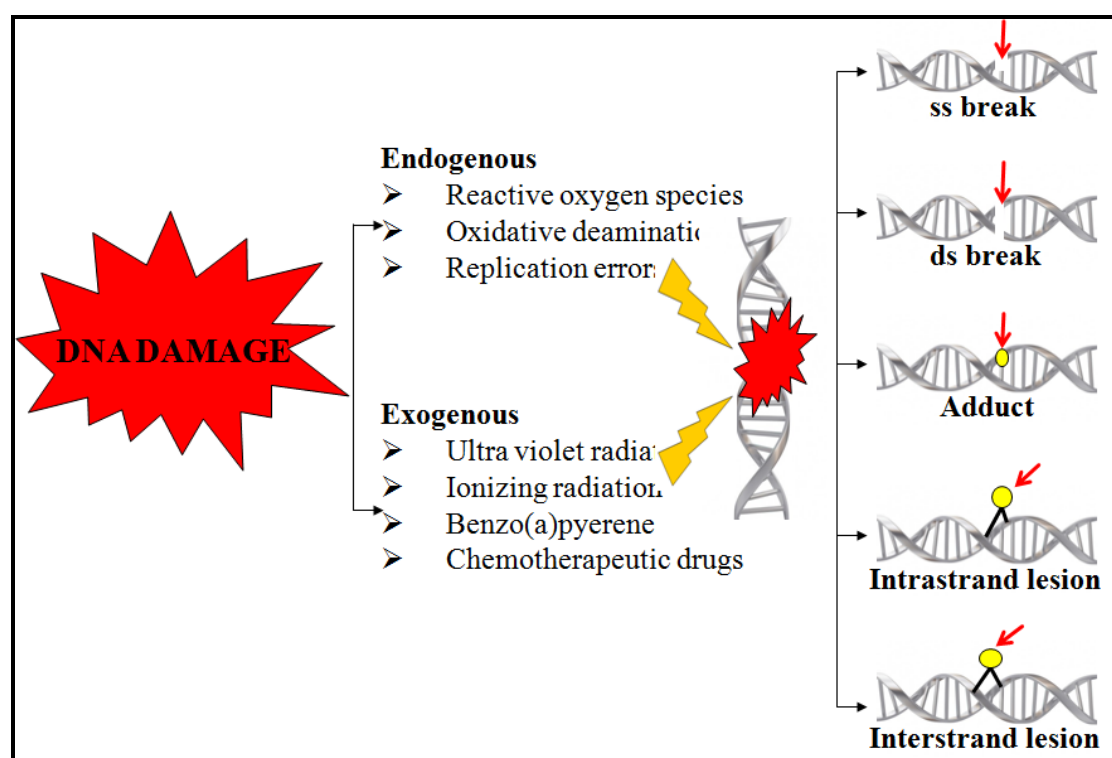


Figure 1.1. Examples of endogenous and exogenous sources of DNA damage, and the different types of DNA damages induced (Hoeijmakers, 2001a).

1.3.1. DNA damage by ultraviolet light (UV)

UV irradiation is a carcinogen, and exposure to UV causes different types of skin cancer that collectively represent approximately 40% of all malignancies diagnosed

every year in US (Detres et al., 2001; Jemal et al., 2010). DNA is one of the key targets for UV-induced radiation damage (Hader and Sinha, 2005). UVC radiation (200-280 nm) is absorbed by the ozone layer in the atmosphere, whereas longer wavelength UVA (320-395 nm) and UVB (280-320 nm) are not. UVA and UVB have significant deleterious effects on DNA (van Kranen and de Gruijl, 1999). Both UVB and UVC radiation induce two types of mutagenic and cytotoxic DNA lesions, cyclobutane pyrimidine dimers (CPDs), and (6–4) photoproducts (6-4PPs) at adjacent pyrimidines (Nakajima et al., 2004). CPDs account for about 75%, and 6–4PPs about 25%, of the total UV-induced DNA lesions (Sinha and Hader, 2002). UVA causes oxidative DNA damage and also plays an important role in skin cancer development (Zhang et al., 1997). UVA causes A:T>C:G transversion mutation in Chinese hamster ovary cells (Huang et al., 2009) and also induces CPDs (Besaratina et al., 2004; Kappes et al., 2006; Rochette et al., 2003). UV-induced CPDs distort the DNA double helix by causing a bend of 9°, while 6–4PPs cause a 44° bend in the DNA double helix (Lee et al., 2004). These lesions result in inhibition of DNA replication and transcription, and are removed by nucleotide excision repair from the genome (Hoeijmakers, 2001a, b).

1.3.2. DNA damage by ionising radiation

Ionising radiation such as γ -rays and X-rays induce double-strand breaks (DSBs) and single-strand breaks (SSBs) in DNA. A DNA double-strand break causes genomic instability such as chromosome aberrations, small deletions and point mutations, which may eventually lead to cancer (Rothkamm et al., 2007). The numbers of DNA lesions per human cell that are detected immediately after a radiation dose of 1 Gy have been estimated to be approximately greater than 1000 damaged bases (Banath et al., 1999). Ionising radiation in the form of radiotherapy is used in the treatment of cancer by inducing DNA damage in cancer cells (Grudzinski et al., 2010). The amount of radiation depends on the type and stage of the cancer being treated. For curative purposes, for example, the typical doses for solid epithelial tumours range from 60-80 Gy in two Gy fractions (Boone, 2009). In the case of breast, head and neck cancer the dose varies between 45-60 Gy delivered in 1.8-2 Gy fractions (Scorsetti et al., 2011).

1.3.3. DNA damage by chemical agents

Cancer development has been closely associated with exposure to a variety of chemical agents that humans come in contact with, either in the natural environment or as a result of occupational exposures (Panacheva et al., 2005). Exposure to DNA reactive genotoxins results in the induction of DNA lesions (O'Brien et al., 2006). An important class of genotoxins that react with DNA are alkylating agents (Pegg et al., 1998). Tobacco smoke results in the formation of alkylating agents that damage DNA by production of DNA adducts leading to mispairing during DNA replication (Pfeifer et al., 2002; Zheng et al., 2001). A good example is benzo(a)pyrene in cigarette smoke, which forms adducts with guanine bases (Denissenko et al., 1996). A number of mutations in the lung cancer cell line H358, were identified using high throughput sequencing technology (Gelhaus et al., 2011). The majority of mutations were found at guanine bases, consistent with a role for benzo(a)pyrene adducts in the formation of mutations in lung cancer cells (Lenne-Samuel et al., 2000).

1.4. DNA damage by chemotherapeutic drugs

Chemotherapy is the use of chemical agents in the treatment of cancer. More than 50% of people diagnosed with cancer are treated with chemotherapeutic drugs (Joensuu, 2008). Common examples include alkylating agents such as methyl methanesulfonate, which attach alkyl groups to the DNA, and crosslinking agents such as cisplatin (Celli and Jaiswal, 2003) and mitomycin C that introduce crosslinks between bases of the same strand (intrastrand crosslinks) or between different strands (interstrand crosslinks) (Ciccia and Elledge, 2010).

1.4.1. Platinum-based chemotherapeutic drugs

The discovery of cisplatin dates back to 1845, when it was called Peyrone's chloride, named after the discoverer Michel Peyrone; Alfred Werner elucidated the structure of cisplatin in 1893 (reviewed in (Kelland, 2007)). Barnett Rosenberg, a biophysist, in 1960 was investigating the effect of electric or magnetic fields on bacterial and mammalian cell division (Rosenberg et al., 1969). He was using platinum electrodes, and discovered that bacterial cells appeared as long filaments about 300 times the usual length when exposed to the electric field. This effect was later shown to be due to the generation of cisplatin during the electrolysis process (Rosenberg et al., 1969).

Although cisplatin therapy has been very effective in treating cancers, especially ovarian and testicular cancer (Higby et al., 1974), there are side-effects due to severe nephrotoxicity, neurotoxicity and ototoxicity (Kelland, 2007; Rabik and Dolan, 2007). This has led to the development of the second-generation drug carboplatin, which has reduced side-effects (Harrap, 1985). Carboplatin is effective against ovarian and non-small cell lung cancer, but has side effects such as myelosuppression (van der Vijgh, 1991). The third generation drug oxaliplatin (Holzer et al., 2006) was found to overcome tumour resistance to cisplatin (Eckardt et al., 2007; Holzer et al., 2006; Jackiewicz et al., 2009). Oxaliplatin is now used as first-line therapy in colorectal cancer treatment (Koshiyama et al., 2005). The structure of cisplatin, carboplatin and oxaliplatin are shown in figure 1.2.

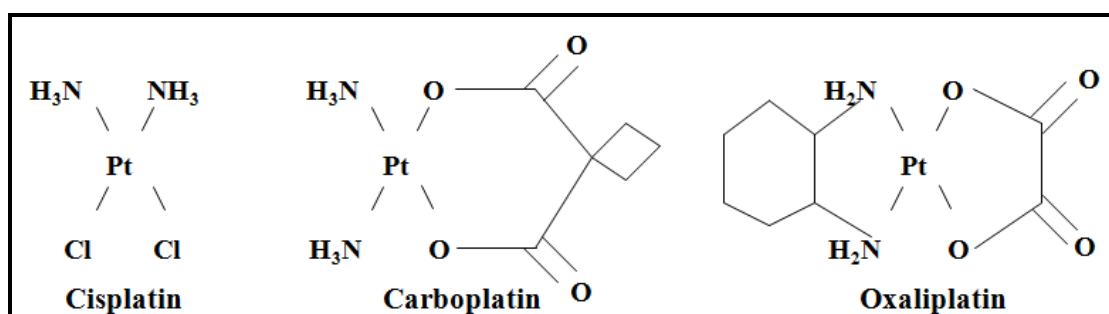


Figure 1.2. Structure of cisplatin, carboplatin and oxaliplatin (Nussbaumer et al., 2011).

The sensitivity to and cytotoxicity of the platinum drug can be explained in part by the adduct levels in the DNA (Bassett et al., 2004; Wu et al., 2004b). Exposure of human XP30R0 fibroblast cells to 5 µg/ml cisplatin for 18 hours resulted in 11.76 pg Pt/µg genomic DNA measured using atomic absorption spectroscopy (Cruet-Hennequart et al., 2008). Similarly when human XP30R0 cells were treated with 4 µg/ml oxaliplatin for 18 hours this resulted in 3.56 pg Pt/µg genomic DNA. Cisplatin adducts block Taq polymerase-mediated DNA synthesis, reducing the amplified product (Bingham et al., 1996). Hence a sensitive SINE (Short Interspersed DNA Element) mediated DNA damage detection assay was adapted for the detection of cisplatin-DNA adducts in cultured mouse 3T3 cells following exposure to cisplatin (Wang and Lippard, 2005). In mice the B1 elements are the most abundant SINEs

with a copy number estimated at 50,000–80,000. Using primers complementary to conserved regions of the B1 elements to anneal the majority of their targets in the genome (Maraia, 1991), large sequences of genomic DNA present between the B1 elements were simultaneously amplified using quantitative polymerase chain reaction (Q-PCR). 3T3 cells were treated with a range of doses from 5–120 μ M cisplatin. The lesion frequencies were from 0.13 lesions/10 kb/5 μ M cisplatin to 2.1 lesions/10 kb/120 μ M cisplatin. In *in vivo* experiments, cisplatin (0, 1, 4, 8 mg/kg body weight) was injected intraperitoneally into mice. After 8 hours, DNA from blood samples was isolated and quantified which show a reduction in the amplified product, which is dependent on the dose of cisplatin. This reduction reflects the damage induced by cisplatin. The corresponding approximate lesion frequencies at 1, 4 and 8 mg/kg body weight were 0.07, 0.17 and 0.45/10 kb of DNA, respectively (Wang and Lippard, 2005).

1.4.2. Cisplatin-induced DNA damage

Cisplatin (cis-diamminedichloroplatinum(II)) is a neutral, square planar coordination complex of platinum(II) having two labile chloride ligands and two inert ammine groups (Todd and Lippard, 2009) as shown in figure 1.2. The *cis* configuration is necessary for the anti-tumour activity of cisplatin (Zamble and Lippard, 1995). The trans isomer, transplatin is clinically inactive because of (i) the type of DNA adducts formed (small amounts of interstrand cross links are formed and no stable intrastrand crosslinks are formed) (ii) chemical reactivity that results in the deactivation of the complex before the drug reaches the tumour site (Kasparkova et al., 2008). Cisplatin is used in the treatment of testicular, ovarian, head and neck, and small cell lung cancers. (Keys et al., 1999; Loehrer and Einhorn, 1984; Morris and Bosl, 1999) It is used in the treatment of testicular germ cell cancers with cure rates of up to 90% (Raghavan, 2003). The mode of action of cisplatin includes four stages: (i) cisplatin is taken up by the cell by both active and passive diffusion; (ii) once inside the cell cisplatin forms activated platinum complexes; (iii) the complexes bind to DNA and form cisplatin-DNA adducts; (iv) adducts block DNA replication and transcription, leading to cell death (Wang and Lippard, 2005).

Cisplatin is actively transported into human cells (Byfield and Calabro-Jones, 1981) by transporters including copper transporter (CTR) protein 1 (Song et al., 2004) and

organic cation transporters (OCTs) belonging to the solute carrier 22 (SLC22) family (Koepsell and Endou, 2004). The SLC22 family consists of several subgroups of carrier proteins. One family comprises the organic cation transporters (OCTs) (Burger et al., 2011), which consist of three members: SLC22A1 (OCT1), expressed in liver and brain, SLC22A2 (OCT2), expressed in brain and kidney, and SLC22A3 (OCT3) expressed primarily in liver, kidney and heart (Koepsell and Endou, 2004). OCT2 plays a role in the uptake and cytotoxicity of various platinum compounds (Burger et al., 2011; More et al., 2010). *In vivo* studies in mice show that OCT2 mediates uptake and transport of cisplatin (Ciarimboli et al., 2010; Filipski et al., 2008). As noted, cisplatin treatment is associated with nephrotoxicity and ototoxicity (Rybak and Whitworth, 2005). OCT2 has been proposed to be involved in potentiating cisplatin-induced nephrotoxicity in the kidney proximal tubule, as OCT2 is expressed in kidneys (Ciarimboli et al., 2010; Gorboulev et al., 1997; Ikari et al., 2005; Rabik and Dolan, 2007). OCT2 also plays a primary role in cisplatin-induced ototoxicity. OCT2 expression in inner and outer hair cells of the cochlea was detected by *in vivo* experiments in mice (Ciarimboli et al., 2010). Cisplatin-treated wild-type mice showed both nephrotoxicity (such as significant increase in polyuria, proteinuria, glucosuria and apoptosis) and ototoxicity (such as significant hearing loss at high frequencies) when compared to OCT1/2^{-/-} knockout mice (Ciarimboli et al., 2010). Hence OCT2 has been identified as a common mediator of cisplatin induced nephro- and ototoxicity by *in vivo* studies.

In addition to uptake, efflux also plays an important role in determining the outcome of cisplatin exposure. ATP7A and ATP7B, two P-type ATPases, are involved in the efflux of platinum compounds (Liu et al., 2010) especially resulting in decreased accumulation of cisplatin in tumour cells, and diminished cytotoxicity. (Nakayama et al., 2001)

Cisplatin undergoes hydrolysis inside the cell. Chloride concentration plays an important role during hydrolysis. Hydrolysis takes place inside the cell because the intracellular chloride concentration (4mM) is lower than the chloride concentration in the blood plasma (103mM) (Sedletska et al., 2005). The chloride ligands are easily substituted by water or hydroxide ions in a process called aquation. It is this aquated, electrophilic, cisplatin that reacts with nucleotides at the N7 position of purine bases

in DNA, resulting in the formation of platinum-DNA adducts (Figure 1.3) (Jamieson and Lippard, 1999). Cisplatin-induced DNA damage includes intrastrand crosslinks, (primarily 1,2-d(GpG) (60-64%), 1,2-d(ApG) (25-29%), and 1,3-d(GpNpG) (5-10%) adducts, interstrand crosslinks (1%), and monoadducts (1-3 (Eastman and Barry, 1987).

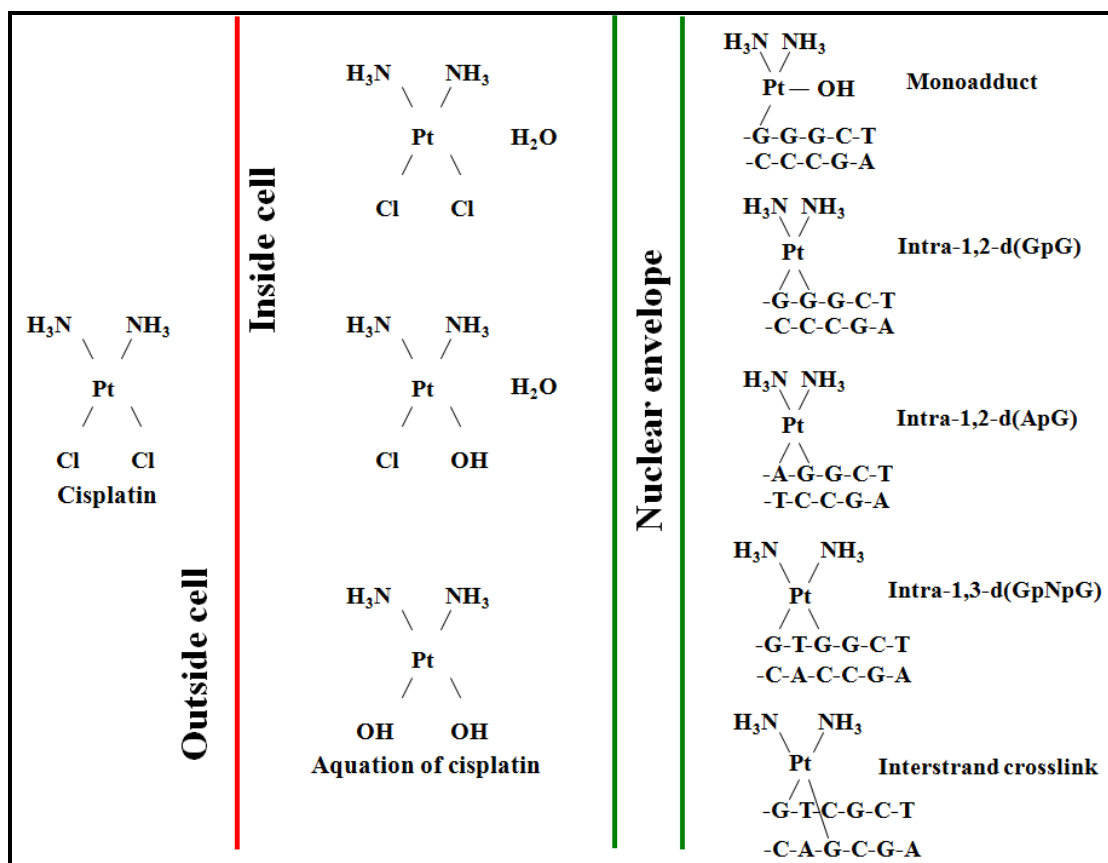


Figure 1.3. Schematic representation of process of aquation of cisplatin inside the cell. The platinum ion binds covalently to the N7 position of purine bases to form intrastrand or interstrand crosslinks (Wang and Lippard, 2005)

While ICLs constitute about 1% of the lesions, they are considered to be the most cytotoxic lesions (Eastman and Barry, 1987). However studies show that intrastrand crosslinks make up to > 95% of the adducts, it is important to understand how cells deal with these adducts. Cisplatin binding to DNA induces structural alterations by bending and unwinding the double helix. X-ray crystallography studies of the 1,2-d(GpG) intrastrand adduct shows that the adduct bends the DNA helix by 40° towards the major groove (Donahue et al., 1990). The 1,3-d(GpNpG) adduct bends the DNA helix by 30° (Malinge et al., 1999). Different cisplatin adducts induce unique

distortions that are differentially recognised by DNA damage repair proteins (Kartalou and Essigmann, 2001a, b; Todd and Lippard, 2009).

As outlined above, cisplatin also generates interstrand crosslinks (ICL) and monoadducts (Fichtinger-Schepman et al., 1985). ICLs prevent the strand separation that is required for essential functions such as DNA replication, transcription, and recombination. Repair of ICLs also results in monoadducts, which will be discussed in Section 1.6.2.1. One of the differences between the interstrand cisplatin crosslink adduct and the intrastrand cisplatin crosslink adduct for example, 1,2-d(GpG) is that, the ICL bends the DNA towards the minor groove and that of the intrastrand adduct bends the DNA towards the major groove (Coste et al., 1999). The ICL binds to the minor groove and bends the helix by 47° in that direction, whereas in the case of the intrastrand crosslink, the adduct binds to the major groove and bends the helix by 40° (Sullivan et al., 2001a, b). The double helix is severely unwound, by 110° , in case of the ICL, resulting in the two cytosine bases opposite the bound guanines being pointed outward, away from the duplex, whereas in the case of the intrastrand adduct the helix is unwound by 15° as revealed by X-ray crystallography and NMR spectroscopy (Coste et al., 1999; Stehlikova et al., 2002).

A number of proteins bind to platinum-DNA adducts with high specificity over unmodified DNA. High-mobility group box protein 1 (HMGB1) is one protein that binds tightly to cisplatin-DNA adducts (Wang and Lippard, 2005). HMGB1 is a non-histone chromosomal protein and plays an important role in many cellular processes involving DNA, including chromatin remodelling, recombination, replication, and transcription (Thomas and Travers, 2001). HMGB1 contains two tandem HMG domains, A and B, and a C-terminal acidic tail. The full-length protein binds the cisplatin intrastrand crosslink (1,2-d(GpG) adduct) primarily through the A domain (Zamble et al., 1996). The repair of 1,2-d(GpG) cisplatin adducts occurs primarily by nucleotide excision repair pathways (Zamble et al., 1996). It is demonstrated that HMGB protein and other B-box-containing proteins including Upstream Binding Factor (UBF), lymphoid enhancer-binding factor LEF-1; the mammalian testis-determining factor SRY; structure specific recognition protein 1 (SSRP1) inhibit NER from repairing the cisplatin adducts both *in vivo* and *in vitro* (Jordan and Carmo-Fonseca, 2000; Reeves and Adair, 2005; Wozniak and Blasiak, 2002).

HMGB1 binds to the DNA and forms a complex, which protects cisplatin adducts from repair by preventing access of NER factors to adduct sites (Arioka et al., 1999). Consistent with this, binding of HMGB1 to cisplatin adducts *in vitro* also inhibits binding of replication protein A (RPA) (Patrick and Turchi, 1999) which, along with xeroderma pigmentosum protein A (XPA), is involved in the initial recognition of DNA lesions in the NER pathway (Hoeijmakers, 2001a). HMGB1 also recognises the interstrand crosslink of cisplatin but with approximately 5-fold lower affinity than the intrastrand crosslinks (Kasparkova et al., 2003).

1.4.3 Carboplatin-induced DNA damage

To find a platinum-based drug with fewer side-effects than cisplatin, in the mid-1980s collaboration between the company Johnson Matthey Plc and the Institute of Cancer Research (ICR) in London, led to the synthesis of the second generation platinum-based drug carboplatin (cis-diammine-[1,1-cyclobutanedicarboxylato]platinum(II) (Figure 1.3) (Harrap, 1985). Carboplatin (Figure 1.2) has a more stable leaving group (cyclobutane dicarboxylate) than cisplatin (chloride) (Harrap, 1985). Clinically, carboplatin has fewer side-effects than cisplatin without affecting the anti-tumour efficacy (Rajeswaran et al., 2008). Carboplatin is used in the treatment of ovarian and lung cancer (Ardizzoni et al., 2007). Carboplatin is different from cisplatin due to the difference in the leaving moiety, which slows the metabolic breakdown of carboplatin in the body (Knox et al., 1986).

The molecular mechanism of interaction of carboplatin with DNA is by the process of aquation, similar to that of cisplatin. However, the rate of adduct formation is about 10-fold slower (Knox et al., 1986). Aquation of carboplatin is the rate-limiting step in its reaction with DNA to form adducts (Hongo et al., 1994). In case of cisplatin, the time taken for mono-aquation and diaquation is the same. However, in the case of carboplatin, the rate of mono-aquation is slower when compared to cisplatin. Once carboplatin is mono-aquated, the time taken for diaquation is 18-fold faster than the formation of the mono-aquated form (Hongo et al., 1994). This is due to the fact that, in carboplatin, the leaving group becomes highly labile after carboplatin becomes mono-aquated (Knox et al., 1986).

In contrast to cisplatin, the major adducts formed by carboplatin are 1,3-d(GpNpG) intrastrand crosslinks, which make up about 46% of the total adducts formed (Blommaert et al., 1995). This adduct distorts double-stranded DNA in a different manner than the cisplatin crosslink (1,2-d(GpG), by bending the DNA by 30° (Todd and Lippard, 2009). Other adducts include 1,2-d(GpG) (33%), 1,2-d(ApG) (19%), as well as a small percentage of interstrand cross-links (1%) and monofunctional adducts (1%) (Blommaert and Saris, 1995; Blommaert et al., 1995).

The largest benefit of using carboplatin over cisplatin is due to its reduced side-effects and lack of nephrotoxicity (Sharma et al., 2011). However the main drawback of carboplatin is its myelosuppressive effects (Calvert et al., 1982). Due to this there is decreased production of blood cells and platelets from the bone marrow resulting in opportunistic infections. Carboplatin has proven to be effective against germ cell cancer, non-small cell lung cancer, ovarian and bladder cancer and acute leukaemia (Aabo et al., 1998). Carboplatin is routinely used for the treatment of ovarian cancer (Skirnisdottir et al., 2007).

1.4.4. Oxaliplatin-induced DNA damage

Oxaliplatin [l-OHP, oxalato(*trans-l*-1,2-diaminocyclohexane) platinum(II)] is a third-generation platinum based chemotherapeutic drug. The oxaliplatin molecular structure consists of a central platinum atom, surrounded by a 1,2-diaminocyclohexane group (DACH) and a bidentate oxalate ligand as shown in figure 1.2 (Kweekel et al., 2005; Woynarowski et al., 2000). Oxaliplatin forms mainly intrastrand crosslinks with DNA between two adjacent guanines (60% GpG) and between an adjacent adenine and guanine (25% ApG) (Saris et al., 1996; Sharma and Smith, 2008). As in the case of cisplatin and carboplatin oxaliplatin also forms a small percentage (1%) of interstrand crosslinks (ICL) (Woynarowski et al., 2000).

The intrastrand DNA adduct generated by cisplatin and oxaliplatin are repaired by similar kinetics by the mammalian nucleotide excision repair (NER) pathway (Reardon et al., 1999). However the adducts are differentially recognised by a number of cellular proteins, such as mismatch repair proteins (Chaney et al., 2005), probably due to the differences in the structure of adducts formed by the two agents (Scheeff et al., 1999). Oxaliplatin is effective in the treatment of cisplatin-resistant tumours and is

approved for the treatment of colon cancer (Chaney et al., 2005).

1.5. Platinum resistance

The clinical efficacy of platinum-based drugs is limited when tumours develop resistance to these drugs. A major mechanism responsible for the development of resistance to cisplatin is the pharmacodynamics of the drug (Shirazi et al., 1996) such that when the interstitial fluid pressures are increased, cisplatin is more easily absorbed by passive diffusion into cells, thereby increasing the efficacy and prolonging patient survival (Siddik, 2003).

Expression of the copper transporter CTR1 increases the cellular uptake of cisplatin. Human small cell lung carcinoma cells that are deficient in *CTR1* (due to a deletion mutation) are resistant to cisplatin (Ishida et al., 2002; Samimi et al., 2004). As noted, the copper-transporting P-type adenosine triphosphatases, ATP7A and ATP7B, play a role in the efflux of cisplatin (Katano et al., 2003; Safaei et al., 2004). In the cytoplasm, platinum-based drugs are aquated and can react with thiol-containing molecules like glutathione (Mukhopadhyay et al., 2003; Rabik and Dolan, 2007). Increased glutathione concentration induces resistance to cisplatin, as the drug is detoxified upon reaction with glutathione (Goto et al., 2002).

1.6. DNA Repair

DNA adducts are repaired by cellular repair pathways. Genetic defects in DNA repair pathways result in inherited human cancer prone-disorders (Hoeijmakers, 2001a). For example, defects in NER proteins causes xeroderma pigmentosum (XP) a recessive photosensitive skin cancer-prone syndrome (Johnson et al., 1999; Masutani et al., 1999). There are seven different complementation groups within the NER-deficient class of XP patients (XP-A to XP-G) (de Boer and Hoeijmakers, 2000). An additional form of XP, xeroderma pigmentosum variant (XPV) results from a defect in replication of UV-induced DNA rather than in NER (Yao et al., 2001), due to deficiency in DNA polymerase η , which is required for error-free bypass of UV-induced cyclobutane pyrimidine dimers (Cordonnier and Fuchs, 1999). Inherited defects in the *pol H* gene encoding polymerase η cause XPV (Johnson et al., 1999; Masutani et al., 1999).

DNA repair proteins could be excellent candidate targets for the development of new therapies to treat cancers (Kirschner and Melton, 2010), which provides a rationale for the use of synthetic lethal approach (Lord et al., 2006). Synthetic lethality occurs when a mutation in either of two genes individually has no effect but combining the mutations leads to cell death because tumour cells often have mutations in key genes (Kaelin, 2005). In cancer therapy, the idea is that suppressing one such gene when the other is defective would be lethal to tumour cells but not to normal cells (Ashworth, 2008). In the context of DNA repair, the best example of this approach is inhibiting PARP (poly(ADP-ribose) polymerase-1). Inhibition of PARP-1 by the specific small molecule AG14361 in BRCA1-mutated mouse embryonic stem cells and in the BRCA2-deficient human cell line V-C8 increased the sensitivity of the cell lines to DNA damaging agents such as ionising irradiation and mitomycin C (Veuger et al., 2003). This has led to the development of PARP inhibitors as therapy for BRCA1- and BRCA2-deficient cancers (Fong et al., 2009). Olaparib is a PARP inhibitor in phase II trials. Breast cancer patients having mutations in BRCA1 or BRCA2 demonstrated an overall response rate of 41% with olaparib (Tutt et al., 2010). Another study with women expressing mutations in BRCA1 and BRCA2 with advanced ovarian cancer demonstrated an overall response rate of 33% (Audeh et al., 2010). This suggests that PARP inhibitors will play a significant role in the treatment of cancer in BRCA1- and BRCA2-mutation carriers (Aly and Ganesan, 2011). However, a small fraction of advanced BRCA1-mutant cancers are resistant to PARP inhibitors (Fong et al., 2010; Tutt et al., 2010).

DNA repair also plays an important role in cisplatin resistance. This is supported by the evidence that cisplatin is effective against testicular cancer because of the reduced ability of these cells to repair cisplatin-induced DNA damage (Koberle et al., 2010; Usanova et al., 2010). It was found that expression levels of ERCC1-XPF endonuclease, an NER protein which is involved in repair of both intrastrand crosslinks and ICLs, is low in testis tumour cell lines compared to other tumour lines (Kirschner and Melton, 2010). It was demonstrated that ERCC1- or XPF-deficient rodent cells are significantly more sensitive to cisplatin than are any other NER-deficient cells (Lan et al., 2004).

1.6.1. Mismatch repair (MMR)

The DNA mismatch repair pathway is mainly responsible for the removal of nucleotides incorrectly inserted during DNA replication (Jiricny, 2000, 2006). The human mismatch repair machinery consists of the MutS α complex (comprising MSH2 and MSH6) and the MutS β complex (comprising MSH2 and MSH3) (Kolodner and Marsischky, 1999). Loss of MMR function, by knocking out MSH2 in *in vivo* mice studies, is associated with cisplatin resistance (Fink et al., 1998). Cisplatin-induced DNA adducts can result in a compound lesion by forming an intrastrand adduct on one strand and a mismatch on the other strand due to misincorporation during DNA replication (Sedletska et al., 2007). MutS α recognises 1,2-GpG intrastrand crosslinks having a misincorporated base opposite one of the cisplatin-adducted purines (Fourrier et al., 2003). MMR proteins bind to cisplatin-DNA adducts and initiate MMR-protein-dependent cell death in the human endometrial carcinoma cell line HEC59 and the human colon cancer cell line HCT116 treated. MMR protein-mediated activation of pro-death signalling involves cytochrome *c*, caspase-9, and caspase-3 following treatment with cisplatin. Cisplatin induces MMR protein-dependent signalling facilitating release of cytochrome *c* into the cytoplasm and cleavage of caspase-9, caspase-3, and PARP (Topping et al., 2009). Chemical inhibition of caspases by the pan-caspase inhibitor z-VAD-FMK inhibits cisplatin-induced, MMR protein-dependent loss of cell viability, indicating a requirement for caspase activation in MMR protein-dependent cytotoxic signalling (Topping et al., 2009).

1.6.2. Nucleotide excision repair (NER)

NER is a DNA repair pathway that removes lesions, which distort DNA and interfere with base pairing, replication and transcription. UV-induced CPDs and 6-4PPs are the major lesions repaired by NER (Sinha and Hader, 2002). Other lesions such as intrastrand DNA adducts and monoadducts formed by cisplatin are also repaired by NER (Gillet et al., 2006). There are two NER sub-pathways. Transcription coupled-NER (TC-NER) repairs mutations in transcribed genes (Sinha and Hader, 2002) while Global genome-NER (GG-NER) repairs on the genome (Auclair et al., 2010). Within the transcribed gene, lesions on the transcribed strand are repaired faster than lesions present in non-transcribed strand (Hanawalt, 2002). Similarly, 6-4PPs are repaired

faster than CPDs as they generate larger distortions in the DNA (Hanawalt, 2002; Svetlova et al., 2002; Takedachi et al., 2010).

As noted above, one NER protein that has been linked to the response of tumours to cisplatin is excision repair cross complementation group 1 (ERCC1). ERCC1 forms a heterodimer with XPF. During NER, this complex carries out incision at the 5' side of the lesion to cleave the damaged strand (Bessho et al., 1997). DNA polymerase ϵ or δ fills the resulting gap in the presence of replication factors, PCNA (Furuta et al., 2002). DNA ligase I ligates the two ends of the DNA (Falik-Zaccai et al., 2009). ERCC1 levels in testicular germ cell tumours influence the response to platinum-based chemotherapy (Welsh et al., 2004). Hence, low levels of ERCC1-XPF in testicular cancer patients respond well to cisplatin (Usanova et al., 2010). Overexpression of ERCC1-XPF in testis germ cell tumour cell lines resulted in the enhanced repair of cisplatin-induced intrastrand crosslinks and decreased cisplatin sensitivity (Usanova et al., 2010).

1.6.2.1. Interstrand crosslink (ICL) repair

ICLs are the most dangerous crosslinks as they prevent strand separation and block both replication and transcription (Muniandy et al., 2010). The repair of ICL involves two general pathways one is the recombination-dependent and the other is the recombination-independent pathway. In recombination-independent pathway the ICL is excised on one strand and the resulting gap is filled by translesion bypass synthesis (Shen et al., 2006; Wang et al., 2001; Zheng et al., 2006). By sequence analysis in avian and mammalian mutants defective in TLS it was detected that deletion of pol ζ and REV1 resulted in a major defect in recombination-independent ICL repair and reduced mutation formation, suggesting that pol ζ and Rev1 play an important role in bypassing the lesion (McCulloch and Kunkel, 2008). The remaining monoadduct is removed by a second round of excision repair. This pathway is clear in bacteria (*E.coli*) (Berardini et al., 1999), but in case of mammals it remains unclear. In cycling mammalian cells recombination-independent pathway is a minor pathway, but in differentiated nonreplicating cells it is the only method of ICL removal (Arora et al., 2010; Muniandy et al., 2009).

In recombination-dependent pathway excision follows homologous recombination (Raschle et al., 2004). Recombination-dependent pathway is a predominant mechanism for ICL removal in cycling mammalian cells during S phase. ICLs can cause the replication fork to stall and then collapse with the formation of a DSB (Yamamoto et al., 2005). Fork stalling recruits FANCM, a Fanconi anemia protein to bind and induce regression of replication fork (de Winter and Joenje, 2009; Gari et al., 2008). Fanconi anemia (FA) is an autosomal recessive genetic disease characterised by short stature, abnormalities of the skin and developmental disabilities. FA is a result of genetic defects in the proteins responsible for DNA repair. FA is a disease caused by mutations in one of 13 distinct genes (*FANCA*, *FANCB*, *FANCC*, *FANCD1*, *FANCD2*, *FANCE*, *FANCF*, *FANCG*, *FANCI*, *FANCI*, *FANCI*, *FANCL*, *FANCM*, and *FANCN*) (Naim and Rosselli, 2009). FANCM is a component of the FA core complex (FANCA, FANCB, FANCC, FANCE, FANCF, FANCG, FANCL, and FANCM) and recruits the entire core complex and monoubiquitinates FANCD2 and FANCI (Thompson and Hinz, 2009). Unhooking of the ICL from one strand of DNA requires two incisions 5' and 3' to the lesion, potentially producing strand breaks at the fork. MUS81-EME1 along with SLX4 is responsible for the first 5' or 3' incision (Hanada et al., 2007). SLX4 is a helicase (Mullen et al., 2001) having anti-recombinogenic function that unwinds and dissolves DNA secondary structures (Wu and Hickson, 2006). SLX4, is capable of efficiently processing HJ structures (Cybulski and Howlett, 2011; Landwehr et al., 2011). The second 5' or 3' incision, or the unhooking of the cross-link is brought about by SLX4 along with ERCC1-XPF (Niedernhofer et al., 2004). This results in the formation of a monoadduct, which is attached to the other strand of the DNA and is bypassed by pol ζ (Niedzwiedz et al., 2004; Nojima et al., 2005). Once the double helix is restored by bypass synthesis the monoadduct is removed by NER (Couve et al., 2009). The restoration of the fork is done by homologous recombination repair (McEachern and Haber, 2006).

USP1/UAF1 is a deubiquitinating enzyme complex, which deubiquitinates FANCD2 and FANCI (Smogorzewska et al., 2007). Although the FA pathway might play a minor role in ICL repair during the G1-phase of the cell cycle (Ben-Yehoyada et al., 2009), its primary function is exerted in S-phase (Knipscheer et al., 2009; Moldovan and D'Andrea, 2009).

1.6.3. Double strand break production

In a normal human cells approximately 50 endogenous double strand break (DSB) per cell per cell cycle is produced (Vilenchik and Knudson, 2003). The presence of γ H2AX (histone H2AX phosphorylated at serine 139) is an indicator for the presence of DSB (Takahashi and Ohnishi, 2005; Ohnishi et al., 2009). DSB and γ H2AX formation were detected after exposure to IR, bleomycin (Banath and Olive, 2003), etoposide (Banath and Olive, 2003) and doxorubicin (Hammond et al., 2003). Exposure to DNA crosslinking agents such as cisplatin (Huang et al., 2004) also results in the production of DSB and γ H2AX formation (Crul et al., 2003). When replication fork collides with the covalently linked topoisomerase I cleavage complex the extension of the leading strand is terminated at the 5' end thereby generating DSB (Strumberg et al., 2000). γ H2AX is formed in response to replication stress induced by UVC and UVB (Halicka et al., 2005). DSBs are also generated endogenously in which H2AX phosphorylation has also been demonstrated. Meiotic recombination (Mahadevaiah et al., 2001), V(D)J recombination (Klein et al., 1996), heavy chain class switching (Petersen et al., 2001) and apoptotic DNA fragmentation (Rogakou et al., 2000) causes DSBs. In addition, the expression of γ H2AX in S- and G2-phase cells could be a response to DSBs or stalled replication forks at damage sites during normal DNA replication (Takahashi et al., 2004).

1.6.3.1. Double strand break recognition

DSBs are cytotoxic lesions and cells initiate a complex DNA damage response wherein the signalling proteins are recruited around the DSB sites forming IR-induced foci (IRIF) (Maser et al., 1997). The mediator of DNA damage checkpoint 1 protein (MDC1) binds to γ H2AX phosphorylated by ATM, and recruits proteins such as p53, Nijmegen breakage syndrome 1 protein (NBS1), and the breast and ovarian cancer susceptibility protein (BRCA1) (Stucki et al., 2005), resulting in the formation of IRIF. MDC1 is phosphorylated in an ATM-dependent manner in response to IR (Stucki et al., 2005). BRCA1 contains two BRCT motifs at its C-terminus and a RING domain at its N-terminus. This RING domain interacts with the RING-motif of BARD1 (BRCA1-associated ring domain protein 1) forming a heterodimer that function as an E3 ubiquitin ligase (Greenberg et al., 2006). BRCA1 interacts with the

receptor associated protein 80 (RAP80) (Sobhian et al., 2007). RAP80 along with its partner BRCA1 co-localises to form the IRIF after IR treatment (Wang and Elledge, 2007; Wang et al., 2007a). Ring finger protein 8 (RNF8) acts as the prime ubiquitin ligase for histone ubiquitination at DSB sites. RNF8 is recruited to DNA damage sites through interactions with MDC1 to promote repair protein assembly and DNA damage signalling (Kolas et al., 2007). The structural maintenance of chromosomes 1 (SMC1) plays an important role in DSB recognition (Kim et al., 2002). SMC1 is phosphorylated on serine 957 by ATM and is co-localised with γ H2AX (Kitagawa et al., 2004). Ubiquitination of H2AX is carried out by ubiquitin-conjugating enzyme 13 (UBC13) (Ikura et al., 2007). Abraxas and RAP80 form a BRCA1 protein complex, which is required for the DNA damage response (Wang and Elledge, 2007; Wang et al., 2007a). UBC13 and RNF8 ubiquitin ligases control foci formation of the RAP80/Abraxas/BRCA1 complex in response to DNA damage (Wang and Elledge, 2007; Wang et al., 2007a).

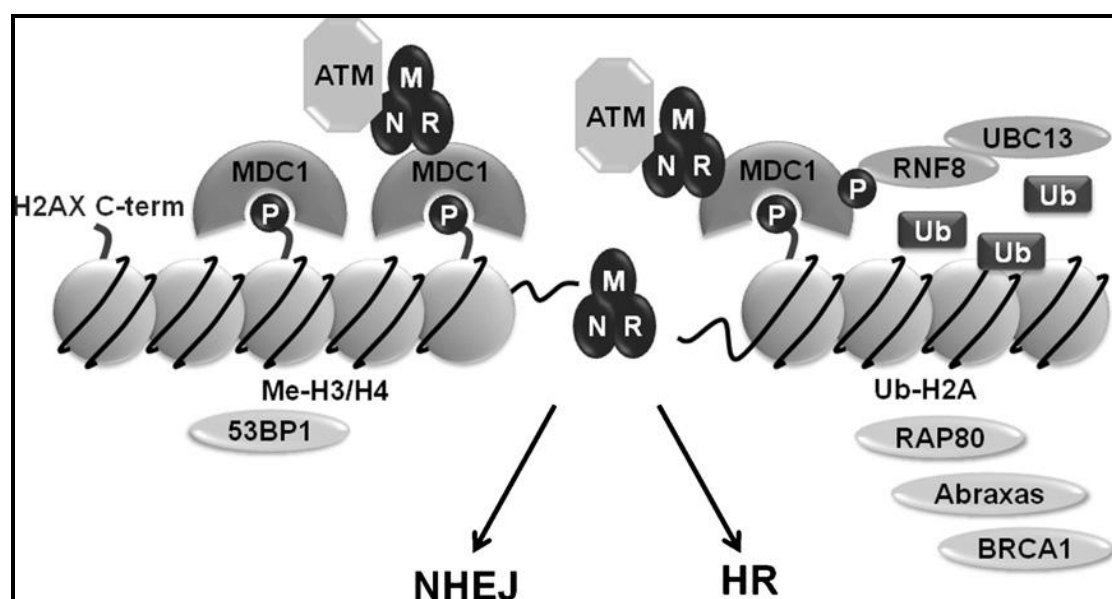


Fig 1.4. Schematic diagram for DSB recognition and signaling pathways (Image adapted from (Ohnishi et al., 2009)).

1.6.3.2. Homologous recombination repair

Homologous recombination (HR) utilises an intact sister chromatid to facilitate DNA double strand break repair. HR is active during the late S- and G2-phases of the cell

cycle (Bohgaki et al., 2010; Takata et al., 1998). HR involves proteins encoded by genes of the RAD52 epistasis group composed of RAD50, RAD51, RAD52, RAD54, RAD55, RAD57, RAD59, MRE11 and Nbs1 (Krogh and Symington, 2004). The MRN complex consists of the Mre11, Rad50 and Nbs1 proteins. Mre11 a DNA nuclease having 3' to 5' exonuclease activity (Moreau et al., 1998; Trujillo et al., 1998) resects DSB ends containing damaged bases or sugar moieties or DNA-protein adducts (Ivanov and Minchenkova, 1994). Rad50 bridges the DNA ends (Lisby et al., 2003a; Lisby et al., 2003b; Lobachev et al., 2004) by maintaining the ends close to each other or closer to a homologous template sequence to facilitate repair (Hopfner et al., 2002a; Hopfner et al., 2002b). The Nbs1 protein is also recruited by MDC1 to regulate the intra-S-phase checkpoint in response to DNA damage (Chapman and Jackson, 2008; Wu et al., 2008) (refer to Section 1.11.4). Another protein involved in HR is CtIp (also known as retinoblastoma-binding protein 8 (RBBP8), is a nuclear protein having endonuclease activity. CtIp cooperates with the MRN complex in the processing of DSB ends (McKee and Kleckner, 1997) to form ssDNA at the ends of the break (Lisby et al., 2004; Lisby and Rothstein, 2004, 2005; Sartori et al., 2007). MRN generates 3' ssDNA overhangs which are coated by the single-stranded DNA binding protein replication protein A (RPA) (Sung and Burns, 2006). DNA strand invasion and homology searching requires binding of Rad51 recombinase to the single-stranded DNA (Bugreev et al., 2011). This requires RPA to be displaced by Rad51, which forms a nucleoprotein filament (Sy et al., 2009; Zhang et al., 2009). Rad51 is loaded onto the DNA by the mediator protein BRCA2 (Sharan et al., 1997; Wong et al., 1997). The Rad51 nucleoprotein filament then captures duplex DNA and searches for homology (Pellegrini et al., 2002). When homology is found, synapsis occurs and the invading strand sets up a D-loop intermediate in the homologous strand resulting in the formation of a Holliday junction (Bianco et al., 1998). There is evidence that DNA polymerase η carries out strand extension at D-loops and polymerase δ extends DNA synthesis from replication forks and also from D-loop extensions (McIlwraith et al., 2005). Eventually, HR results in the formation of two intact DNA strands (Wesoly et al., 2006).

1.6.3.3. Non-homologous end-joining repair (NHEJ)

The non-homologous end-joining pathway repairs DSBs especially in G1-phase of the cell cycle, and in non-proliferating cells where HR cannot occur because there is no homologous sister chromatid available (Delacote and Lopez, 2008). NHEJ is initiated by the binding of a heterodimeric protein complex composed of Ku70 and Ku80 to both ends of the broken DNA molecule (Spagnolo et al., 2006). The Ku-DNA complex recruits DNA-PK_{cs}, which binds to DNA and forms a molecular bridge between the two DNA ends (DeFazio et al., 2002). Artemis is recruited to the DSB and interacts with DNA-PK_{cs}. Artemis possesses both a DNAPK_{cs}-independent 5'-to-3' exonuclease activity and a DNA-PK_{cs}-dependent endonuclease activity, and trims the overhangs (Ma and Lieber, 2002; Ma et al., 2005). The X- family DNA polymerases, polymerase λ and polymerase μ fill the gaps formed. Both polymerases μ and λ have BRCT domains in the N-terminus. Ku recruits polymerase μ and polymerase λ by binding to their BRCT domains, which mediates interaction with other DNA repair proteins (Gu et al., 2007; Lieber, 2010). NHEJ is completed by ligation of the DNA ends, a step that is carried out by XRCC4, DNA ligase IV and XLF (Gu et al., 2007).

1.7. Translesion synthesis (TLS)

Some types of DNA damage cannot be completely removed, for example not all CPDs are removed before cells enter S-phase. Such lesions can result in the blockage of replication fork progression because polymerase α , δ or ϵ cannot bypass lesions. Cells have evolved mechanisms for continuing replication past DNA lesions, a process designated as translesion synthesis or TLS (Goodman, 2002; Lehmann, 2005; Livneh, 2001). TLS is a form of post-replication repair. The translesion mode of DNA synthesis is carried out by specialised DNA polymerases, especially Y-family DNA polymerases (Ohmori et al., 2001). There are four Y-family polymerases in human cells: polymerases η , ι , κ and Rev1. In addition, the B-family DNA polymerase ζ also plays an important role in TLS in eukaryotes (Neal et al., 2010). Several other DNA polymerases (polymerase μ , λ , θ and ν) may also have roles in TLS (Balsamo et al., 2003; de la Casa-Esperon and Sapienza, 2003; Lehmann et al., 2007; Vaisman et al., 2004).

The conserved active site of the Y-family polymerases is located in the N-terminal of the protein. The C-terminal is not conserved between the different Y-family polymerases and is involved in recruitment of the protein to blocked replication forks (Lehmann, 2005). Y-family DNA polymerases have a palm, thumb and finger domain, and also a fourth domain called the “little finger” or PAD (polymerase associated domain) region (Silvian et al., 2001; Trincao et al., 2001). Specialised DNA polymerases have a more open active site when compared to the replicative polymerases α , δ or ϵ , and can therefore accommodate structurally altered bases, thus allowing replication past DNA adducts (Alt et al., 2007; Biertumpfel et al., 2010; Stallons and McGregor, 2010).

Proliferating cell nuclear antigen (PCNA) is a ring-shaped homotrimeric protein that surrounds ssDNA and binds to DNA polymerases. PCNA plays a vital role in DNA replication past lesions (McCulloch et al., 2004). PCNA interacts with a large number of proteins involved in replication, repair, cell cycle regulation and sister chromatid cohesion (Moldovan et al., 2007). PCNA is mono- and polyubiquitinated in primary human skin fibroblasts after UV irradiation (Hoege et al., 2002). Damage-induced PCNA-ub is important for recruitment of specialised DNA polymerases to sites of stalled forks. PCNA is ubiquitinated by covalently attaching ubiquitin residues to the protein in a process involving three enzymes: Ub-activating enzyme (Uba or E1), Ub-conjugating enzyme (Ubc or E2) and Ub ligase (E3) (Hershko and Ciechanover, 1998). PCNA is monoubiquitinated at Lys-164 by the E2-E3 complex upon DNA damage in humans (Hishiki et al., 2009; Kannouche et al., 2004; Stelter and Ulrich, 2003; Watanabe et al., 2004). PCNA can also be sumoylated by a small ubiquitin-like modifier (SUMO1) at the Lys-164 residue by the SUMO-specific E2 conjugating enzyme Ubc9 and the SUMO E3 ligase Siz1 (Hoege et al., 2002; Stelter and Ulrich, 2003). It was also reported that PCNA monoubiquitination is subject to regulation by the deubiquitinating enzyme (DUB) USP1 (Komander et al., 2009). DUBs are cysteine proteases that cleave ubiquitin from mono- and polyubiquitinated substrates. USP1 deubiquitinates PCNA in the absence of DNA damage in order to regulate TLS (Huang et al., 2006; Komander et al., 2009; Reyes-Turcu and Wilkinson, 2009). Deubiquitination of PCNA by USP1 is one way in which TLS is regulated.

PCNA is monoubiquitinated when replicative polymerases stalls at the blocking lesion, and this serves as an anchor for targeting specialised polymerases specifically to the location of the DNA damage (Livneh, 2006). Monoubiquitination of PCNA increases its affinity for pol η , pol ι , and Rev1 (Bienko et al., 2005; Guo et al., 2006b; Kannouche and Lehmann, 2004; Plosky et al., 2006; Watanabe et al., 2004). All these polymerases contain one or two ubiquitin-binding domains (UBD) or a ubiquitin-binding zinc finger (UBZ). Both domains are involved in mediating the interaction of the polymerases with ubiquitinated PCNA (Bienko et al., 2005). Ubiquitin-binding domains bring about the polymerase switch (Friedberg et al., 2005). The TLS polymerases bind PCNA at its interdomain connector loop (IDCL) via their PCNA-interacting protein (PIP) domain. TLS polymerase also binds to PCNA ubiquitinated at lys 164 via their UBD/UBZ domain. However, binding of ubiquitin (Ub) on PCNA is crucial for the TLS polymerase to function in lesion bypass (Bienko et al., 2005; Guo et al., 2006b; Plosky et al., 2006). Genetic studies with yeast polymerase η have shown that mutational inactivation of the PIP domain abolishes the ability of polymerase η to function in TLS *in vivo* (Haracska et al., 2001a). Mutational inactivation of the PIP domain results in defects in the function of polymerase η in TLS *in vivo*. Hence, it was concluded that the binding of the ubiquitin moiety on PCNA via the UBZ domain is a prerequisite for human polymerase η to interact with PCNA (Bianco et al., 1998).

DNA polymerases belonging to Y-family are involved in TLS across the cisplatin 1,2 d(GpG) adduct. This was studied in human fibroblasts using siRNA to knock down the expression of one or more TLS polymerases (Livneh et al., 2010). Knocking down the expression of Rev3 caused a five-fold decrease in the extent of TLS across the cisplatin adduct. Knocking down the expression of *POLH* (encoding pol η), or *POLK* (encoding pol κ) had individually a small effect on TLS extension. However, when the expression of both *POLK* and *POLH* was simultaneously knocked-down, TLS extension decreased by 5-fold, similar to the effect of knocking down polymerase ζ alone (Shachar et al., 2009). This shows that polymerase ζ cooperates with either polymerase η or polymerase κ to carry out TLS, and that the three polymerases are responsible for most of the TLS across cisplatin 1,2 d(GpG) adducts in human fibroblast cells.

Rev1 also plays a role in TLS in human XPV cells. Rev1 requires monoubiquitinated PCNA to bypass UV induced CPDs in XPV cells (Guo et al., 2006b). The C-terminal 100 amino acids of Rev1 interact with pol η , pol ι , pol κ as well as with Rev7, which is the regulatory subunit of polymerase ζ (Acharya et al., 2007; Haracska et al., 2005; Kannouche et al., 2004). In the case of bypassing UV-induced CPDs in XPV cells, it was shown using siRNA knock-down studies, that three polymerases, polymerase ζ , polymerase κ and polymerase ι were involved in TLS in the absence of polymerase η (Wang et al., 2007b). Polymerase κ and/or polymerase ι carry out the insertion step, whereas polymerase ζ carries out the extension step (Livneh et al., 2010).

1.7.1. DNA polymerase zeta (ζ)

As noted above, human polymerase ζ plays an important role in TLS. Polymerase ζ , a B-family polymerase, comprises the Rev3 catalytic subunit and Rev7 accessory subunit (Gan et al., 2008). Polymerase ζ is highly specialised for extending from nucleotides inserted opposite a lesion site by another DNA polymerase (Prakash et al., 2005). Studies indicate that polymerase ζ can extend efficiently from a diverse array of DNA lesions, such as CPDs (Johnson et al., 2000), (6-4) PP (Johnson et al., 2001), and an abasic site (Haracska et al., 2001b). *In vitro* studies have shown the sequential use of purified polymerase η and polymerase ζ in replication past cisplatin 1,2d(GpG) adducts (Shachar et al., 2009). Disruption of *Rev3* is lethal to mouse embryogenesis (Van Sloun et al., 2002). Chicken DT40 cells deficient in *Rev3* exhibit significant chromosome instability and hypersensitivity to a wide variety of DNA damaging agents including cisplatin (Mizutani et al., 2004; Nojima et al., 2005; Sonoda et al., 2003; Wu et al., 2006). Human fibroblast cells expressing reduced levels of REV3 were also found to be more sensitive to cisplatin (Wu et al., 2004a). The sensitisation to cisplatin caused by the reduction in REV3 level is a result of the role of REV3 in the TLS of both intra- and interstrand DNA crosslinks (Hicks et al., 2010). It was also found that REV3 depletion in a highly chemoresistant mouse model of lung adenocarcinoma cell line, sensitised the cells to cisplatin (Doles et al., 2010). Thus a potential benefit of reduced cisplatin-induced cytotoxicity can be achieved by reducing REV3 activity.

1.7.2. DNA polymerase kappa (κ)

Polymerase κ is unable to efficiently bypass UV-induced (6-4) PPs or CPDs (Ohashi et al., 2000; Zhang et al., 2000b). However polymerase κ performs error-free TLS when encountering 8-oxoguanine (Zhang et al., 2000a), etheno-deoxyadenine (Levine et al., 2001), thymine glycol (Fischhaber et al., 2002) and benzo(a)pyrene (Zhang et al., 2000a) lesions suggesting an important role played by polymerase κ in the bypass of either oxidative damage or aromatic DNA adducts. Benzo(a)pyrene (Suzuki et al., 2002) is present in cigarette smoke and causes p53 mutations detected in lung tumours of smokers (Ogi et al., 2002). Under *in vitro* conditions, polymerase κ efficiently bypasses benzo(a)pyrene lesions in a mostly error-free manner, by inserting C opposite the lesion, when compared to polymerase η which bypasses in an error-prone manner (Ogi et al., 2002). Studies using siRNA-mediated *POLK*-knockdown showed that this reduces the efficiency of TLS past BPDE adducts in human U2OS cells (Shachar et al., 2009). This results in increased DSB formation at stalled replication forks and increased toxicity in U2OS cells without functional polymerase κ (Stallons and McGregor, 2010). siRNA knock-down of one or more TLS polymerases was carried out in human fibroblast cells and TLS across cisplatin 1,2d(GpG) adducts was measured. Knocking down *POLK* had a mild effect on inserting a base opposite the lesion in an error-prone manner (Livneh et al., 2010).

1.7.3. DNA polymerase iota (ι)

Polymerase ι is closely related at the DNA and aminoacid sequence level to polymerase η . Following the original identification of *RAD30* (*POLH*) encoding pol η it was reported that human cells contained a second *RAD30* orthologue, designated *RAD30B* (McDonald et al., 2001). The human *RAD30B* gene was localised to chromosome 18q21 by FISH analysis (McDonald et al., 2001). *RAD30B* gene was renamed as *POLI* (Tissier et al., 2000). Polymerase ι can insert a base opposite various damaged bases (Tissier et al., 2000) and acts in association with another extender DNA polymerase to carry out TLS past different lesions (Johnson et al., 2000). Pol ι has very low processivity and has a high error rate on undamaged DNA (Gening, 2011). Pol ι inserts a G particularly opposite a template T (Tissier et al., 2000). Purified mouse pol ι displays extremely error-prone properties during synthesis

opposite all four undamaged template bases *in vitro* (McDonald et al., 2003). Pol ι interacts with polymerase η after UV-induced DNA damage, and is co-localised in replication foci (Kannouche et al., 2003) in human fibroblast cells. This accumulation in foci is dependent on PCNA, since mutation of a PCNA-binding motif in pol ι abolishes its interaction with PCNA *in vitro*, and its localisation into replication foci in response to damage by UV (Vidal et al., 2004). Localisation of polymerase ι in foci is also largely dependent on the presence of polymerase η , as it is reduced in pol η -deficient XPV cells (Kannouche et al., 2002). In XPV cells, pol ι is responsible for the high frequency of UV-induced mutagenesis in these cells (Wang et al., 2007b). In human cells, pol ι is effective in the initial insertion step opposite an AP site (Choi et al., 2010b). There is no known human disorder involving deficiency of pol ι . However, Pol ι is overexpressed in some lung cancer cell lines as well as in primary human gliomas (Hicks et al., 2010).

1.7.4. Rev 1

Rev1 is a member of the Y-family DNA polymerases but is not a true DNA polymerase, but is a dCMP transferase, capable of inserting dCMP opposite either Gs or abasic sites in template DNA (Nelson et al., 1996). Rev1 also differs from the other TLS polymerases in having a BRCA1 C-terminal (BRCT) domain close to its N-terminus (Murakami-Sekimata et al., 2010). The BRCT domain is important for binding of Rev1 to PCNA. Deletion of the BRCT domain of Rev1 reduces survival after UV-irradiation in both *S.pombe* and DT40 cells (Guo et al., 2006a). Rev1 co-localises with polymerase η , polymerase ι and PCNA in replication foci after DNA damage (Tissier et al., 2004). The C-terminal of Rev1, consisting of 150 amino acids, interacts with polymerase η , polymerase ι , polymerase κ and Rev7 (Guo et al., 2003; Murakumo et al., 2001; Ohashi et al., 2004; Tissier et al., 2004), which suggest a role for Rev1 in TLS as a platform for switching between TLS polymerases (Kannouche and Strydom, 2003). Studies in yeast have shown that Rev1 plays only a minor role in TLS past CPDs, but is required for bypass of (6-4) PPs and abasic sites (Gibbs et al., 2005). Rev1 bypasses (6-4) PPs by interacting with polymerase ζ via its noncatalytic Rev7 subunit (Murakumo et al., 2001). Mutation in WRN gene causes Werner syndrome associated with premature aging and predisposition to cancer. WRN belongs to the RecQ DNA helicase family and plays an important role in maintaining

genomic stability. WRN also plays a role in Rev1-dependent translesion synthesis at the replication fork, based on studies carried in chicken DT40 cells (Phillips and Sale, 2010).

1.7.5. DNA polymerase eta (η)

Xeroderma pigmentosum (XP) is an autosomal recessive disorder characterised by extreme skin sensitivity to sunlight and skin-cancer susceptibility (Bootsma and Hoeijmakers, 1991). As outlined above (Section 1.6) there are eight complementation groups, XP-A through XP-G, and XP variant (XPV). Cells from XP-A through XP-G patients are defective in nucleotide excision repair that removes UV-induced DNA damage from the genome (van Steeg and Kraemer, 1999). In contrast, XPV cells, which make up about 20% of XP patients, carry out normal nucleotide excision repair (Section 1.6.2) but are deficient in bypass of CPDs as they lack the ability to carry out translesion synthesis because of the defect in the *POLH* gene encoding DNA polymerase η (Lehmann et al., 1975). The human *POLH* gene is located on the chromosome 6p21.1-6p12 (Thakur et al., 2001), spans 40kb of DNA, and consists of 11 exons.

DNA polymerase η is a 78 kDa protein first identified in 1999 as a factor that could complement defective replication of UV-irradiated plasmids in xeroderma pigmentosum variant cell extracts *in vitro* (Johnson et al., 1999; Masutani et al., 1999). Polymerase η can carry out replication past CPDs in the template by incorporating the correct base, adenine, despite the distortion caused by the CPD (Masutani et al., 2000; McCulloch et al., 2004). It was shown that TLS by pol η is the most efficient way for the bypass of UV-induced CPDs (Yoon et al., 2009). Defects in human polymerase η are linked to increased susceptibility to UV-induced skin cancer development in XPV patients (Broughton et al., 2002; Inui et al., 2008; Tanioka et al., 2007).

In human cells, translesion synthesis carried out by pol η reduces cellular sensitivity to platinum-based chemotherapeutic drugs (Chen et al., 2006). Pol η is also involved in other functions such as somatic hypermutation and replication of D-loops and at DNA fragile sites (Betous et al., 2009; Rey et al., 2009). Somatic hypermutation is a mutagenic process, in which the immunoglobulin (Ig) genes are diversified during B-

cell differentiation (Longo and Lipsky, 2006). Error-prone DNA polymerases generate mutations at A/T base pairs from an initial deamination event. The Ig gene mutation pattern in B-cells from XPV patients was reduced in A/T mutagenesis (Faili et al., 2004; Zeng et al., 2004; Zeng et al., 2001). Inactivation of polymerase η in the mouse also resulted in a reduction in the proportion of A/T mutations in B-cells (Delbos et al., 2007; Delbos et al., 2005; Martomo et al., 2006; Martomo et al., 2005) suggesting that pol η plays a role in B-cell differentiation.

As outlined in Section 1.6.3.2, homologous recombination repair is essential for the repair of naturally occurring DSBs that arise by replication-fork collapse during normal DNA replication (Kraus et al., 2001). Restart of a collapsed replication fork involves strand invasion mediated by HR proteins, and requires DNA synthesis by polymerase η as shown in Section 1.6.3.2 (Cox et al., 2000; Plosky and Woodgate, 2004). Polymerase η co-localises with Rad51 at stalled replication forks (Kannouche et al., 2002). Extracts prepared from polymerase η -defective XPV cell lines exhibited severely reduced D-loop extension activity, indicating that polymerase η is important in promoting primer extension of an invading strand present in a D-loop structure (McIlwraith et al., 2005). Rad51 mediates strand invasion also stimulates polymerase η , which extends DNA synthesis at the sites of stalled replication forks (McIlwraith et al., 2005). However, further investigation of the role of pol η in HR is required.

Human osteosarcoma U2OS cells, in which the expression of polymerase η was silenced using short hairpin RNAs were used to study the role of polymerase η in DNA replication during S-phase. Chromosomal fragile sites (CFSs) are several hundred kilobase regions of chromosomal DNA that are replicated in late S-phase (Ciullo et al., 2002). Polymerase η -depleted cells demonstrated both altered replication and elevated instability of a CFS measured by using replication track analysis (RTA) on stretched DNA. This could be due to delayed completion of bulk replication occurring in early S-phase, or to impaired onset of late replication (Rey et al., 2009).

1.7.6. Role of DNA polymerase η in replication past platinum adducts

Polymerase η is efficient in bypassing cisplatin-DNA adducts, in particular intrastrand 1,2d(GpG) adducts (Albertella et al., 2005a; Bassett et al., 2002; Masutani et al.,

2000; Vaisman and Chaney, 2000; Vaisman et al., 2000) both *in vitro* and *in vivo* (Bassett et al., 2004; Shachar et al., 2009). In *in vitro* studies, purified pol η accurately inserted two cytosines opposite the 1,2d(GpG) adduct produced by cisplatin in an oligonucleotide template (Shachar et al., 2009). The high-resolution crystal structure of human polymerase η during TLS of platinum adducts was reported recently. Polymerase η acts as a molecular splint to stabilise damaged DNA in the B-form (Biertumpfel et al., 2010). In XPA cell lines, the predominant 1,2d(GpG) adducts formed by cisplatin contribute to the cytotoxicity of cisplatin (Albertella et al., 2005b; Shachar et al., 2009; Szymkowski et al., 1992). SV40-transformed, XP30RO fibroblast cells lacking DNA polymerase η have reduced survival when compared to the normal fibroblast upon treatment with UV and cisplatin (Albertella et al., 2005b; Chen et al., 2006; Cruet-Hennequart et al., 2008).

The major adduct of carboplatin is 1,3-d(GpNpG), which makes up about 46% of the total adducts formed (refer to Section 1.4.3). *In vitro* studies showed that human polymerase η incorporated nucleotides opposite the first G-residue (3') of a 1,3-d(GpNpG) adduct (Chijiwa et al., 2010). However, pol η was unable to incorporate any nucleotides opposite the second residue that is not bound to carboplatin, or the third (5') G-residue attached to the 1,3-d(GpNpG) (Chijiwa et al., 2010). It was shown in *in vitro* studies that replication comes to a halt when encountering an adduct induced by carboplatin which results in cell death in human tumour cells lacking ERCC1, one of the key factors of NER. Hence, treatment of NER-negative tumour cell lines with carboplatin has highly beneficial outcomes (Shachar et al., 2009).

1.7.7. The polymerase switch

DNA polymerase switching is a process by which one DNA polymerase replaces a second polymerase at the 3'-OH end of a primed DNA template (Friedberg et al., 2005). Polymerase switching is influenced by several factors such as the relative expression levels of the different polymerases, changes in the sub-cellular localization of the different polymerases (Kannouche et al., 2003), interactions of polymerases with their sliding clamp proteins, association with other polymerases, post-translational modification of polymerases and clamp proteins (Hoege et al., 2002), and the relative affinities of the different polymerases for the DNA. As noted above, certain specialised polymerases are capable of bypassing specific classes of DNA

lesions in a relatively accurate manner, while others bypass the same lesion in a largely error-prone manner (Abdulovic and Jinks-Robertson, 2006). Thus, recruitment of the inappropriate specialised polymerases during TLS could result in genomic instability.

Switching during TLS is complex, and may involve at least one or two switches (Figure 1.5) (Plosky and Woodgate, 2004). One specialised polymerase inserts a base opposite the lesion, but may not be able to extend the nascent strand further. A second specialised polymerase is therefore required to extend the nascent strand, and subsequently returns the 3'-OH end of the DNA template back to the replicative polymerase (Lehmann et al., 2007).

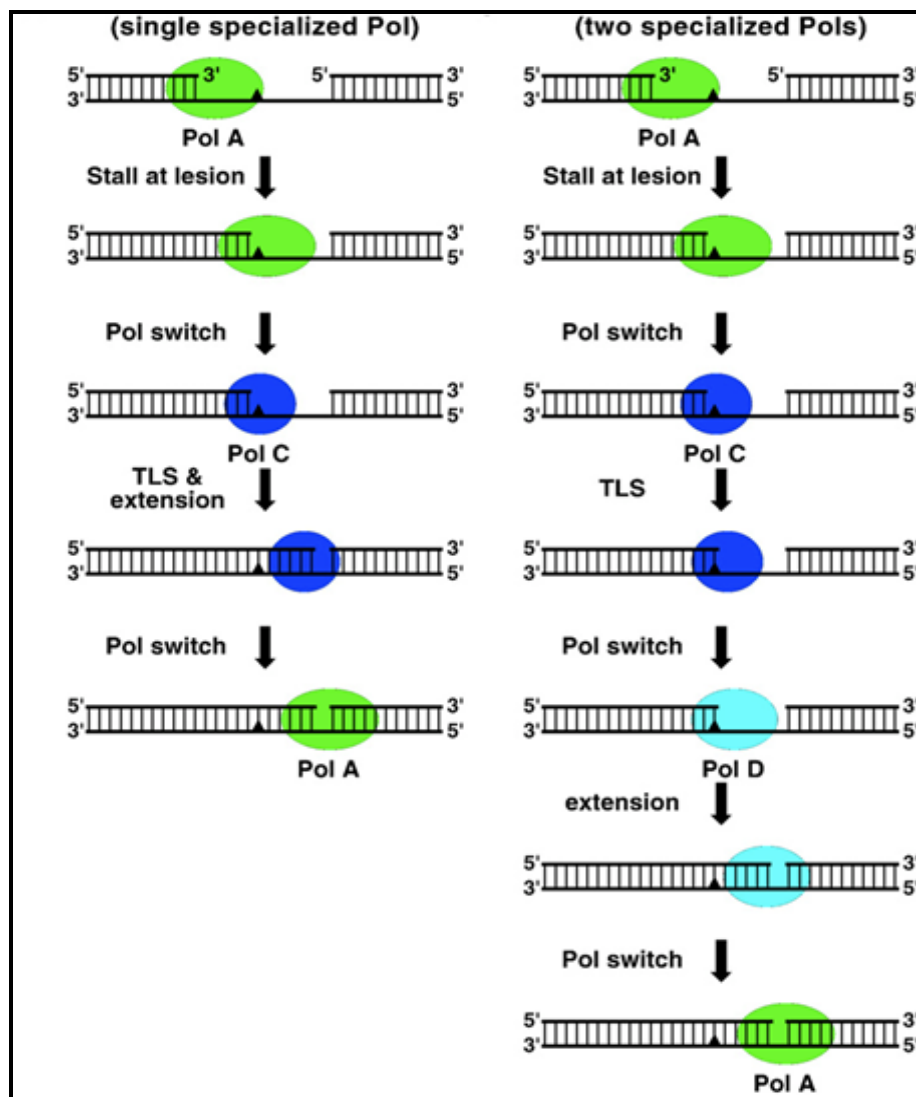


Figure 1.5. Schematic representation of polymerase switching during translesion synthesis using one or two specialised polymerases (Plosky and Woodgate, 2004).

1.8. The DNA damage responses (DDR)

The DNA damage response, like most cellular signalling pathways is a complex process that involves first sensing the damage and then transducing a signal to downstream effectors that elicit the appropriate cellular response, in this case to maintain genomic stability or to activate apoptosis if the damage is too great to be repaired (Mahmoudi et al., 2006) (Figure 1.6). A better understanding of the DNA damage response pathway may improve the efficacy of existing cancer therapies, and aid in the development of novel anticancer compounds.

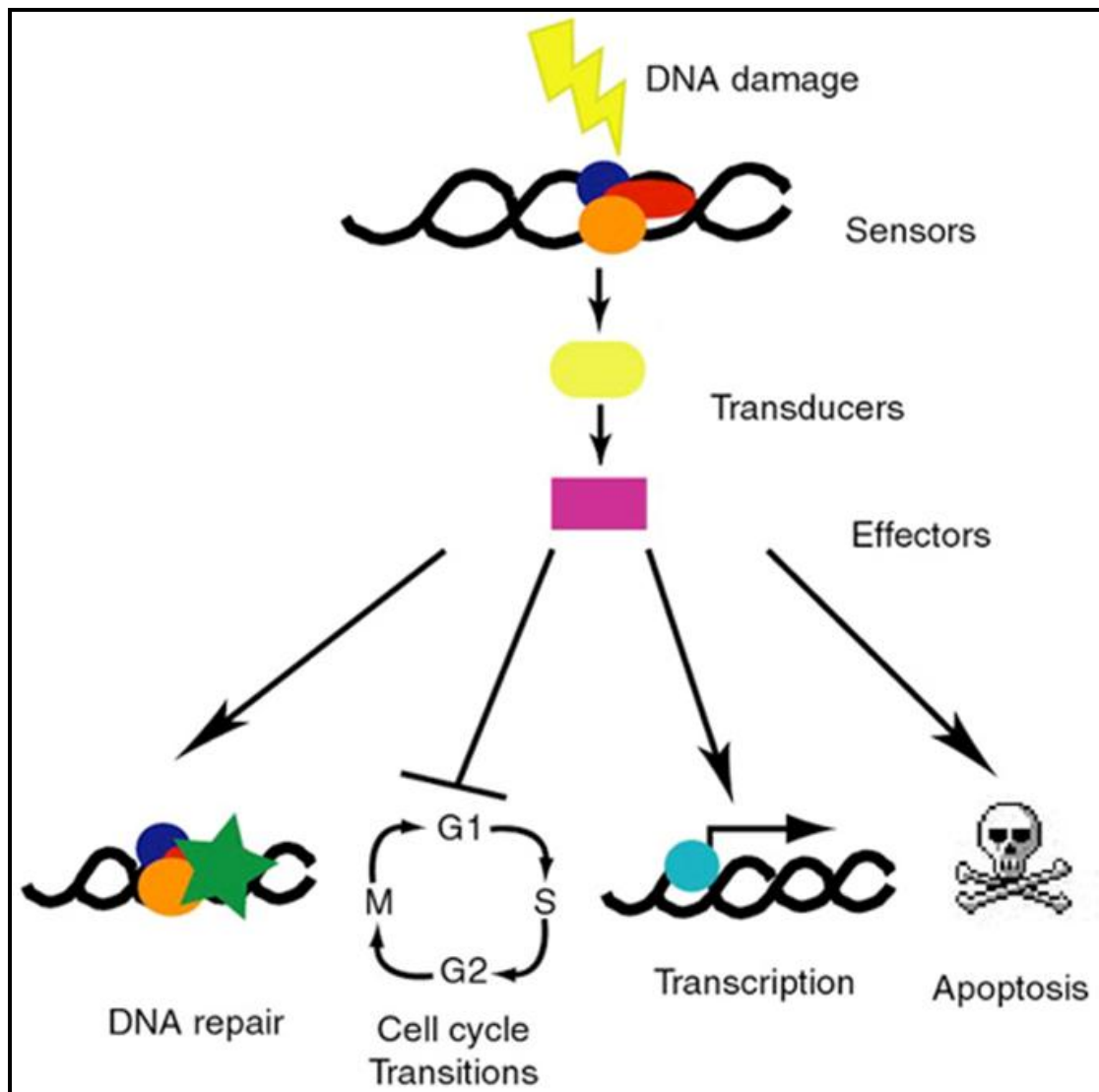


Figure 1.6. Schematic diagram of the DNA damage response pathway in eukaryotic cells (Mahmoudi et al., 2006).

1.8.1. DNA damage sensor proteins

A DNA damage sensor is a protein that senses the damage and activates a cascade of downstream events resulting in the execution of a metabolic or transcriptional programme. In order to identify a protein as a sensor of DNA damage it has to fulfil a number of criteria (Mahmoudi et al., 2006). A sensor protein should be physically associated with the DNA damage upon its induction. It should independently modify other proteins, and mutations in the sensor protein should stop downstream of cell cycle checkpoint activation. A sensor protein should also be able to identify incorrect signals that are sent in the absence of the damage or that amplify the signal when there is minimal damage of the DNA (Negayama et al., 1992).

As described in Section 1.6.3, in DSB repair in mammalian cells, the MRN protein complex (Mre11, Rad50 and Nbs1) is an important damage sensor that activates ATM (Lavin, 2007; You et al., 2005). The MRN complex has both endo- and exonuclease activities (Budd and Campbell, 2009; Mimitou and Symington, 2008; Stracker et al., 2004; Zhu et al., 2008). Mre11 binds to DNA, which further allows the activation of Nbs1 (Limbo et al., 2007; Williams et al., 2009) and RAD50. RAD50 holds the broken ends of the DNA together while Nbs1 protein mediates several protein-protein interactions with other proteins including ATM kinase (Falck et al., 2005), MDC1 adaptor protein (Goldberg *et al.*, 2003; Lukas *et al.*, 2004) and CtIP tumour suppressor protein (Chailleux et al., 2010; Eid et al., 2010). These interactions further activate the ATM-Chk2 signalling cascade and homologous recombination repair (Adams and Carpenter, 2006; Cimprich and Cortez, 2008; Jazayeri et al., 2006).

Human ortholog of Rad9A belongs to the family of DNA damage sensor proteins. Rad9 forms a ring-like complex with Rad1 and Hus1 forming the trimeric 9-1-1 complex (Bermudez et al., 2003; Bonilla et al., 2008; Burtelow et al., 2001; Rauen et al., 2000; Shiomi et al., 2002). Rad9 is constitutively phosphorylated but in the presence of damage is hyperphosphorylated (Chen et al., 2001; St Onge et al., 1999). Rad9 activates Chk1, which phosphorylates proteins that regulate the checkpoint response (Furuya et al., 2004; Roos-Mattjus et al., 2003). The 9-1-1 complex also interacts with DNA polymerase β and flap endonuclease 1 (FEN1) to repair the damage (Touaille et al., 2004).

Mediator of DNA damage checkpoint protein 1 (MDC1) is a chromatin-associated protein that interacts with the MRN complex in a DNA damage-independent manner (Lou et al., 2003). Since MDC1 is required for the intra-S-phase and G2/M DNA damage checkpoints it plays an important role in cell cycle regulation (Lou et al., 2004). MDC1 co-localises with ATM (Kim et al., 2006; Mochan et al., 2003). MDC1-mediated activation of ATM, which induces phosphorylation of Chk2 at Thr 68 which re-localises to the DNA damage sites, suggesting that MDC1 has a critical role in Chk2-mediated DNA damage response (Lou et al., 2003). Chk2 phosphorylates Cdc25C protein at serine 216 leading in turn to the inhibition of Cdc2 kinase. This consequently blocks cells from entering M-phase (Kastan and Bartek, 2004; Niida and Nakanishi, 2006). In addition, Chk2 phosphorylates Cdc25A protein phosphatase on serine 123. Cdc25A is degraded and can no longer phosphorylate cyclin/CDK2, inhibiting the DNA replicative CDK2 and consequently S-phase delay (Falck et al., 2002; Motoyama and Naka, 2004).

1.8.1.1. γ H2AX

Histone H2AX is a subunit of the nucleosome that is rapidly phosphorylated at DSBs in mammalian chromatin (Kobayashi et al., 2009; Pilch et al., 2003; Redon et al., 2002). Phosphorylated H2AX on serine 139 in humans is termed γ H2AX (Sedelnikova et al., 2002). Phosphorylated H2AX covers up to 2 Mbp of chromatin per DSB, thus providing a useful marker of damage, detected by immunofluorescence (Bonner et al., 1993). Human γ H2AX is phosphorylated on Ser139 located within the C-terminal tail of the protein (Redon et al., 2002). Phosphorylation of H2AX by ATM occurs upon DNA damage and γ H2AX is considered a mediator, downstream of DSB sensing. H2AX is phosphorylated by ATR in response to UV, hydroxyurea and aphidicolin, and by ATM in response to IR. DNA-PK also phosphorylates H2AX in response to DNA fragmentation during apoptosis, and in response to UV radiation (Helt et al., 2005; Mukherjee et al., 2006; Ward and Chen, 2004). H2AX phosphorylation plays a key role in DNA damage checkpoint activation, while its dephosphorylation by tyrosine phosphatase, EYA is important to allow the cell cycle to resume (Burma et al., 2001; Celeste et al., 2003; Cook et al., 2009; Downey and Durocher, 2006).

1.8.2. Transducers: the PIK kinases

Once DNA damage is sensed, the cell must transduce this signal to appropriate effector proteins. In human cells, activation of phosphoinositide kinases is essential for the proper transduction of a signal from DNA damage. The major PIK kinases in the DNA damage response are ATM (ataxia telangiectasia mutated), ATR (ATM and Rad3-related) and DNA-PK (DNA-dependent protein kinase) (Elledge, 1996; Vesterdal, 1991).

1.8.2.1. Activation of phosphoinositide kinases (PIK Kinases)

In eukaryotes, the PIK kinases (phosphatidylinositol kinases) co-ordinate the cellular response to DNA damage and play critical roles in the control of cell growth, gene expression and V(D)J recombination (Durocher and Jackson, 2001; Yang et al., 2003). PIK kinase members are high molecular mass proteins. Ataxia-telangiectasia mutated (ATM), ataxia- and Rad3-related (ATR), mammalian target of rapamycin (mTOR), DNA-dependent protein kinase catalytic subunit (DNA-PKcs), suppressor of morphogenesis in genitalia (SMG-1) and transformation/transcription domain-associated protein (TRRAP) (Lempiainen and Halazonetis, 2009) are the six members found in mammals. In the context of DDR, ATM, ATR and DNA-PK are considered the most important PIK kinases. ATM, ATR and DNA-PK function as protein serine/threonine kinases (Savitsky et al., 1995a; Shiloh and Rotman, 1996). At the cellular level, ATM and DNA-PK_{cs} respond to DSBs (Tomita, 2010), while ATR is activated in response to DNA replication blocks that lead to formation of long stretches of single-stranded DNA (Choi et al., 2010a).

1.8.2.2. Ataxia telangiectasia, mutated (ATM)

Ataxia telangiectasia (AT) is a rare autosomal recessive human disease and a predisposition to cancer. Ataxia refers to uncoordinated movements. Talangiectasias are enlarged blood vessels just below the surface of the skin, which appear as tiny, red, spider-like veins (Strigini et al., 1991). AT patients have increased risk of breast cancer as ATM regulates phosphorylation of BRCA1 following DNA damage (Lavin, 2008). ATM defects are also associated with certain lymphomas and leukemias (Gronbaek et al., 2002; Van et al., 2001). It was found that a mutation in the *ATM* gene caused this disease (Savitsky et al., 1995a). The *ATM* gene is located on

chromosome 11q22.3, and the ataxia telangiectasia mutated protein (ATM, 350 kDa and 3056 aa) is a central player in the cellular response to various damaging agents in particular agents that induce DSBs (Lavin and Shiloh, 1997; Savitsky et al., 1995b; Shiloh, 2003). ATM plays a critical role in the activation of checkpoints that lead to DNA damage-induced cell cycle arrest at S-, G2- and M-phases (Hurov et al., 2010). ATM protein consists of a focal adhesion targeting (FAT) domain, a phosphoinositide 3,4-kinase (PI3K) domain and a FAT carboxy-terminal (FAT-C) domain (Bakkenist and Kastan, 2003; Kim et al., 1999; O'Neill et al., 2000). Upon exposure to IR, ATM kinase activity increases and results in the autophosphorylation of ATM at serine 1981 (Bakkenist and Kastan, 2003). Activation of ATM results in the phosphorylation of a number of downstream targets such as serine 15 of p53, and serine 139 of histone H2AX in response to DNA damage (Kozlov et al., 2003; Matsuoka et al., 2007).

Electron microscopic analysis revealed the structure of ATM to consist of a large head domain of approximately 115 Å by 75–140 Å and a long arm that protrudes from the head region (Llorca et al., 2003). ATM forms an inactive dimer or a multimer in non-damaged cells. Bakkenist and Kastan (2003) reported that induction of DSBs causes a relaxation in chromatin structures that promotes the intermolecular phosphorylation of ATM dimers or multimers leading to dissociation into active ATM monomers (Bakkenist and Kastan, 2003). Serine367 and Serine1893 have also been identified as autophosphorylation sites in ATM (Kozlov et al., 2006; So et al., 2009). All three autophosphorylation sites have been demonstrated to be physiologically significant because mutations in these phosphorylation sites led to defects in ATM signalling (Kozlov et al., 2006). Both ATM and ATR phosphorylate proteins to initiate a signalling cascade that includes many substrates that initiate the secondary wave of phosphorylation events to extend signalling. A vast network of over 700 human and mouse proteins substrates phosphorylated in response to DNA damage were discovered by using peptide IP with anti phosphotyrosine followed by mass spectrometry methods (Matsuoka et al., 2007).

1.8.2.3. Ataxia telangiectasia and Rad-3-related (ATR)

ATR is another member of the PIK kinase family and is encoded by *ATR* gene. The human *ATR* gene is located on chromosome 3q22-24. ATR is required for checkpoint responses after treatment of cells with agents that cause DNA damage like IR or block

replication due to bulky adducts or stall replication fork and generate ssDNA (Cortez, 2003; Durocher and Jackson, 2001; Shiloh, 2001). Homozygous deletion of ATR in mice causes early embryonic lethality showing that ATR is essential during development (O'Driscoll, 2009).

ATR has a molecular weight of 303 kDa with 2466 amino acids (Cortez et al., 2001). ATR forms a complex with ATR-interacting protein (ATRIP), which is a 791 amino acid protein with a molecular size of 86 kDa that can be immunoprecipitated along with ATR (Itakura et al., 2004). ATRIP and ATR expression is interdependent on each other. This mutual dependency for expression suggests that the amount of ATR and ATRIP in cells is tightly coordinated (Ball et al., 2005; Cliby et al., 1998; Tibbetts et al., 2000).

Inactivation of ATR kinase by siRNA in HeLa cells increases the sensitivity of human cells to cisplatin (Cliby et al., 1998; Nghiem et al., 2002; Wagner and Karnitz, 2009). The ATR substrate BRCA1 (Tibbetts et al., 2000) and the Chk1 substrate Rad51 (Pedram et al., 2009) are also localised to cisplatin-damaged DNA (Bhattacharyya et al., 2000). ATR plays an important role in S-phase arrest in cisplatin-treated human fibroblast and osteosarcoma cells (Lewis et al., 2009).

Mutations in the ATR gene causes seckel syndrome, was identified in 2000 from two inbred Pakistani families (Goodship et al., 2000). Cells from ATR-seckel patients (ATR^{-/-}) demonstrated impaired phosphorylation of ATR-dependent substrates following UV radiation. Seckel cells treated with cisplatin (1µM) showed decreased cell survival using clonogenic assay and was arrested in the beginning of the S-phase of the cell cycle (Wilsker and Bunz, 2007). ATR or ATM phosphorylates many substrates on serine or threonine that are followed by glutamine, so-called SQ/TQ motifs (Douglas et al., 2007).

1.8.2.4. DNA-dependent protein kinase (DNA PK)

DNA-PK is a multiprotein complex comprising a 470 kDa catalytic subunit (DNA-PK_{cs}) and the DNA end-binding proteins Ku 70 and Ku 80 (Walker et al., 2001). The human DNA-PK gene (*PRKDC*) localises to 8q11 and is estimated to comprise about 100 exons covering around 180 kbp of DNA (Collis et al., 2005). DNA-dependent protein kinase (DNA-PK) binds to DNA and must be DNA-bound to be catalytically

active. The N-terminal region of the protein consists of a leucine zipper motif that mediates dimerisation and interactions with Ku or other proteins (Brewerton et al., 2004). The C-terminal kinase domain consists of 500 amino acid residues (Bosotti et al., 2000). Electron crystallographic studies indicate DNA-PK and Ku bound to DNA has an open ring-like shape with the DNA threaded through the opening (Sibanda et al., 2010). Ku first binds to the DNA end and translocates inwardly by one helical turn. This then recruits DNA-PK_{cs} which stabilises its binding to DNA (Hammarsten et al., 2000). DNA-PK recruits and activates proteins involved in DNA end-processing and ligation and thereby plays a critical role in DSB repair by NHEJ (Goodarzi et al., 2006; Ma et al., 2005).

DNA-PK phosphorylates a number of substrates, including itself, in response to IR (Matsuoka et al., 2007). Two major clusters of *in vitro* autophosphorylation sites in DNA-PKcs are the ABCDE cluster and the PQR cluster. The ABCDE cluster contains phosphorylation sites at serines 2612 and 2624 and threonines 2609, 2620, 2638, and 2647 (Douglas et al., 2001), and the PQR cluster contains phosphorylation sites at serines 2023, 2029, 2041, 2053, and 2056 (Cui et al., 2005). Threonines 2609, 2638, and 2647 in the ABCDE cluster and serine 2056 in the PQR cluster are phosphorylated in human cells *in vivo* in response to DNA damage (Chan et al., 2002; Chen et al., 2005; Yajima et al., 2006). Autophosphorylation of DNA-PK at Thr 2609 plays a major role in regulation of NHEJ (Dobbs et al., 2010). DNA-PK_{cs} autophosphorylation could lead to conformational change in DNA-PK_{cs} leading to DNA-PK and Ku complex dissociation. The dissociation facilitates interaction of DNA-PK_{cs} with other damage-responsive proteins, DNA-PK_{cs} substrates, subsequently leading to repair of the DSB (Douglas et al., 2001). *In vitro*, DNA-PK phosphorylates many substrates on serines or threonines that are followed by a hydrophobic residue (Lees-Miller et al., 1992; Matsumoto et al., 1999).

DNA-PK plays an important role in apoptosis (Sand-Dejmek et al., 2011). DNA-PK_{cs}-deficient mouse cells are resistant to apoptosis (Bharti et al., 1998). In irradiated mouse thymocytes, p53-dependent apoptosis is significantly suppressed in the absence of DNA-PK_{cs} (Wang et al., 2001). DNA-PK phosphorylates p53 at serine 18 in mouse embryonic fibroblast cells, in response to IR. When serine 18 was mutated to alanine in these cells failure to initiate apoptosis confirmed that p53-dependent

apoptotic response was mediated by DNA-PK (Wu et al., 2008). DNA-PK also plays an important role in apoptotic signalling by phosphorylating p53 at serine 15 in response to DNA damage (Lees-Miller et al., 1992; Wang et al., 1992). DNA-PK_{cs}, while regulating the early stages of apoptosis, itself becomes a target for proteases later on in the apoptotic process (Burma and Chen, 2004; Lincz, 1998).

With regards to cisplatin, DNA-PK plays an important role in both NHEJ and apoptosis (Sand-Dejmek et al., 2011). DNA-PK is capable of phosphorylating nucleosomal H2AX (Park et al., 2003) following cisplatin treatment of human ovarian cancer A2780 cells. Depletion of DNA-PK_{cs} reduced PARP-1 cleavage in A2780 cells treated with cisplatin, suggesting a role of DNA-PK in controlling the induction of apoptosis by cisplatin (Bernstein et al., 2002). DNA-PK-depleted cells, generated using shRNA directed against DNA-PK_{cs}, were more sensitive to cisplatin treatment cells than control cells (Sand-Dejmek et al., 2011).

DNA-PK_{cs}, ATM and ATR proteins crosstalk in response to DNA damage, and elicit cell cycle arrest, DNA repair or cell death. DNA-PK also plays an important role in V(D)J recombination in B- and T-lymphocytes to generate hypervariable antigen binding sites (Gao et al., 1998; Williams et al., 2001). Inhibitors such as wortmannin and LY294002, also inhibit DNA-PK in a non-competitive and competitive manner, respectively (Izzard et al., 1999). These inhibitors retard NHEJ by inhibiting DNA-PK_{cs} and enhance the cytotoxicity of DNA damaging agents such as IR and topoisomerase II poisons (Boulton et al., 2000; Rosenzweig et al., 1997). More potent and specific inhibitors such as NU7026 (2-(morpholin-4-yl)-benzo[h]chromen-4-one) (Veuger et al., 2003; Willmore et al., 2004) and NU7441 (2-N-morpholino-8-dibenzothiophenyl-chromen-4-one) have led to a better understanding of the function of DNA-PK (Hardcastle et al., 2005; Leahy et al., 2004). NU7441 is a specific inhibitor of DNA-PK, with an IC₅₀ of 14 nmol/L, with at least 100-fold higher selectivity for this enzyme compared with other inhibitors (Zhao et al., 2006). NU7441 also increased the cytotoxicity of IR and etoposide in Chinese hamster ovary cells (Hardcastle et al., 2005; Leahy et al., 2004). It also increased the persistence of γ H2AX foci. Treatment of cells with NU7441 prolonged G2 arrest in human colon cancer cell lines after IR and etoposide, and increased the antitumour activity of IR in a human colon cancer xenograft model (Zhao et al., 2006).

The glioblastoma cell lines MO59J and MO59K differ in their DNA-PK status. The DNA-PK-deficient MO59J cells are 30-fold more sensitive to radiation when compared to MO59K cells, which are DNA-PK-proficient cells (Fischer et al., 2001). This difference in sensitivity is also seen in other chemotherapeutic drugs (Allalunis-Turner et al., 1993).

1.9. Replication protein A (RPA)

RPA is an important PIKK substrate, and an effector protein with roles in DNA replication, checkpoint activation and DNA repair. RPA is a heterotrimeric single-stranded DNA binding protein that was first identified as a human cell factor that was essential for cell-free replication of plasmids containing the SV40 origin of replication (Kenny et al., 1990; Umbricht et al., 1993). RPA homologues have been identified in all eukaryotes (Wobbe et al., 1987; Wold, 1997). Human RPA is composed of 70-, 32-, and 14-kD subunits, commonly referred to as RPA1, RPA2, and RPA3, respectively (Figure 1.7) (Iftode et al., 1999). Each of the three subunit contains an oligonucleotide/oligosaccharide-binding fold (OB-fold) that is commonly seen in other single-stranded DNA binding proteins. In RPA, these OB-folds are referred to as DNA binding domains (DBDs) (Bochkarev and Bochkareva, 2004).

RPA1 contains four OB-folds (DBD A-C and F) (Wyka et al., 2003). The majority of DNA binding activity is found in DBD-A and DBD-B, referred to as the ssDNA-binding core (Arunkumar et al., 2003). RPA1 also contains an OB-fold at each terminus, DBD-F at the N-terminus, and DBD-C at the C-terminus. DBD-F interacts with a large number of other proteins and is required for DNA repair, recombination, and cell cycle regulation in yeast and humans (Braun et al., 1997; Iftode et al., 1999; Longhese et al., 1996; Umezue et al., 1998). DBD-C interacts with DNA and is involved in recognition of DNA damage (Gomes and Wold, 1995; Lao et al., 2000).

RPA2 contains DBD-D that can be cross-linked to DNA at the primer-template junction (Pestryakov et al., 2004) and is also involved in heterotrimeric complex formation (Gomes and Wold, 1995). The RPA2 subunit contains multiple phosphorylation sites within the N-terminal region. RPA2 is phosphorylated on serine 23 and serine 29 by CDKs during normal cell cycle progression (Dutta and Stillman,

1992). RPA2 is also hyperphosphorylated upon DNA damage at serines 4, 8 and 33 and threonine 21 by PIK kinases (Carty et al., 1994; Liu and Weaver, 1993).

RPA3 contains DBD-E which interacts with DBD-C of RPA1 and DBD-D of RPA2 to form the heterotrimeric complex (Bochkareva et al., 1998). RPA3 is therefore involved in heterotrimer formation and is responsible for the polarity of binding to DNA (Bochkareva et al., 2002; Pestryakov et al., 2004; Pestryakov et al., 2003; Salas et al., 2009).

A single alternative form of RPA2 called RPA4 has been identified in human cells (Kemp et al., 2010; Keshav et al., 1995). The *RPA4* gene is located on the X chromosome and is devoid of introns (Tomkiel et al., 2002). RPA4 interacts with RPA1 (Zou and Elledge, 2003). The RPA4 subunit is 63% similar to RPA2 and has similar domain organisation at the protein level (Mason et al., 2010). It is either RPA2 or RPA4 that interacts with RPA1 and RPA3 to form a complex. Thus RPA1, RPA3 and RPA4 can form an alternative stable heterotrimeric complex, which interacts with ssDNA but cannot support DNA replication *in vitro* (Mason et al., 2010). RPA4 is expressed in all normal human tissues including the brain, heart, liver, kidney, ovary, placenta and prostate. However, the expression of RPA4 is reduced in cancer tissues compared to its corresponding normal tissue (Kemp et al., 2010).

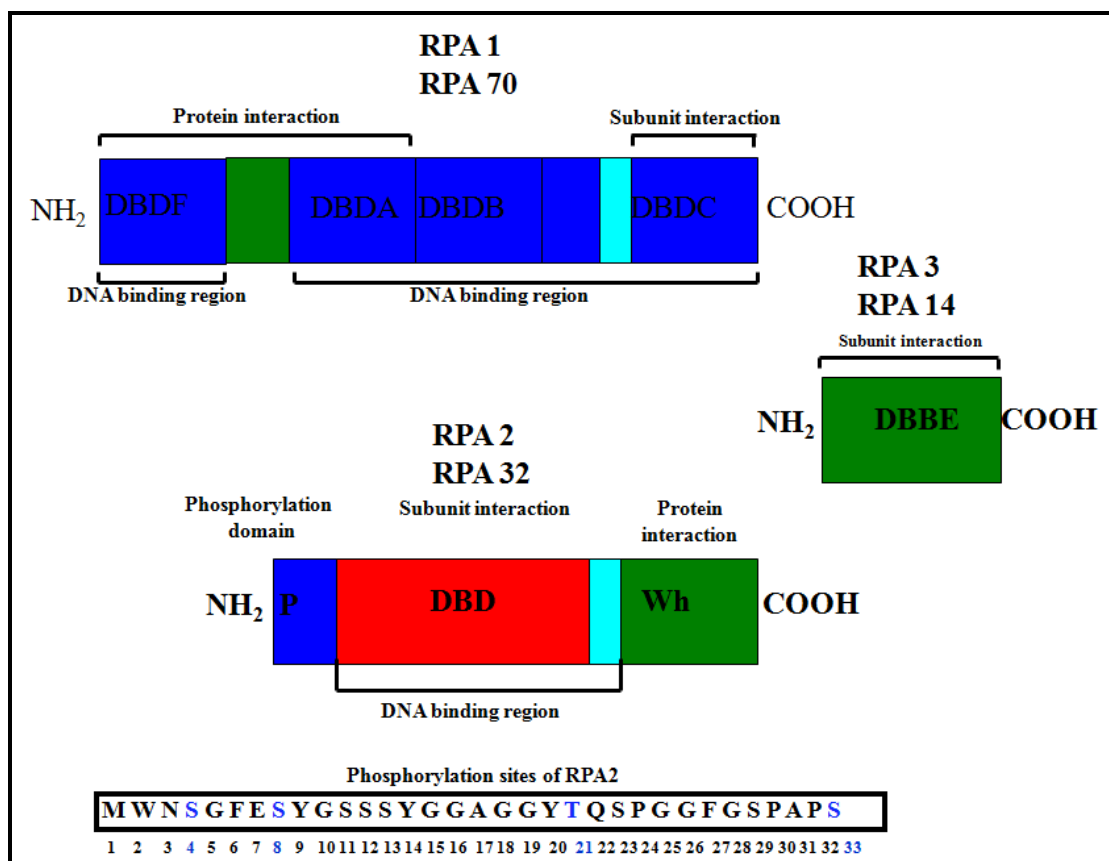


Figure 1.7. Domain structure of the subunits of replication protein A, and phosphorylation domain of RPA2 (Fanning et al., 2006).

1.9.1. Binding of RPA to ssDNA, protein-protein interactions and repair

RPA plays an important role in DNA replication (Haring et al., 2008) including assembly of pre-replication complexes and stabilisation of ssDNA following unwinding of DNA by helicases (Anciano Granadillo et al., 2010; De Vlaminck et al., 2010). RPA promotes an initial opening of the DNA, and is required for loading of DNA polymerase α and additional replication fork proteins. Once replication forks are established, RPA remains bound at the forks during elongation (Walther et al., 1999; Yuzhakov et al., 1999).

RPA2 plays an important role in DNA repair. Studies in human, *Xenopus* and yeast systems indicate that RPA recruits ATR to ssDNA generated by DNA repair or replication, through the interaction with ATRIP (Ball et al., 2007; Ball et al., 2005; Choi et al., 2010a; Kim et al., 2005; Zou and Elledge, 2003). RPA forms nuclear foci after DNA damage and plays an important role in DNA repair pathways including

base excision repair, nucleotide excision repair and double-strand break repair (Iftode et al., 1999; Krokan et al., 1977; Riedl et al., 2003). During HR, BRCA2 displaces RPA and facilitates Rad51 nucleoprotein filament formation (Bochkarev and Bochkareva, 2004; Wong et al., 2003) by interacting with Rad52 protein (Grimme et al., 2010; Shinohara and Ogawa, 1998). The role of RPA in NHEJ is not well defined, but it appears that RPA binds to ssDNA regions at or near a dsDNA end allowing DNA-PK to phosphorylate RPA2, resulting in RPA2 dissociating from the Ku-DNA-PK complex (Allen et al., 2011). In NER, XPA and RPA both bind to the 5' end of the damaged DNA and XPA facilitates the recruitment of ERCC1-XPF for the incision of the damaged strand (Krasikova et al., 2010; Orelli et al., 2010).

1.9.2. Cell cycle-dependent RPA phosphorylation

In human and yeast cells, RPA2 is phosphorylated in a cell-cycle dependent manner. Cdk1-cyclin B or Cdk2-cyclin A phosphorylate RPA2 during S- and M-phase at serine 23 and serine 29 (Anantha et al., 2007; Dutta and Stillman, 1992a; Oakley et al., 2003). RPA2 is phosphorylated at serine 23 in S-phase and remains phosphorylated during M-phase whereas, serine 29 phosphorylation takes place only during M-phase (Stephan et al., 2009). RPA purified from mitotic cells showed reduced binding to ATM, DNA polymerase α , and DNA-PK as compared to unphosphorylated recombinant RPA (Oakley et al., 2003). The RPA2 anti-phosphoserine 23 antibody recognises the phosphorylated RPA2, which is characterised by a small reduction in the RPA2 mobility in western blotting and is present in S-phase HeLa cells (Brush et al., 2001; Oakley et al., 2003)

1.9.3. Role of RPA in the DNA damage response

RPA1 is phosphorylated *in vitro* on Thr 180 in response to HU, UV and IR (Nuss et al., 2005).

RPA2 is phosphorylated on a number of N-terminal sites in response to DNA damaging agents including IR (Carty et al., 1994; Liu and Weaver, 1993), UV and chemotherapeutic agents (Niu et al., 1997; Nuss et al., 2005). Damage-induced phosphorylation of RPA2 generates a slow-mobility form of the protein (by SDS-PAGE) termed hyperphosphorylated RPA2. DNA damage induced by IR in HeLa cells leads to RPA2 hyperphosphorylation on threonine 21, serines 4, 8, 33 and/or at

least one phosphoserine in residues 11–13 (Boubnov and Weaver, 1995; Fried et al., 1996; Liu and Weaver, 1993; Zernik-Kobak et al., 1997).

RPA2 hyperphosphorylation plays an important role in DNA repair (Binz et al., 2004; Vassin et al., 2004). In particular, hyperphosphorylation of RPA2 may modulate RPA interactions with DNA and proteins involved in the DNA repair and signalling pathways in response to DNA damage (Binz et al., 2004). For instance, hyperphosphorylated RPA2 has shown decreased interactions with simian virus 40 (SV40) large T-antigen, DNA polymerase α , DNA-PK, ATM, and p53 *in vitro* whereas, hyperphosphorylation has no effect on RPA interactions with XPA and Rad52 (Binz et al., 2004; Jackson et al., 2002; Oakley et al., 2003; Patrick et al., 2005; Wu et al., 2005). In *in vitro* studies, it was shown that hyperphosphorylated RPA2 interacts with Rad51 (Wu et al., 2006b). Hyperphosphorylated RPA also binds double-stranded DNA with a reduced affinity when compared to that of ssDNA (Binz et al., 2004; Oakley et al., 2003).

DNA-damage-induced phosphorylation is carried out by PIK kinase (Binz et al., 2004; Carty et al., 1994). RPA2 binds to ssDNA intermediates (Namiki and Zou, 2006) formed during the repair of double-strand breaks and at blocked replication forks. Binding of RPA mediates binding of the ATR-ATRIP complex to the DNA and activates ATR kinase. ATR phosphorylates RPA2 at serine 33 (Anantha et al., 2007; Jazayeri et al., 2006). Cyclin-dependent kinase is also required for DNA damage-induced RPA2 hyperphosphorylation (Anantha et al., 2007). This indicates that RPA2 phosphorylation catalysed by CDKs and PIK kinases may be interdependent (Anantha et al., 2007). Cisplatin-induced RPA hyperphosphorylation, on serine 4 and 8 is DNA-PK-dependent (Cruet-Hennequart et al., 2008).

The mitotic form of RPA2 can be further phosphorylated by both ATM and DNA-PK (Stephan et al., 2009). Mitotic RPA2 hyperphosphorylation plays a role both in cellular exit from a damaged mitosis into a normal 2N state G1-phase, and in decreasing cell death from DNA damage-dependent apoptosis (Anantha et al., 2008). Mitotic phosphorylation at Serine23 and Serine29 primes RPA2 to undergo additional phosphorylation events in response to DSBs induced due to bleomycin in human osteosarcoma cells (Anantha et al., 2007).

Proteins that are phosphorylated in response to DNA damage have to be dephosphorylated by phosphatases. Phosphatase PP4C dephosphorylates both γ -H2AX generated during DNA damage and hyperphosphorylated RPA2 (Lee et al., 2010). Dephosphorylation of hyperphosphorylated RPA2 is necessary to resume DNA synthesis after DNA damage, which allow cells to continue cycling (Olson et al., 2006). Dephosphorylation of RPA2 was also required for completion of HR (Lee et al., 2010).

1.10. DNA damage and cell cycle progression

The process of replication of damaged DNA and TLS must be considered in the overall context of cell cycle progression, and the processes that regulate the cell cycle following DNA damage. The cell cycle is a process by which a cell replicates its genome, and distributes the cell contents evenly to the two daughter cells (Zhou and Elledge, 2000). This process is further subdivided into four phases: gap 1 (G1), synthesis (S) and gap 2 (G2), together called the interphase, and mitosis (M). Terminally differentiated cells such as nerve and muscle cells exit the cell cycle and enter a quiescent state known as G0-phase, where cells do not divide (Tiainen et al., 1996). Because the biochemical processes differ between cells in G1-, S-, G2- and M-phases, the responses of individual cells to DNA damage may differ depending on the phase of the cell cycle at the time of exposure (Sakaue-Sawano et al., 2011). In the context of cancer treatment, this could impact the response of tumour cells to treatment. Terz *et al.*, (1977) studied the cycling and non-cycling cell populations by injecting tritiated thymidine methyl (H_3 -TRD) in human solid tumours to label replicating DNA. The study concluded that in solid tumours, 50-60% of the cells were in S phase (Terz et al., 1977).

1.10.1. Role of cyclins in cell cycle regulation

Cyclins are important regulators of cell cycle progression, and are synthesised and degraded in a cell-cycle dependent manner (Hunt, 1991; Traganos, 2004) (Figure 1.8). A protein complex consisting of cyclins and associated cyclin-dependent kinases (CDKs) regulates the cell cycle (Krylov et al., 2003; Malumbres and Barbacid, 2009). Cyclin-CDK complexes consist of four cyclins: D, E, A and B and four CDKs: 4, 6, 2 and 1 (Hunt, 1991) (Figure 1.8). CDKs belong to a family of serine/threonine protein kinases. CDK-cyclin complexes are regulated by phosphorylation and

dephosphorylation of the CDK subunit (Malumbres and Barbacid, 2005) by CDK-activating kinases (CAK), which phosphorylate the CDK-cyclin complex on the CDK subunit (Lees, 1995).

The nuclear protein retinoblastoma (Rb), the product of the tumour suppressor gene *RB*, is an important target of cyclin-CDKs during cell cycle progression (Taya, 1997). In G₀-cells, as well as in early G₁-phase cells, pRb is hypophosphorylated and therefore active (Mihara et al., 1989). Hypophosphorylated pRb binds both the E2F transcription factor and histone deacetylase (Luo et al., 1998). Free E2F activates transcription of several genes such as PCNA, topo 1, c-Myc, cyclin D1, cyclin A (Soucek et al., 1997), cyclin E (Geng et al., 1996), p21Cip1 (Hiyama et al., 1997), CDK2 (Helin et al., 1993), CDK1, and Cdc25, whose products are important for S-phase entry and for DNA replication. In mid-to late-G₁-phase of the cell cycle, pRb is phosphorylated by cyclin-CDKs and releases E2F, and becomes inactive until M-phase, when it is dephosphorylated by a PP1-type phosphatase (Ludlow, 1993) and binds to E2F and HDAC again.

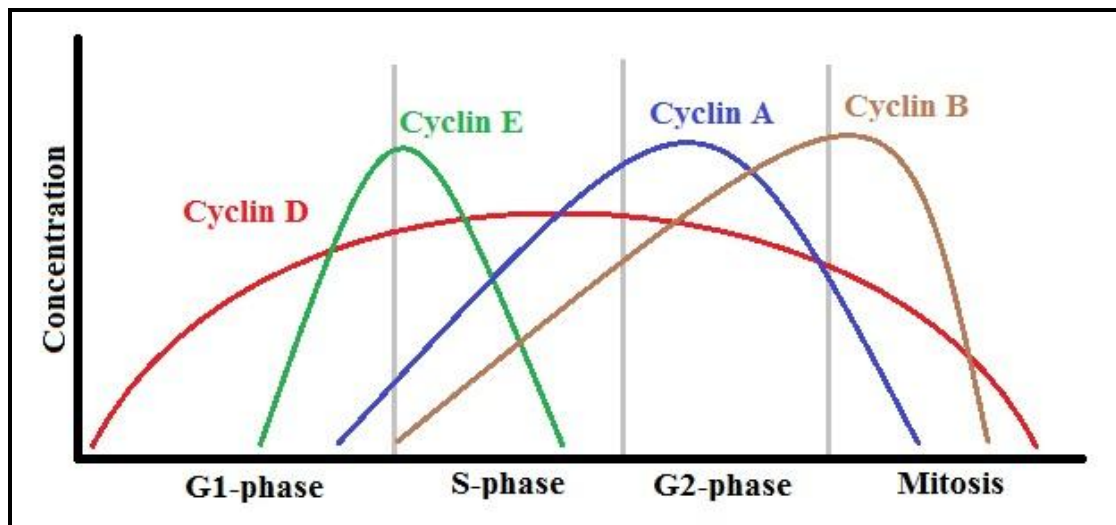


Figure 1.8. The eukaryotic cell cycle showing the key cyclins and cyclin-dependent kinases (CDKs) at each stage (redrawn from (Sullivan and Morgan, 2007)).

Cyclin D synthesis begins during early G₁-phase, and the level of cyclin D is high at late G₁-phase, near the G₁-S boundary (Sherr, 1994) (Figure 1.8). CDK4, the CDK partner of cyclin D, is phosphorylated on a single threonine residue (Threonine 161) (Sherr, 1994) by CDK-activating kinase (CAK). This phosphorylation stimulates the

kinase activity. Phosphorylation of Threonine 14 and Tyrosine 15 by Wee1 and Myt1 on the other hand, inhibits and inactivates the kinase (Terada et al., 1995).

While CDK4 and CDK6 in complex with D-type cyclins are responsible for G1 progression, CDK2 activity increases rapidly in mid-to-late G1-phase. CDK2 in complex with cyclin E plays a vital role at the G1-to-S transition and during S-phase (Reed, 1996). In addition to activating phosphorylation events carried out by CAKs, phosphorylation of CDKs by Wee1 and Myt1 can inhibit CDK activity. These inhibitory phosphorylations are removed by the Cdc25 phosphatase family members (Cdc25 A-C) (Hoffmann et al., 1994), which are dual-specificity phosphatases that remove inhibitory phosphate residues from CDKs. Cdc25A-C control entry to and progression through various phases of the cell cycle. Cdc25A is expressed predominantly in late G1-phase, and increases in S-phase. Cdc25A undergoes CDK2-cyclin E-dependent phosphorylation during S-phase, resulting in an increase in its phosphatase activity (Hoffmann et al., 1994).

Cyclin A, on the other hand, binds to and activates CDK2 in G2- and M-phases (Pagano et al., 1992). During interphase, CDK2 activity is down-regulated by Wee1- and Myt1-dependent phosphorylation on Threonine 14 and Tyrosine 15 (Terada et al., 1995). Phosphorylation of Cdc25C by polo-like kinase 1 increases CDK1/cyclin B activity and promotes entry into mitosis (Lindqvist et al., 2005). Exit from mitosis requires inactivation of cyclin B/CDK1, by proteosomal-mediated degradation of cyclin B, which occurs during the metaphase-to-anaphase transition (Cimini et al., 2003).

CDK activity is also modulated by negative regulators known as cyclin-dependent kinase inhibitors (CKIs). CKIs can be divided into two family of proteins: the INK4 family and the Kip/Cip family (Aprelikova et al., 1995; Harper et al., 1993). p16 belongs to the INK4 family that inhibits CDK4 and CDK6 activity by binding in competition with D-type cyclins (Aprelikova et al., 1995). Other members of the INK4 family are p15, p18 and p19 (Hirai et al., 1995). CDK2 is inhibited by members of the Kip/Cip family (p21, p27, and p57). p21 was the first characterised member of this family and plays a role in the p53-dependent DNA damage response (Harper et al., 1993). Small molecule inhibitors of CDKs have also been identified. For example, flavopiridol, a synthetic flavone that has high affinity for CDKs, was shown

to bind to and directly inhibit CDK 1, 2, 4 and 6 and induce cell cycle arrest in breast cancer cells (Losiewicz et al., 1994). Roscovitine, a small molecule aminopurine, is also a potent inhibitor of CDK2 (McClue et al., 2002) and CDK1 (Meijer et al., 1997).

1.10.2. Cell cycle synchronisation

In order to study cell cycle progression, methods have been developed to bring cells in culture to the same stage of the cell cycle, a process known as synchronisation (Tobey et al., 1990). Cell synchronisation methods are broadly classified into two types: physical and chemical methods. Physical methods can be based on cell size (for example, centrifugal elutriation), cell density, affinity to antibody, and fluorescence emission by labelled cells (using fluorescence activated cell sorting-FACS) (Merrill, 1998). In centrifugal elutriation, cells are separated based on the principle that cell size differs at different stages of the cell cycle. During the separation process cells are separated based on the sedimentation coefficient of individual cells. However, in this method, large numbers of cells (up to 10^7) are needed to obtain enriched cell populations. This is more feasible with cells in suspension than with adherent cells (Futcher, 1999).

Chemical methods include those based on blocking metabolic reactions, such as double thymidine block, and prevention of microtubule function during mitosis (such as the use of nocodazole) (Davis et al., 2001). In the case of the double thymidine block procedure, DNA synthesis is inhibited by the addition of thymidine as it has a negative feedback on nucleotide biosynthesis and cells are arrested in S-phase. Removal of thymidine results in exit of cells from S-phase arrest. Then, high concentration of thymidine is added to impose a block again, to obtain cells in late G1-phase (Bostock et al., 1971). Another chemical method to obtain cells arrested in G1-phase is by growth factor deprivation, by removal of serum from the culture medium (Kues et al., 2000). Cells are grown in culture medium without serum, causing cells to arrest in G1-phase. Synchrony is reversed by addition of serum to the culture medium (Kues et al., 2000).

Cells can also be synchronised in mitosis by the addition of nocodazole (methyl [5-(2-thienylcarbonyl)-1H-benzimidazole-2-yl]), a mitotic inhibitor (Harper, 2005; Kung

et al., 1990; Ludlow et al., 1993). Nocodazole binds to β -tubulin in microtubules, resulting in microtubule depolymerisation, thereby arresting cells in prometaphase (Jordan et al., 1992). This approach can be used to generate an enriched population of mitotic cells. Arrested cells can be released into the cell cycle by removal of the drug, to obtain enriched population of cells in different phases of the cell cycle (Jordan et al., 1992). In mitosis, microtubules play a critical role in the separation of chromosomes between the two daughter cells. Microtubules are composed of dimers of α -tubulin and β -tubulin (Schiebel, 2000). Tubulin dimers are polar structures, which assemble and disassemble to form microtubules (Dammermann et al., 2003; Howard and Hyman, 2003). Microtubules are dynamic structures, which continuously undergo assembly and disassembly (Vaughan and Dawe, 2011). In mitotic cells, kinetochore microtubules, which attach to the centromeres of condensed chromosomes, are the targets of nocodazole treatment (Fukagawa, 2004). Microtubules also contribute to chromosome movement by pushing the spindle poles apart resulting in the formation of two daughter cells (Maiato et al., 2004).

Since microtubules play a central role in mitosis, drugs that affect microtubule assembly have been used clinically in the treatment of cancer, and are also useful tools in cell synchronisation studies in experimental settings (Cimini et al., 2002; Neumann et al., 2001; Shen et al., 2005). For example, the drugs colchicine and colcemid bind to β -tubulin (Wolff et al., 1996) and inhibit microtubule polymerisation, which blocks mitosis (Screpanti et al., 2010). In contrast, vincristine, vinblastine and taxols stabilise microtubules, preventing disassembly, and block cell division (Bhattacharyya et al., 2011). All these drugs are used in cancer treatment. Nocodazole causes microtubule depolymerisation, thereby preventing formation of metaphase spindles (De Brabander et al., 1977). The absence of microtubule attachment to kinetochores activates the spindle assembly checkpoint (SAC) causing the cell to arrest in prometaphase. The effect of nocodazole on microtubules is reversible (De Brabander et al., 1977) so that, following washout of the drug, cells in culture can resume cell cycle progression.

1.11. DNA damage-induced cell cycle checkpoints

Cell cycle checkpoints are biochemical control mechanisms that ensure the fidelity of cell division in eukaryotic cells (Hartwell and Weinert, 1989). Checkpoints monitor whether the processes at each phase of the cell cycle have been accurately completed before the cell progresses to the next phase (Nakanishi et al., 2006). In mammalian cells, the checkpoint response to DNA damage or replication stress regulates cell cycle progression (Melo and Toczyski, 2002) (Figure 1.9). The DNA damage-activated cell cycle checkpoint kinases Chk1 and Chk2 are activated by ATR and ATM respectively, thereby linking the DNA damage response with the checkpoint machinery (Stiff et al., 2006; Zhao and Piwnicka-Worms, 2001) (Figure 1.9).

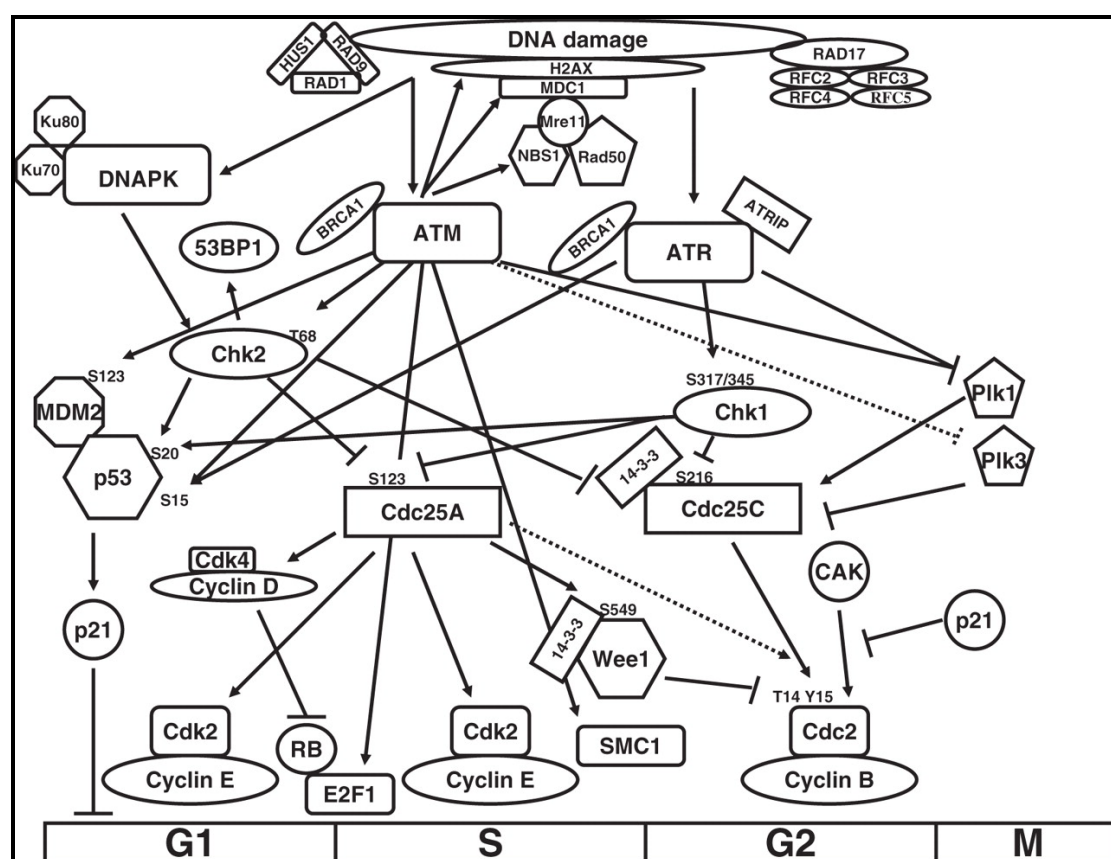


Figure 1.9. Schematic diagram of DNA damage-induced cell cycle checkpoints in human cells (from Niida and Nakanishi, 2006).

Human Chk1 and Chk2 are structurally and functionally distinct but contain highly conserved protein kinase domains (O'Neill et al., 2002). There is significant crosstalk between the ATR-Chk1 and ATM-Chk2 signalling cascades (Garcia-Muse and

Boulton, 2005; Gatei et al., 2003; Goudelock et al., 2003; Hirao et al., 2002; Matsuoka et al., 2000; McSherry and Mueller, 2004; Stracker et al., 2008) as represented in figure 1.9. Both these effector kinases play an important role in the regulation of cell cycle arrest. Chk1 and Chk2 phosphorylate the Cdc25 family of phosphatases that remove inhibitory phosphorylations from CDKs (Boutros et al., 2006; Karlsson-Rosenthal and Millar, 2006).

1.11.1. Checkpoint kinase 1 (Chk1)

DNA damage occurring in S-phase, or DNA replication stress, triggers checkpoint responses which delay entry into mitosis by arresting DNA replication (Zhao et al., 2002). Chk1 is a 54 kDa, chromatin-associated protein expressed in normal growing cells (Yilmaz et al., 2011). In response to ssDNA produced following DNA damage-induced replication arrest, Chk1 is recruited to sites of damage through interaction with Rad17 (Bao et al., 2001), which is activated by the binding of the protein claspin (Gao et al., 2009). Chk1 is then phosphorylated by ATR on at least two residues, serine 317 and serine 345 (Kulkarni and Das, 2008). Chk1, as outlined in figure 1.9, is an important regulator of both S-phase progression and mitotic entry. Chk1 phosphorylates Cdc25C on serine 216, inhibiting Cdc25C. This prevents activation of the Cdc2-cyclin B complex and inhibits mitotic entry (Loffler et al., 2006). Alterations in Chk1 play an important role in the etiology of cancer (Menoyo et al., 2001). The *Chk1* gene is essential since knock-out of *Chk1* in mice is embryonically lethal (Lam et al., 2004). Cells examined from mice that were conditional for Chk1 expression in mammary glands showed abnormal cell cycle progression, in particular accumulation of cells in S-phase, and premature chromatin condensation, resulting in premature mitotic entry and induction of apoptosis (Lam et al., 2004). Phosphorylation may both participate in Chk1 activation and promote its degradation. The turning off of Chk1 activity can be mediated by the proteasomal degradation of the adaptor protein claspin which is impeded by ubiquitin-specific peptidase 7 (USP7) deubiquitinase (Faustrop et al., 2009).

1.11.2. Checkpoint kinase 2 (Chk2)

Human Chk2, is a 60 kDa protein that controls G1/S (Figure 1.9) and G2/M checkpoint (Castedo et al., 2004). Chk2 is phosphorylated on Threonine 68 by ATM

in response to IR-induced DNA damage (Buscemi et al., 2004; Matsuoka et al., 2000; Oliver et al., 2007). Activated Chk2 mediates radiation-induced G1 arrest and inhibition of DNA synthesis in S-phase cells, through phosphorylation of Cdc25A phosphatase, which triggers the ubiquitination and proteasomal degradation of Cdc25A (Chehab et al., 2000; Falck et al., 2001). Ubiquitination of Chk2 itself has also been reported and is controlled by phosphorylation of serine 379 and serine 456 by ATM (Kass et al., 2007; Lovly et al., 2008). Chk2 plays a critical role in DNA damage-induced apoptosis, as studies using Chk2 knock-out mice showed that Chk2-null cells were resistant to IR-induced apoptosis (Hirao et al., 2000; Takai et al., 2002). In addition, Chk2 participates in G2/M arrest by phosphorylating Cdc25C phosphatase (Castedo et al., 2004) facilitating binding of the molecular chaperone 14-3-3, which leads to inactivation of Cdc25C by the ubiquitin-dependent proteasome pathway. Since Cdc25C is required for activation of CDK1-cyclin B and entry into mitosis, Cdc25C inactivation activates the G2/M checkpoint (Timofeev et al., 2010).

1.11.3. The G1-phase checkpoint

A DSB occurring in the genome of a cell in G1-phase can activate the G1 checkpoint (Kanaar and Wyman, 2008). ATM or ATR-dependent activation of Chk1 or Chk2 leads to phosphorylation of Cdc25A and to activation of the G1 checkpoint (Mailand et al., 2000). p53 activation is required for maintenance of the G1 checkpoint. p53 is phosphorylated by both ATR and ATM inhibiting the nuclear export and degradation of p53 (Zhang and Xiong, 2001). p53 is also stabilised by phosphorylation and inhibition of the p53-associated ubiquitin-protein ligase E3, MDM2 (de Toledo et al., 2000). p53 upregulates p21, which in turn inhibits CDK2, thereby maintaining the G1/S checkpoint (Section 1.10.1) (Lukas et al., 2003). p21 binds and inhibits the cyclin E-CDK2 complex and the cyclin D-CDK4 complex thereby, preventing phosphorylation of retinoblastoma protein (Rb) (Section 1.10.1) (Harper et al., 1993; Maitra et al., 2001). As outlined in Section 1.10.1, phosphorylation of Rb results in the release of the E2F transcription factor which is required for transcription of genes that are required for S-phase progression (Bartek and Lukas, 2001; Talluri et al., 2010); inhibition of E2F release prevents S-phase entry (He et al., 2000). Defects in the G1 checkpoint play a vital role in human cancers as mutations in G1 checkpoint proteins including p53 is commonly seen in many cancers (Foster et al., 2010; Kastan

and Bartek, 2004).

1.11.4. DNA damage-induced S-phase checkpoints

DNA replication in eukaryotes occurs in S-phase and is initiated at multiple replication origins. In mammalian cells, ionising radiation-induced strand breaks cause an immediate arrest of DNA synthesis (Bartek et al., 2004; Savell et al., 2001). However, in cells from patients with ataxia telangiectasia, DNA synthesis is not inhibited by radiation and the cells progress through S-phase without any delay demonstrating a role for ATM in mediating IR-induced cell cycle arrest. There are three checkpoints associated with S-phase: the replication checkpoint, the intra-S-phase checkpoint and the S/M checkpoint (Bartek et al., 2004). All three checkpoints are p53-independent (Bartek et al., 2001).

The replication checkpoint is activated in response to stalled replication forks during S-phase (Segurado and Tercero, 2009). This occurs in response to collision of replication forks with DNA damage or aberrant DNA structures (Mirkin, 2008). Stalled replication forks lead to ATR-dependent, Chk1-mediated phosphorylation of Cdc25C preventing activation of cyclin E/CDK2, and inhibiting S-phase progression by blocking loading of Cdc45 onto chromatin (Luciani et al., 2004).

The intra-S-phase checkpoint delays S-phase progression. The firing of new origins of replication is inhibited, but this does not slow the extension of actively progressing replication forks. In the intra-S checkpoint response, CDK2 activity is inhibited by the phosphorylation and degradation of Cdc25A, which is regulated by Chk1- and Chk2-induced phosphorylation (Falck et al., 2002).

The S/M checkpoint ensures that cells do not enter mitosis with incompletely replicated DNA (Nghiem et al., 2002). ATR phosphorylates and activates Chk1 resulting in phosphorylation of Cdc25C. Phosphorylated Cdc25C is unable to dephosphorylate CDK1; failure to activate CDK1 causes premature chromatin condensation (PCC), which inhibits entry to mitosis (Niida et al., 2005).

1.11.5. G2- and M-phase checkpoints

The G2-phase checkpoint is critical in preventing the entry of cells into mitosis in the presence of DNA damage (Deckbar et al., 2007). As outlined above, during DNA damage ATR phosphorylates Chk1, while ATM phosphorylates Chk2. Chk1 and Chk2 phosphorylate and inactivate Cdc25C, which is necessary for cyclin B/CDK2 complex activation. Lack of cyclin B/CDK2 activity blocks the cell cycle transition from G2 to M (Smits and Medema, 2001). Although Chk1 signalling initiates G2 arrest, the maintenance of the arrest requires Chk2 signalling. Mutation of BRCA1 by substituting alanine on serine 1423 in the Brca1-mutant human breast cancer cell line HCC1937 demonstrated that ATM-mediated phosphorylation of BRCA1 on this site is also a key event in the G2 checkpoint (Xu et al., 2003) by analysing histone H3 levels using flow cytometry. Mutated BRCA1 thereby failed to rescue G2 checkpoint defects in HCC1937 cells (Xu et al., 2003). p53 also plays an important role in the maintenance of G2 arrest and in the control of entry into mitosis (Taylor and Stark, 2001). p53 is required for ATM-dependent phosphorylation events in G2 following exposure to irradiation (DiTullio et al., 2002). In prolonging G2 arrest, the p53-regulated CDK inhibitor, p21, as well as the transcriptional target of p53, *GADD45* are upregulated. The G2 checkpoint also requires signalling by the MAPK kinase p38 to Cdc25B (Deng et al., 2002). Inactivation of p38 by genetic deletion restored G2-to-M progression following UVC-induced DNA damage in human fibroblasts (Deng et al., 2002).

Protein phosphatase 2A (PP2A) (Wang et al., 2004) dephosphorylates cyclin B-CDK1 substrates, and this dephosphorylation event is regulated during mitotic entry and exit (Mochida et al., 2004). During G2-phase, PP2A activity is high and cyclin B-CDK1 activity is low, which prevents phosphorylation of mitotic substrates (Burgess et al., 2010). When cells enter mitosis, PP2A activity decreases and cyclin B-CDK1 activity increases (Burgess et al., 2010) allowing mitotic substrates of cyclin B-CDK1 to be phosphorylated and mitosis to proceed (Burgess et al., 2010).

The spindle assembly checkpoint (SAC) plays an important role when cells enter mitosis by preventing premature metaphase-to-anaphase transition (Musacchio and Salmon, 2007). The SAC consists of sensor proteins, the mitotic checkpoint complex (MMC), the anaphase-promoting complex/cyclosome (APC/C) and Cdc20. Sensor

proteins include Mad1, Bub1 and Mps1. The MCC includes Mad2, Bub3, BubR1 and Cdc20. During anaphase, in the normal cell cycle, APC is activated through decreasing MCC activity which polyubiquitinates the anaphase inhibitor securin (Ciosk et al., 1998). Ubiquitination and destruction of securin at the end of metaphase releases the active protease separase, which cleaves the cohesion molecules that hold the sister chromatids together, to activate anaphase (Nasmyth and Haering, 2005). The SAC is deactivated by APC activation and is not reactivated by the loss of sister-chromatid cohesion during anaphase. The proteolysis of cyclin B and inactivation of the CDK1-cyclin-B kinase also inhibits SAC activity. Degradation of Mps1 during anaphase prevents the reactivation of SAC after removal of sister-chromatid cohesion.

1.12. Cell cycle effects of cisplatin

As described in Section 1.4.1, platinum-based drugs remain critical in many cancer therapy approaches. There is considerable evidence that cell cycle progression is altered when cells are treated with cisplatin and related platinum-based chemotherapeutic agents. Therefore, studies of the effects of cisplatin on cell cycle progression have been carried out to understand the complex network of proteins that determine the outcome of exposure (Ubezio et al., 2009). Cisplatin can affect cells by inducing cell death (cytotoxic effect) or by delaying cell cycle progression (cytostatic effect). Hence, to gain insight into the response of cells to cisplatin, in the present study both the cytotoxic and cytostatic effects were investigated. In considering the relationship between the cell cycle and exposure to platinum-based DNA damaging agents, there are two related aspects: (i) effects of DNA damaging agents on cell cycle progression, and (ii) effects of cell cycle stage at the time of exposure on the response to DNA damaging agents.

1.12.1 Effects of DNA damaging agents on cell cycle progression

As outlined above (Section 1.11), normal cells have the capacity to arrest in G1-, S-, G2- or M-phases of the cell cycle in response to DNA damage. The arrest allows time for repair of potentially lethal DNA damage prior to replication or mitosis (Bartek and Lukas, 2001). Most normal cells in culture are in G1-phase of the cell cycle; hence, in these cells, G1-phase arrest occurs post-DNA damage (Vermeulen et al., 2003). In contrast, many cancer cells lack the DNA damage-induced G1 checkpoint because of

p53 inactivation, and consequently arrest occurs in the S- or G2-phases of the cell cycle (Vermeulen et al., 2003).

Cisplatin induces a number of DNA adducts, as outlined in Section 1.4.2. Cisplatin-induced intra- and inter-strand DNA adducts produce severe local distortions in the DNA double helix, and prevents DNA replication by blocking replicative DNA polymerases (Section 1.7.6) or preventing strand separation, in the case of ICLs (Section 1.6.2.1) (Bhana et al., 2008; Pillaire et al., 1995). The pathways used to repair cisplatin-induced ICLs differs depending on the cell cycle stage, in that ICLs are repaired in G1-phase by NHEJ (Mogi et al., 2008; Smeaton et al., 2009), and in a replication-dependent process in S-phase by HR. Robinson et al., (2007) demonstrated that in HeLa cells synchronised using a double-thymidine block, following etoposide treatment RPA2 foci were observed in S-phase cells, while phosphorylated Nbs1-foci was observed in G1-phase cells. This is consistent with homologous recombination repair occurring in S-phase, and MRN-dependent non-homologous end joining repair occurring in G1-phase (Robinson et al., 2007).

Cisplatin strongly inhibited cell cycle progression in phytohemagglutinin-activated (PHA) peripheral blood lymphocytes (Kubbies et al., 1991). Using flow cytometry to elucidate the effects on cell cycle progression, it was found that when lymphocytes were treated with cisplatin (1 µg/ml) inhibition of cell cycle progression in the S- and G2-phases occurred (Kubbies et al., 1991). When the cells were treated with a higher dose of cisplatin (3 µg/ml) only S-phase arrest was observed, without G2 arrest, as cells did not progress from S-phase into G2-phase (Kubbies et al., 1991). Cisplatin also induced S-phase arrest in the human breast cancer cell line, MCF-7 (Lee et al., 1999) within six hours of treatment (Xu et al., 2005). By inhibiting ATR activity using caffeine, it was shown that ATR plays a major role in cisplatin-induced S-phase arrest (Abraham, 2001; Cliby et al., 1998; Lewis et al., 2009). S-phase arrest was also reported in the human hepatoblastoma cell line HepG2 treated with cisplatin (2 µg/ml) (Qin and Ng, 2002). In S-phase cells, cisplatin-induced intrastrand adduct are bypassed by specialised polymerases in the process of translesion synthesis (Section 1.7.6). Polymerase η plays a role in bypassing cisplatin-adducts, as depletion of polymerase η protein in HeLa cells using siRNA leads to the accumulation of cells in S- and G2-phase of the cell cycle (Rojas et al., 2010). S-phase arrest was also

demonstrated in pol η -deficient XP30R0 human fibroblast cells following cisplatin and carboplatin treatment (Cruet-Hennequart et al., 2008; 2009).

In murine leukaemia L1210 cells, cisplatin induced a slowdown in S-phase, and G2 arrest (Sorenson and Eastman, 1988). Cisplatin (1 $\mu\text{g/ml}$) caused a short G2-phase arrest, detected by flow cytometry (Sorenson and Eastman, 1988). Exposure of L1210 cells to a higher dose of cisplatin (8 $\mu\text{g/ml}$) resulted in an irreversible Chk1-dependent G2 arrest, followed by apoptosis (Dai and Grant, 2010).

Thus, the main effects of cisplatin are S-phase and G2-phase arrest, as described above. However, more recently, G1 checkpoint activation by cisplatin has also been demonstrated. Cisplatin induced G1 arrest in p53-defective HeLa cells (Koprinarova et al., 2010) and p53-proficient ovarian A2780 cells (He et al., 2011), demonstrating that cisplatin-induced G1 arrest is p53-independent. Kuang et al. (2001) demonstrated that treatment of A2780 cells with 1R, 2R-diaminocyclohexane (trans-diacetato)(dichloro)platinum(IV) (DAP), a platinum analogue led to arrest of the cells in G1-phase (Kung et al., 1990). He et al (2011) compared the effects of DAP and cisplatin on cell cycle progression. A2780 cells were first exposed to DAP which arrested the cells in G1-phase. Cells were then exposed to nocodazole to arrest cells in G2/M. DAP-treated cells remained strongly arrested in G1-phase (He et al., 2011). In contrast, when cells were treated with cisplatin rather than DAP, G2/M accumulation was detected and a decrease in G1-phase cells was seen (He et al., 2011). Thus following cisplatin treatment, cells were primarily arrested in S- and G2/M-phases, and G1 arrest was not as strong as following DAP treatment.

1.12.2 Effects of cell cycle stage at the time of exposure on the response to DNA damaging agents

The effect of cell cycle stage at the time of treatment on the outcome of exposure to cisplatin and other DNA damaging agents is important to understand the DNA damage response pathways that are activated, and how this may influence the outcome of exposure. In a study using CHO, cells in early S-phase were generated by nocodazole arrest and release, followed by arrest at the G1/S boundary using aphidicolin (Mutomba and Wang, 1996). Treatment of these cells with cisplatin resulted in G2-phase arrest (Sorenson and Eastman, 1988). This is consistent with

inhibition of CDK1-cyclin B dephosphorylation, which is required for mitotic entry (Pondaven et al., 1990).

In another study, Ubezio et al (2009) treated an asynchronous population of the human ovarian cancer cell line, IgroV1, with cisplatin to investigate the effects of the drug on cells in different stages of the cell cycle. Employing a mathematical model, the cytostatic and cytotoxic effects of cisplatin on cells in each phase of the cell cycle was characterised. In this model, flow cytometry was used to identify cells in different phases. S-phase cells were labelled with BrdU, and BrdU-labelled cells were followed over time using flow cytometry. Checkpoint activity was measured by analysing the endpoints including growth, cell viability, fraction of BrdU-labelled cells, and the percentage of cells in each phase. The model incorporated the cell proliferation difference between drug-treated and control cells. IgroV1 cells were treated for 1 hour with cisplatin at different drug concentrations up to 100 μ M, and harvested between 6 and 96 hours. When IgroV1 cells were treated with <10 μ M cisplatin, checkpoints in all the phases were activated and no cell death was observed (Ubezio et al., 2009). At higher concentrations of cisplatin (100 μ M), cell death occurred from 24-96 hours post-treatment in arrested S and G2/M cells (Ubezio et al., 2009).

In another study, CHO cells synchronised by centrifugal elutriation, were treated with nitrogen mustard to investigate the cell cycle-dependence of DNA crosslink formation (Murray and Meyn, 1986). When the levels of nitrogen mustard-induced crosslinks were analysed using the alkaline elution technique there was no significant difference in the levels of adducts formed in cells in different phases (Murray and Meyn, 1986). However, it was determined by clonogenic assays that cell populations enriched in G1 were the most sensitive to nitrogen mustard treatment, and those enriched in late S- and G2-phases were more resistant (Murray and Meyn, 1986). Thus, the cell cycle stage rather than levels of ICLs determined the outcome of exposure.

Diamant et al. (2011) has provided further evidence that the response of human cells to UV-induced lesions is different between S- and G2-phases. Human osteosarcoma cells were synchronised by centrifugal elutriation, and cells at the G1/S boundary were treated with UV radiation, and allowed to progress through the cell cycle (Diamant et al., 2011). To measure TLS during different phases of the cell cycle, cells were transfected with gapped plasmids carrying either a single CPD or a cisplatin-

GG adduct (Diamant et al., 2011). It was demonstrated that TLS was higher in G2-phase cells compared to S-phase cells (Diamant et al., 2011). RPA2 foci were detected in S-phase indicating the formation of ssDNA upon UV irradiation. RPA2 foci disappeared 20 hours post-irradiation indicating that cells in G2-phase, identified by γ -tubulin staining, have filled in the gaps.

1.13. Research objectives

The cell cycle stage-dependence of cisplatin toxicity, cell cycle arrest and DDR activation in human cells was investigated. The present study focused on the effects of cisplatin and carboplatin on pol η -deficient cells following treatment in different phases of the cell cycle.

Specific Aims:

1. To investigate whether cell cycle phase affects sensitivity and cell cycle progression in pol η -deficient and expressing human cells exposed to cisplatin and carboplatin.
2. To characterise the activation of key DNA damage response pathways following treatment of cells in different phases of the cell cycle with cisplatin and carboplatin.

Chapter 2: Materials and Methods

2.1. Cell lines

The XP30RO cell line (Volpe and Cleaver, 1995) is an SV40-transformed human fibroblast line, and was obtained from the Coriell Institute for Medical Research, New Jersey (repository number GM0317A). XP30RO cells lack pol η as a result of a 13-base pair deletion in exon 2 of the *POLH* gene. TR30-2 was derived from XP30RO cells by Dr. Seamus Coyne (DNA damage response lab, NUIG). In TR30-2 cell line pol η is expressed constitutively (Cruet-Hennequart et al., 2006).

2.2. Cell culture

Cell culture reagents were obtained from Sigma (Dorset, UK), and sterile plasticware was obtained from Sarstedt AG (Nümbrecht, Germany), unless otherwise stated. XP30RO and TR30-2 cells were grown in Minimal essential media (MEM) supplemented with 2X essential and non-essential amino acids (Gibco), 2X vitamins (Gibco), 2 mM L-glutamine, 15% uninactivated foetal bovine serum (FBS) (Biosciences) and 1% penicillin-streptomycin. All cell lines were grown as adherent cultures in 75 cm² flasks. All cell culture procedures were carried out in a class III Bio-Safety cabinet (Medical Supply Company, Dublin, Ireland). Surfaces and plasticwares were sprayed with 70% industrial methylated spirit (IMS) before carrying out any cell culture procedures in the tissue culture hood. Cells were passaged once they were 80% confluent, or the media was changed once after three days if the cells were not ready to be passaged. The cells were treated with 2X trypsin-EDTA in Hanks balanced salt solution (HBSS) for four minutes. Fresh complete culture medium was added to inactivate trypsin and the cells were centrifuged at 1,200 r.p.m. for five minutes in a Rotanta 400 centrifuge (Hettich International, Kirchleugern, Germany). The cell pellet obtained was gently resuspended in 10 ml of fresh complete medium, and mixed well. Cells were counted using a Kova[®] Glasstic[®] slide 10 combination coverslip-microscope slide (Hycor Biomedical Ltd, CA, USA). 4×10^5 cells were added to 20 ml of pre-warmed medium in a sterile 75 cm² flask and incubated in the incubator.

2.3. Cryopreservation

Cells were removed from flasks by treatment with 2X trypsin-EDTA in HBSS, (Sigma) for four minutes. Complete media was added to inactivate trypsin and the cells were then centrifuged at 1200 r.p.m. for five minutes, counted and resuspended

in freezing media. Freezing media contains culture media (without addition of amino acids, vitamin supplements or antibiotics), 20% uninactivated FBS and 10% dimethylsulfoxide (DMSO, Sigma). Cell lines were frozen down in labelled 1.5 ml cryovials (Nunc, Wiesbaden, Germany) at a concentration of $1.5\text{--}2 \times 10^6$ cells per ml. 1 ml aliquots of cells was added to each cryovials and placed in a Cryo 1°C freezing container (Nalgene[®], Rochester, NY, USA) containing 250 ml of 100% isopropanol. Cells were stored at -80° C overnight to maintain the intact cell membrane. After 48 hours later cells were transferred to a liquid nitrogen storage container (Jencons-PLS, Bedfordshire, UK).

2.4. Resuscitation

All cell lines were resuscitated quickly by thawing the cryovials in a water bath at 37° C. The contents of the cryovial were then mixed with 5 ml of pre-warmed complete cell culture media in a 15 ml sterile tube. Following centrifugation at 1000 r.p.m for 5 minutes the freezing media containing DMSO was removed. The resulting cell pellet was resuspended in 6 ml of fresh complete cell culture media, mixed well and dispensed into a 25 cm² flask. The flask was then incubated in an autoflow CO₂ water-jacketed incubator (Nuaire, Plymouth, MN, USA) at 37° C and 5% CO₂. The cell culture medium was changed the next day.

2.5. Cell synchronisation mitotic arrest

Cells were treated with the microtubule inhibitor nocodazole (0.1 µM, Sigma) dissolved in DMSO, for 16 hours. Mitotic cells were collected by shake-off. Nocodazole was removed by washing the cells twice with serum-free media. The cells were then centrifuged at 1200 r.p.m and the cell pellet was resuspended in 10 ml fresh complete culture medium. Cells were counted and 4×10^5 cells were seeded in 60 mm cell culture dishes. Cells were cultured for 6 hours to generate cells in G1-phase, and for 12 hours to generate cells in S-phase. Cells were treated with cisplatin or carboplatin as indicated in individual experiments.

2.6. Treatment with platinum-based drugs and inhibitors

Cells were counted and 4×10^5 cells were seeded in 60 mm cell culture dishes. When cells reached approximately 70% confluence, as determined using light microscopy they were treated with 1.66 μM cisplatin (cis-Diammineplatinum (II) Dichloride, Ebewe, 1mg/ml solution) or 50 μM carboplatin (cis-diammine(1,1 cyclobutanedicarboxylato) platinum). A 20 mM stock solutions of carboplatin was prepared in distilled water and stored at 4° C. The chemotherapeutic drug solutions were added directly to the cell culture medium. Control cells were treated with an equal volume of distilled water. In case of experiments with inhibitors, they were added directly along with cisplatin or carboplatin. DNA-PK inhibitor NU7441 (10 μM), ATM inhibitor KU55933 (10 μM) from KuDOS and cyclin dependent kinase (CDK) inhibitor Roscovitine (15 μM) from Sigma were used in the experiments. Cells were incubated for the period of time indicated for each experiment. Stock solutions of 10 mM of inhibitor (NU7441 and KU55933) and 25 mM of inhibitor (Roscovitine) were prepared by mixing them in DMSO. The cells were treated with these solutions and incubated at 37° C and 5% CO₂ for the period of time indicated in individual experiments. Control cells were treated with an identical amount of DMSO or dH₂O as appropriate.

2.7. XTT cell viability assay

Cell viability was determined using the XTT assay. XTT is a colorimetric assay for the non-radioactive quantification of cell proliferation and viability based on the metabolism of tetrazolium salt to a water-soluble formazan salt by viable cells. Cells were counted and 5×10^3 cells were seeded in 96-well plate in triplicate using a multichannel pipette. Control wells containing only culture medium, and untreated cells were also plated in triplicate. Following mock-treatment, or treatment with 1.66 μM cisplatin or 50 μM carboplatin for the indicated time period, medium containing the drugs was removed. Fresh complete culture medium was replaced, and the cells were incubated for an additional 4 days (96 h). To assess cell survival following drug treatment, the medium was removed and XTT reagent (XTT cell proliferation kit II, XTT, Roche) was added to the wells that consist of XTT labelling reagent and electron coupling reagent. Both reagents are thawed at 37° C in the water bath before use. The 96-well plate was replaced back in to the incubator for 4 hours. Cell viability was assessed, by measuring the absorbance at 490 nm (for 0.1 s) using a

plate reader (Victor² 1420 Multilabel Counter, Wallac, MA, USA). Optical density (OD value) from triplicate wells was averaged. The blank value (wells containing only medium) was subtracted from the values for all the other wells. Cell survival was expressed as a percentage of the survival of corresponding untreated cells using the equation:

$$(\text{OD value of treated cells} \div \text{OD value of control cells}) \times 100$$

2.8. Trypan blue assay

Following treatment of cells seeded in 60 mm dishes (Sarstedt) at different stages of the cell cycle, they were harvested by adding 2X trypsin-EDTA in HBSS for five minutes. Cells were centrifuged at 1200 r.p.m. for 5 minutes and the cell pellet was gently resuspended in 1 ml of sterile 1X PBS. 10 µl was transferred to a 1.5 ml eppendorf (Sarstedt) and 10 µl of 0.4% trypan blue solution (Sigma) was added. The contents of the tube were mixed and 8 µl was placed in a Kova[®] Glasstic[®] 10 Slide (Hycor Biomedical Ltd., Garden Grove, CA, USA). The total number of viable (transparent) and non-viable (blue) cells were counted. The percentage of non-viable cells was calculated using the equation:

$$(\text{Non-viable cell number} \div \text{total cell number}) \times 100$$

2.9. Preparation of cell extracts

60 mm culture dishes were placed on ice and the culture medium was removed. The cells were washed once with 2 ml of ice-cold 1X PBS pH 7.6. PBS was removed completely and 60 µl of cell lysis buffer (PBS pH 7.6, 1% Triton (Sigma), 0.5% deoxycholic acid (DOC, Sigma), 0.1% SDS (Bio-Rad Laboratories, CA, USA) containing protease inhibitors aprotinin (2 µg/ml, Sigma), leupeptin (1 µg/ml, Sigma), phenylmethylsulfonyl fluoride (PMSF, 1 mM, Sigma), and phosphatase inhibitors sodium fluoride (NaF, 5 mM, Sigma), sodium orthovanadate (Na₃VO₄, 1 mM, Sigma), was added. Cells were scraped from the dishes using 39 cm cell scrapers (Sigma) incubated for five minutes on ice. The lysate was scraped down by placing the dishes vertically and transferred into a 1.5 ml eppendorf tube. The tubes were vortexed at high speed for 20 seconds, incubated on ice for 15 minutes and centrifuged at 14,000 r.p.m for 15 minutes in a Sigma 1-15K centrifuge (Sigma

Laborzentrifugen, Osterode am Harz, Germany). Supernatants were transferred to another sterile labelled eppendorf and stored at -70° C until used.

2.10. Protein assay

The protein concentration of cell lysates was determined by using the DC Protein Assay (Bio-Rad Laboratories). A standard curve was prepared using Bovine Serum Albumin (BSA) as a protein standard, as outlined in Table 2.1 (below). Both the standards and the protein samples were analysed in duplicate.

BSA concentration (mg/ml)	0	0.2	0.4	0.6	0.8	1
BSA Stock Solution at 2mg/ml (µl)	0	5	10	15	20	25
Lysis Buffer (µl)	50	45	40	35	30	25

Table 2.1. DC protein assay standard preparation.

5 µl of each BSA standard, and 2 µl of cell lysate plus 3 µl of cell lysis buffer (test samples) was pipetted into individual wells, in duplicate, in a flat-bottomed 96-well plate (Sarstedt). Buffer A' was prepared by adding 20 µl of Reagent S to 1 ml of Reagent A. To each of the wells (standards and test samples) 25 µl of Buffer A' was added. Then 200 µl of Buffer B was added to all the wells. The plate was incubated on the bench at room temperature for 15 minutes and the absorbance of each well was read at 490 nm using a Victor² 1420 Multilabel Counter (Wallac, MA, USA). Using MS Excel software, a linear standard curve was plotted of the absorbance versus BSA concentration. The R² value was calculated and any curves having a R² value below 0.95 were discarded, and the assay was repeated. Using MS Excel, the slope of the line was calculated, and the equation $y = mx + c$ (where y = absorbance, m = slope of the line, x = BSA concentration and c = line intercept on the y-axis) was used to calculate the protein concentration of individual cell lysates.

2.11. Sodium dodecyl sulphate polyacrylamide gel electrophoresis (SDS-PAGE)

The Mini Protean III was used for gel electrophoresis. The running and the stacking gel were prepared as outlined in Table 2.2.

Running gel	10 mls/1mm gel (12%) (ml)	Stacking gel	2mls/gel (ml)
d.H ₂ O	3.3	d.H ₂ O	1.4
30% w/v acrylamide/bis-acrylamide	4	30% w/v acrylamide/bis-acrylamide	0.33
Tris 1.5 M, pH 8.8	2.5	Tris 1.0 M, pH 6.8	0.25
10% w/v SDS	0.1	10% w/v SDS	0.02
10% w/v APS	0.1	10% w/v APS	0.02
TEMED	0.004	TEMED	0.002

Table 2.2. SDS-PAGE preparation.

The components of the running gel were mixed well in a 50 ml falcon tube and pipetted in between the two glass plates and allowed to polymerise. The gel is overlaid with ethanol to exclude oxygen and promote polymerisation. It also prevents bubble formation and ensure a flat surface. After polymerisation the ethanol was removed. The gel surface was rinsed well, the stacking gel mixture was pipetted in between the plates and the comb of 1.0 mm width was inserted. Once the gel had polymerised the comb was removed and the wells were washed well.

For each sample prepared previously, a volume equivalent to 20 µg of protein was pipetted into small 0.5 ml PCR tubes. It was then mixed with 4X Laemmli SDS reducing buffer (62.5mM Tris-HCl pH 6.8, 20% glycerol, 2% SDS, 5% β-mercaptoethanol, 1% bromphenol blue) (Laemmli, 1970). Samples were boiled for five minutes to denature proteins, and were loaded on to the SDS-PAGE gel using Gel Saver II tips (Fisher Scientific, UK). Pre-stained broad-range protein marker of 5 µl (Fermentas) was loaded in the first well followed by samples. Empty wells were filled with 1X Laemmli SDS reducing buffer. Electrophoresis was carried out in 1X running buffer (19.2mM glycine, 2.5mM Tris, 0.01% SDS, pH 8.3) at 130V (current limit, 400 mA), for approximately 2.5-3 hours.

2.12. Western immunoblotting

Following electrophoresis, the SDS-PAGE gel was removed from the glass plates and submerged in 1X transfer buffer (19.2 mM glycine, 2.5 mM Tris, 20% methanol) thereby preventing it from drying out. Immobilon-P polyvinylidene fluoride (PVDF, Millipore, MA, USA) membrane was cut to the appropriate size and activated by

submerging in methanol, followed by dH₂O and transfer buffer for three minute each. The Mini Trans-Blot[®] Cell System from Bio-Rad was used for all western immunoblotting procedures. The transfer cassette was assembled with its black side down followed by a sponge and a stack of five; cut Whatman filter papers soaked in used transfer buffer. The gel was placed on the filter paper and the activated PVDF membrane was positioned on the gel so that it completely covers the gel. A stack of five filter papers and a sponge is placed on top of the membrane and the cassette is closed. The PVDF membrane is placed on the cathode side and the SDS-PAGE gel on the anode side of the transfer apparatus.

The transfer apparatus was placed in the running tank, with an ice pack and filled with freshly-made ice-cold 1X transfer buffer. Transfer was carried out at 100V for 45 minutes. The transfer of proteins was confirmed by the presence of the pre-stained protein markers on the membrane. To visualise proteins transferred to the membrane, in certain cases the membranes were also stained with Ponceau S (Sigma) solution for 5 minutes and rinsed three times with T-TBS (100 mM Tris, 68 mM NaCl, 0.05% Tween-20) for 5 minutes on a rocker (Stuart Scientific, Surrey, UK) at medium speed, at room temperature.

The membranes were then blocked by incubating in blocking solution (100 mM Tris, 68 mM NaCl, 0.05% Tween-20, 5% w/v non-fat powdered milk) for one hour with rocking at room temperature. The membranes were probed with primary antibody by diluting the antibody solution to the appropriate dilution (shown in the Table 2.3) in 5% blocking solution. Membranes with the primary antibody solution were placed in plastic bags, heat-sealed using a vacuum sealer and placed on the rocker overnight at 4° C.

Primary antibody	Source (Company)	Protein size (kDa)	Secondary antibody	Working dilutions of primary antibody
Anti-Pol eta (B-7)	Santa Cruz	78	Anti-mouse	1:100
Anti-Cyclin E (M-20)	Santa Cruz	53	Anti-rabbit	1:1000
Anti-Cyclin B1	Thermo Scientific	62	Anti-rabbit	1:2000
Anti-phospho Ser317 Chk1	Cell Signaling	51	Anti-rabbit	1:1000
Anti-RPA2	Oncogene	34	Anti-mouse	1:4000
Anti-phospho Ser4/Ser8 RPA2	Bethyl Laboratories	34	Anti-rabbit	1:4000
Anti-phospho-H2AX (ser139) JBW301	Upstate	15	Mouse	1:2000
Anti-actin	Sigma	42	Rabbit	1/5000

Table 2.3. Primary and secondary antibodies used in western immunoblotting.

Primary antibodies that were bound to the membrane were detected using horseradish peroxidase (HRP)-linked secondary antibodies (Jackson ImmunoResearch Laboratories, Inc., PA, USA). The appropriate secondary antibody was diluted 1/10000 in 3% milk, and the membranes were incubated in this solution for one hour at room temperature with rocking. The membranes were then washed three times in T-TBS, for seven minutes each time. HRP activity was visualised using the ECL+ Western Blotting chemiluminescent detection system (Amersham Biosciences, Buckinghamshire, UK). 2 ml of detection solution was prepared for each membrane by combining reagent A and B in the ratio 1:40. The detection solution was then pipetted onto the membrane and incubated for 5 minutes. The membranes are then transferred to a film cassette (Sigma) and taken to the dark room. Kodak[®] BioMax MR Scientific Imaging Film (Sigma) was used to detect chemiluminescence emitted by the ECL+ reaction. The imaging film was developed using a CP1000 automatic film processor (Agfa, Mortsel, Belgium) with Devalex[®] X-ray developer and Fixaplex[®] X-ray fixer (both from Champion Photochemistry, Essex, UK).

2.13. Cell cycle analysis by flow cytometry

Cells were seeded in 60 mm culture dishes for the respective timepoints. One hour prior to harvesting at individual timepoints, cells were pulse labelled with 10 μ M bromodeoxyuridine (BrdU, Becton Dickinson Immunocytometry Systems, CA,

USA). To harvest cells for flow cytometry, culture medium was discarded and the cells were washed with 2 ml of pre-warmed 1X PBS. The PBS was removed, 500 μ l of 2X trypsin-EDTA was added and cells were incubated for 5 minutes at room temperature. Trypsin was inactivated by the addition of 1.5 ml of complete cell culture medium, and the cells were transferred to a 15 ml tube. The cell pellet was collected by centrifuging the 15 ml tube at 1200 r.p.m for 5 minutes in a Rotanta 400 centrifuge. The cell pellet was resuspended in 1 ml of cold PBS, and the cells were fixed by the addition of 3 ml ice-cold 100% ethanol in a dropwise manner. Fixed cells were stored at -20° C. On the day of analysis, the cells were thawed at room temperature for 10 minutes and centrifuged at 1200 r.p.m for 10 minutes in a Rotanta 400 centrifuge. 1 ml 2N HCl/0.5% Triton X-100 was added in a dropwise manner to the cell pellet, and the cells were placed on the rocker at room temperature for 30 minutes. The cells were centrifuged at 1200 r.p.m. for 10 minutes, and HCl was neutralised by resuspending the cell pellet in 1 ml neutralising buffer (0.1 M Na₂B₄O₇·10H₂O, pH 8.5). Cells were transferred to a 1.5 ml eppendorf tube and centrifuged at 1000 r.p.m. for 10 minutes. The cells were permeabilised by resuspending the cell pellet in 1 ml PBS, 1% w/v BSA, 0.5% v/v Tween-20. 20 μ l anti-BrdU-FITC antibody (Becton Dickinson Immunocytometry Systems, CA, USA) was added to all the samples, except to the control sample. The cells were then placed on a rocker at room temperature for 30 minutes in the dark. The cells were then washed by addition of 1 ml PBS, 1% w/v BSA, 0.5% v/v Tween-20. Cells were then centrifuged at 1200 r.p.m. for 5 minutes. Cellular DNA was stained by resuspending the cell pellet in 500 μ l of propidium iodide containing RNase (PI/RNase Staining Buffer, Becton Dickinson Biosciences, NJ, USA), and incubated for 15 minutes in the dark. Analysis was done using a FACS Calibur flow cytometer (Becton Dickinson Biosciences). Data was analysed using Cell Quest™ software. Histograms were generated by plotting cell counts against PI content. BrdU profiles were generated by plotting PI content against FITC fluorescence using a scatter plot. The distribution of cells in each phase of the cell cycle was calculated using Cell Quest™ software, and is expressed as a percentage of the total number of cells analysed.

2.14. Immunofluorescence

Cells were grown on 22x 22 mm glass coverslips (BDH, Mumbai, India) placed in the 60 mm culture dishes. The coverslips were prepared by washing in dH₂O and degreasing by placing in concentrated HCl overnight. The coverslips were rinsed with distilled H₂O three times and then dried under UV light in the class III cell culture hood. Coverslips were stored in sterile petri dishes (Sigma) until required. Cells were pre-permeabilized using a hypotonic solution (20 mM HEPES (pH 8.0), 20 mM NaCl, 5 mM MgCl₂) containing inhibitors of phosphatase (1 mM ATP, 0.1 mM Na₃VO₄, 1 mM NaF and 0.5% NP40) for 15 minutes on ice. The cells were then fixed in 4% (v/v) paraformaldehyde (PFA) in PBS for 10 min. Excess PFA was removed by rinsing the coverslips twice with 1X PBS. Coverslips were then stored at 4° C in PBS. On the day of immunostaining, PBS was removed and the coverslips were washed once with PBS. Cells were then permeabilized with 0.1% (v/v) Triton X-100 (Sigma) in PBS for 10 minutes and washed once with PBS. Cells were blocked for 30 minutes using a blocking solution (1% (w/v) BSA and 0.1% (v/v) Triton X-100) at room temperature. The cells were then incubated for 1 hour with 200 µl of the primary antibody, diluted in the blocking solution.

Primary antibody	Dilution	Company
Anti-phospho Ser4/Ser8 RPA p34	1:4000	Bethyl
Anti- Phospho-H2AX (ser139)	1:1000	Upstate

Table 2.4, Dilutions of the primary antibodies used for immunofluorescence.

The coverslips were washed twice in 1ml PBS for seven minutes. Secondary antibodies were diluted in blocking solution. 200 µl of the secondary antibody was added on the coverslips and incubated in the dark for 45 minutes.

Secondary antibody	Dilution	Company
Anti-rabbit - FITC	1:1000	Jackson Immunochemicals
Anti-mouse -Cy3	1:1000	Jackson Immunochemicals

Table 2.5. Dilutions of the secondary antibodies used for immunofluorescence.

The coverslips were washed twice in 1 ml PBS for seven minutes with rocking at room temperature in the dark

Nuclear DNA was subsequently stained with DAPI (4',6-diamidino-2-phenylindole, Sigma, 100 ng/ml DAPI in dH₂O) for five minutes in the dark. Coverslips were washed twice with PBS. A final rinse with water was done to completely remove the buffer attached to the coverslips. The coverslips were then inverted and mounted on SuperFrost glass slides (BDH) using SlowFade (Invitrogen). The edges of the coverslips were fixed on the slides using nail varnish. Slides were stored at 4° C. Immunofluorescence was visualised, at 100X magnification, using an Olympus fluorescence microscope. Images were analysed using CellR imaging software (Olympus, Essex, UK). About 200 cells were counted per coverslip and the number of cells positive for nuclear foci was determined. The percentage of cells with foci was calculated using the equation:

$$(\text{Number of cells with foci} \div \text{total number of cells counted}) \times 100$$

Chapter 3: Results

Platinum-based drugs such as cisplatin and carboplatin induce DNA damage by forming adducts, and inhibit DNA replication (Wang and Lippard, 2005). Bypass of cisplatin-induced intrastrand crosslinks by specialised DNA polymerases such as DNA pol η is one way in which cells can tolerate DNA damage by platinum-based drugs. Studies have reported the effects of cisplatin-induced DNA damage on various cell types (Section 1.12) (Basu and Krishnamurthy, 2010) but only a few studies have reported the effects of cisplatin on pol η -deficient cells (Cruet-Hennequart et al., 2008, Cruet-Hennequart et al., 2009) and none reported the role played by pol η in response to cisplatin in different cell cycle stages. Hence, in this study, the cell cycle phase-dependence of cisplatin and carboplatin sensitivity, and cell cycle arrest was investigated in pol η -deficient (XP30R0) cells and pol η -expressing (TR30-2) cells. Downstream DNA damage responses were also characterised following treatment of cells in different phases of cell cycle with cisplatin and carboplatin.

3.1. Pol η expression in XP30R0 and TR30-2 cells

In the present study, two cell lines were used: XP30R0 cells which lack pol η , as a result of a 13-base pair deletion in exon 2 of the *POLH* gene which encodes pol η (Johnson et al., 1999, Masutani et al., 2000) and TR30-2 cells, which were derived from XP30R0 cells by stable transfection with the wild-type *POLH* gene. To verify the expression of pol η protein in the XP30R0 and TR30-2 cells used in this study, western blotting was performed. Pol η protein was undetectable by western blotting in XP30R0 cell extracts, and was detectable in TR30-2 cell extracts, as indicated by the presence of a band corresponding to the expected molecular size of human pol η (78 kDa) using anti-pol η antibody (Figure 3.1.)

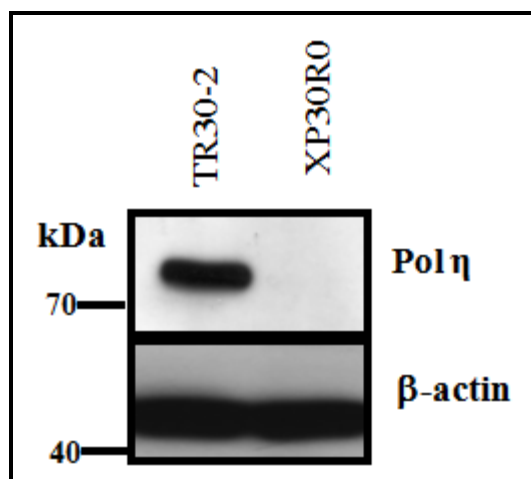


Figure 3.1. Pol η expression in XP30R0 and TR30-2 cells. XP30R0 and TR30-2 cell extracts were prepared. Proteins were analysed by SDS-PAGE and Western blotting using an anti-pol η antibody. β -actin was used as a loading control. The blot shown is representative of data obtained from three independent experiments.

3.2. Analysis of nocodazole toxicity

In the present study, nocodazole was used to generate populations of XP30R0 and TR30-2 cells enriched in the G1-, S- or M-phases. The effect of nocodazole on cell viability was first determined using the trypan blue dye-exclusion assay in order to define a dose of nocodazole, which was not highly toxic to these cell lines, and was compatible to recovery of viable cells to allow release of cells into the cell cycle. The trypan blue dye-exclusion assay differentiates between viable and non-viable cells as non-viable cells display increased cell membrane permeability, thus allowing the dye to enter. Non-viable cells therefore are stained blue, while viable cells exclude the dye and appear as unstained cells.

XP30R0 and TR30-2 cells did not differ in sensitivity to nocodazole (Figure 3.2). The percentage of non-viable XP30R0 cells following treatment with 0.1 μ M nocodazole for 16 hours was 17%, compared to 4% for control cells (Figure 3.2). 16 hours after treatment with 0.3 μ M nocodazole, 21% of XP30R0 cells were non-viable while after exposure to 0.5 μ M nocodazole, 47% of XP30R0 cells were non-viable.

The percentage of non-viable TR30-2 cells following treatment with 0.1 μ M nocodazole for 16 hours was 15%, compared to 4% of control cells (Figure 3.2). 16 hours after treatment with 0.3 μ M nocodazole, 19% of TR30-2 cells were non-viable, while after 0.5 μ M nocodazole, 45% of TR30-2 cells were non-viable (Figure 3.2).

Thus, following exposure to 0.1 μM nocodazole for 16 hours 82% of cells were viable (Figure 3.2). Following longer exposure to 0.1 μM nocodazole, for 36 hours, XP30R0 and TR30-2, cell viability was reduced by approximately 45% in both cell lines (data not shown).

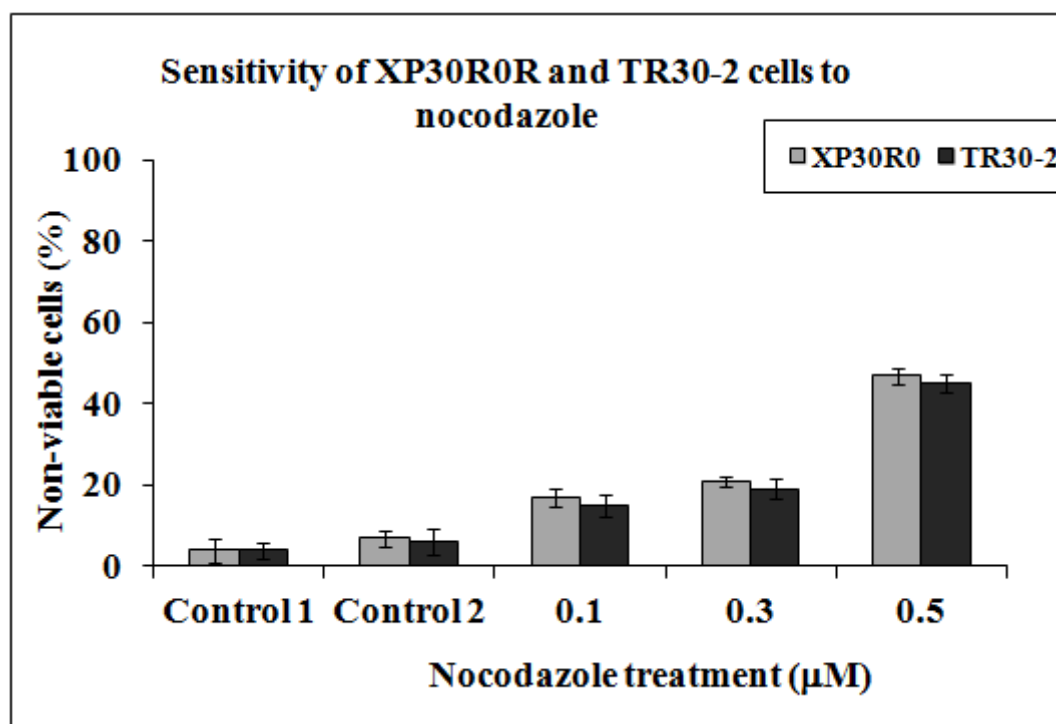


Figure 3.2. Dose-dependence of nocodazole-toxicity in XP30R0 and TR30-2 cells. Cells were either untreated (control 1), mock-treated (control 2) or treated with 0.1-0.5 μM nocodazole. The graph presents the percentage of non-viable cells in the total cell population (both adherent and in suspension) at the time of harvest. Cells were incubated with trypan blue dye and scored as either viable or non-viable. The data presented is the mean of three experiments. Error bars represent one standard deviation.

3.3. Cell synchronisation using nocodazole

Based on the cell viability data shown in figure 3.2, XP30R0 and TR30-2 were exposed to 0.1 μM nocodazole for 16 hours to synchronise cells in M-phase (Oakley et al., 2001, Oakley et al., 2003, Harper, 2005, Harper and Elledge, 2007, Stephan et al., 2009). Nocodazole arrests cells in mitosis as formation of metaphase spindles is inhibited and cells are therefore arrested in pro-metaphase (Harper, 2005). XP30R0 and TR30-2 cells were treated with 0.1 μM nocodazole for 16 hours and cell synchronisation was analysed by flow cytometry. Mitotic cells were collected by the shake-off method, as the nocodazole-treated cells rounded up and could be readily

detached from the flask. As determined by flow cytometry, this procedure generated an enriched M-phase population (91% in M-phase in XP30R0 cells; 87% in M-phase in TR30-2 cells) suitable for use in further experiments. Cells arrested in mitosis were represented by a single peak at 4N DNA content consistent with arrest in mitosis (Figure 3.3, right panels). Cells having more than 4N DNA content was observed in mitotic shake-off cells which could be due to endoreduplication.

As an alternative to nocodazole arrest, the effectiveness of thymidine block to synchronise XP30R0 and TR30-2 cells in G1/S-transition was also examined (Bostock et al., 1971). However, the use of double-thymidine block was not effective in synchronising XP30R0 cells at the G1/S border (data not shown).

Flow cytometry cannot distinguish G2- and M-phase cells containing (4N) DNA content.

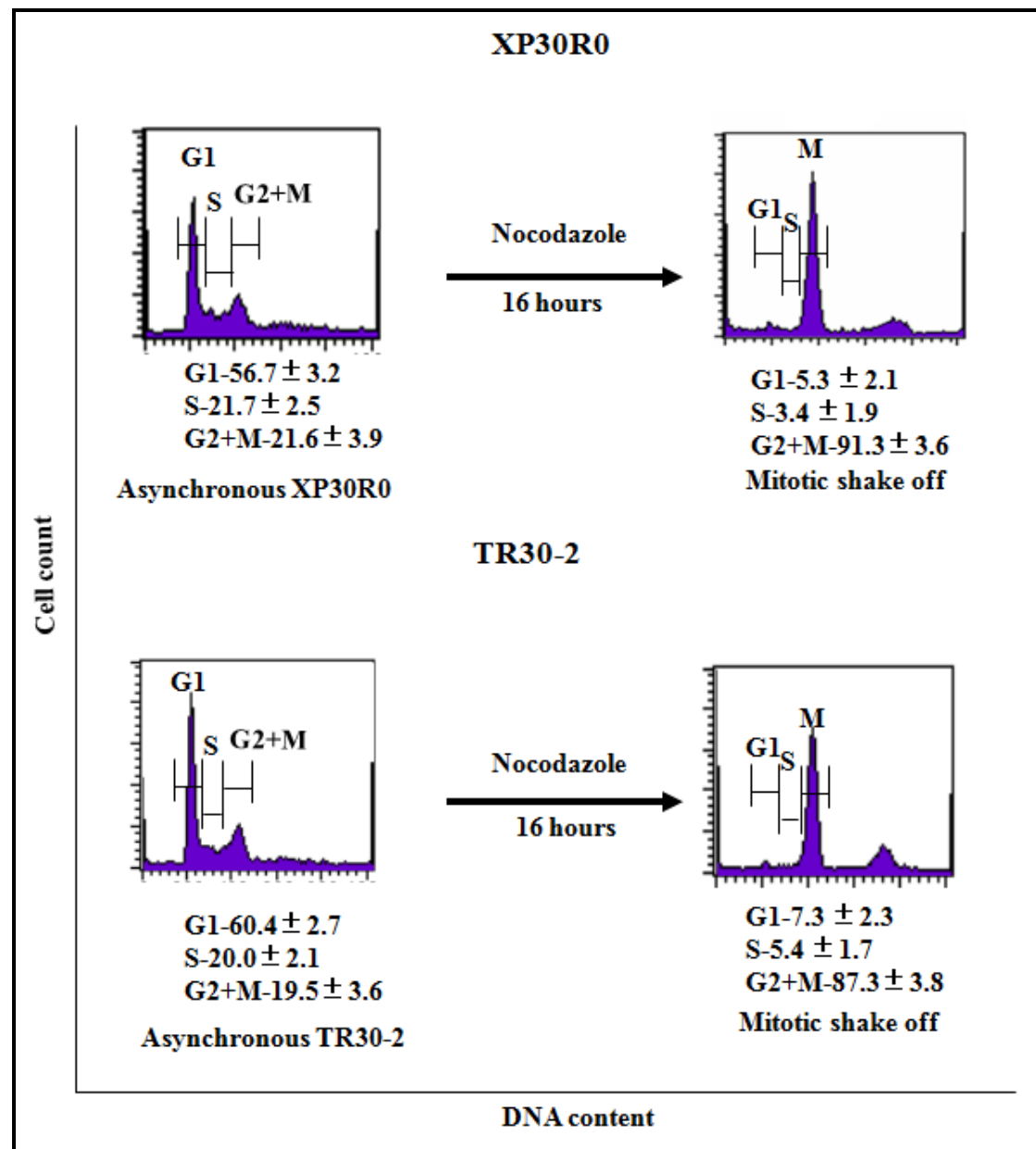


Figure 3.3. Cell synchronisation using nocodazole. (A) XP30R0 and TR30-2 cells were treated with nocodazole (0.1 μ M) for 16 hours to obtain a synchronous mitotic population. Asynchronous cells were collected by trypsinisation, and mitotic cells were collected by shake-off method from separate dishes. Cells were analysed by flow cytometry using a FACS Calibur instrument, and data was analysed using Cell QuestTM software. Ungated profiles are shown. The percentage of cells in each phase was marked and only the percentage of the cells marked by the markers 'G1', 'S' and 'G2+M' were used in calculating the final distribution. Data represents an average of three experiments \pm one standard deviation.

3.3.1. Effect of nocodazole treatment on subsequent cell cycle progression

Since the objective of the present study was to investigate the cell cycle-dependence of the effects of platinum-based drugs, nocodazole arrest and release was used to generate cell populations enriched in the G1-, S- or M-phases. To determine whether treatment with nocodazole alone affected subsequent progression through the cell cycle, the ability of mitotic cells released from nocodazole arrest to progress into the G1- and S-phases was compared to that of mitotic cells collected by shake-off from an asynchronously growing culture in the absence of nocodazole treatment. The yield of mitotic cells obtained following nocodazole treatment was 4.5-fold higher than the mitotic cells obtained from shake-off of asynchronously growing cells, without prior nocodazole treatment (Table 3.1). The doubling time of XP30R0 was approximately 24 hours, as the cells completed one full cell cycle as derived from cell numbers in figure 3.3.1A. Nocodazole was removed from the cells by washing cells in serum-free media. Cells were harvested at 6, 12, 24 and 36 hours after reseeding of the mitotic cells. Mitotic cells collected from asynchronously growing cultures, and following nocodazole treatment progressed into G1-phase and continued into the cell cycle (Figure 3.3). While the percentage of cells in S-phase, 24 hours after re-seeding, was higher in cells released from nocodazole arrest compared to mitotic cells reseeded from asynchronously growing cultures, overall, release from nocodazole arrest did not affect cell cycle progression significantly in XP30R0 cells (Figure 3.3.1A and B).

Table 3.1. Number of cells collected by shake-off with or without nocodazole treatment.

Cell type	Nocodazole	Cell number
XP30R0	+	7×10^6
	-	1.55×10^6

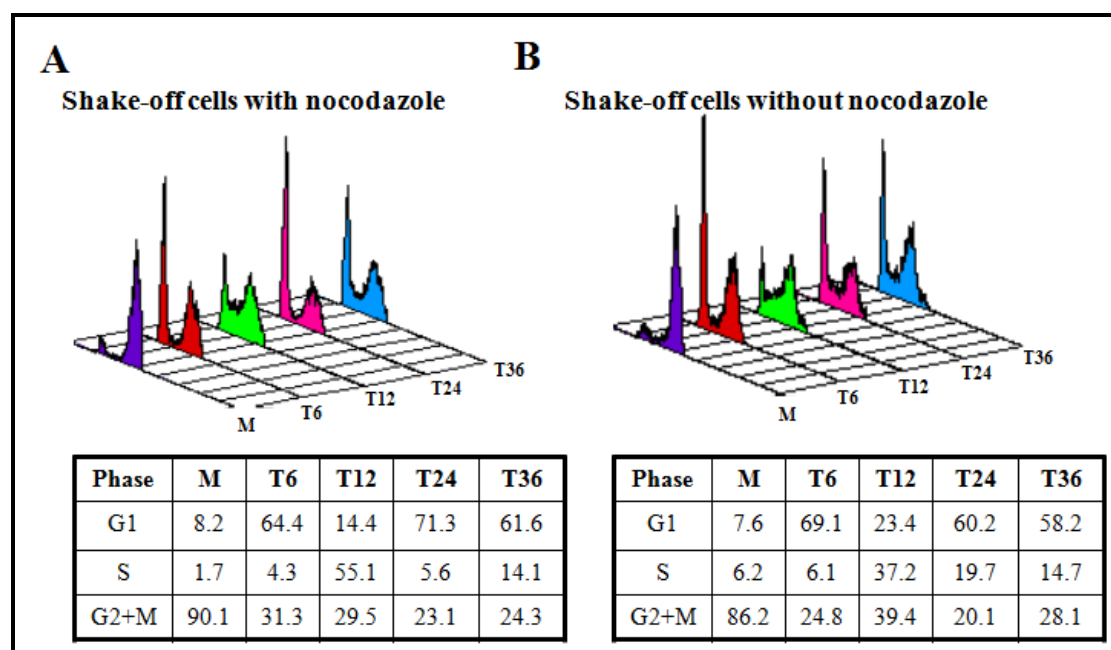


Figure 3.3.1. Time-course of release from nocodazole arrest. Cell cycle progression of mitotic cells (M) collected by mitotic shake-off, either (A) following nocodazole treatment or (B) from normal cell cultures without prior nocodazole treatment. Cells were collected, reseeded and harvested at 6, 12, 24 and 36 hours following mitotic shake-off. Cells were gated in the overlay plots. The percentage in each cell cycle phase is shown; data is an average of three experiments.

3.3.2. Identification of G1- and S-phase cells, post-nocodazole treatment and release

XP30R0 and TR30-2 cells were synchronised in mitosis using nocodazole, and collected by the shake-off method as shown in figure 3.3.2. Nocodazole was then removed by washing the mitotic cells in nocodazole-free media. The synchronous mitotic cells were reseeded in drug-free medium, and harvested at specific time points to obtain a cell population enriched in cells in either G1- or S-phase. The cells were cultured for 6, 8, 12 or 15 hours and analysed by flow cytometry (Figure 3.3.2). The representative histograms shown were not gated. Only the percentage of cells marked in each phase was calculated. Six hours after release from nocodazole arrest, the percentage of XP30R0 and TR30-2 cells in G1-phase was similar, with an average of 72% of XP30R0 cells and 76% of TR30-2 cells in this phase (Figure. 3.2.2). 12 hours after release from nocodazole, 53% of XP30R0 cells and 54% of TR30-2 cells were in S-phase, (Figure 3.3.2). It should be noted that not all cells had exited M-phase upon release from nocodazole for 6 hours (Figure 3.3.2); about 21% of cells remained in

M-phase (Figure 3.3.2). Nonetheless release of cells for 6 hours or 12 hours generated cell populations that were enriched in G1- or S-phase cells, respectively (Figure 3.3.2). These will be referred to as ‘G1-phase’ and ‘S-phase’ cells respectively in subsequent experiments.

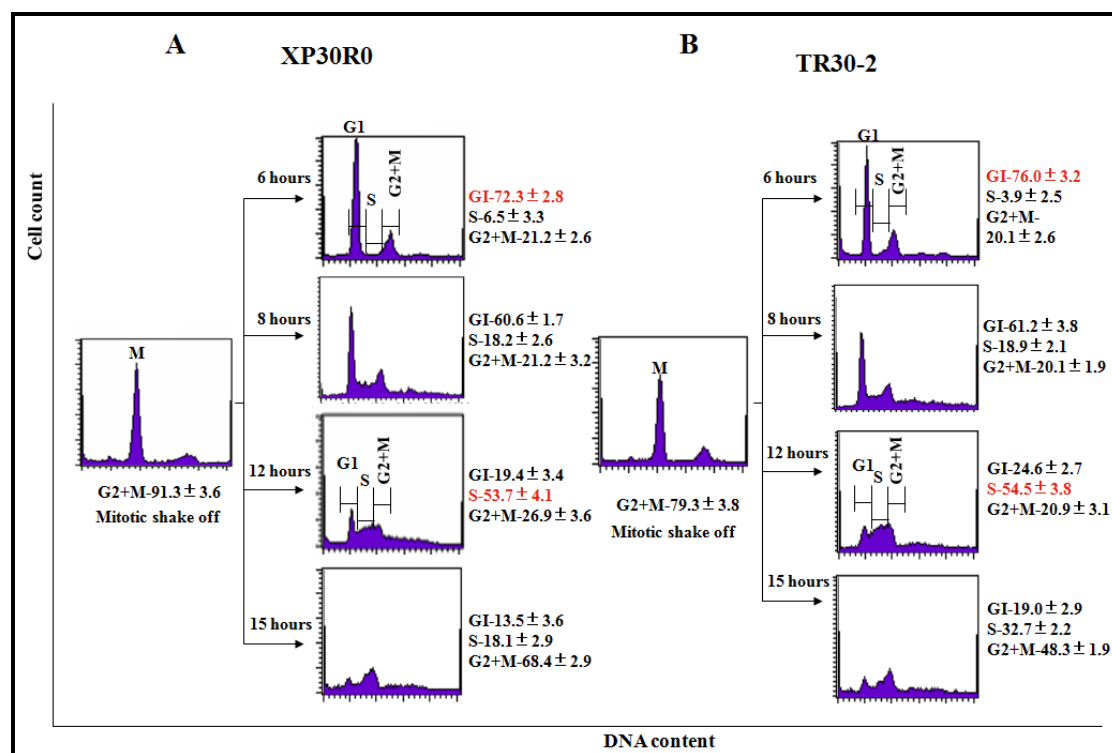


Figure 3.3.2. Cell cycle progression after release from nocodazole arrest. (A) XP30R0 cells and (B) TR30-2 cells were cultured for 24 hours. Cells were treated with nocodazole (0.1 μ M) for 16 hours. Mitotic cells were collected by the shake-off method. The drug was removed by washing the cells in serum-free media. The cells were reseeded in drug-free medium for 6, 8, 12 or 15 hours. Flow cytometry was used to analyse cell cycle distribution using a FACS calibur instrument, and data was analysed using Cell QuestTM software. The representative histograms shown were not gated. The percentage of cells marked in each phase was calculated. Data represents an average of three experiments \pm one standard deviation.

3.4. Cell cycle-dependence of cisplatin and carboplatin toxicity

To investigate the cell cycle dependence of cisplatin and carboplatin toxicity, XP30R0 and TR30-2 cells were treated with cisplatin (1.66 μ M) or carboplatin (50 μ M). These doses were previously determined to be equitoxic by the XTT cell viability assay, in experiments using asynchronously growing XP30R0 cells (Cruet-Hennequart et al., 2009). Following treatment of asynchronously growing XP30R0

cells with cisplatin for 24 hours, viability was reduced to 45% (Figure 3.4A) consistent with previous reports (Cruet-Hennequart et al., 2008, Cruet-Hennequart et al., 2009). TR30-2 cells were more resistant to cisplatin than XP30R0 cells (Figure 3.4A). Following carboplatin treatment viability of asynchronously growing XP30R0 cells reduced to 36% compared to 52% in TR30-2 cells. While under these conditions, cells were slightly more sensitive to 50 μ M carboplatin than to 1.66 μ M cisplatin but no statistically significant. The observed toxicity was in general agreement with previous studies using XP30R0 cells (Cruet-Hennequart et al., 2008, Cruet-Hennequart et al., 2009) (Figure 3.4A). There was no statistically significant difference between XP30R0 and TR30-2 cells.

To investigate the cell cycle phase-dependence of cisplatin and carboplatin toxicity the viability of cells treated with cisplatin or carboplatin in the G1-, S- or M-phases was determined. Following cisplatin treatment, viability of XP30R0 cells treated in G1-phase was 35%, compared to 51% in TR30-2 cells ($p < 0.05$; Figure 3.4). The viability of XP30R0 cells treated in S-phase was 15% compared to 43% in TR30-2 cells ($p < 0.005$; Figure 3.4). When cells were treated in M-phase, viability was 45% in XP30R0 cells compared to 55% in TR30-2 cells. Statistically significant differences were observed in the viability of XP30R0 cells and TR30-2 cells when the cells were largely in G1- or S-phase at the time of treatment with cisplatin (Figure 3.4B). Overall, XP30R0 cells treated with cisplatin in S-phase were more sensitive compared to G1- and M-phase cells. The biggest difference between XP30R0 and TR30-2 cells was observed in cells that were treated in S-phase.

Following carboplatin treatment, the viability of XP30R0 cells treated in G1-phase was 30% compared to 45% in TR30-2 cells ($p < 0.05$; Figure 3.4). The viability of XP30R0 cells treated in S-phase was 12%, compared to 34% in TR30-2 cells ($p < 0.005$; Figure 3.4). When cells were treated in M-phase viability was 35% in XP30R0 cells compared to 47% in TR30-2 cells (Figure 3.4). Again, as in the case of cisplatin treatment, there was a statistically significant difference in cell viability between XP30R0 and TR30-2 cells treated with carboplatin in the G1- or S-phase (Figure 3.4C), and XP30R0 cells treated with carboplatin in S-phase were sensitive than cells treated in the G1- and M-phases.

Overall, both XP30R0 and TR30-2 cells treated in S-phase were more sensitive to cisplatin and carboplatin compared to cells in G1- or M-phase at the time of treatment ($p < 0.005$). The S-phase sensitivity occurred in both pol η -deficient and pol η -expressing cells, but the effect was more pronounced in XP30R0 cells, indicating a role for pol η in modulating the toxic effects of cisplatin and carboplatin in S-phase cells (Figure 3.4D and E).

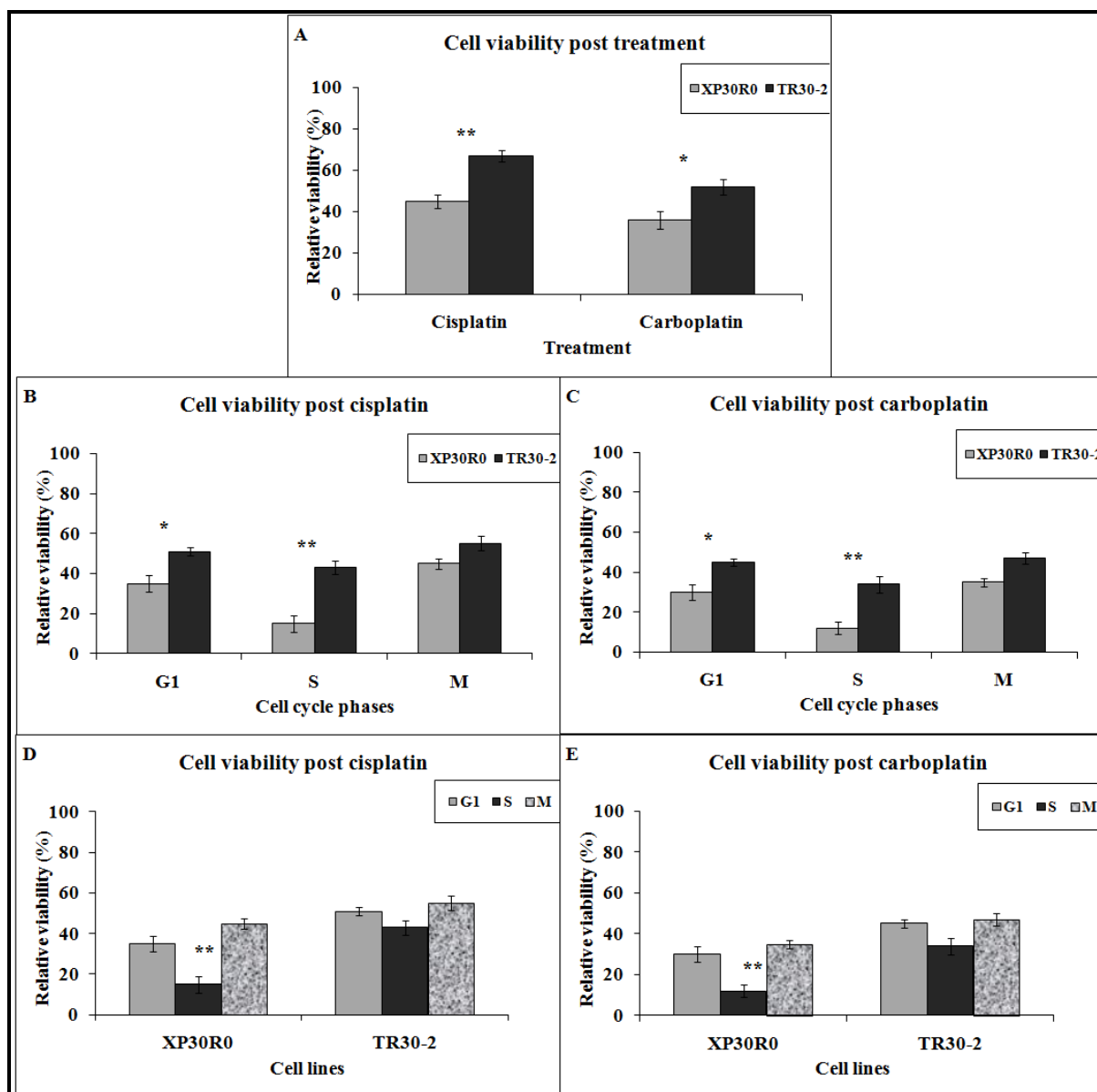


Figure 3.4. Analysis of cell viability following treatment of cells at different phases of the cell cycle with either cisplatin or carboplatin. (A) Asynchronous populations of XP30R0 and TR30-2 cells were treated with cisplatin (1.66 μ M) or carboplatin (50 μ M) for 24 hours. The drugs were removed, and 5×10^3 cells were reseeded in 96-well plates and incubated for 4 days. Cell viability was determined using the XTT assay. B and D, viability of XP30R0 and TR30-2 cells in the G1-, S- or M-phase of the cell cycle treated with cisplatin for 24 hours. C and E, viability of XP30R0 and TR30-2 cells in the G1-, S- or M-phase of the cell cycle treated with carboplatin for 24 hours. Each data point represents a mean of three experiments, and error bars represent one standard deviation. Significant differences in cell viability between XP30R0 and TR30-2 cells treated at the G1-, S- and M-phase of the cell cycle were determined using Students t-test and Anova, and are shown by * ($p < 0.05$) and ** ($p < 0.005$).

Summary

XP30R0 cells were more sensitive to cisplatin and carboplatin treatment than TR30-2 cells, and XP30R0 cells in S-phase at the time of treatment were more sensitive to cisplatin and carboplatin compared to cells in G1- or M-phase. The enhanced sensitivity of S-phase cells was stronger in pol η -deficient XP30RO cells.

3.5. Characterisation of the effects of cisplatin and carboplatin on cell cycle progression and DNA damage responses in G1-phase cells

As outlined above, to obtain cells enriched in G1-phase cells, following nocodazole arrest, mitotic cells were collected by shake-off, washed, reseeded and harvested 6 hours later. The experiments described in this section were performed on XP30R0 and TR30-2 cells treated with cisplatin and carboplatin when the cells were in G1-phase.

3.5.1. Effect of cisplatin and carboplatin on cell cycle progression in G1-phase cells lacking or expressing DNA pol η

XP30R0 and TR30-2 cells in G1-phase were treated with cisplatin or carboplatin to investigate the effect on cell cycle progression after treating cells in G1-phase. XP30R0 and TR30-2 cells were synchronised using nocodazole as described in Section 3.3.2. Mitotic cells collected through the shake-off method were reseeded. After 6 hours, G1-phase cells were treated with cisplatin (1.66 μ M) or carboplatin (50 μ M), and harvested after 12, 24 and 36 hours. Cell cycle progression was analysed using flow cytometry, as shown in figure 3.5.1A. Western blot analysis showed the absence of pol η in XP30R0 cells, and expression of pol η in TR30-2, up to 36 hours post-treatment (Figure 3.5.1B). The percentage of cells in each cell cycle phase was determined using Cell QuestTM and is shown graphically in figure 3.5.2A (cisplatin-treated cells) and figure 3.5.2B (carboplatin-treated cells). Both G2- and M-phase cells were included in the population of cells with 4N DNA content. The sub G1 population was gated and only the ungated cell population was used for calculating the percentage of cells in each phase of the cell cycle.

The major effects on cell cycle progression when XP30R0 cells in G1-phase were treated with cisplatin were (i) an increased percentage of cells in G1-phase 12 hours after treatment, compared to untreated cells. This is consistent with a delay in exiting G1-phase (Figure 3.5.1.1A, panel 1), and (ii) delayed progression through S-phase for up to 36 hours after exposure, shown by a statistically significant increase in the percentage of cells remaining in S-phase at 24 and 36 hours post-treatment (Figure 3.5.1.1A, panel 3). Consistent with arrest of cell cycle progression, and failure of cells

to complete the cell cycle and re-enter G1-phase, the percentage of cells in G1-phase was reduced at later times (24 and 36 hours) after cisplatin treatment (Figure 3.5.1.1A, panel 1). The effect of cisplatin on cell cycle progression in G1-phase TR30-2 cells that express pol η was broadly similar to that of pol η -deficient cells, in that at later times (24 and 36 hours) post-treatment, the percentage of cells in S-phase was increased compared to controls (Figure 3.5.1.1A, panel 3) consistent with cell arrest in S-phase. However, there was no statistically significant difference in the percentage of cells in G1-phase 12 hours post cisplatin in TR30-2 cells, unlike the case in XP30R0 cells.

The effect of carboplatin on G1-phase XP30R0 cells was generally comparable to that of cisplatin, in that exit from G1-phase was delayed, evidenced by an increased percentage of cells in G1-phase at 12 hours post-treatment (Figure 3.5.1.1B, panel 1), and arrest of cells in S-phase, shown by a significant increase in the percentage of cells remaining in S-phase. Thus, compared to untreated cells, 24 hours after cisplatin treatment, there was an 8-fold increase in the percentage of cells in S-phase and at 36 hours there was a 2.6-fold increase (Figure 3.5.1.1B, panel 3). In the case of carboplatin treatment, there was a difference in the response of XP30R0 and TR30-2 cells, in that there was no difference in the percentage in S-phase at 12 hours in TR30-2 cells (Figure 3.5.1.1B, panel 4), while a statistically significant difference was observed in XP30R0 cells (Figure 3.5.1.1B, panel 3).

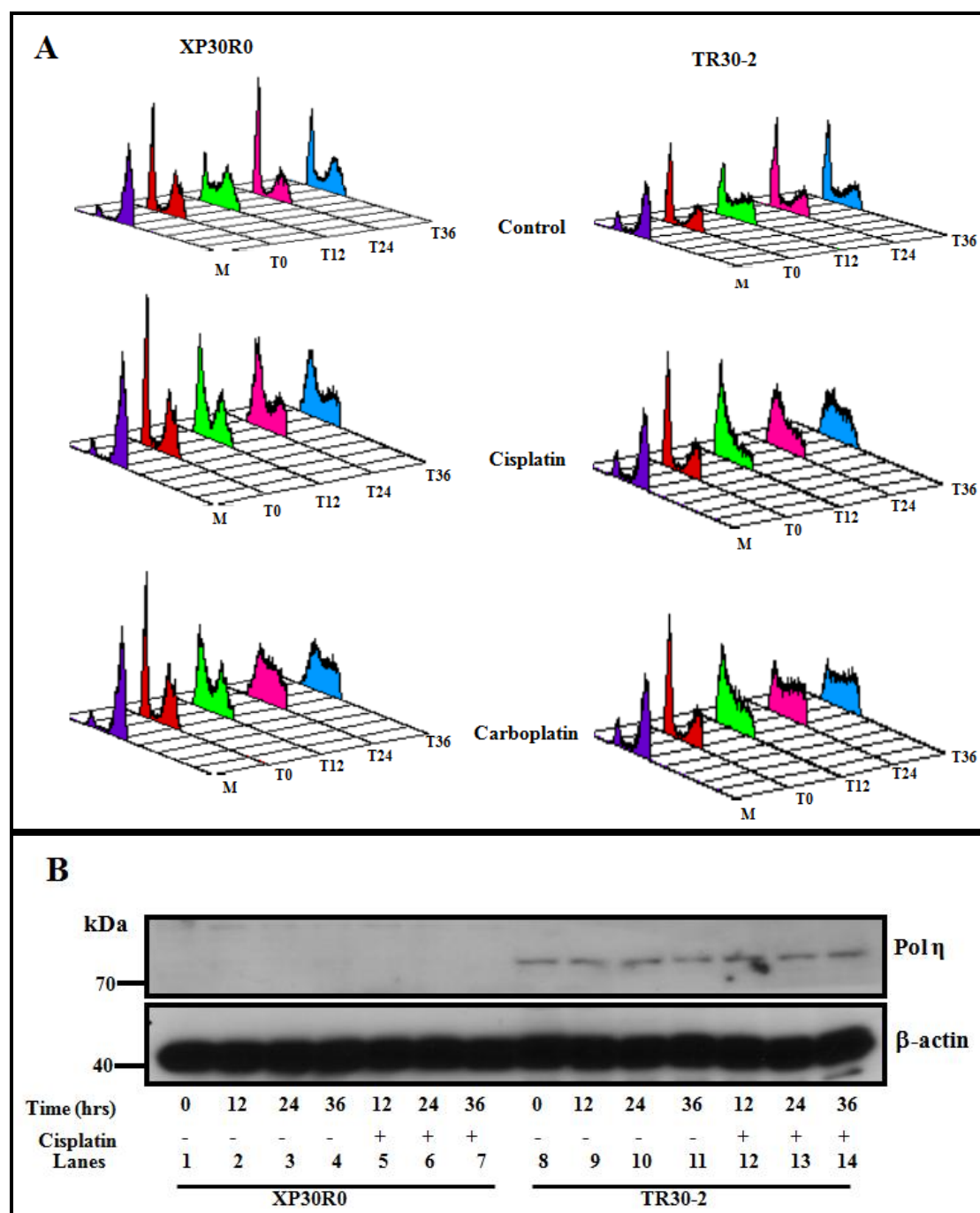
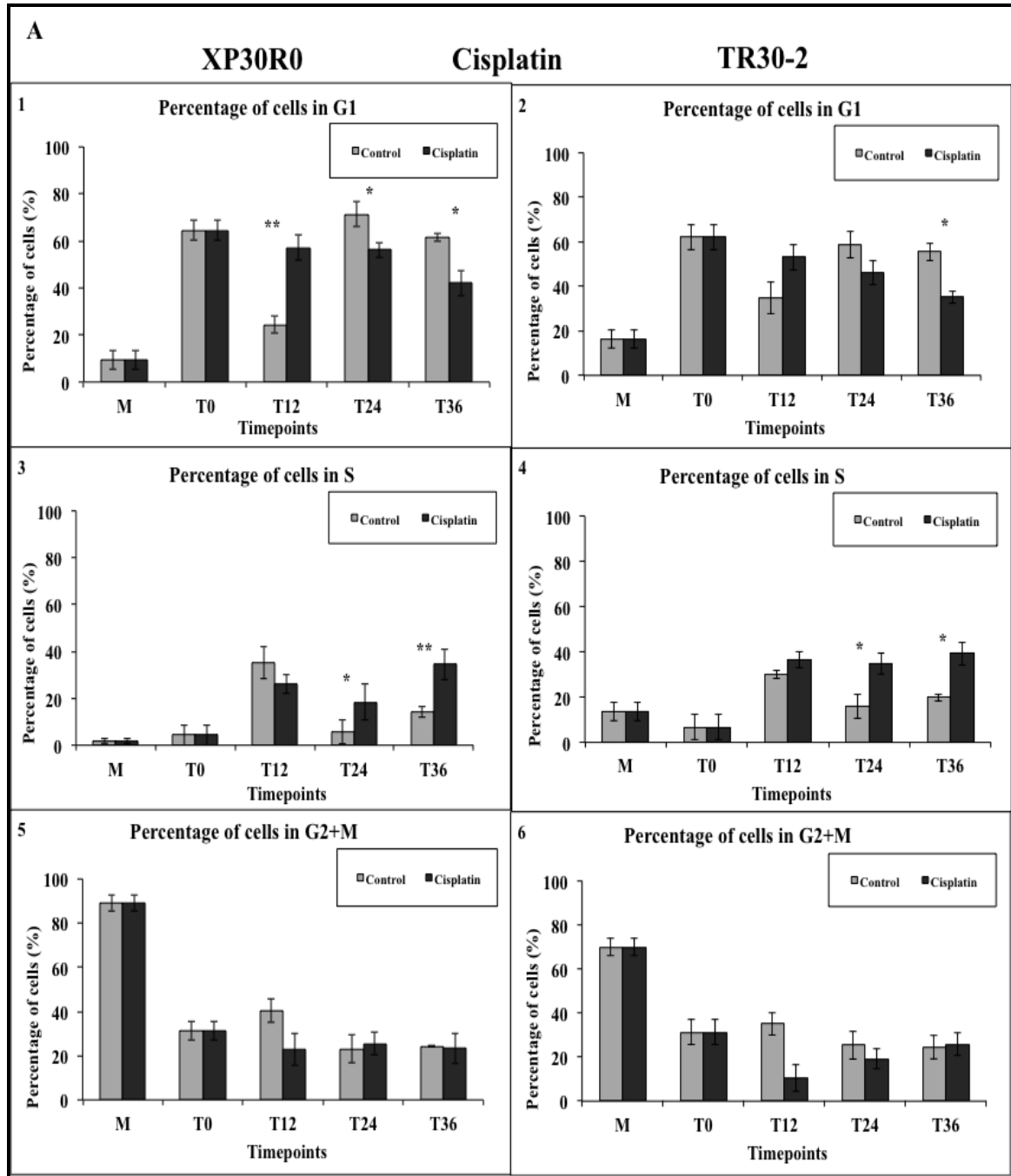


Figure 3.5.1. Cell cycle distribution of XP30R0 and TR30-2 cells in G1-phase treated with cisplatin or carboplatin. (A) XP30R0 and TR30-2 cells in G1-phase were treated with cisplatin (1.66 μ M) or carboplatin (50 μ M). Cells were harvested at 0 (G1-phase cells), 12, 24 and 36 hours post-treatment. The cells were stained with propidium iodide and analysed by flow cytometry. The histogram profiles show the distribution of cells in different phases of the cell cycle, including mitotic shake-off cells (M). (B) Western blot analysis of pol η expression in XP30R0 and TR30-2 cells, without or with cisplatin treatment. Actin was used as a loading control.



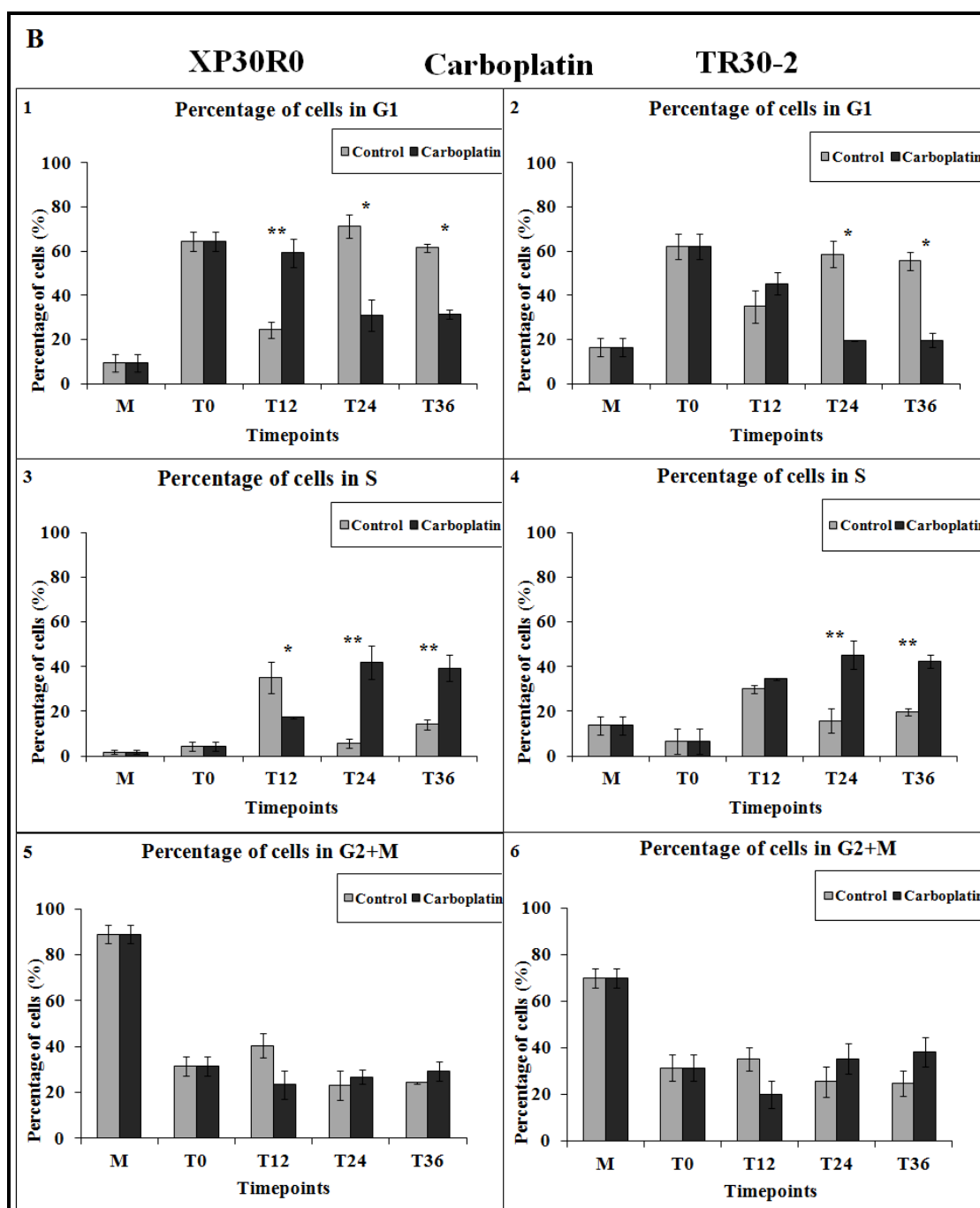


Figure 3.5.1.1. Bar graphs showing percentage of XP30R0 and TR30-2 cells in each cell cycle phase, following treatment of G1-phase cells with cisplatin or carboplatin. Bar graphs shows the percentage of XP30R0 and TR30-2 cells in each phase of the cell cycle, in (A) control (untreated), and cisplatin-treated cells, and in (B) control and carboplatin-treated cells. Each data point represents a mean of three experiments; error bars represent one standard deviation. Statistically significant differences in the percentage of cells in G1- and S-phase XP30R0 and TR30-2 cells between control and post-cisplatin or carboplatin treatment, were determined using Student t-test, and are shown by * ($p < 0.05$) and ** ($p < 0.005$).

Summary

Following treatment of G1-phase XP30R0 and TR30-2 cells with cisplatin and carboplatin, the strongest effect observed was prolonged arrest in S-phase, for up to 36 hours post-treatment. When cisplatin-treated G1-phase XP30R0 cells were compared to TR30-2 cells, the percentage of cells in G1-phase was slightly higher at 12 hours post-cisplatin and -carboplatin treatments in XP30R0 cells.

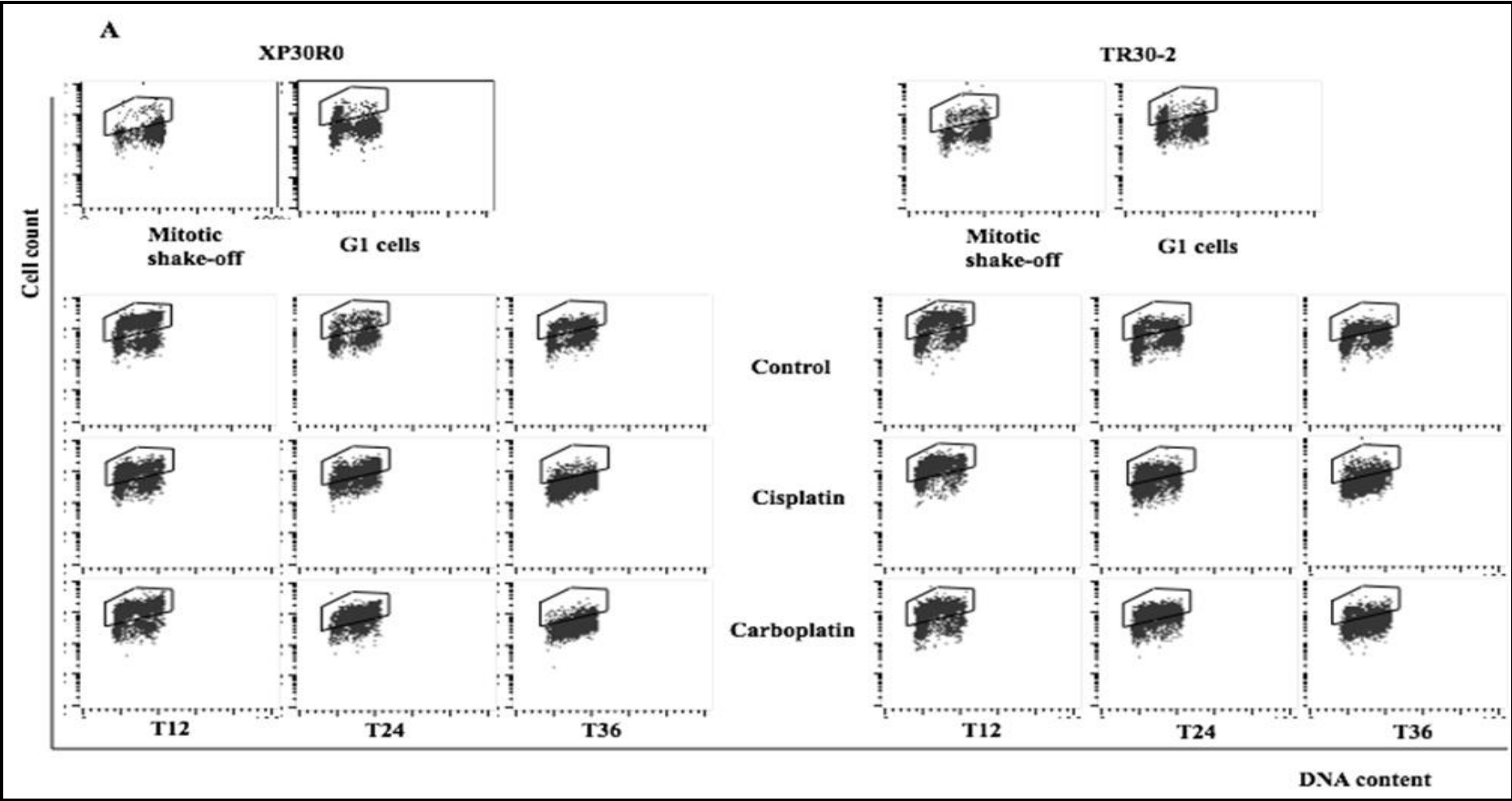
3.5.2. BrdU incorporation after cisplatin and carboplatin treatment of G1-phase cells lacking or expressing DNA pol η

BrdU is a thymidine analogue that can be incorporated into newly synthesised DNA instead of thymidine during replication in S-phase (Hyatt and Beebe, 1992). Anti-BrdU-specific antibodies are used to detect BrdU incorporation in cells that are actively replicating DNA (Hyatt and Beebe, 1992). To investigate the effect of treating G1-phase cells with cisplatin or carboplatin on DNA replication, XP30R0 and TR30-2 cells were treated with cisplatin or carboplatin and harvested after 0 hours ('S-phase cells'), and after 12, 24 and 36 hours. Cells were pulse-labelled with BrdU one hour prior to harvesting at the respective time points. BrdU incorporation was analysed using flow cytometry (Figure 3.5.2A).

In untreated XP30R0 cells, there was an increase in the percentage of BrdU-positive cells from 10% to 35%, 12 hours after release from nocodazole arrest (Figure 3.5.2B, panel 1). This is consistent with entry of cells into S-phase, as shown above by propidium iodide staining and FACS analysis (Figure 3.5.1A and 3.5.1.1). Consistent with progress through S-phase, 24 hours after G1-phase, the percentage of BrdU-positive control cells decreased (Figure 3.5.2B, panel 1 and 3). Treatment with cisplatin or carboplatin did not change the percentage of BrdU-positive cells 12 hours post-treatment, although the distribution of labelled cells was shifted towards early S-phase cells (Figure 3.5.2B, panel 1 and 3). The major effects of cisplatin and carboplatin on BrdU incorporation in XP30R0 cells was that BrdU incorporation was sustained up to 24 hours following drug treatment, while at this time, control cells had exited S-phase (Figure 3.5.2B, panel 1 and 3). This is consistent with S-phase arrest, as shown by an increased percentage of cells in S-phase 24 hours after treatment

(Figure 3.5.2B, panel 1 and 3). By 36 hours, control cells had returned to S-phase, reflected by an increase in the percentage of BrdU-positive cells, while in drug-treated cells, the percentage of BrdU-positive cells was greatly reduced, reflecting continued arrest of cells in S-phase, associated with inhibition of ongoing DNA replication (Figure 3.5.2B, panel 1 and 3).

In TR30-2 cells that express pol η , the pattern of BrdU incorporation was broadly similar. Control cells showed an increased in the percentage of BrdU cells at 12 hours (Figure 3.5.2B, panel 2 and 4), consistent with the majority of cells being in S-phase (Figure 3.5.2B, panel 2 and 4). However, following cisplatin and carboplatin treatment, the percentage of BrdU-positive cells increased at 24 hours relative to untreated cells, consistent with S-phase arrest in these cells (Figure 3.5.2B, panel 2 and 4). At 36 hours post-treatment, the difference between the percentage of BrdU-positive cells between control and cisplatin- or carboplatin-treated cells was less pronounced in TR30-2 than in XP30R0 cells (Figure 3.5.2B, panel 2 and 4). This may reflect ongoing DNA replication at late times post-exposure in pol η -expressing cells; however the basis of this difference requires further investigation.



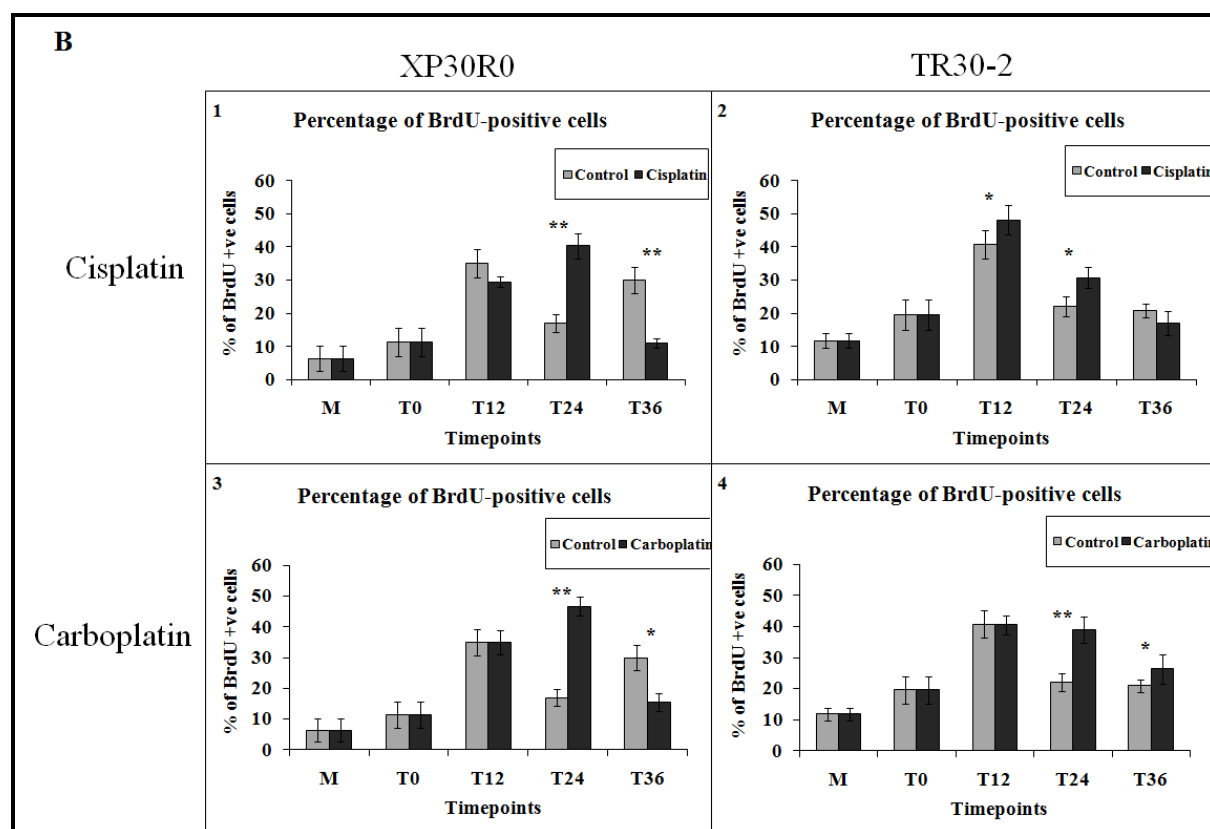


Figure 3.5.2. BrdU incorporation in XP30R0 and TR30-2 cells treated with cisplatin or carboplatin in G1-phase. (A) XP30R0 and TR30-2 cells were treated with cisplatin (1.66 μ M) or carboplatin (50 μ M) in G1-phase, and harvested at 12, 24 and 36 hours post-treatment. Cells were pulse-labelled with BrdU 1 hour prior to harvesting at the respective time-points. The cells were stained with propidium iodide and with FITC-labelled anti-BrdU antibody, and analysed by flow cytometry. Dual-labelling plots of BrdU-positive staining versus propidium iodide staining are shown. (B) Bar graphs show the percentage of BrdU-positive cells in control (untreated), and cisplatin- or carboplatin-treated XP30R0 and TR30-2 cells. Each data point represents a mean of three experiments; error bars represent one standard deviation. Significant differences in the percentage of BrdU-positive XP30R0 and TR30-2 cells post-cisplatin-or carboplatin treatment compared to control cells, determined using Student t-test, are shown by * ($p < 0.05$) ** ($p < 0.005$).

Summary

Following treatment with cisplatin or carboplatin in G1-phase, BrdU-positive XP30R0 and TR30-2 cells accumulated up to 24 hours post-treatment, when untreated cells were no longer strongly labelled. The percentage of BrdU-positive pol η -deficient XP30R0 cells was increased compared to the percentage of TR30-2 cells, consistent with a role for pol η in S-phase progression.

3.5.3. Expression of cyclin B and cyclin E after treatment of G1-phase XP30R0 and TR30-2 cells with cisplatin

To further characterise the effect of cisplatin on cell cycle progression, G1-phase XP30R0 and TR30-2 cells were treated with cisplatin (1.66 μ M), and the levels of cyclin B and cyclin E were analysed by western blotting. Cyclin B and cyclin E play an important role in G2/M (Hyatt and Beebe, 1992) and G1/S (Sheaff et al., 1997) transitions, respectively. Cell extracts were prepared 12, 24 and 36 hours post-treatment, and the levels of cyclins B and E were analysed by SDS-PAGE and Western blotting. In the present study, only cyclin B and cyclin E expression was characterised (Cruet-Hennequart et al., 2009).

The levels of cyclin B and cyclin E varied between control XP30R0 and TR30-2 cells and cisplatin-treated cells, as determined using densitometric analysis of western blots. In both untreated XP30R0 cells and TR30-2 cells, cyclin E and cyclin B expression increased at 12 hours as cells progressed through S-phase and into G2/M (Figure 3.5.3 A and B). However, in cisplatin-treated G1-phase XP30R0 and TR30-2 cells, expression of both cyclin E and cyclin B was lower at 12 hours compared to control cells, consistent with delayed cell cycle progression (Figure 3.5.3 A and B). The peak of cyclin B expression in XP30R0 cells following cisplatin treatment was at 36 hours (Figure 3.5.3B, panel 1) while in the case of TR30-2 cells, expression was similar at 24 and 36 hours post-treatment (Figure 3.5.3B, panel 2).

Following cisplatin treatment, cyclin E expression in XP30R0 cells was highest at 24 and 36 hours post-treatment (Figure 3.5.3B, panel 3), while in the case of TR30-2 cells, the highest-level occurred at 36 hours (Figure 3.5.3B, panel 4). Pol η -dependence was observed in cisplatin-treated TR30-2 cells where cyclin B expression peaked at 24 hours (Figure 3.5.3B, panel 2), while in XP30R0 cells at 36 hours (Figure 3.5.3B, panel 1). In cisplatin-treated TR30-2 cells, cyclin E expression was highest at 36 hours (Figure 3.5.3B, panel 4), while in XP30R0 this occurred at 24 and 36 hours (Figure 3.5.3B, panel 3).

Overall, the major effect of cisplatin on cyclin B and cyclin E levels was to delay the timing of peak expression compared to untreated cells, in particular in pol η -deficient XP30RO cells (Cruet-Hennequart et al., 2009). This is consistent with delayed cell cycle progression as shown by flow cytometry in the previous section.

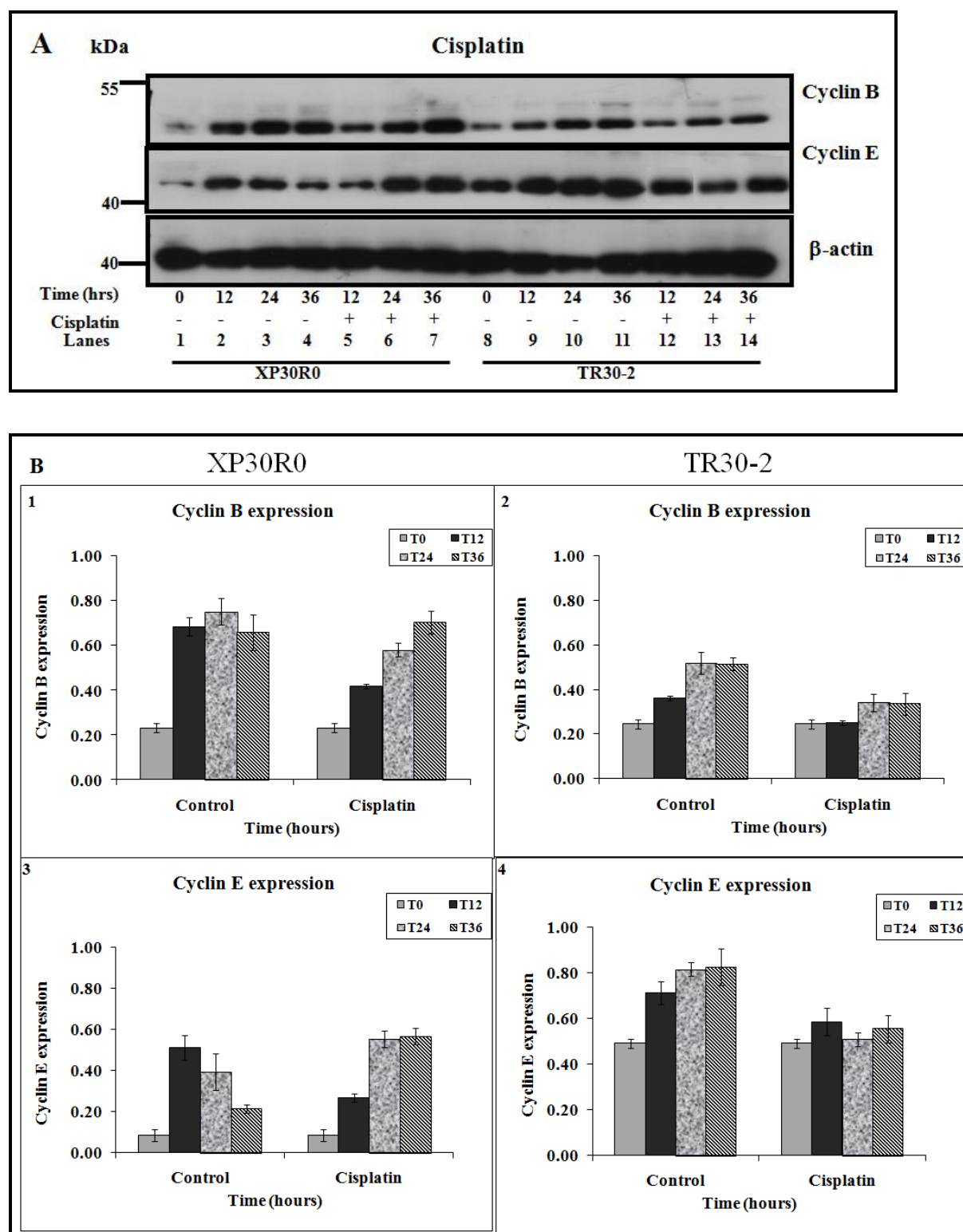


Figure 3.5.3. Effect of cisplatin treatment on cyclin B and cyclin E expression. (A) G1-phase XP30R0 and TR30-2 cells were treated with cisplatin (1.66 μ M) and harvested after 12, 24 and 36 hours. Cell extracts were analysed by SDS-PAGE and western blotting. Panels 1, 2 and 3 show western blots of cyclin B, cyclin E and actin respectively. Western blots are representative of three experiments. (B) Graph, calculated using densitometry analysis, represents expression of cyclin B in XP30R0 and TR30-2 cells treated with cisplatin (panel 1 and 2), and expression of cyclin E in XP30R0 and TR30-2 cells treated with cisplatin (panel 3 and 4). Cyclin band

intensities were normalised to the respective actin levels in the sample. The values are an average of data from three experiments, and error bars represent one standard deviation. There was no statistical significance observed between control and cisplatin-treated cells.

3.5.4. Expression of cyclin B and cyclin E after treatment of G1-phase XP30R0 and TR30-2 cells with carboplatin

XP30R0 and TR30-2 cells were treated with carboplatin (50 μ M) and the expression of cyclins B and E was analysed. As was the case following cisplatin treatment, expression of cyclins B and E varied between control cells and carboplatin-treated cells in both XP30R0 and TR30-2 cells (Figure 3.10A).

In both control XP30R0 and TR30-2 cells, cyclin E and cyclin B expression increased at 12 hours as the cells progressed through S-phase and into G2/M (Figure 3.5.4 A and B). However, following treatment of G1-phase XP30R0 and TR30-2 cells with carboplatin, cyclin E and cyclin B expression was lower at 12 hours compared to control cells, consistent with delayed cell cycle progression (Figure 3.5.4A and B). In XP30R0 cells following carboplatin treatment, cyclin B expression peaked at 24 and 36 hours (Figure 3.5.4B, panel 1), while in TR30-2 cells the expression peaked at 24 hours but was reduced at 36 hours (Figure 3.5.4B, panel 2).

In both XP30R0 and TR30-2 cells following carboplatin treatment, cyclin E expression peaked at 36 hours (Figure 3.5.4B, panel 3 and 4). However, the level of cyclin E was considerably higher at the time of treatment (T0) in TR30-2 cells compared to XP30RO cells (Figure. 3.5.4B). Overall, as in the case of cisplatin treatment, following treatment of G1-phase cells with carboplatin treatment, the peak of expression of cyclins E and B was delayed, consistent with cell cycle arrest, and this effect was more pronounced in pol η -deficient cells.

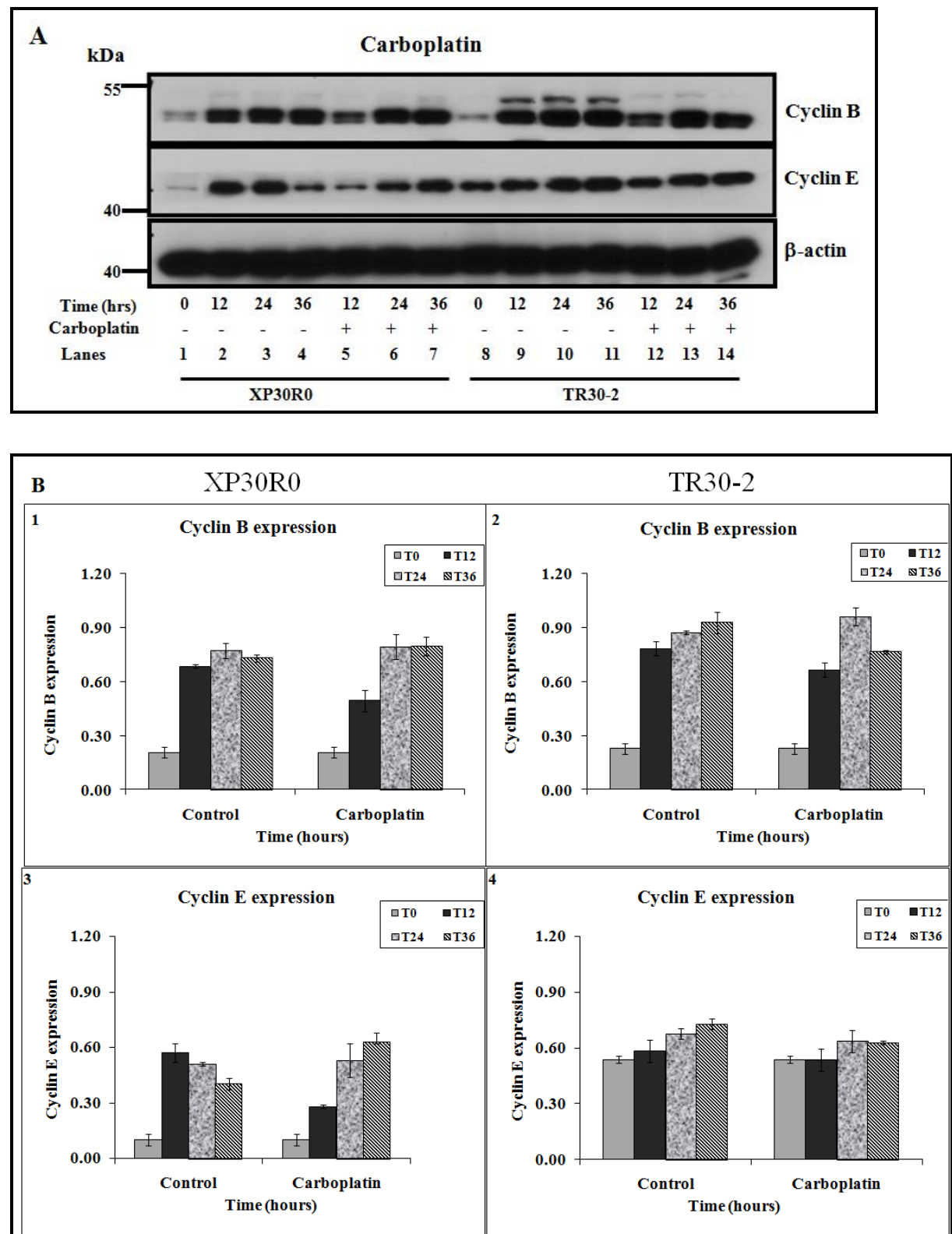


Figure 3.5.4. Effect of carboplatin treatment on cyclin B and cyclin E levels. (A) G1-phase XP30R0 and TR30-2 cells were treated with carboplatin (50 μ M) and harvested at 12, 24 and 36 hours. Cell extracts were prepared and analysed by SDS-PAGE and Western blotting. Panels 1, 2 and 3 show Western blots of cyclin B, cyclin E and actin respectively. Western blots are representative of three experiments. (B) Graph, calculated using densitometry analysis, represents expression of cyclin B in XP30R0 and TR30-2 cells treated with carboplatin (panel 1 and 2), and expression of

cyclin E in XP30R0 and TR30-2 treated with carboplatin (panel 3 and 4). Cyclin band intensities were normalised to the respective actin levels in the sample. The values are an average of data from three experiments, and error bars represent one standard deviation. There was no statistical significance observed between control and carboplatin-treated cells.

3.6. Activation of DNA damage responses

3.6.1. H2AX phosphorylation in cisplatin- and carboplatin-treated G1-phase XP30R0 cells

As shown above, cisplatin and carboplatin cause replication arrest, which can lead to replication fork collapse, thereby generating DNA strand breaks (Burma et al., 2001). In response to DNA strand breaks, histone H2AX is phosphorylated by ATM at serine 139, generating γ H2AX (Kobayashi et al., 2009). To investigate cisplatin- or carboplatin-induced H2AX phosphorylation, pol η -deficient XP30R0 cells in G1-phase were treated with cisplatin or carboplatin, and harvested after 12, 18, 24 and 36 hours. Cell extracts were prepared and analysed by SDS-PAGE and Western blotting. In control XP30R0 cells (Figure 3.6.1A and B, panel 1, lanes 1-5) no phosphorylation of H2AX on serine 139 was detected. In cisplatin-treated cells, phosphorylation of H2AX occurred at 12 hours and the protein remained phosphorylated up to 36 hours post-treatment (Figure 3.6.1A, panel 1, lanes 6-9). In the case of carboplatin treatment, phosphorylation of H2AX on serine 139 was also detected at 12 hours, increased at 18 hours, and the protein remained phosphorylated for up to 36 hours (Figure 3.6.1B, panel 1, lanes 6-9). H2AX phosphorylation was only detected only in pol η -deficient XP30R0 cells.

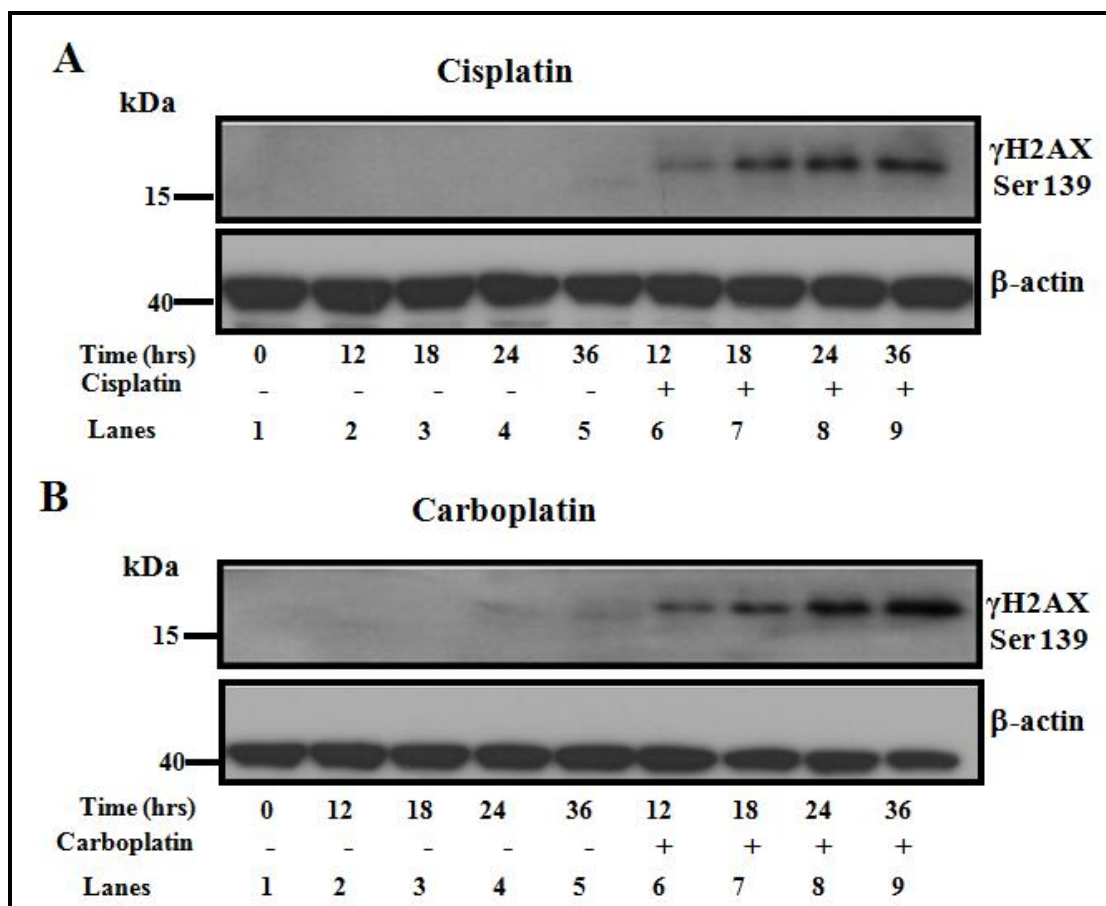


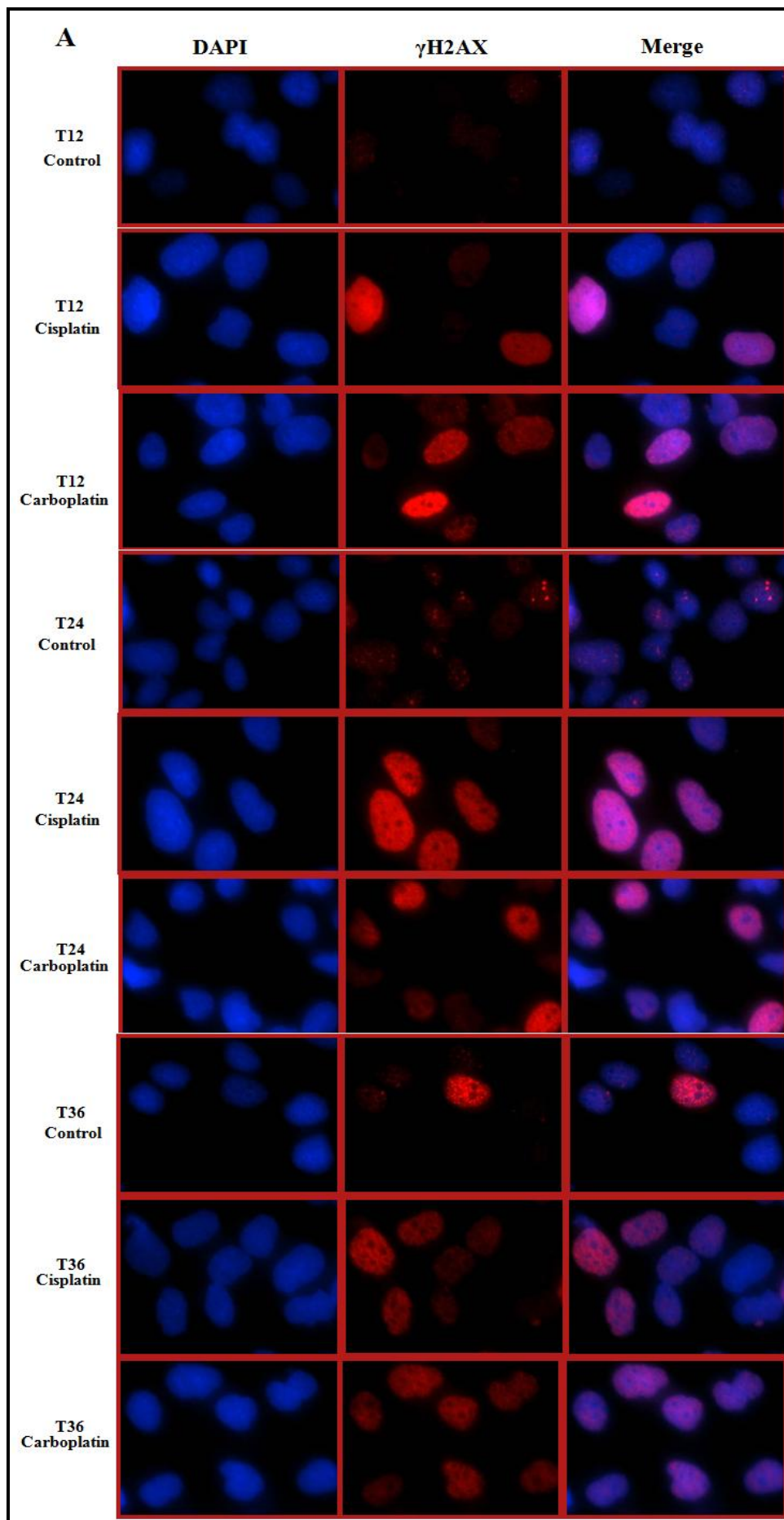
Fig 3.6.1. H2AX phosphorylation in cisplatin and carboplatin-treated G1-phase XP30R0 cells. G1-phase XP30R0 cells were treated with (A) cisplatin (1.66 μ M) or (B) carboplatin (50 μ M) and harvested at 12, 18, 24 and 36 hours. Cell extracts were prepared and analysed by SDS-PAGE and Western blotting. The upper panel in A and B show H2AX phosphorylated at serine 139, detected using an anti- γ H2AX antibody. Actin was used as a loading control. Western blots are representative of three independent experiments.

3.6.1.1 Nuclear staining for γ H2AX in cisplatin- and carboplatin-treated G1-phase XP30R0 cells.

To further investigate cisplatin- and carboplatin-induced H2AX phosphorylation associated with cell cycle arrest, immunofluorescence staining for γ H2AX was carried following treatment of G1-phase XP30R0 cells with cisplatin (1.66 μ M) or carboplatin (50 μ M). As shown by Western blotting, there was strong induction of H2AX phosphorylation in both cisplatin- and carboplatin-treated cells up to 36 hours post-treatment (Figure 3.6.1A and B). Consistent with this, in control cells, at 12 hours post mock-treatment, little γ H2AX staining was detectable by

immunofluorescence, indicating that release from nocodazole does not generate significant levels of strand breaks. 24 and 36 hours post mock-treatment, 8% and 3% of cells were γ H2AX-positive, respectively (Figure 3.6.1.1A and B, panel 1 and 2). In the case of cisplatin-and carboplatin-treated cells, 25% of the total cells counted were stained positively for γ H2AX 12 hours post-treatment ($p < 0.0005$ versus control), 35% were γ H2AX-positive 24 hours post-treatment ($p < 0.0005$ versus control), and 20% of the total cells counted were positive for γ H2AX staining 36 hours post-treatment ($p < 0.0005$ versus control) (Figure 3.6.1.1B, panel 1 and 2).

γ H2AX staining was detected at 12 hours post-treatment consistent with the formation of cisplatin and carboplatin-induced DNA strand breaks, possibly due to the replication fork collapse as a result of arrest in S-phase. γ H2AX staining was found to be increased at 24 hours and was still detectable at 36 hours post-treatment with cisplatin and carboplatin, consistent with continued arrest of cells in S-phase as shown by flow cytometry (Figure 3.5.1.1A and B, panel 3) (Cruet-Hennequart et al., 2008). The percentage of γ H2AX-stained cells was found to be similar in cisplatin -and carboplatin-treated cells (Figure 3.6.1.1B, panel 1 and 2). All values in treated cells were significantly different from the corresponding untreated samples ($p < 0.0005$).



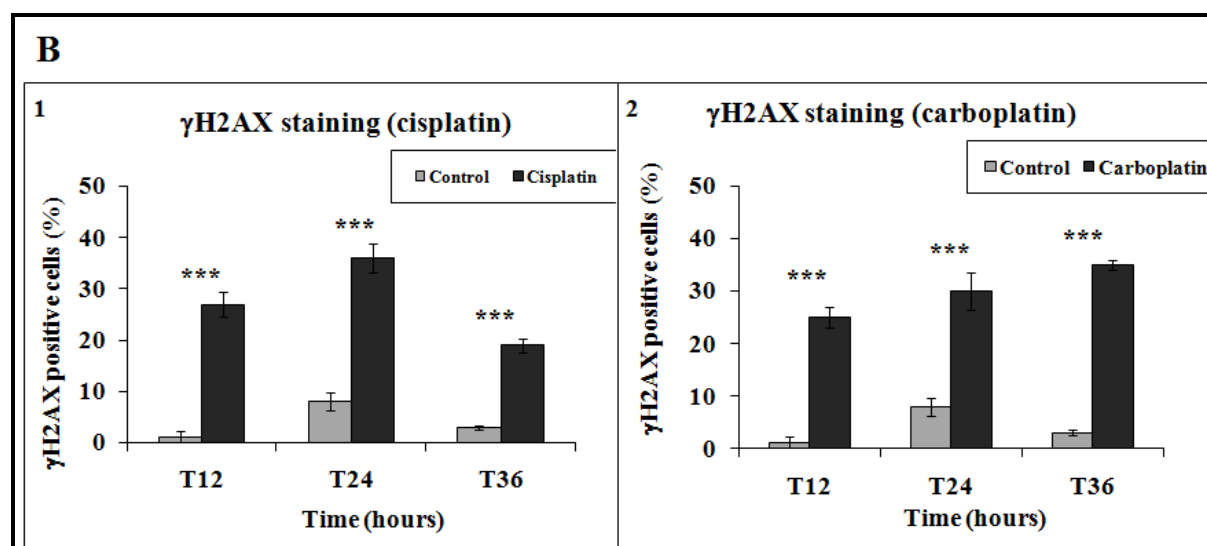


Figure 3.6.1.1. Nuclear γ H2AX staining following treatment of G1-phase XP30R0 cells with cisplatin and carboplatin. (A) XP30R0 cells in G1-phase were treated with cisplatin or carboplatin. (B) Bar graph represents the percentage of cells positive for γ H2AX staining post treatment with (1) cisplatin or (2) carboplatin. Cells were grown on glass coverslips in culture medium, and treated with cisplatin (1.66 μ M) or carboplatin (50 μ M) for 12, 24 and 36 hours. Cells were stained for H2AX phosphorylated at serine139 using a phosphospecific antibody, and detected using a FITC-labelled secondary antibody. DNA was counter-stained using DAPI. The total number of cells counted was 200. The number of cells positive for nuclear γ H2AX staining was counted and expressed as a percentage of the total number of cells counted. Each data point represents an average of three experiments, and error bars represent one standard deviation. Significant differences between the percentage of γ H2AX-positive control and drug-treated cells were determined using Students t-test, and are shown by *** ($p < 0.0005$).

3.6.2. Phosphorylation of RPA2 on serine 4/serine 8 in cisplatin- and carboplatin-treated G1-phase XP30R0 and TR30-2 cells

Cisplatin activates PIK kinase-dependent DNA damage responses, leading to phosphorylation of a number of substrates including RPA2 and Chk1 (Cruet-Hennequart et al., 2008, Cruet-Hennequart et al., 2009). In response to DNA damage, RPA2 is phosphorylated on N-terminal serines 4, 8 and 33 and on threonine 21 (Binz et al., 2004). Cisplatin-induced RPA2 phosphorylation on serine 4/serine 8 was enhanced in pol η -deficient XP30R0 cells compared to normal GM00637 cells expressing pol η (Cruet-Hennequart et al., 2008). To investigate the relationship between RPA2 phosphorylation and cell cycle phase at the time of treatment, cells in G1-phase were treated with cisplatin or carboplatin. The pol η -dependence of this

response was investigated by comparison of RPA2 phosphorylation on serine 4/serine 8 between XP30R0 and TR30-2 cells. Cells in G1-phase were treated with cisplatin or carboplatin, and harvested 12, 24 or 36 hours later. Cell extracts were prepared and analysed by SDS-PAGE and Western blotting. RPA2 phosphorylated on serine 4/serine 8 in XP30R0 cells was strongly detected at 24 and 36 hours post-cisplatin and carboplatin treatment (Figure 3.6.2A and B, panel 2, lanes 6 and 7). The peak of carboplatin-induced RPA2 phosphorylation was later than that of cisplatin-induced RPA2 phosphorylation, consistent with reported data on platinum-induced RPA2 phosphorylation in asynchronously growing XP30R0 cells (Cruet-Hennequart et al., 2009). In the case of TR30-2 cells, the level of RPA2 phosphorylation on serine 4/serine 8 was reduced compared to that in XP30R0 cells, 24 and 36 hours post-cisplatin and carboplatin treatment (Figure 3.6.2A and B, panels 2, lanes 13 and 14). Thus, while RPA2 serine 4/serine 8 phosphorylation was detected in both XP30R0 and TR30-2 cells at 24 and 36 hours post-treatment with both cisplatin and carboplatin, RPA2 phosphorylation was more strongly induced in pol η -deficient cells. This may be consistent with a role for RPA phosphorylation in repair of double strand breaks occurring as a result of replication fork collapse (Cruet-Hennequart et al., 2006) in cells arrested in S-phase (Figure 3.5.1.1A and B, panel 3). In cells lacking pol η , fork stalling at sites of lesions, and fork collapse are enhanced (Cruet-Hennequart et al., 2008).

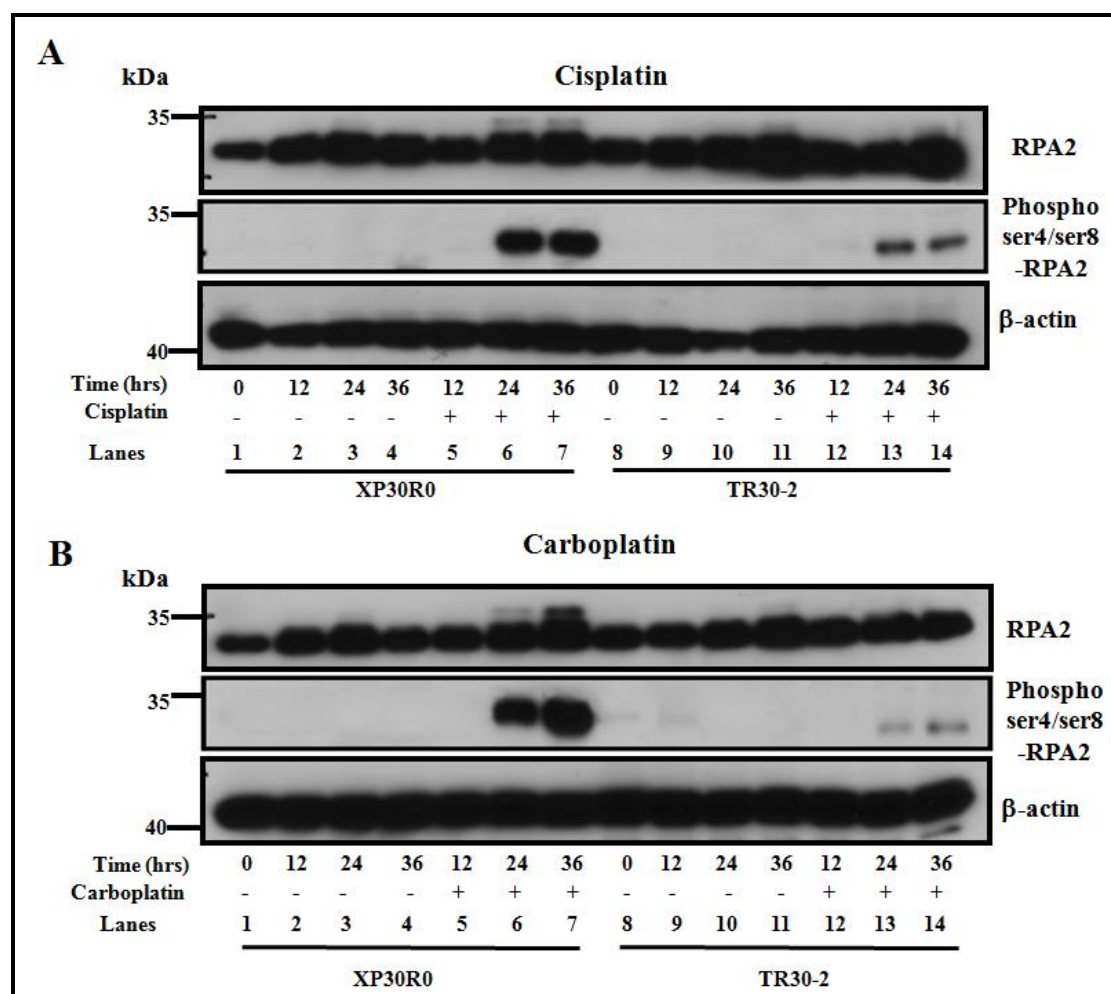


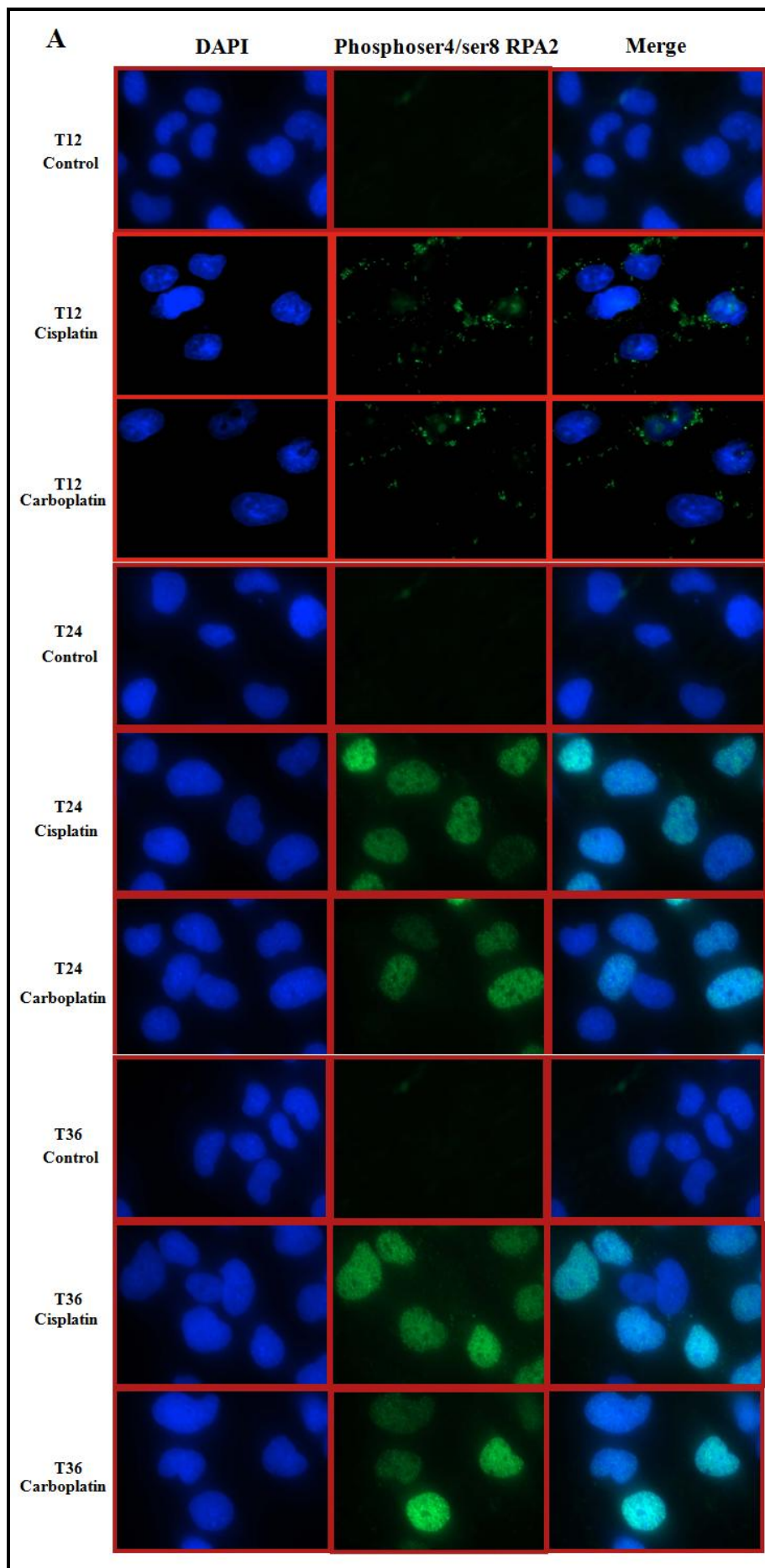
Figure 3.6.2. Time-course of RPA2 phosphorylation in G1-phase XP30R0 and TR30-2 cells treated with cisplatin and carboplatin. XP30R0 and TR30-2 cells in G1-phase were treated with (A) cisplatin (1.66 μ M) or (B) carboplatin (50 μ M) and harvested at 12, 24 and 36 hours. Cell extracts were prepared and analysed by SDS-PAGE and Western blotting. Panels 1, 2 and 3 shows Western blots of RPA2, RPA2 phosphorylated on serine 4/serine 8, and β -actin, respectively. Western blots are representative of three experiments.

3.6.2.1. Nuclear RPA2 serine 4/serine 8 staining in cisplatin- and carboplatin-treated G1-phase XP30R0 cells

To further investigate RPA2 phosphorylation in G1 phase XP30R0 cells following treatment with cisplatin (1.66 μ M) or carboplatin (50 μ M), immunofluorescence staining of RPA2 phosphorylated on serine 4/serine 8 was carried out. RPA2 phosphorylation on serine 4/serine 8 was detectable by immunofluorescence after treatment of G1-phase XP30R0 cells with cisplatin and carboplatin. In control cells at 12 hours post-mock treatment, there was no detectable staining of phosphorylated

serine 4/serine 8 on RPA2, whereas at 24 and 36 hours post-mock treatment about 5% cells stained positive for phosphorylated serine 4/serine 8 on RPA2 (Figure 3.6.2.1A and B). Phosphoserine 4/serine 8 staining was first detectable at 24 hours post-cisplatin treatment, and was sustained for up to 36 hours. About 20% of cells were positive for RPA2 phosphorylation by 36 hours (Figure 3.6.2.1B, panel 1). RPA2 phosphorylation post-carboplatin was delayed relative to cisplatin-induced RPA2 phosphorylation (Figure 3.6.2.1B, panel 3) with the peak of RPA2-positive cells occurring after 36 hours (Figure 3.6.2.1B, panel 2). This is consistent with Western blot data (Figure 3.6.2A and B) and with previous reports (Cruet-Hennequart et al., 2009). The basis of the difference in the timing of RPA2 phosphorylation after carboplatin compared to cisplatin is not clear, but may reflect differential use of specific repair pathways in response to carboplatin compared to cisplatin (Cruet-Hennequart et al., 2009). Overall, the immunofluorescence data supports the interpretation that RPA2 phosphorylation on serine 4/serine 8 is a relatively late event after cisplatin or carboplatin treatment, and is sustained for up to 36 hours.

The differences between the frequency of cisplatin- or carboplatin-treated RPA phosphoserine 4/serine 8-positive XP30R0 cells and control cells were statistically significant (Fig. 3.6.2.1.). A significant difference between the percentage of RPA phosphoserine 4/serine 8 positive cisplatin-treated and carboplatin-treated XP30R0 cells was also observed at 24 hours post-treatment (Fig. 3.6.2.1.).



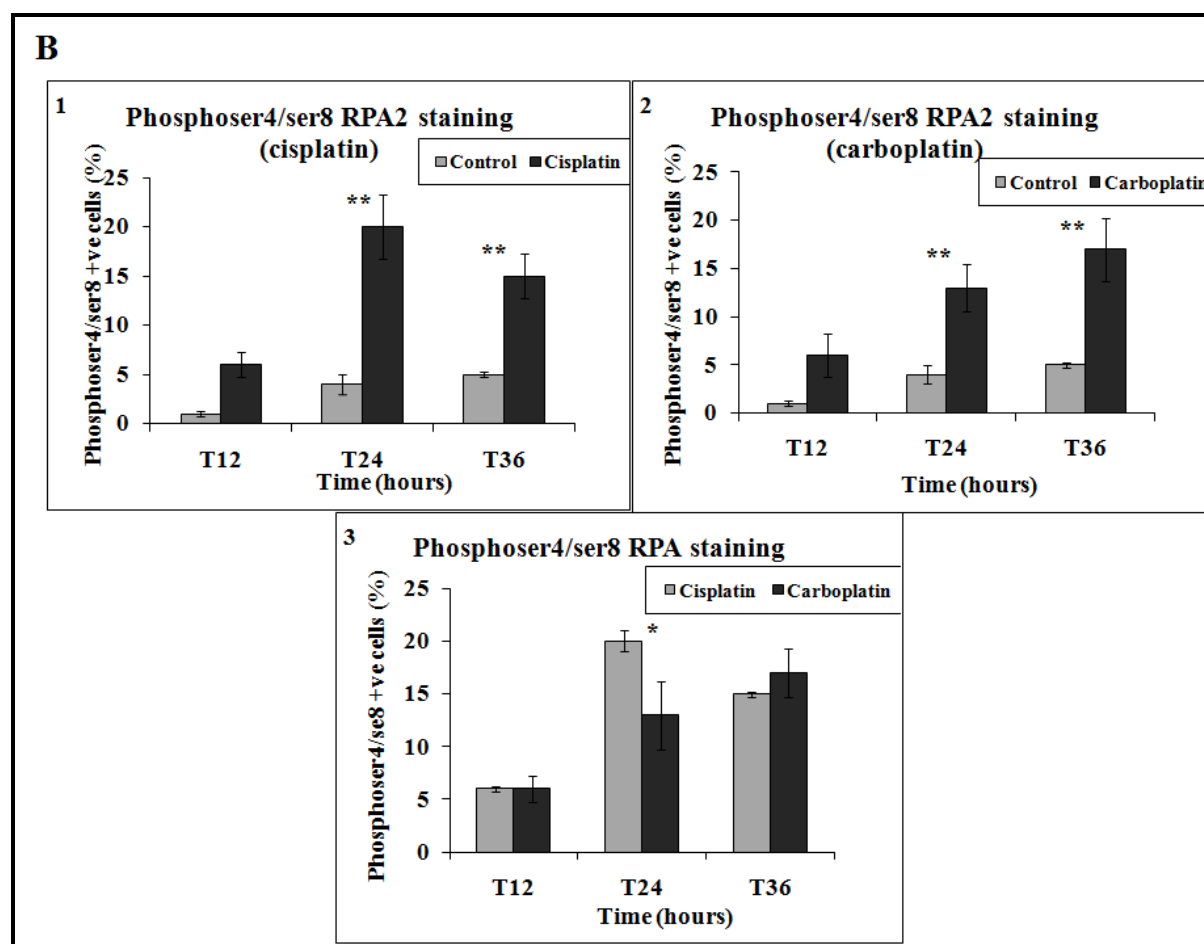


Figure 3.6.2.1. Detection of nuclear serine4/serine8 phosphorylated RPA2 staining in XP30R0 cells. (A) XP30R0 cells in G1-phase were treated with cisplatin (1.66 μ M) or carboplatin (50 μ M). Cells were grown on glass coverslips in culture medium and treated with cisplatin or carboplatin for 12, 24 and 36 hours. Cells were stained for phosphoserine 4/serine 8 RPA2 using a phosphospecific antibody, and staining was detected using a FITC-labelled secondary antibody. DNA was counter-stained using DAPI. (B) The bar graphs show the percentage of cells positive for RPA2 phosphorylated on serine 4/serine 8. The number of cells positive for nuclear phosphoserine 4/serine 8 RPA2 staining were counted and expressed as a percentage of the total number of cells counted. (1) Percentage of control or cisplatin-treated XP30R0 cells positive for nuclear phosphoserine 4/serine 8 RPA2 staining; (2) percentage of control and carboplatin-treated XP30R0 cells positive for phosphoserine 4/serine 8 RPA2 staining; (3) comparison of RPA2 phosphorylation in cisplatin- and carboplatin-treated XP30R0 cells. Each data point represents an average of three experiments, and error bars represent one standard deviation. Significant differences in phosphoserine 4/serine 8 RPA2 staining between control and drug-treated cells, and between cisplatin- and carboplatin-treated cells were determined using Students t-test, and are shown by * ($p < 0.05$) and ** ($p < 0.005$).

3.6.2.2. Effect of inhibition of PIK kinases or CDKs on cisplatin-and carboplatin-induced RPA2 hyperphosphorylation in G1-phase XP30R0 cells

PIK kinases including ATM, ATR and DNA-PK, are a family of serine/threonine protein kinases that phosphorylate downstream targets in response to DNA damage (Lempiainen and Halazonetis, 2009) (Section 1.8.2.1). ATR, is activated following damage-induced replication arrest while ATM and DNA-PK are activated by DNA strand breaks (Abraham, 2004). RPA2 is phosphorylated by CDKs on serine 23 and serine 29 (Stephan et al., 2009) during the normal cell cycle. Serine 23 phosphorylation occurs in S-phase while serine 29 phosphorylation may occur in M-phase (Stephan et al., 2009). In the case of phosphorylation of RPA2 on serine 4/serine 8, it is known that this is DNA-PK-dependent (Section 1.9.3). To investigate the roles of DNA-PK, ATM and CDKs in cisplatin- and carboplatin-induced RPA2 phosphorylation on serine 4/serine 8, XP30R0 cells were co-treated with cisplatin or carboplatin and with either NU7441, a small molecule inhibitor of DNA-PK_{cs}; with KU55933, an inhibitor of ATM kinase (Veuger et al., 2003, Hickson et al., 2004, Cowell et al., 2005), or with roscovitine, an inhibitor of CDK1/2 (Anantha et al., 2007, Stephan et al., 2009). The IC₅₀ value for the inhibition of ATR kinase activity by NU7441 and KU55933 is greater than 100 µM (Veuger et al., 2003, Hickson et al., 2004, Cowell et al., 2005); at the dose of 10 µM used in the present study, ATR should not be inhibited by either NU7441 or KU55933. Phosphorylation of RPA2 on serine 4/serine 8 was detected in cells treated with cisplatin and carboplatin (Figure 3.6.2.2A and B, panel 1, lane 3, 6 and 9). When cells were co-treated with either cisplatin or carboplatin and with NU7441, damage-induced phosphorylation of RPA2 was reduced, consistent with previous reports that DNA-PK plays an important role in cisplatin-induced phosphorylation of RPA2 on serine 4/serine 8 (Cruet-Hennequart et al., 2009) (Figure 3.6.2.2A and B, panel 1, lane 2).

There was no reduction in RPA2 phosphorylation in cells treated with cisplatin or carboplatin and KU55933, compared to the corresponding cisplatin- or carboplatin-treated cells (Figure 3.6.2.2A, panel 1, lane 5 and 6), which indicates that ATM does not play a role in phosphorylation of cisplatin- or carboplatin-induced RPA2 on serine 4/serine 8, consistent with previous reports (Cruet-Hennequart et al., 2008). There was also a reduction in RPA2 phosphorylation when cisplatin- or carboplatin-treated cells were co-treated with roscovitine (Figure 3.6.2.2A, panel 1, lane 8 and 9),

indicating that inhibition of CDK1/2 by roscovitine also inhibited cisplatin- and carboplatin- induced RPA2 phosphorylation on serine 4/serine 8. While there is currently no evidence that CDKs directly phosphorylate RPA2 on serine 4/serine 8, this may be consistent with a requirement for phosphorylation of RPA2 on serine 23 or serine 29 before serine 4/serine 8 phosphorylation can occur (Olson et al., 2006, Anantha et al., 2008). In all cases following treatment with inhibitor alone (NU7441 or KU55933 or roscovitine) resulted in RPA2 phosphorylation.

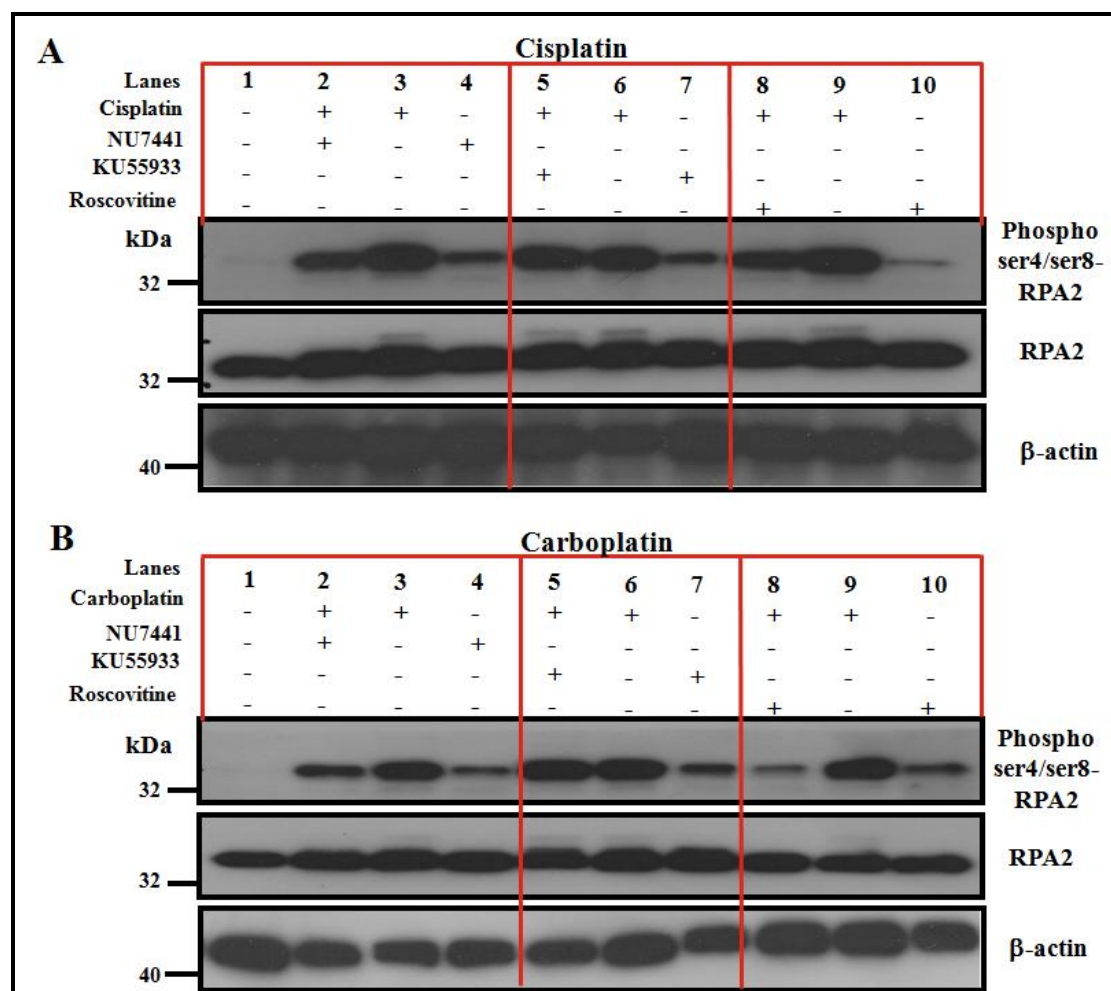


Figure 3.6.2.2. Effect of NU7441, KU55933 and roscovitine on cisplatin- and carboplatin-induced RPA2 phosphorylation in XP30R0 cells treated in G1-phase. Western blots of XP30R0 cells treated in G1-phase with (A) cisplatin (1.66 μ M) or (B) carboplatin (50 μ M) in the presence or absence of NU7441 (10 μ M); KU55933 (10 μ M), or roscovitine (15 μ M), for 24 hours. Cell extracts were prepared and analysed by SDS-PAGE and Western blotting. Panels 1, 2 and 3 shows Western blots of RPA2 phosphorylated at serine 4/serine 8, RPA2 and β -actin respectively. Western blots are representative of three experiments.

3.6.3. The timing of cisplatin- and carboplatin-induced Chk1 and RPA2 phosphorylation in XP30R0 cells treated in G1-phase

DNA replication arrest results in the ATR-mediated phosphorylation of the checkpoint kinase, Chk1, as well as phosphorylation of RPA2 in a DNA-PK-dependent manner (Zhou and Elledge, 2000, Matsuoka et al., 2007). ATR-mediated phosphorylation of Chk1 on serine 317 regulates replication arrest and entry into mitosis (Matsuoka et al., 2007, Cimprich and Cortez, 2008). To compare the timing of Chk1 and RPA2 phosphorylation, pol η -deficient XP30R0 cells in G1-phase were treated with cisplatin (1.66 μ M) or carboplatin (50 μ M). Cells were harvested after 12, 18, 24 and 36 hours. Cell extracts were analysed by SDS-PAGE and Western blotting. In control XP30R0 cells (Figure 3.6.3A and B, panel 2, lanes 1-5), slight phosphorylation of Chk1 was detectable at 18 hours post-treatment (Figure 3.6.3A and B, panel 2, lane 3). In both cisplatin- and carboplatin-treated cells, phosphorylation of Chk1 was detected at 12 hours, increased at 18 hours and the protein remained phosphorylated for up to 24 hours (Figure 3.6.3A and B, panel 2, lane 6, 7 and 8). At 36 hours, Chk1 phosphorylation was strongly reduced (Figure 3.6.3A and B, panel 2, lane 9).

In control cells, no phosphorylation of RPA2 at serine 4/serine 8 was detected (Figure 3.6.3A and B, panel 3, lanes 1-5). In cisplatin-treated cells, phosphorylation of RPA2 at serine 4/serine 8 was not detected at 12 hours but was detectable at 18 hours and increased at 24 and 36 hours (Figure 3.6.3A, panel 3, lanes 6-9). In carboplatin-treated cells, phosphorylation of RPA2 at serine 4/serine 8 was not detected at 12 hours post-treatment but was detected at 18 hours, and increased at 24 and 36 hours (Figure 3.6.3B, panel 3, lanes 6-9).

Phosphorylation of Chk1 was an earlier event, and was detected at 12 hours post-treatment of G1-phase XP30R0 cells with both cisplatin and carboplatin, while RPA2 phosphorylation on serine 4/serine 8 was a later event and was detected at 18 hours post-treatment with both cisplatin and carboplatin. Thus, the peak of Chk1 phosphorylation at serine 317 clearly precedes the peak of RPA2 phosphorylation on serine 4/serine 8, and activation of the ATR-mediated Chk1 checkpoint precedes DNA-PK-dependent RPA2 phosphorylation. This is consistent with blockage of replication fork progression occurring in S-phase phase cells, which may result in

generation of strand breaks that activate RPA2 phosphorylation (Cruet-Hennequart et al., 2008).

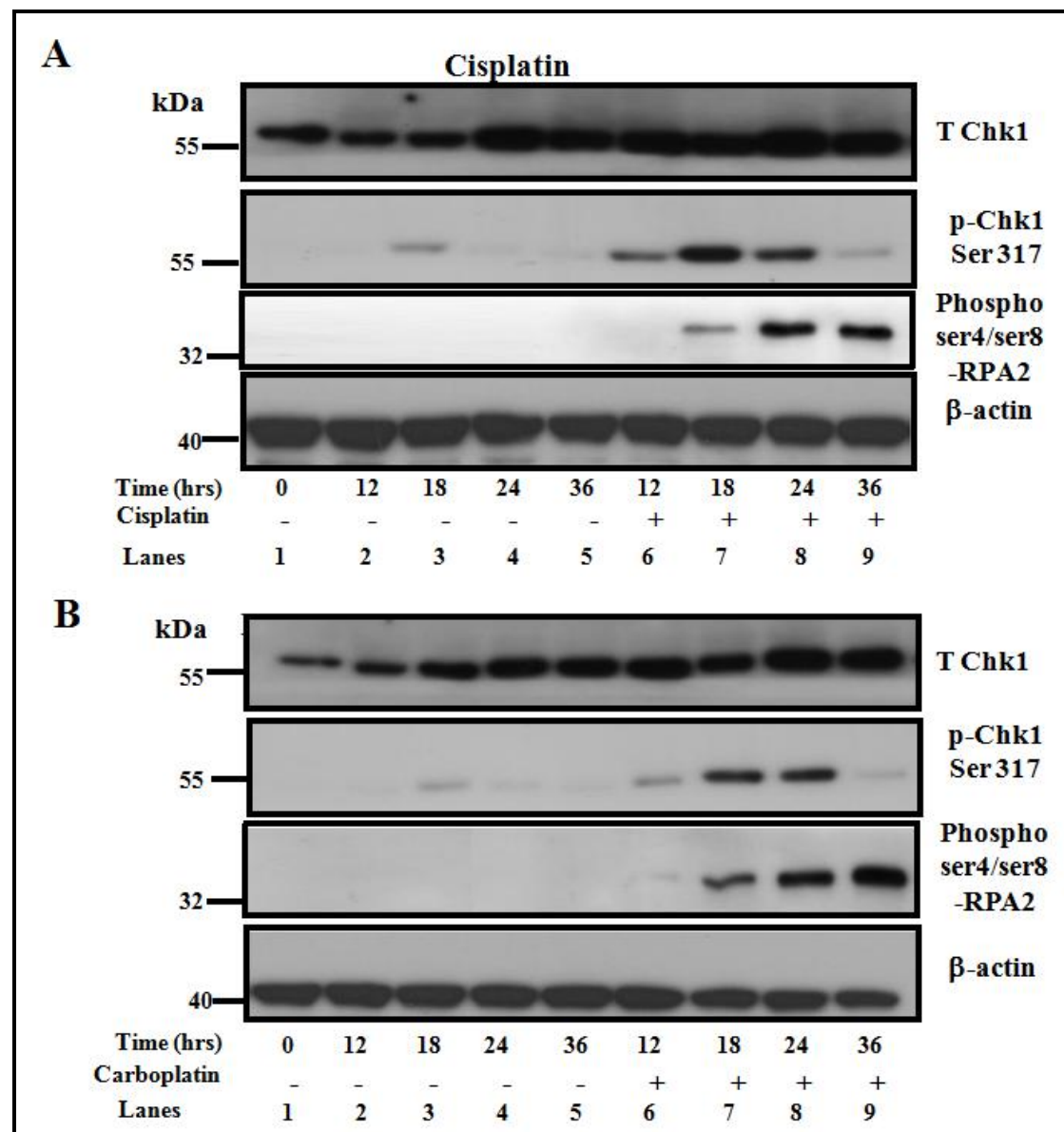


Figure 3.6.3. Chk1 and RPA2 phosphorylation in cisplatin and carboplatin-treated G1-phase XP30R0 cells. G1-phase XP30R0 cells were treated with (A) cisplatin (1.66 μ M) or (B) carboplatin (50 μ M) and harvested at 12, 18, 24 and 36 hours. Cell extracts were prepared and analysed by SDS-PAGE and Western blotting. Panels 1, 2 and 3 show Western blots of Chk1, Chk1 phosphorylated at serine 317, RPA2 phosphorylated at serine 4/serine 8, and β -actin, respectively. Western blots are representative of three experiments.

Summary of effects of cisplatin and carboplatin on G1-phase cells.

XP30R0 cells were more sensitive to cisplatin and carboplatin treatment, compared to TR30-2 cells. Cells treated in S-phase were more sensitive to cisplatin and carboplatin compared to cells treated in G1 and M-phase. Analysis of cell cycle progression showed that XP30R0 cells had a slight delay in exiting G1-phase following treatment compared to TR30-2 cells. Both XP30R0 and TR30-2 cells were strongly arrested in S-phase post-cisplatin and carboplatin-treatment, but the percentage of S-phase accumulation was significantly higher in XP30R0 cells compared to TR30-2 cells, consistent with a role for pol η in cell cycle progression in S-phase. The expression of cyclin B and E was altered post treatment compared to the control cells in both XP30R0 and TR30-2 cells. In XP30R0 cells cisplatin- and carboplatin-induced RPA2 phosphorylated on serine 4/serine 8 was strongly detected at 24 and 36 hours, by both Western blotting and IF. In TR30-2 cells, the level of platinum-induced RPA2 phosphorylation on serine 4/serine 8 was reduced compared to XP30R0 cells. RPA2 phosphorylation on serine 4/serine 8 was a late event, compared to phosphorylation of Chk1 on serine 317. Chk1 phosphorylation was detected 12 hours post-treatment of G1-phase XP30R0 cells, while RPA2 phosphorylation on serine 4/serine 8 was a later event peaking at 24 to 36 hours post-treatment. γ H2AX staining was detected at all timepoints post-treatment with both cisplatin- and carboplatin. DNA-PK and CDK1/2 play an important role in cisplatin- and carboplatin-induced phosphorylation of RPA2 in G1-phase XP30R0 cells. On the other hand, ATM did not play a role in the phosphorylation of RPA2.

3.7. Characterisation of the effects of cisplatin and carboplatin on cell cycle progression and DNA damage responses in S-phase cells

As explained earlier (Section 3.3.2), to obtain cells enriched in S-phase cells, following nocodazole arrest, mitotic cells were collected by shake-off, washed, reseeded and harvested 12 hours later. The experiments described in this section were performed on XP30R0 and TR30-2 cells treated with cisplatin and carboplatin when in S-phase.

3.7.1. Effect of cisplatin and carboplatin on cell cycle progression in S-phase cells lacking or expressing DNA pol η

XP30R0 and TR30-2 cells in S-phase were treated with cisplatin or carboplatin to investigate the effect on cell cycle progression after treating S-phase cells with cisplatin and carboplatin. XP30R0 and TR30-2 cells were synchronised using nocodazole as described in Section 3.3. Mitotic cells were collected following shake-off and reseeded. 12 hours after release from nocodazole, cells in S-phase were treated with cisplatin (1.66 μ M) or carboplatin (50 μ M), and harvested after 0 (S-phase cells), 12, 24 and 36 hours. The absence of pol η expression in XP30R0 cells; expression of pol η in TR30-2 cells was confirmed by Western blotting. Cell cycle progression was analysed using flow cytometry (Figure. 3.7.1A), and the percentage of cells in each cell cycle phase was determined using Cell QuestTM (Figure 3.7.1.1A and B). Both G2- and M-phase cells were included in the population of cells with 4N DNA content.

As shown in figure 3.7.1A, at T0, corresponding to 12 hours after release from nocodazole arrest, the majority of XP30R0 and TR30-2 cells were in S-phase, as determined using PI staining and flow cytometry. After a further 12 hours, cells were in G2- and M-phases. By 24 and 36 hours, cells had returned to a distribution typical of asynchronously growing XP30R0 and TR30-2 cells (Figure 3.7.1A, panel 1). The major effect of cisplatin on S-phase XP30R0 cells was induction of a strong delay in S-phase progression. The percentage of cells in S-phase increased compared to untreated cells, 12 hours after treatment. This increase was sustained for up to 36 hours post-treatment (Figure 3.7.1.1A, panel 3). The difference between the percentage of untreated and cisplatin-treated cells in S-phase was statistically

significant at 12, 24 and 36 hours post-treatment. Prolonged S-phase arrest and delayed cell cycle progression is supported by the fact that the percentage of cells in G1-phase was greatly reduced 36 hours after cisplatin-treatment (Figure 3.7.1.1A, panel 1), while the percentage of cells in G2+M-phases was increased significantly (Figure 3.7.1.1A, panel 5). Overall, the data indicates that cisplatin induces prolonged arrest in S-phase, with delayed progression through cell cycle, such that cells have not re-entered G1-phase by 36 hours (Figure 3.7.1.1A, panel 1).

When XP30R0 cells were treated with carboplatin, initially cell cycle progression was less strongly inhibited, compared to post cisplatin treatment (Figure 3.7.1A). 36 hours after carboplatin treatment, the percentage of cells in S-phase was significantly increased compared to control cells (Figure 3.7.1.1B, panel 3). This could indicate that S-phase arrest is more pronounced if cells re-enter S-phase during the second cell cycle following carboplatin exposure. In the case of TR30-2 cells, cisplatin and carboplatin had less dramatic effects on cell cycle progression. There was no significant difference between the percentage of control and cisplatin-treated (Figure 3.7.1.1A, compare panels 2 and 6) or carboplatin-treated cells (Figure 3.7.1.1B, compare panels 2 and 6), except in the percentage of cells in S-phase 36 hours post-treatment. At this time, there was a significant difference between the percentage of cells in S-phase in cisplatin-treated (Figure 3.7.1.1A, panel 4) and carboplatin-treated cells compared to untreated cells. Again, this may be indicative of arrest in S-phase during a second cell cycle (Figure 3.7.1.1B, panel 4). This effect was seen in other studies when cells were treated with O⁶ methylguanine leads to reduced replication rate in the second cell cycle (Mojaś et al., 2007). Pol η may play a role in replication of damaged DNA generated upon exposure of S-phase cells in TR30-2 cells.

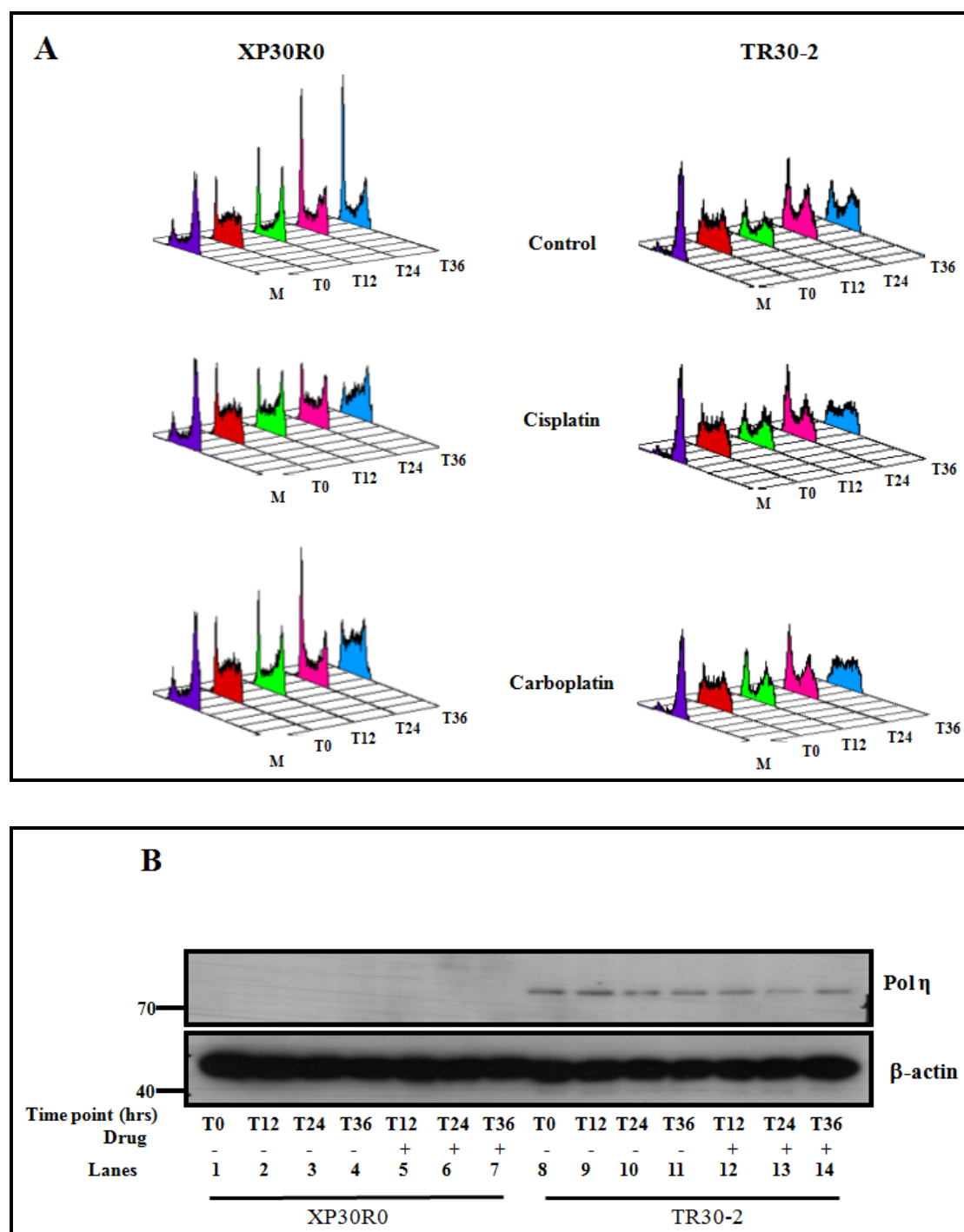
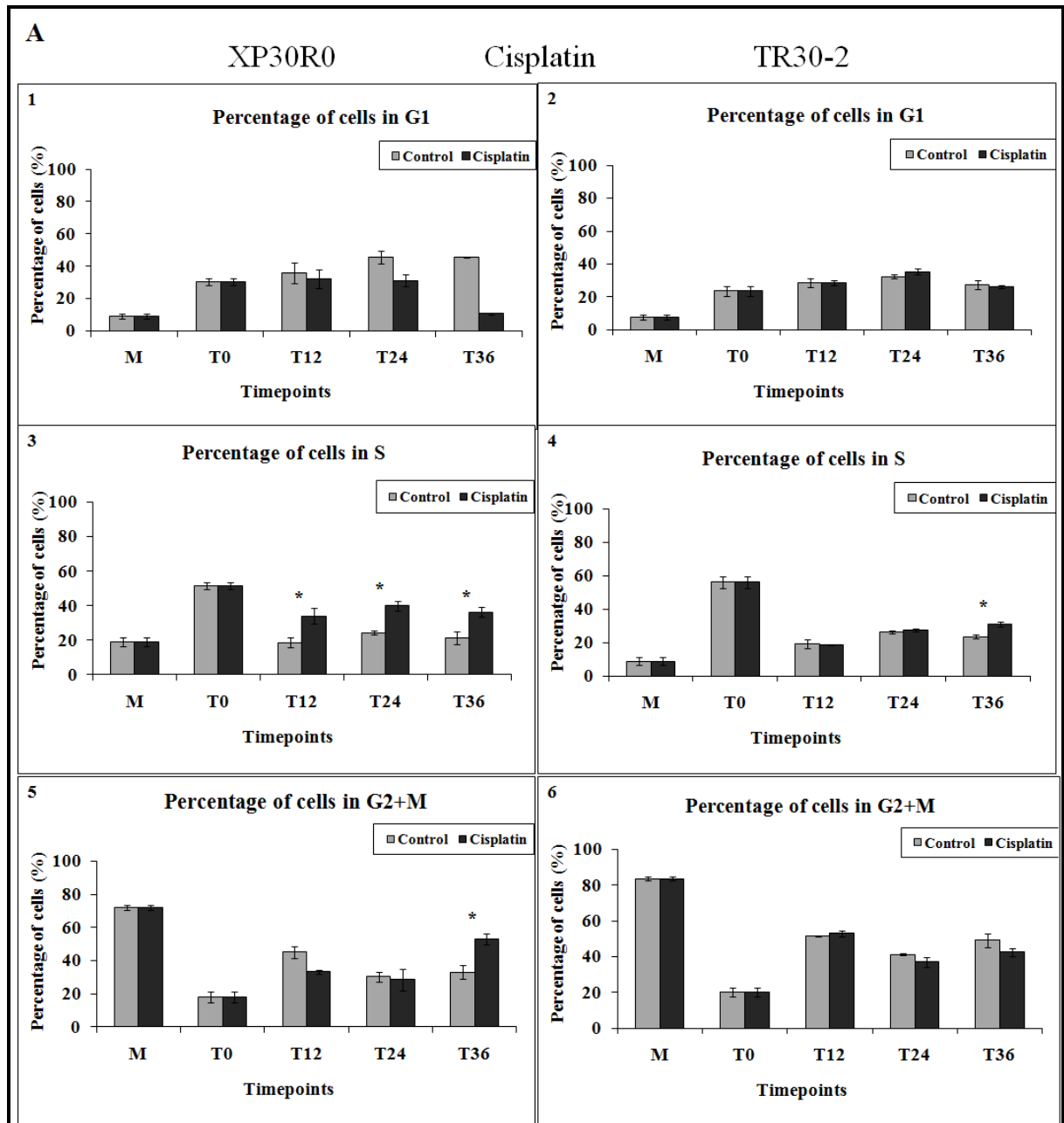


Figure 3.7.1. Cell cycle distribution of XP30R0 and TR30-2 cells in S-phase treated with cisplatin or carboplatin. (A) XP30R0 and TR30-2 cells in S-phase were treated with cisplatin (1.66 μ M) or carboplatin (50 μ M). Cells were harvested at 0 (S-phase cells), 12, 24 and 36 hours post-treatment. The cells were stained with propidium iodide and analysed by flow cytometry. The histogram profiles show the distribution of cells in different phases of the cell cycle, including mitotic shake-off cells (M). (B) Western blot analysis of pol η expression in XP30R0 and TR30-2 cells, without or with drug treatment. Actin was used a loading control.



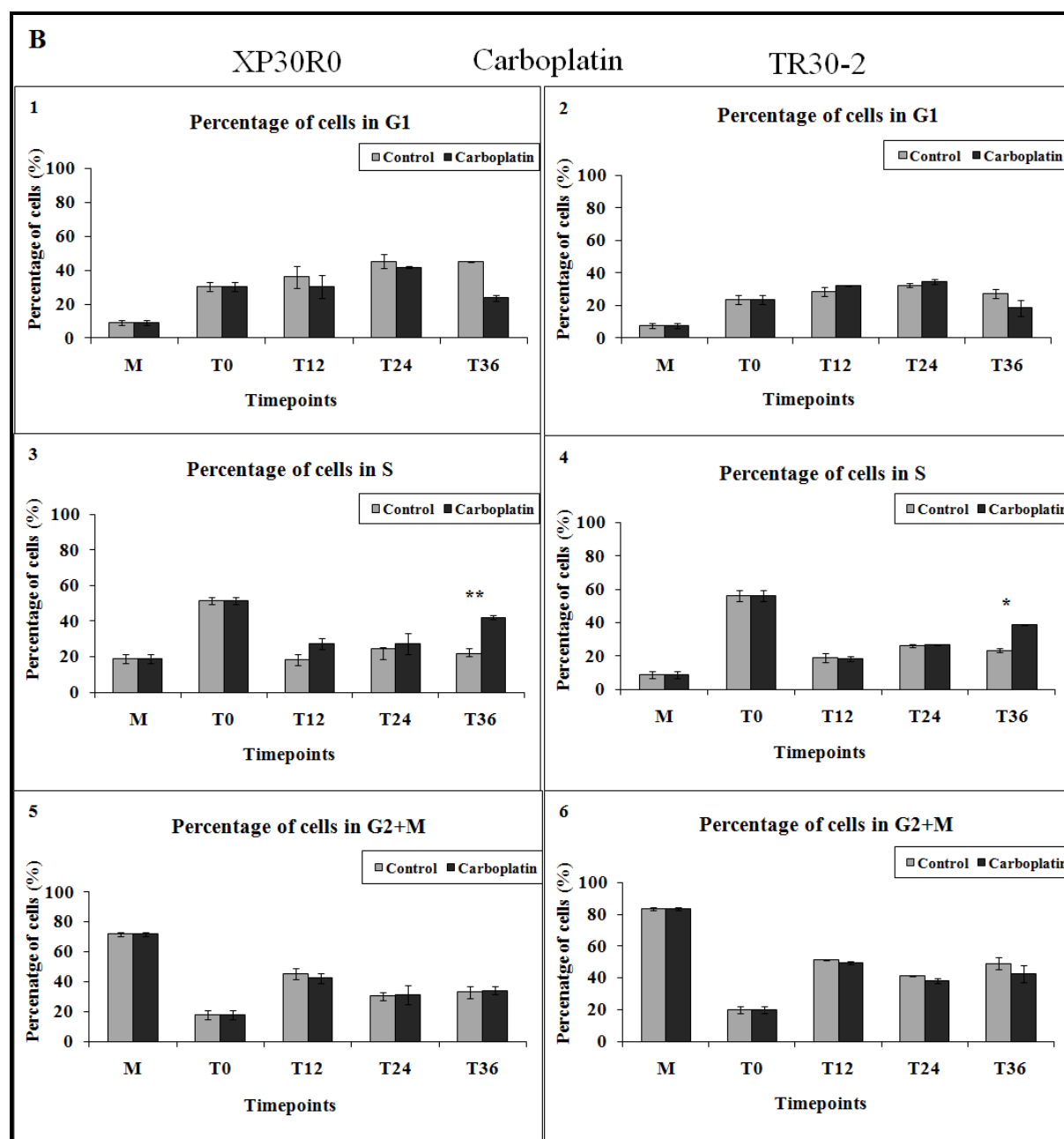


Figure 3.7.1.1. Bar graphs showing percentage of XP30R0 and TR30-2 cells in each cell cycle phase, following treatment of S-phase cells with cisplatin or carboplatin. (A) Bar graphs shows the percentage of XP30R0 and TR30-2 cells in each phase of the cell cycle, (A) in control (untreated), and cisplatin-treated cells, and (B) in control and carboplatin-treated cells. Each data point represents a mean of three experiments; error bars represent one standard deviation. Statistically significant differences in the percentage of cells in S-phase in XP30R0 and TR30-2 cells between control and post-cisplatin or carboplatin treatment, were determined using Student t-test, and are shown by * ($p < 0.05$) and ** ($p < 0.005$).

Summary

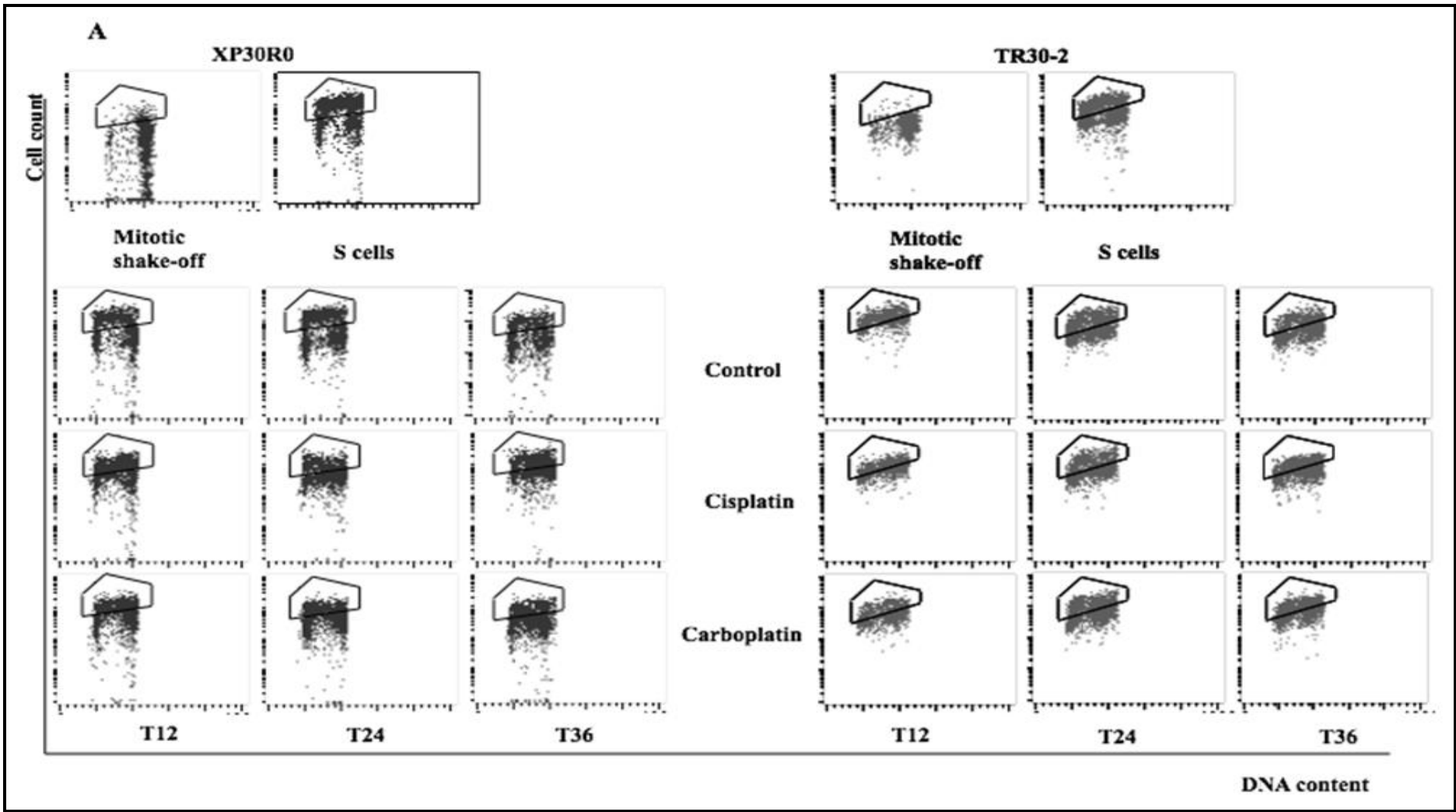
Following treatment of S-phase XP30R0 cells with cisplatin, cells were strongly arrested in S-phase. Up to 24 hours following carboplatin treatment, S-phase arrest was less pronounced than following cisplatin treatment. However, at 36 hours post-treatment, cells strongly arrested in S-phase, possibly due to effects in cells undergoing a second round of replication. Cisplatin- and carboplatin-induced cell cycle arrest was reduced in TR30-2 cells expressing pol η compared to the pol η -deficient cell line, but cells arrested in S-phase, 36 hours post-treatment.

3.7.2. BrdU incorporation after cisplatin and carboplatin treatment at S-phase cells lacking or expressing DNA pol η

To investigate the effect on DNA replication of treating cells in S-phase with cisplatin or carboplatin, XP30R0 and TR30-2 cells were treated with cisplatin or carboplatin and harvested after 0 (S-phase cells), 12, 24 and 36 hours. Cells were pulse-labelled with BrdU one hour prior to harvesting at the respective timepoints. BrdU incorporation was analysed using flow cytometry (Figure 3.7.2A), and the percentage of cells incorporating BrdU was determined (Figure 3.7.2B).

In untreated XP30R0 cells the percentage of BrdU-positive cells decreased from 70% at the time of treatment to 30% after 12 hours (Figure 3.7.2B, panels 1 and 3), consistent with cells exiting S-phase and entering G2/M, as shown also using propidium iodide staining (Figure 3.7.1A). The major effects of cisplatin on BrdU incorporation in XP30R0 cells were a decrease in the overall level of BrdU incorporated, and an increase in the percentage of BrdU-positive cells 12, 24 and 36 hours following drug treatment. This is consistent with arrest of cells in S-phase, while control cells exit S-phase (Figure 3.7.2B, panel 1). The increased percentage of cells in S-phase is consistent with S-phase arrest (Figure 3.7.2B, panel 1). However, following treatment of S-phase XP30R0 cells with carboplatin, a statistically significant difference in the percentage of BrdU-positive cells between control and treated cells was only observed at 36 hours post-treatment (Figure 3.7.2B, panel 3). In TR30-2 cells expressing pol η , the pattern of BrdU incorporation was broadly similar. Control cells showed a high percentage of BrdU-positive cells at T0 (Figure

3.7.2B, panel 2 and 4), when the majority of cells were in S-phase, and 12 hours later the percentage of BrdU-positive cells decreased as cells exited S-phase (Figure 3.7.2B, panel 2 and 4). However, following cisplatin and carboplatin treatment, a statistically significant difference between the percentages of BrdU-positive cells in control and treated cells were only observed at 36 hours post-treatment. Thus, there was a difference between S-phase XP30R0 and TR30-2 cells treated with cisplatin (Figure 3.7.2B, panel 1 and 2), in that of the percentage of BrdU-positive cells was increased over controls by cisplatin treatment in XP30RO cells at 12, 24 and 36 hours post-treatment, but not in TR30-2 cells. This may reflect reduced S-phase arrest in pol η -expressing cells at the earlier timepoints, consistent with data from PI staining (Figure 3.7.1).



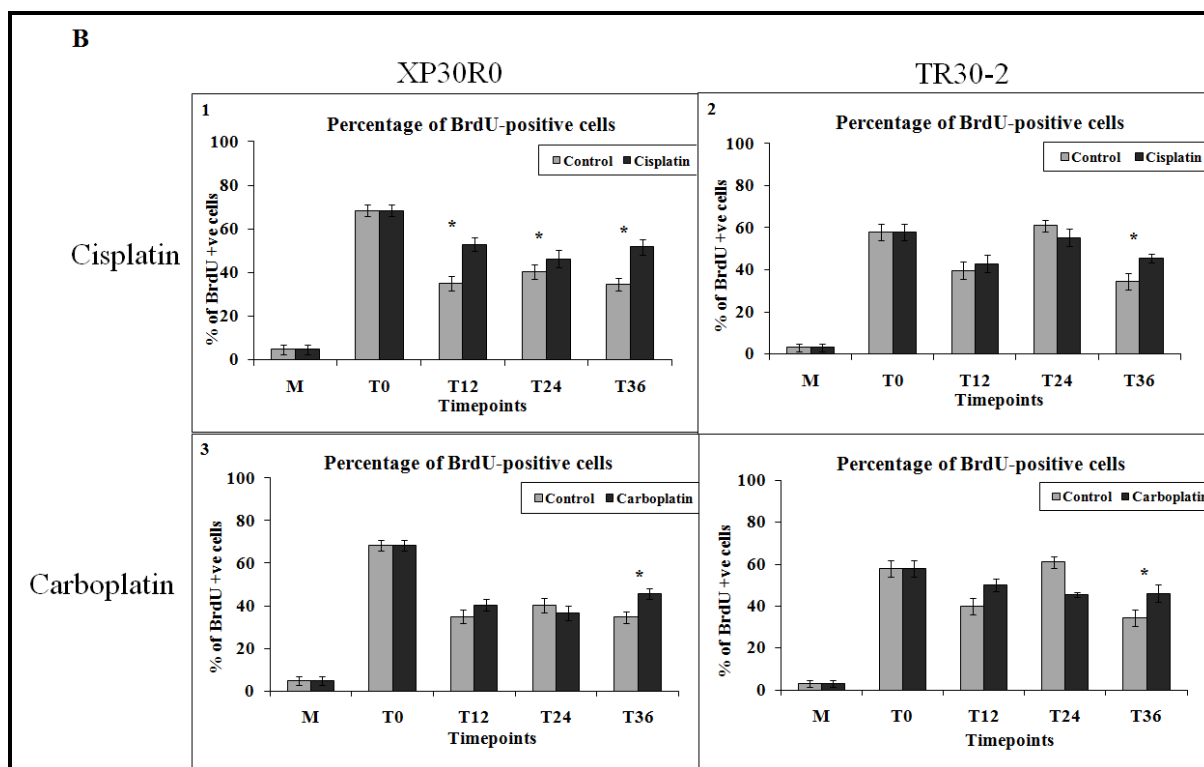


Figure 3.7.2. BrdU incorporation in XP30R0 and TR30-2 cells treated with cisplatin or carboplatin in S-phase. (A) XP30R0 and TR30-2 cells were treated with cisplatin (1.66 μ M) or carboplatin (50 μ M) in S-phase, and harvested at 0, 12, 24 and 36 hours post-treatment. Cells were pulse-labelled with BrdU 1 hour prior to harvesting at the respective time-points. The cells were stained with propidium iodide and with FITC-labelled anti-BrdU antibody, and analysed by flow cytometry. Dual-labelling plots of BrdU-positive staining versus propidium iodide staining are shown. (B) Bar graphs show the percentage of BrdU-positive cells in control (untreated), and cisplatin- or carboplatin-treated XP30R0 and TR30-2 cells. Each data point represents a mean of three experiments; error bars represent one standard deviation. Significant differences in the percentage of BrdU-positive XP30R0 and TR30-2 cells post-cisplatin-or carboplatin treatment compared to control cells, determined using Student t-test, are shown by * ($p < 0.05$).

Summary

When S-phase XP30R0 cells were treated with cisplatin, the percentage of BrdU-positive cells was increased over control cells, between 12 and 36 hours post-exposure, indicative of arrest of cells in S-phase. Following carboplatin treatment, the percentage of BrdU-positive cells was statistically different from control values only at 36 hours post-treatment. The extent of arrest in S-phase was less in TR30-2

cells than in XP30R0 cells, consistent with a role for pol η in ongoing DNA synthesis in S-phase.

3.7.3. Expression of cyclin B and cyclin E after treatment of S-phase XP30R0 and TR30-2 cells with cisplatin

To further characterise the effect of cisplatin on cell cycle progression, XP30R0 and TR30-2 cells, in S-phase were treated with cisplatin (1.66 μ M), and the levels of cyclin B and cyclin E were analysed, by SDS-PAGE and western blotting, 12, 24 and 36 hours post-treatment. Levels of cyclin B and cyclin E varied between control cells and cisplatin-treated XP30R0 and TR30-2 cells, as determined using densitometric analysis of the western blots.

In untreated XP30R0 cells cyclin B expression was low, when cells were in S-phase (T0) and increased 24 and 36 hours later, as cells progressed through S-phase and into G2/M (Figure 3.7.3B, panel 1). Following treatment with cisplatin, cyclin B expression did not change significantly, as cells were arrested in S- and G2/M-phases (Figure 3.7.3B, panel 1). In untreated TR30-2 cells, cyclin B expression increased with time. Following cisplatin treatment cyclin B expression was lower at 36 hours compared to control cells, consistent with cells being arrested in S-phase (Figure 3.7.3B, panel 2).

In untreated XP30R0 cells, cyclin E expression decreased at 12 hours as cells exited S-phase, and increased at 24 and 36 hours, consistent with cell cycle progression. Following cisplatin treatment, cyclin E expression remained unaltered between 12 and 36 hours post-treatment, as cells were arrested in S-phase (Figure 3.7.3B, panel 3). In TR30-2 cells, following cisplatin treatment, cyclin E expression was slightly higher at 36 hours compared to 24 hours, consistent with S-phase arrest (Figure 3.7.3B, panel 4). Overall, the level of cyclin E in S-phase cells was generally higher in TR30-2 cells than in XP30R0 cells; however, the basis of this difference was not investigated further.

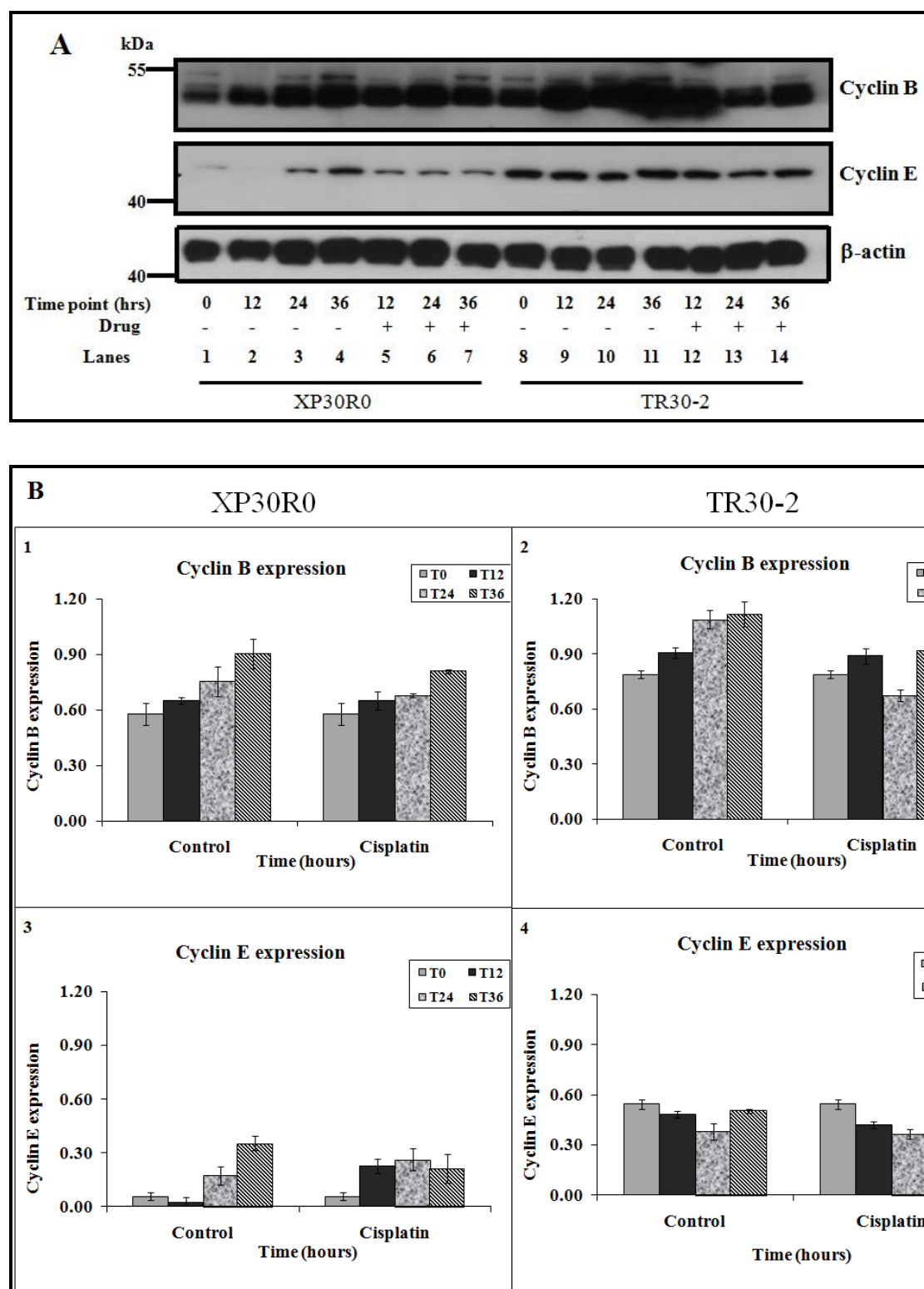


Figure 3.7.3. Effect of cisplatin on cyclin B and cyclin E expression. (A) S-phase XP30R0 and TR30-2 cells were treated with cisplatin (1.66 μ M) and harvested after 0, 12, 24 and 36 hours. Cell extracts were analysed by SDS-PAGE and Western blotting. Panels 1, 2 and 3 show Western blots of cyclin B, cyclin E and actin respectively. Cyclin B and cyclin E expression was compared between control and cisplatin-treated in both XP30R0 and TR30-2 cells. Western blots are representative of three experiments. (B) Graph, calculated using densitometry analysis, represents expression of cyclin B in XP30R0 and TR30-2 treated with cisplatin (panel 1 and 2)

and cyclin E in XP30R0 and TR30-2 treated with cisplatin (panel 3 and 4) normalised to the respective actin levels in the sample. The values are an average of data from three experiments and error bars represent one standard deviation. There was no statistical significance observed between control and cisplatin-treated cells.

3.7.4. Expression of cyclin B and cyclin E after treatment of S-phase XP30R0 and TR30-2 cells with carboplatin

XP30R0 and TR30-2, cells were treated with carboplatin (50 μ M) and the expression of cyclins B and E were analysed by Western blotting. Expression of cyclins B and E varied between the control cells and carboplatin-treated population in both XP30R0 and TR30-2 cells (Figure 3.20A), as determined by densitometric analysis of the Western blots.

In untreated XP30R0 cells, cyclin B expression was low when cells were in S-phase (T0) and increased at 24 and 36 hours as the cells progressed through the cell cycle (Figure 3.7.4B, panel 1). Following carboplatin treatment, cyclin B expression increased at 24 and 36 hours as the cells progressed through S-phase and into G2/M but decreased slightly at 36 hours (Figure 3.7.4B, panel 1). In untreated TR30-2 cells, cyclin B expression increased with time, while following carboplatin treatment, cyclin B expression decreased at 36 hours consistent with cells being arrested in S-phase (Figure 3.7.4B, panel 2). Cyclin E expression in XP30R0 control cells, decreased after 12 hours, as cells had exited S-phase, and increased at 24 and 36 hours consistent with ongoing cell cycle progression (Figure 3.7.4B, panel 3). Following carboplatin treatment, the level of cyclin E was lower at 24 and 36 hours post-treatment in XP30R0 cells, consistent with a delay in cell cycle progression in these cells (Figure 3.7.4B, panel 3 and 4).

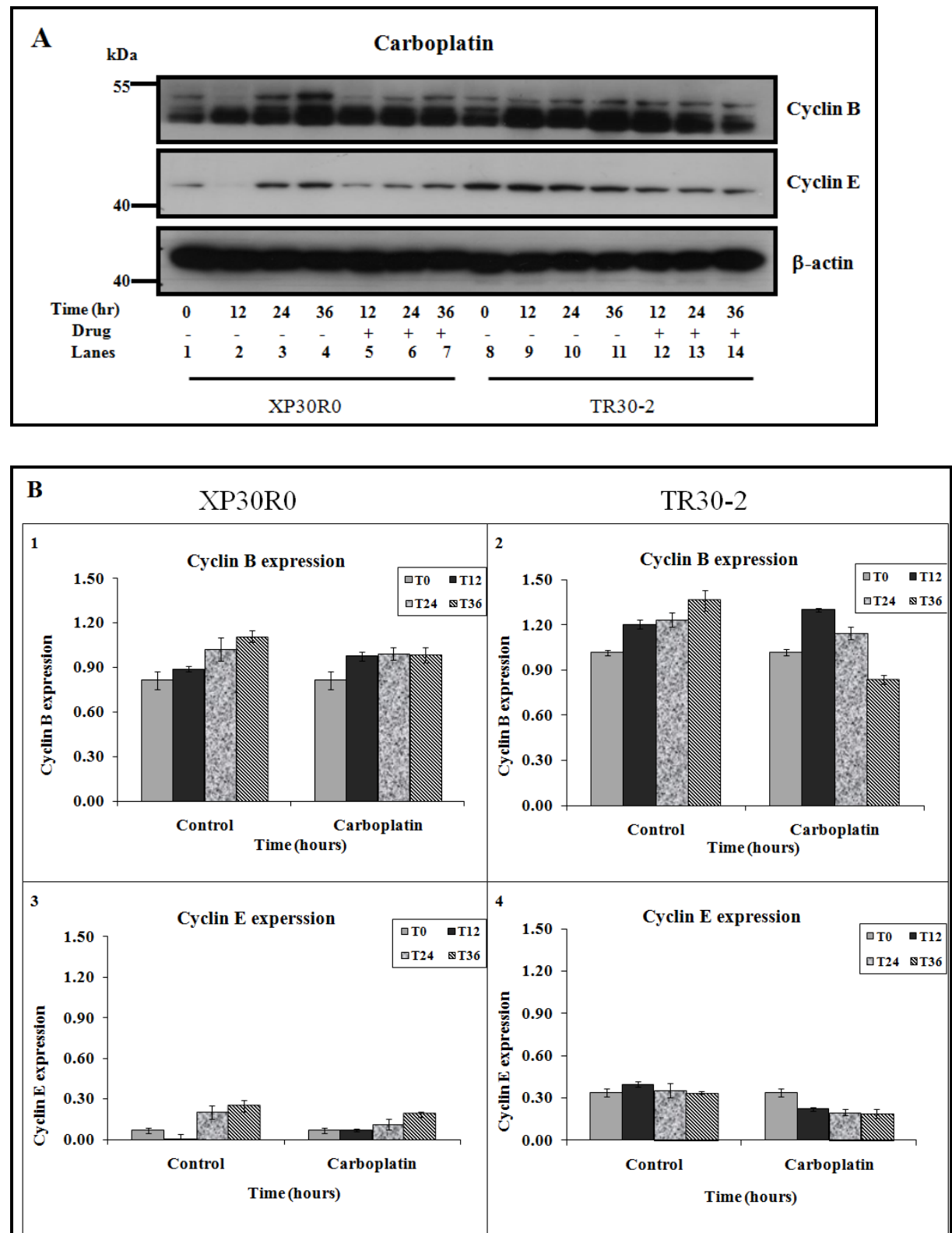


Figure 3.9.4. Effect of carboplatin on cyclin B and cyclin E levels. (A) S-phase XP30R0 and TR30-2 cells were treated with carboplatin (50 μ M) and harvested at 0, 12, 24 and 36 hours. Cell extracts were prepared and analysed by SDS-PAGE and Western blotting. Panels 1, 2 and 3 show Western blots of cyclin B, cyclin E and actin

respectively. Cyclin B and cyclin E expression was compared between control and carboplatin-treated in XP30R0 and TR30-2 cells. Western blots are representative of three experiments. (B) Graph, calculated using densitometry analysis, represents expression of cyclin B in XP30R0 and TR30-2 treated with carboplatin (panel 1 and 2) and cyclin E in XP30R0 and TR30-2 treated with carboplatin (panel 3 and 4) normalised to the respective actin levels in the sample. The values are an average of data from three experiments and error bars represent one standard deviation. There was no statistical significance observed between control and carboplatin-treated cells.

3.8. Activation of DNA damage responses

3.8.1. H2AX phosphorylation in cisplatin- and carboplatin-treated S-phase XP30R0 cells

Histone H2AX is phosphorylated at serine 139 in response to DNA strand breaks, generating γ H2AX (Rogakou et al., 1998, Kobayashi et al., 2009). To investigate H2AX phosphorylation in S-phase cells, pol η -deficient XP30R0 cells were released from nocodazole arrest for 12 hours and treated with cisplatin (1.66 μ M) or carboplatin (50 μ M). Cells in S-phase were treated with drug, and cell extracts were prepared 0, 12, 18, 24 and 36 hours later and analysed by SDS-PAGE and Western blotting. In control XP30R0 cells (Figure 3.8.1A and B, panel 1, lanes 1-5), no γ H2AX was detectable by Western blotting. Following treatment of cells with cisplatin or carboplatin, H2AX phosphorylation was strongly induced by 12 hours and sustained for up to 36 hours post-treatment (Figure 3.8.1A and B, panel 1, lanes 6-9). The timing of γ H2AX formation is consistent with induction of DNA strand breaks in S-phase cells as a result of prolonged replication arrest. A contribution of DNA repair, in particular ICL repair, can also not be ruled out.

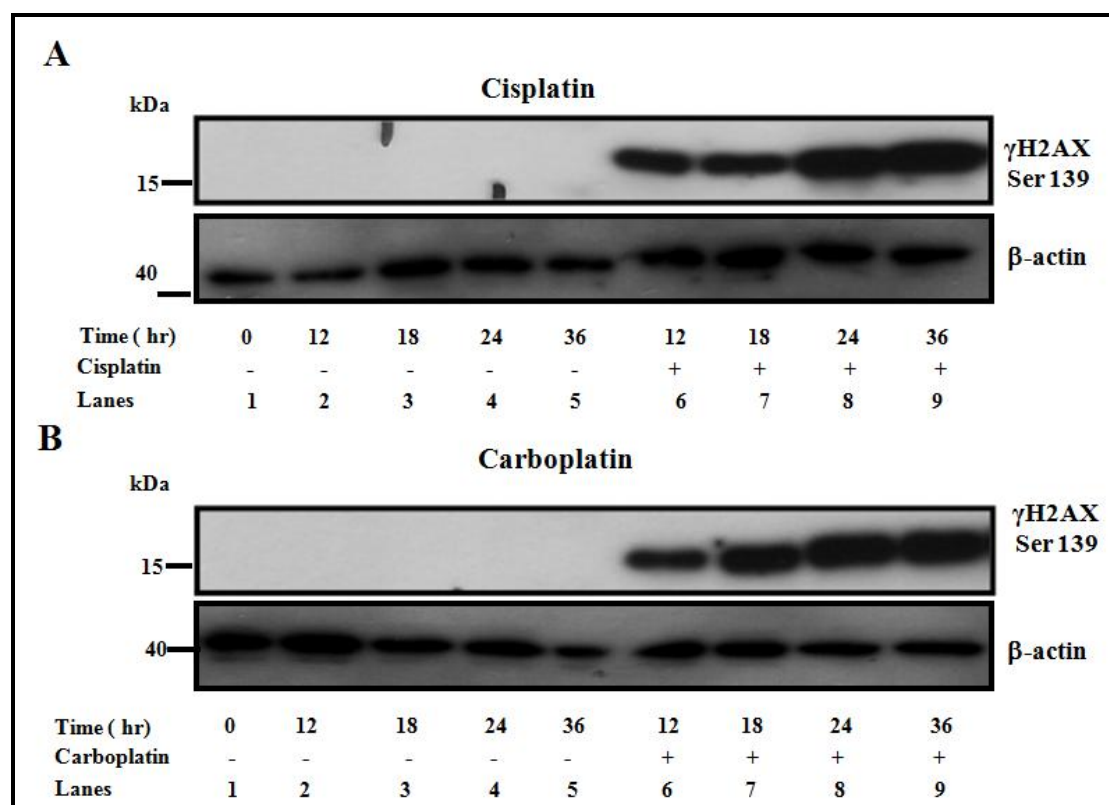
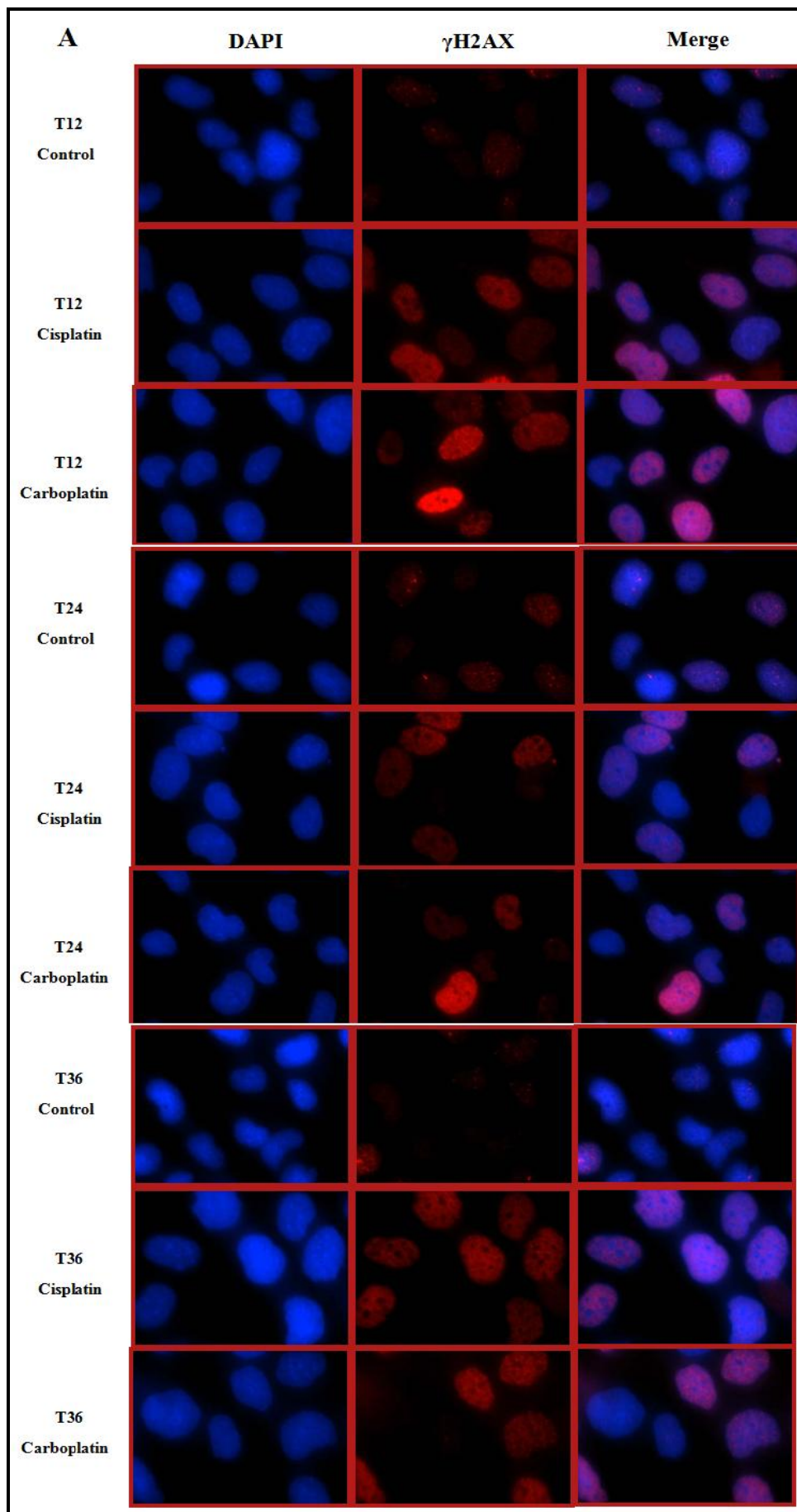


Figure 3.8.1. H2AX phosphorylation in cisplatin- and carboplatin-treated S-phase XP30R0 cells. S-phase XP30R0 cells were treated with (A) cisplatin (1.66 μ M) or (B) carboplatin (50 μ M) and harvested at 0, 12, 18, 24 and 36 hours. Cell extracts were prepared and analysed by SDS-PAGE and Western blotting. Panel 1 shows Western blot of H2AX phosphorylated at serine 139 detected using anti- γ H2AX antibody. Actin was used as a loading control. Western blots are representative of three experiments.

3.8.1.1. Nuclear staining for γ H2AX in cisplatin- and carboplatin-treated S-phase XP30R0 cells

To further investigate γ H2AX induction, immunofluorescence staining of γ H2AX was carried out, following treatment of S-phase XP30R0 cells with cisplatin (1.66 μ M) or carboplatin (50 μ M). As shown by Western blotting, H2AX phosphorylation was induced in both cisplatin- and carboplatin-treated cells, up to 36 hours post-treatment (Figure 3.8.1A and B). However, Western blotting does not provide information on the fraction of cells showing γ H2AX staining. To determine the percentage of cells that showed H2AX phosphorylation, all γ H2AX stained cells were scored as γ H2AX-positive, whether staining was in discrete foci or pan-nuclear. In control cells, 12 hours post mock-treatment, 3% of cells were γ H2AX-positive, while 24 and 36 hours

post mock-treatment, 5% and 2% cells were γ H2AX positive, respectively (Figure 3.8.1.1B, panel 1 and 2). Thus the background of γ H2AX-positive XP30RO cells in the S-phase population is low. Following cisplatin-treatment, 20% of cells were γ H2AX-positive 12 hours post-treatment. 28% were γ H2AX-positive 24 hours post-treatment ($p < 0.005$ versus control), and 32% were γ H2AX-positive 36 hours post-treatment ($p < 0.05$ versus control) (Figure 3.8.1.1B, panel 1). Following carboplatin-treatment, there was an increase in γ H2AX staining up to 36 hours. 14% of cells were γ H2AX-positive 12 hours post-treatment, 23% were positive for γ H2AX 24 hours post-treatment ($p < 0.005$ versus control) and 28% were γ H2AX-positive after 36 hours post-treatment ($p < 0.005$ versus control) (Figure 3.8.1.1B, panel 2). Thus, the peak of cisplatin- and carboplatin-induced γ H2AX staining was at 36 hours (Figure 3.8.1.1B). There were statistically significant differences between the percentage of γ H2AX-positive cells in controls and cisplatin- or carboplatin-treated XP30RO cells, at 24 and 36 hours post treatment.



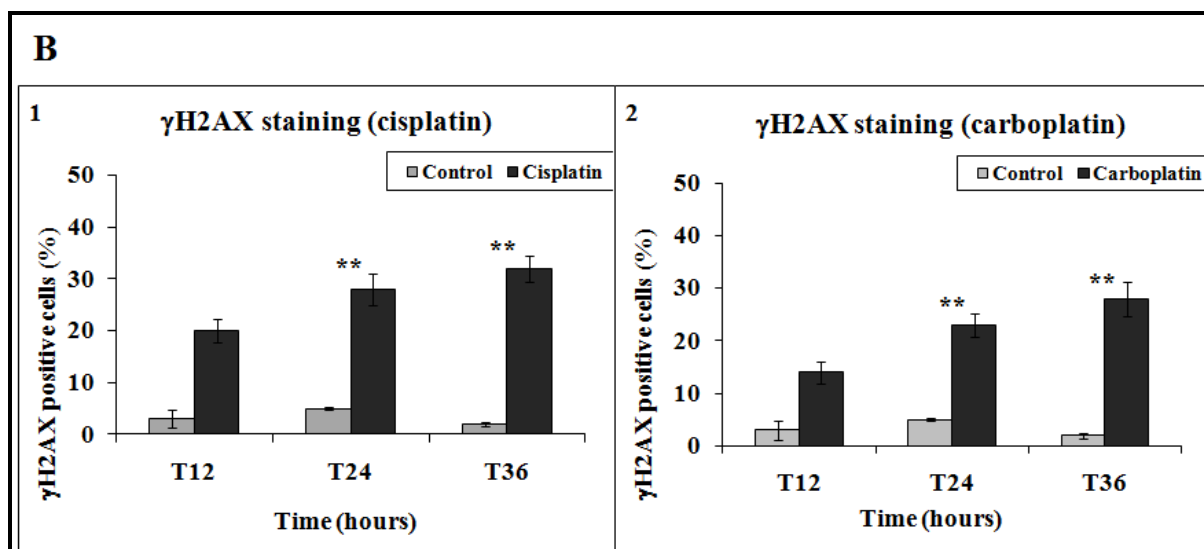


Figure 3.8.1.1. Detection of nuclear γ H2AX staining following treatment of S-phase XP30R0 cells with cisplatin and carboplatin. (A) XP30R0 cells were treated with cisplatin or carboplatin in S-phase. (B) Bar graph represents the percentage of cells positive for γ H2AX staining post treatment with (1) cisplatin or (2) carboplatin compared to untreated cells. Cells were grown on glass coverslips in culture medium and treated with cisplatin (1.66 μ M) or carboplatin (50 μ M) for 12, 24 and 36 hours. Cells were stained for H2AX phosphorylated at serine 139 using a phosphospecific antibody, and detected using a FITC-labelled secondary antibody. DNA was counter-stained using DAPI. The number of cells positive for nuclear γ H2AX staining was counted and is expressed as a percentage of the total number of cells counted. Each data point represents an average of three experiments, and error bars represent one standard deviation. Significant differences in γ H2AX staining between control and cisplatin- or carboplatin-treated cells were determined using Students t-test, and are shown by ** ($p < 0.005$).

3.8.2. Phosphorylation of RPA2 on serine 4/serine 8 in cisplatin and carboplatin-treated S-phase XP30R0 and TR30-2 cells

As shown earlier (Figure 3.6.2), the RPA2 subunit of RPA was strongly phosphorylated on serine4/serine8 in XP30R0 cells when the cells were treated in G1-phase and allowed to progress through the cell cycle. To further investigate the relationship between RPA2 phosphorylation and cell cycle phase at the time of drug exposure, cells in S-phase were treated with cisplatin or carboplatin. The pol η -dependence of this response was investigated by comparison of RPA2 phosphorylation on serine4/serine8 in XP30R0 and TR30-2 cells. Cells were treated at S-phase with cisplatin or carboplatin; 12, 24 and 36 hours later, cell extracts were prepared and analysed by SDS-PAGE and Western blotting. In untreated cells, little

RPA2 phosphorylation on serine4/serine8 was detectable. However, following cisplatin treatment, RPA2 phosphorylated on serine4/serine8 in XP30R0 cells was strongly detected at 24 hours and 36 hours post-treatment (Figure 3.8.2A, panel 2, lanes 6 and 7). Following carboplatin treatment RPA2 phosphorylated on serine4/serine8 was again detected at 24 hours, with an increased level detected at 36 hours post-treatment (Figure 3.8.2B, panel 2, lanes 6 and 7). In TR30-2 the timing of cisplatin and carboplatin-induced RPA2 phosphorylation on serine4/serine8 was similar to that in XP30R0 cells; however, the levels were greatly reduced. (Figure 3.8.2B, panels 2, lanes 6, 7, 13 and 14). RPA2 phosphorylation was detected in XP30R0 cells 24 and 36 hours post-treatment with both cisplatin and carboplatin. However, the peak of carboplatin-induced RPA2 phosphorylation was later than that of cisplatin-induced phosphorylation.

RPA2 phosphorylation thus represents a late event in the response of S-phase cells to cisplatin or carboplatin-induced DNA damage, and corresponds to the time at which the majority of XP30R0 and TR30-2 cells are arrested in S-phase (Figure 3.7.1.1A and B). This may be consistent with a role for RPA phosphorylation in repair of double strand breaks occurring as a result of replication fork collapse in cells arrested in S-phase (Cruet-Hennequart et al., 2006, Cruet-Hennequart et al., 2008, Cruet-Hennequart et al., 2009).

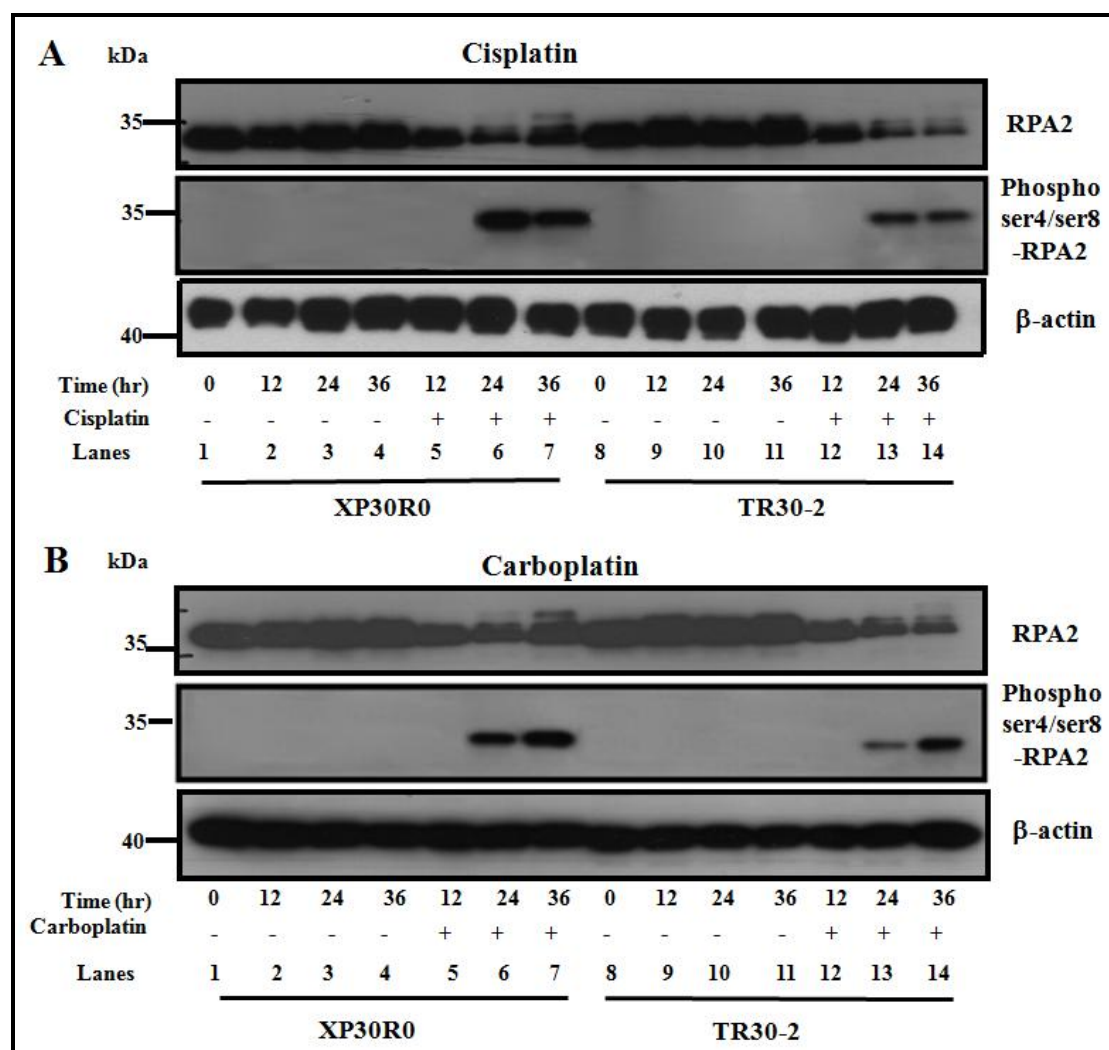


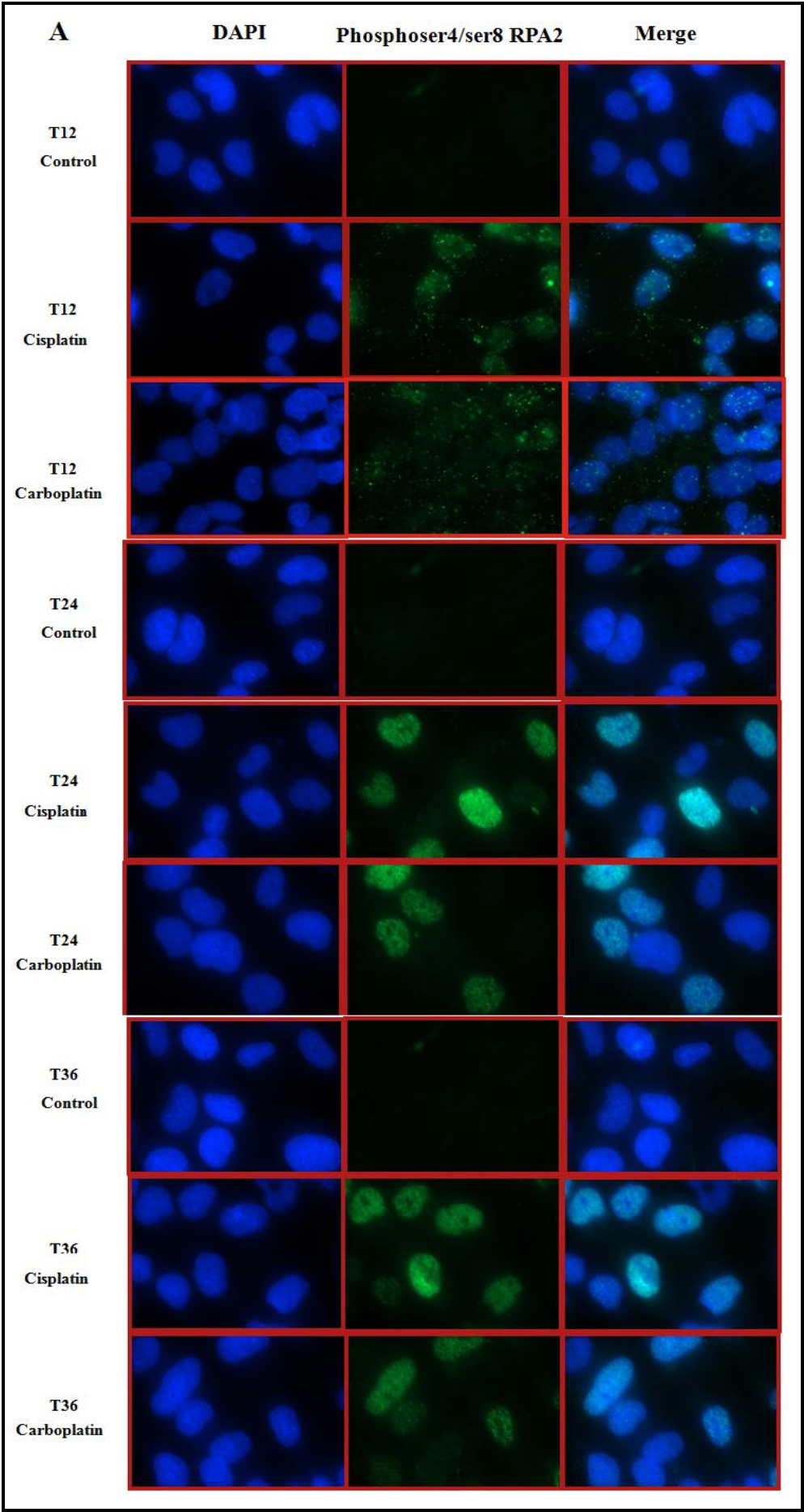
Figure 3.8.2. Time-course of RPA2 phosphorylation in S-phase treated XP30R0 and TR30-2 cells treated with cisplatin and carboplatin. XP30R0 and TR30-2 cells in S-phase were treated with (A) cisplatin (1.66 μ M) or (B) carboplatin (50 μ M) and harvested at 0, 12, 24 and 36 hours. Cell extracts were prepared and analysed by SDS-PAGE and Western blotting. Panels 1, 2 and 3 shows Western blots of RPA2, RPA2 phosphorylated on serine4/serine8 and actin respectively. Western blots are representative of three experiments.

3.8.2.1. Nuclear RPA2 serine 4/serine 8 staining in cisplatin-and carboplatin-treated S-phase XP30R0

Immunofluorescence staining of phosphorylated RPA2 on serine4/serine8 was carried out following treatment of XP30R0 cells at S-phase with cisplatin (1.66 μ M) or carboplatin (50 μ M). As demonstrated by Western blotting there was strong induction of RPA2 phosphorylation of serine4/serine8 in both cisplatin- and carboplatin-treated XP30R0 cells, 24 and 36 hours post-treatment (Figure 3.8.2A and B). In post-mock

treated cells, there was low, background RPA2 phosphoserine 4/serine 8-positive cells, with 7% of cells staining positive 24 hours post-mock-treatment (Figure 3.8.2.1A and B). 12 hours post-cisplatin treatment, 15% of cells stained positive (Figure 3.8.2.1A), while following carboplatin treatment 16% of the cells stained positive (Figure 3.8.2.1B). Consistent with the late onset of RPA2 phosphorylation on serine4/serine8, shown by Western blotting data, at 24 and 36 hours post-cisplatin treatment, 29% of cells stained positive for RPA2 phosphorylated on serine4/serine8 (Figure 3.8.2.1A). Following carboplatin treatment about 26% ($p < 0.005$ versus control) at 24 hours and 32% at 36 hours stained positive for RPA2 phosphorylated serine4/serine8 (Figure 3.8.2.1B). Statistically significant difference between the percentage of phosphorylated RPA2-positive cells in cisplatin- and carboplatin-treated XP30RO cells and control cells were detected at 24 and 36 hours post-treatment.

Overall, this data confirms that RPA2 phosphorylation on serine4/serine8 is a late event, even when XP30RO cells are in S-phase when treated with cisplatin or carboplatin. Thus prolonged arrest or fork collapse may be required to generate RPA2 phosphorylation on serine4/serine8.



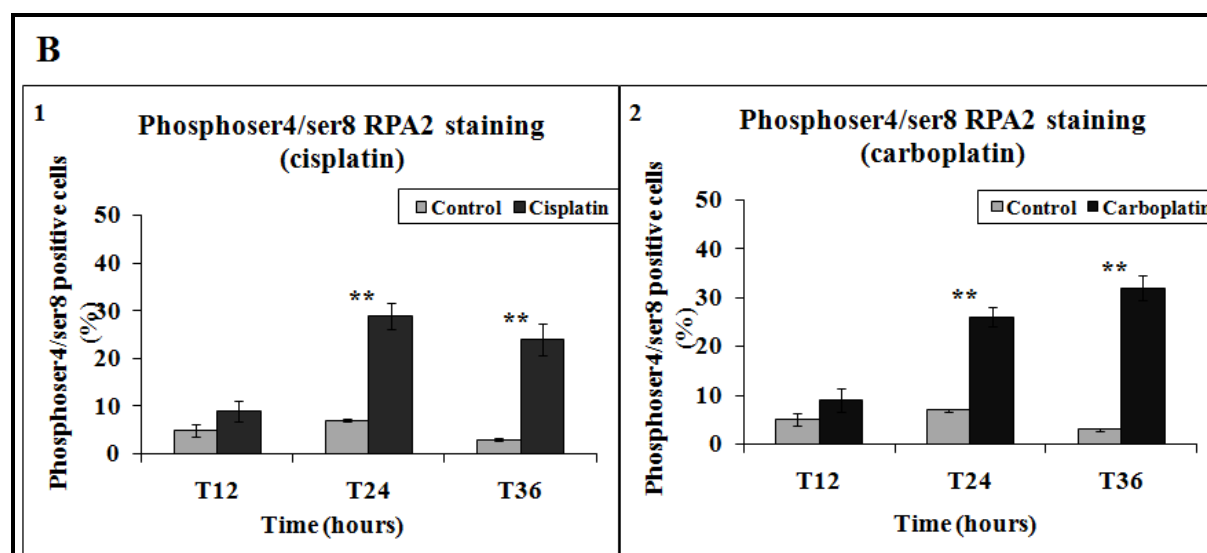


Figure 3.8.2.1. Detection of nuclear staining of serine4/serine8 for phosphorylated RPA2 in S-phase-treated XP30R0 cells. (A) XP30R0 cells were treated in S-phase with cisplatin or carboplatin. Cells were grown on glass coverslips in culture medium and treated with cisplatin (1.66 μ M) or carboplatin (50 μ M) for 12, 24 and 36 hours. Cells were stained for RPA2 phosphorylated on serine4/serine8 using a phosphospecific antibody, and detected using a FITC-labelled secondary antibody. DNA was counter-stained using DAPI. (B) Bar graphs represent the percentage of cells positive for serine4/serine8 staining. The number of cells positive for nuclear phosphoserine4/serine8 RPA2 staining were counted, and expressed as a percentage of the total number of cells counted. (1) Percentage of XP30R0 cells positive for nuclear phosphoserine4/serine8 RPA2 staining in controls and cisplatin treated cells (2) Percentage of XP30R0 cells positive for nuclear phosphoserine4/serine8 RPA2 staining in controls and carboplatin treated cells. Each data point represents an average of three experiments, and error bars represent one standard deviation. Significant differences in serine4/serine8 RPA2 staining between the control and drug-treated cells were determined using Students t-test and are shown by ** ($p < 0.005$).

3.8.2.2. Effect of PIK kinase and CDK on cisplatin- and carboplatin-induced RPA2 hyperphosphorylation in S-phase XP30R0 cells

To investigate the roles of DNA-PK, ATM and CDKs in RPA2 phosphorylation, S-phase XP30R0 cells were co-treated with cisplatin or carboplatin and with either NU7441, a small molecule inhibitor of DNA-PK_{cs}; with KU55933, an inhibitor of ATM kinase (Veuger et al., 2003, Hickson et al., 2004, Cowell et al., 2005) or with roscovitine, an inhibitor of CDK1/2 (Anantha et al., 2007, Stephan et al., 2009). Both cisplatin and carboplatin induced phosphorylation of RPA2 on serine4/serine8 (Figure 3.8.2A and B, panel 2, lane 6 and 7). When cells were treated with both cisplatin or

carboplatin and NU7441, 24 hours later phosphorylation of RPA2 was reduced (Figure 3.8.2.2A and B, panel 1, lane 2) consistent with previous reports that DNA-PK plays an important role in cisplatin-induced RPA2 phosphorylation on serine4/serine8 (Cruet-Hennequart et al., 2008).

There was no reduction in RPA2 phosphorylation on serine4/serine8 in cells co-treated with cisplatin or carboplatin and KU55933 compared to the corresponding cisplatin- or carboplatin-treated cells, which shows that ATM does not play a role in phosphorylation of RPA2 on serine4/serine8, consistent with previous report (Cruet-Hennequart et al., 2008) (Figure 3.8.2.2A, panel 1, lane 5 and 6). There was a reduction in RPA2 phosphorylation on serine4/serine8 when cells were co-treated with cisplatin or carboplatin and roscovitine (Figure 3.8.2.2A, panel 1, lane 8 and 9). As noted previously, this could be possibly due to a requirement of phosphorylation of RPA2 on serine 23 or serine 29 before it can be phosphorylated on serine4/serine8 (Olson et al., 2006, Anantha et al., 2007).

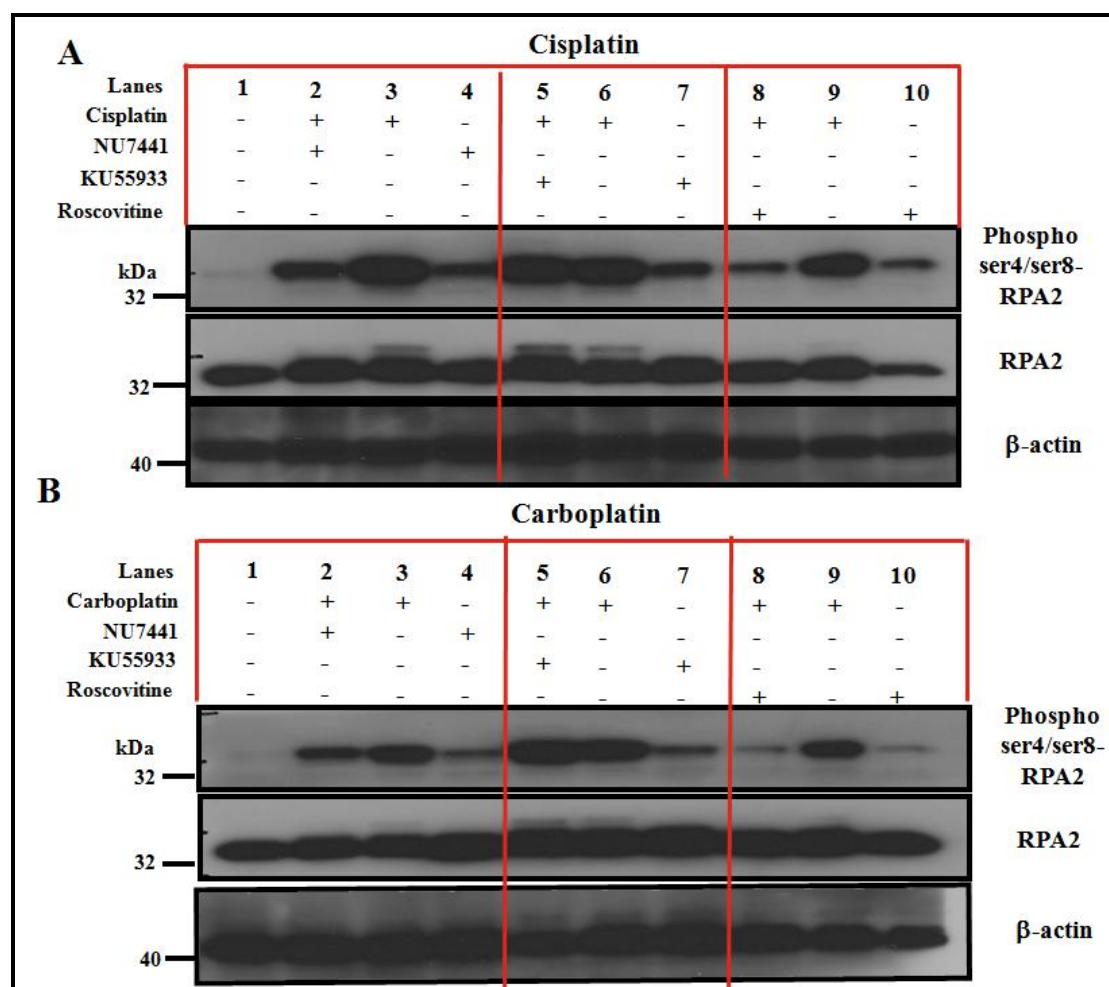


Figure 3.8.2.2. Effect of NU7441, KU55933 and roscovitine on S-phase XP30R0 cells treated with cisplatin or carboplatin-induced RPA2 phosphorylation. Western blots of S-phase XP30R0 cells treated with (A) cisplatin (1.66 μ M) or (B) carboplatin (50 μ M), in the presence or absence of NU7441 (10 μ M); or KU55933 (10 μ M) or roscovitine (15 μ M) for 24 hours. Cell extracts were prepared and analysed by SDS-PAGE and Western blotting. Panels 1, 2 and 3 shows Western blots of RPA2 phosphorylated at serine4/serine8, RPA2 and actin respectively using anti-RPA2 serine4/serine8, anti-RPA2 and anti- β -actin antibodies. Western blots are representative of three experiments.

3.8.3. The timing of cisplatin- and carboplatin-induced Chk1 and RPA2 phosphorylation in XP30R0 cells treated in S-phase

Chk1 is phosphorylated by ATR in response to replication arrest, while RPA2 phosphorylation on serine4/serine8 is DNA-PK dependent (Zhou and Elledge, 2000, Matsuoka et al., 2007). To compare the timing of Chk1 and RPA2 phosphorylation following treatment of S-phase XP30R0 cells with cisplatin and carboplatin, cells in S-phase were treated with drug, harvested after 0, 12, 18, 24 and 36 hours, and

analysed by SDS-PAGE and Western blotting. In control XP30R0 cells slight phosphorylation of Chk1 was detectable 24 and 36 hours after mock-treatment (Figure 3.8.3A and B, panel 2, lanes 1-5). In both cisplatin- and carboplatin-treated cells, phosphorylation of Chk1 was detected at 12 hours and the protein remained phosphorylated for up to 24 hours (Figure 3.8.3A and B, panel 2, lane 6, 7 and 8). While Chk1 phosphorylation was slightly reduced by 36 hours following cisplatin treatment, there was no decrease at 36 hours following carboplatin treatment (Figure 3.8.3A and B, panel 2, lane 9).

In control cells, phosphorylation of RPA2 at serine4/serine8 was detected at T0, T12 and T18 (Figure 3.8.3A and B, panel 3, lanes 1-5). In cisplatin-treated cells, phosphorylation of RPA2 at serine4/serine8 was detected between 18 hours and 36 hours, with a peak at 24 hours, as described above (Figure 3.8.3A, panel 2, lanes 6-9). In carboplatin-treated cells phosphorylation of RPA2 at serine4/serine8 was delayed relative to cisplatin-treatment, and was not detectable until 24 hours after treatment (Figure 3.8.3B, panel 3, lanes 6-9). Overall, this demonstrates that cisplatin- and carboplatin-induced phosphorylation of Chk1 is an earlier event than phosphorylation of RPA2 on serine4/serine8, even when cells are in S-phase at the time of treatment. Thus the peak of Chk1 phosphorylation at serine 317 clearly precedes the peak of RPA2 phosphorylation on serine4/serine8, indicating that activation of the ATR-mediated Chk1 checkpoint precedes damage-induced RPA2 phosphorylation on serine4/serine8 in S-phase cells.

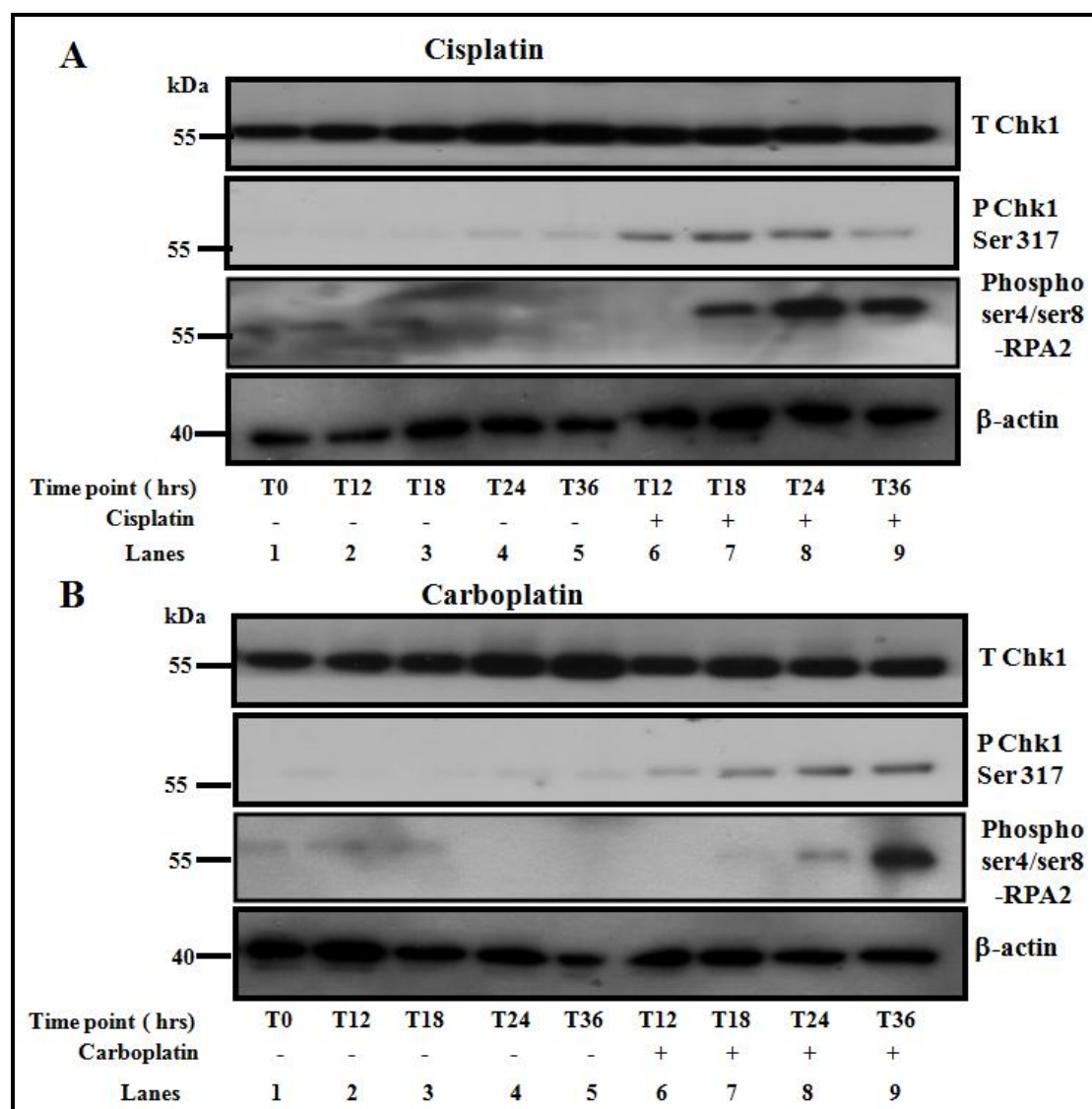


Figure 3.8.3. Chk1 and RPA2 phosphorylation in cisplatin and carboplatin-treated S-phase XP30R0 cells. S-phase XP30R0 cells were treated with (A) cisplatin (1.66 μ M) or (B) carboplatin (50 μ M) and harvested at 0, 12, 18, 24 and 36 hours. Cell extracts were prepared and analysed by SDS-PAGE and Western blotting. Panels 1, 2 and 3 show Western blots of Chk1 phosphorylated at serine 317, RPA2 phosphorylated at serine4/serine8 and β -actin respectively. Western blots are representative of three experiments.

Summary of effects of cisplatin and carboplatin on S-phase cells

Following treatment S-phase XP30R0 cells with cisplatin, cells were arrested in S-phase immediately post-treatment. Following carboplatin treatment, the arrest was not as pronounced, but there was evidence that cells were arrested in S-phase at the second round of replication, 36 hours post treatment. Following treatment of TR30-2 cells expressing polh with cisplatin, cell cycle arrest was less than in polh-deficient

XP30R0 cells, but cells arrested 36 hours post-treatment. This indicates a role for pol η in cell cycle progression in S-phase cells treated with cisplatin in particular. The expression of cyclin B and E was altered post treatment compared to the control cells in both XP30R0 and TR30-2 cells. Following treatment of XP30R0 cells with cisplatin and carboplatin, H2AX was phosphorylated by 12 hours post-treatment, and the protein remained phosphorylated up to 36 hours post-treatment. In comparison to Chk1 phosphorylation on serine 317, RPA2 phosphorylation was a late event in both XP30R0 and TR30-2 cells, occurring at 24 and 36 hours post-treatment. The peak of cisplatin-induced RPA2 phosphorylation was at 24 hours post treatment while the peak of carboplatin-induced RPA2 phosphorylation was at 36 hours post-treatment. A role for DNA-PK and CDK1/2 in the RPA2 phosphorylation on serine4/serine8 in S-phase XP30R0 cells was identified, while ATM did not play a role in the RPA2 phosphorylation.

3.9. Characterisation of the effects of cisplatin and carboplatin on cell cycle progression and DNA damage responses in M-phase cells

3.9.1. Effect of cisplatin and carboplatin on cell cycle progression in M-phase cells lacking or expressing DNA pol η .

To investigate the effect of cisplatin and carboplatin on cell cycle progression in M-phase cells, XP30R0 and TR30-2 cells were synchronised using nocodazole (Section 3.3), collected using the shake-off method, and exposed to cisplatin (1.66 μ M) or carboplatin (50 μ M). Cells were either harvested immediately (T0; M-phase), or after 8, 12, 24 and 36 hours. Cell cycle progression was analysed using flow cytometry (Figure 3.9.1A), and the percentage of cells in each cell cycle phase was determined using Cell QuestTM (Figure 3.9.1.1,A and B). Pol η was expressed in TR30-2 cells, and not in XP30RO cells (Figure 3.9.1B).

The major effects on cell cycle progression when XP30R0 cells in M-phase were treated with cisplatin were an increase in the percentage of cells in G1-phase 12 hours after treatment, consistent with a delay in exiting G1-phase (Figure 3.9.1.1A, panel 1), and delayed progression through S-phase for up to 36 hours after exposure (Figure 3.9.1.1A, panel 3). Consistent with arrest of cell cycle progression, the percentage of cells in G1-phase was reduced at late times after cisplatin treatment (24 and 36 hours) (Figure 3.9.1.1A, panel 1), due to failure of cells to traverse the cell cycle and re-enter G1-phase. The effect of cisplatin on cell cycle progression in M-phase TR30-2 cells that express pol η was broadly similar to that of pol η -deficient cells, in that at later times (24 and 36 hours) post-treatment, the percentage of cells in S-phase was increased compared to controls (Figure 3.9.1.1A, panel 4), consistent with strong cell cycle arrest. However, 12 hours post-cisplatin treatment there was no statistically significant difference in the percentage of TR30-2 cells in S-phase, unlike the case in XP30R0 cells. Thus, a slight delay in exiting S-phase occurs in XP30RO cells but not in TR30-2 cells. The basis of this delay has not been investigated further, but could suggest a role for pol η in G1-phase, possibly in repair of adducts (Soria et al., 2009).

The effect of carboplatin on M-phase XP30R0 cells was generally comparable to that of cisplatin, in that exit from G1 was delayed, evidenced by an increased percentage of cells in G1 at 12 hours post-treatment (Figure 3.9.1.1B, panel 1). Cells were then

arrested in S-phase, with a strong increase in the percentage of cells remaining in S-phase at 24 hours and 36 hours post-treatment, compared to untreated cells (Figure 3.9.1.1B, panel 3).

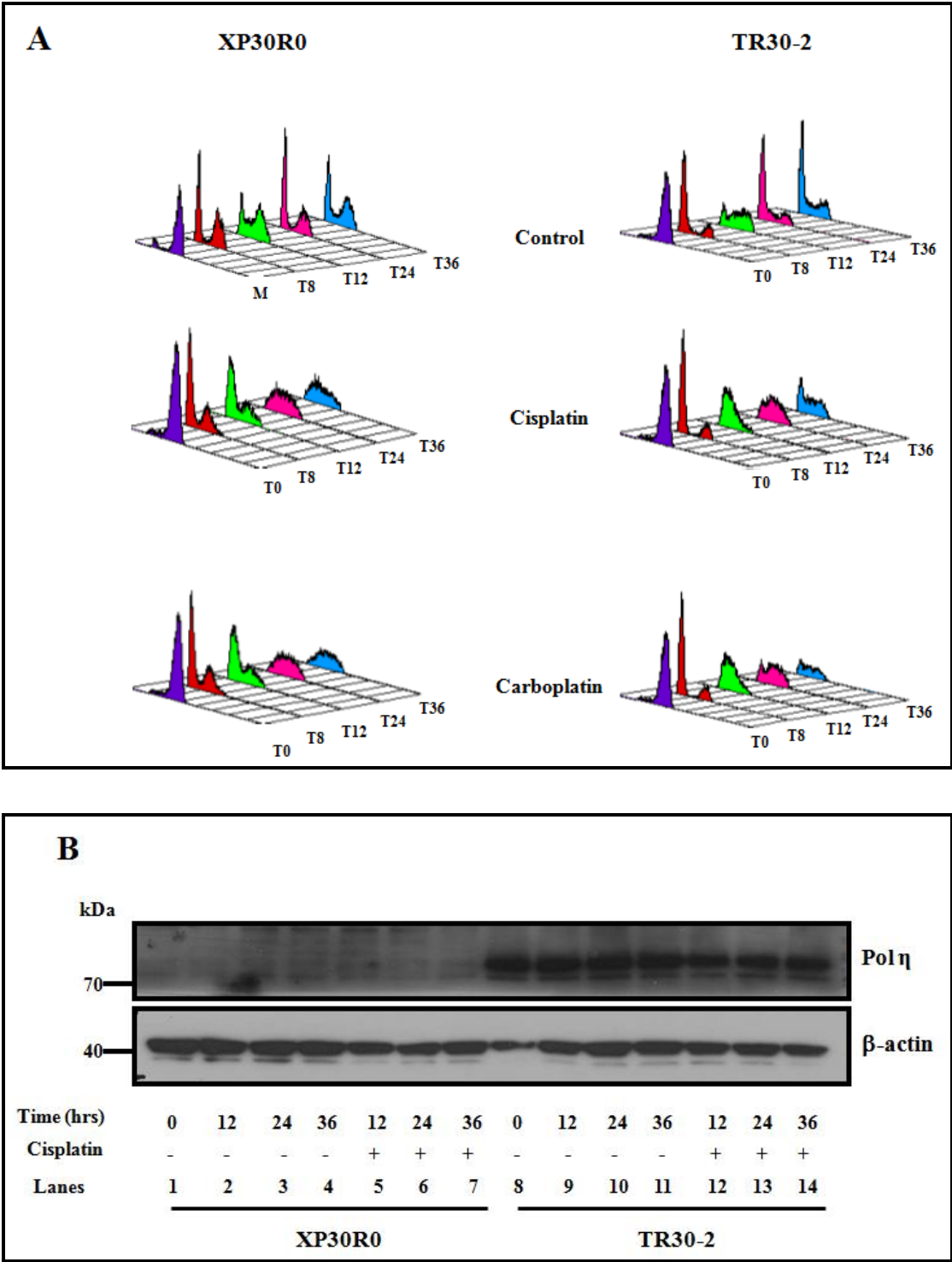
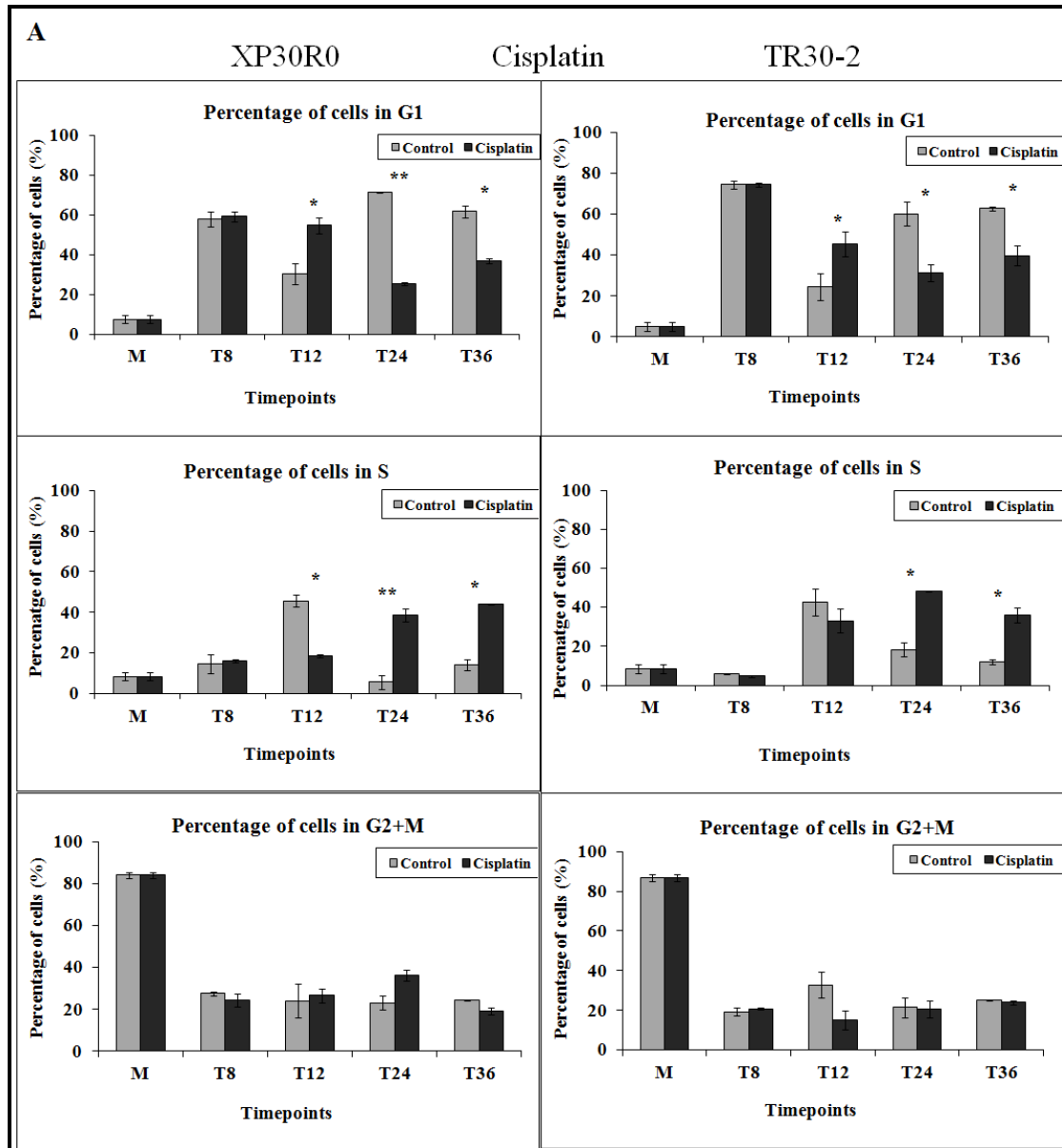


Figure 3.9.1 Histogram profiles showing cell cycle distribution of XP30R0 and TR30-2 cells treated with cisplatin or carboplatin in M-phase. (A) XP30R0 and TR30-2 cells in M-phase were treated with cisplatin (1.66 μ M) or carboplatin (50 μ M) and cells were harvested at 0 (M-phase cells), 12, 24 and 36 hours post-

treatment. The cells were stained with propidium iodide and analysed by flow cytometry. The histogram profiles show the distribution of cells in different phases of the cell cycle. (B) Western blot showing pol η levels in TR30-2 cells across these timepoints.



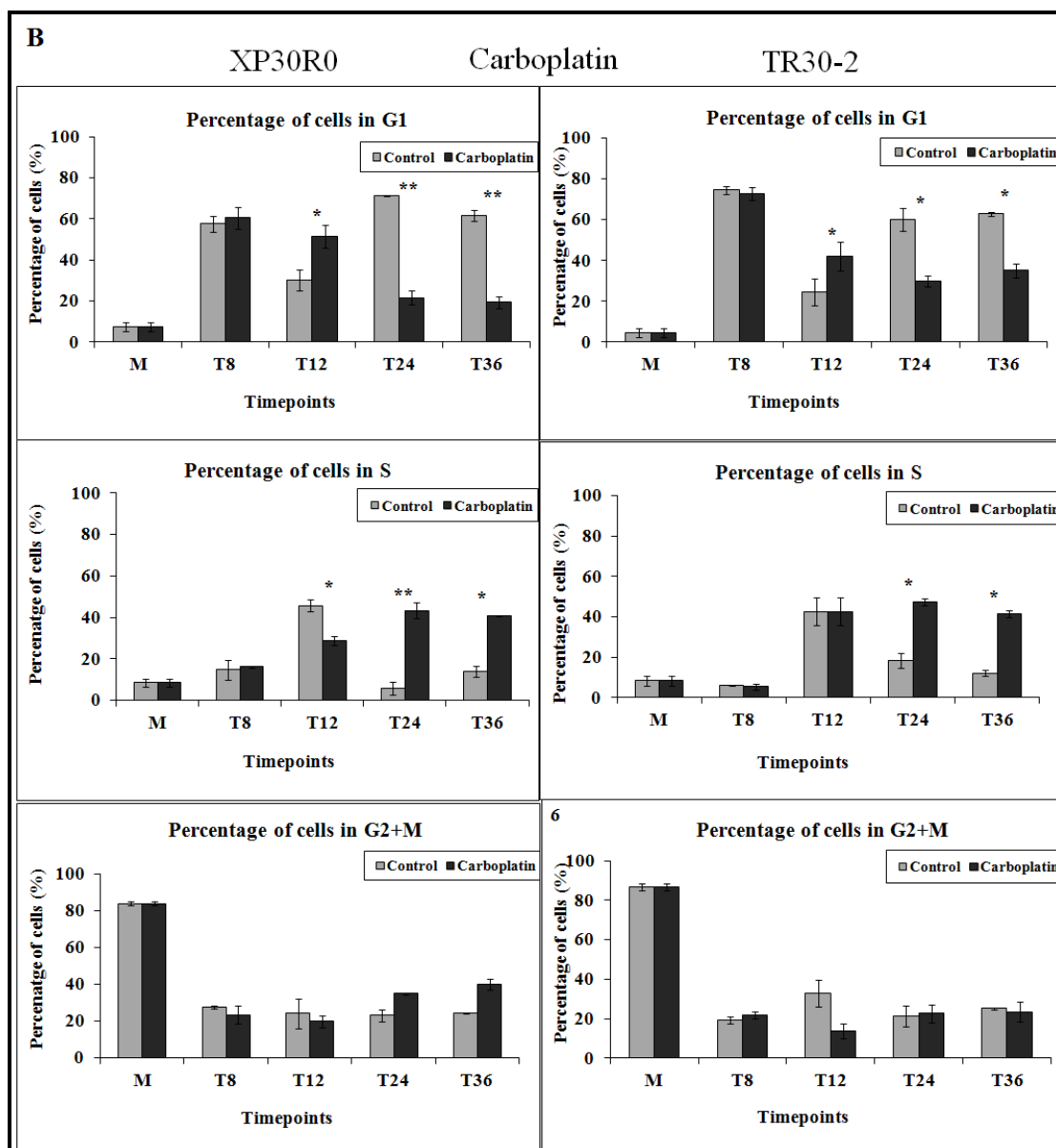


Figure 3.9.1.1. Cell cycle distribution of XP30R0 and TR30-2 cells treated with cisplatin or carboplatin in M-phase. (A) XP30R0 and TR30-2 cells in M-phase shows the percentage of cells in each phase of the cell cycle, in control (untreated), and in cisplatin- or (B) carboplatin-treated XP30R0 and TR30-2 cells. Each data point represents a mean of three experiments; error bars represent one standard deviation. Significant differences in the percentage of cells in G1- and S-phase between control and treated XP30R0 and TR30-2 cells was, determined using Student t-test are shown by * ($p < 0.05$) and ** ($p < 0.005$).

Summary

Following treatment of M-phase XP30R0 and TR30-2 cells with cisplatin and carboplatin, cisplatin-treated XP30R0 cells showed a delay in exiting G1 phase; this effect was less pronounced in TR30-2 cells. This may indicate a role for pol η in G1-phase. At later times, 24 and 36 hours post treatment; XP30R0 and TR30-2 cells were arrested in S-phase.

3.9.2. Determination of BrdU incorporation after cisplatin and carboplatin treatment in M-phase cells lacking or expressing DNA pol η

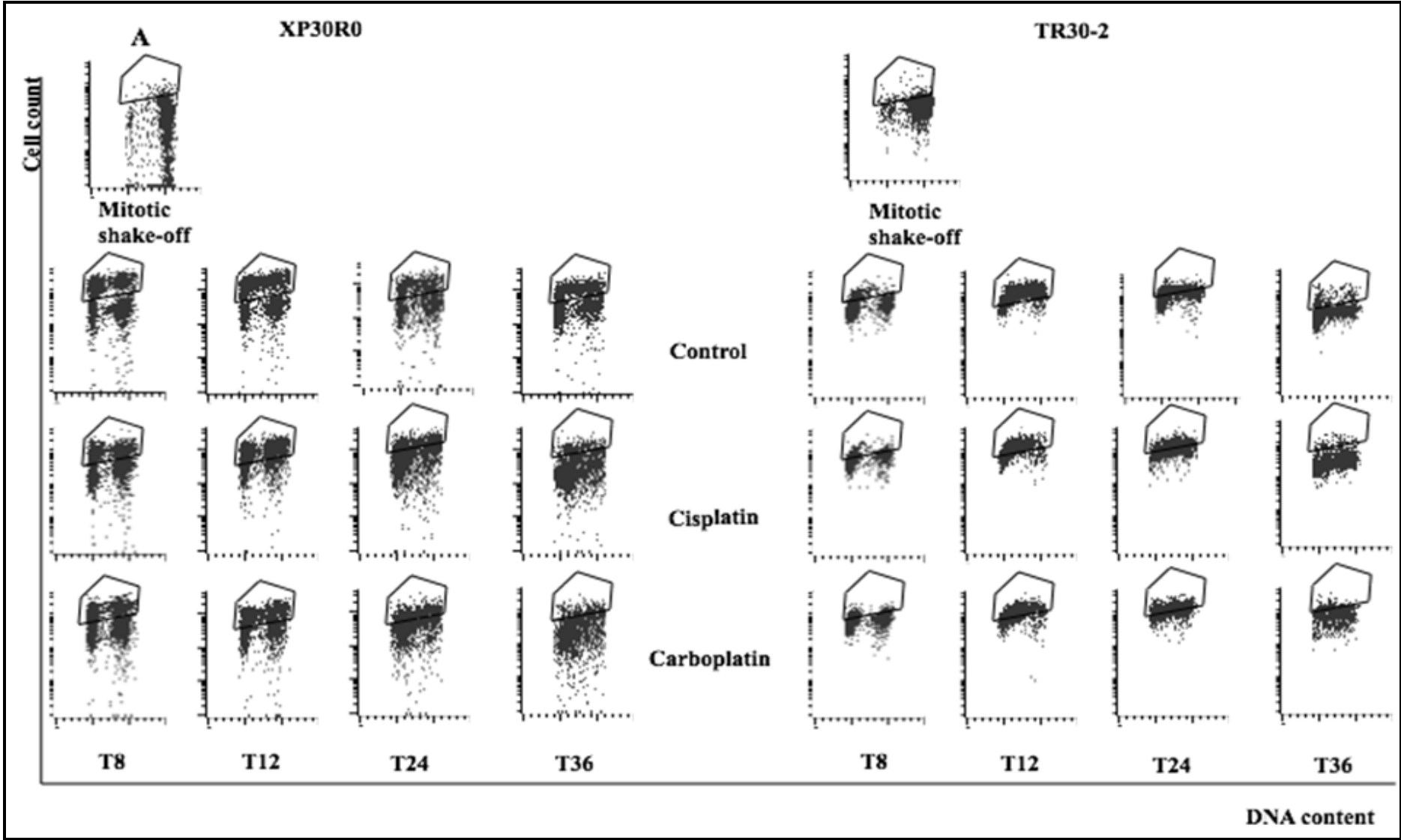
To investigate the effect on DNA replication of treating M-phase cells with cisplatin or carboplatin, XP30R0 and TR30-2 cells were treated with cisplatin or carboplatin and harvested after 8, 12, 24 and 36 hours. Cells were pulse-labelled with BrdU one hour prior to harvesting. BrdU incorporation was analysed by flow cytometry (Figure 3.9.2A), and the percentage of cells incorporating BrdU was determined (Figure 3.9.2B).

In untreated XP30R0 cells, there is an increase in the percentage of BrdU-positive cells from 5% to 70% 12 hours after release from nocodazole arrest (Figure 3.9.2B, panel 1 and 3). This is consistent with entry of the majority of cells into S-phase at this time as shown also by propidium iodide staining and FACS analysis (Figure 3.9.1.1A and B). Treatment with cisplatin or carboplatin decreased the percentage of BrdU-positive cells. The decrease was statistically significant in the case of cisplatin-treated cells (Figure 3.9.2B, panel 1 and 3). Consistent with progress through and exit from S-phase, 24 and 36 hours after nocodazole release, the percentage of BrdU-positive control cells decreased (Figure 3.9.2B, panel 1 and 3).

The major effects of cisplatin and carboplatin on BrdU incorporation in XP30R0 cells was that sustained BrdU incorporation was observed at 24 hours following drug treatment, while at this time control cells had exited S-phase (Figure 3.9.2B, panel 1 and 3). This is consistent with strong S-phase arrest, as shown by an increased percentage of cells in S-phase (Figure 3.9.1.1B). By 36 hours, control cells had returned to S-phase, reflected in an increase in percentage of BrdU-positive cells,

while in drug-treated cells, the percentage of BrdU-positive cells was greatly reduced (Figure 3.9.2B, panel 1 and 3). This is consistent with arrest of cells in S-phase, associated with inhibition of ongoing DNA replication.

In TR30-2 cells expressing pol η , the pattern of BrdU incorporation was broadly similar. Control cells showed an increased in the percentage of BrdU-positive cells at 12 hours (Figure 3.9.2B, panel 2 and 4), consistent with the majority of cells being in S-phase 12 hours after nocodazole release (Figure 3.9.2B, panel 2 and 4). However, following cisplatin and carboplatin treatment, the percentage of BrdU-positive cells was increased at 24 hours relative to untreated cells, consistent with S-phase arrest in these cells (Figure 3.9.2B, panel 2 and 4). At 36 hours post-treatment, the difference between the percentage of BrdU-positive cells in control and cisplatin or carboplatin treated cells is less pronounced in TR30-2 than in XP30R0 cells (Figure 3.9.2B, panel 3, 4, 1 and 2), possibly reflecting ongoing replication in pol η -expressing cells. However, this effect was small and requires further investigation.



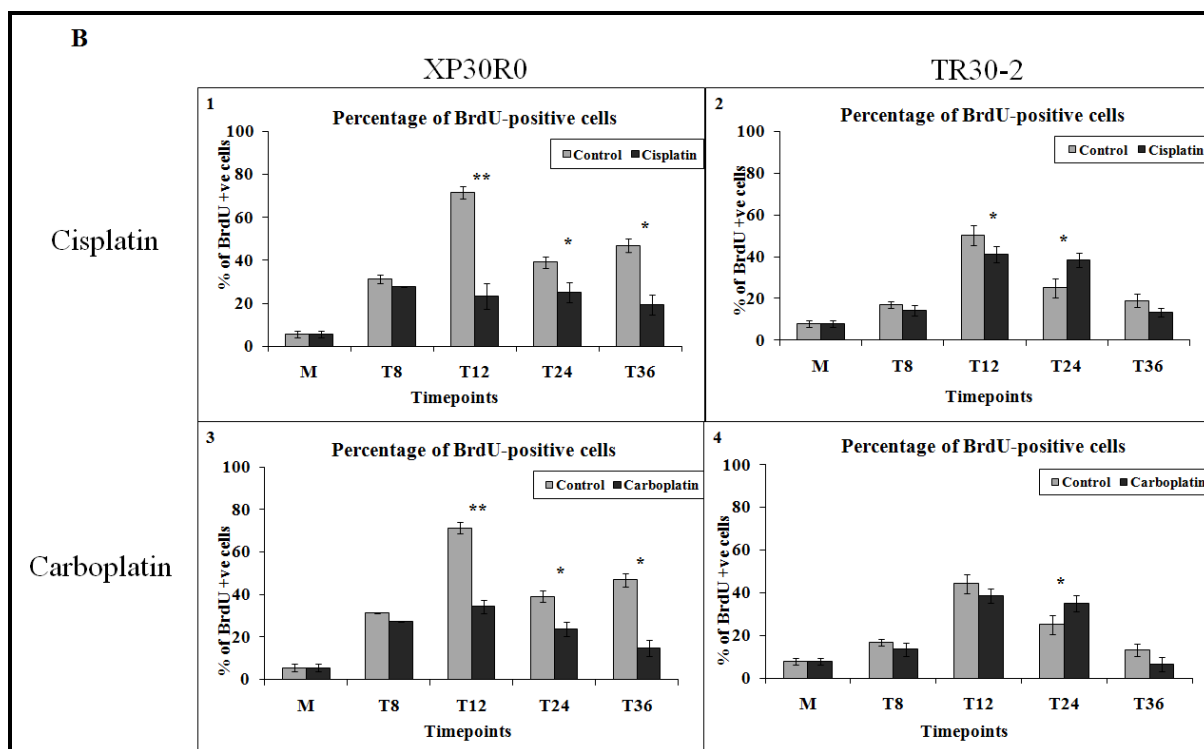


Figure 3.9.2. BrdU incorporation in XP30R0 and TR30-2 cells treated with cisplatin or carboplatin at M-phase. (A) XP30R0 and TR30-2 cells were treated with cisplatin (1.66 μ M) or carboplatin (50 μ M) in M-phase and harvested at 8, 12, 24 and 36 hours post-treatment. Cells were pulse-labelled with BrdU 1 hour prior to harvesting at the respective time points. The cells were stained with propidium iodide and with FITC labelled anti-BrdU antibody and analysed by flow cytometry. The dot blots show the distribution of BrdU-positive cells in S-phase of the cell cycle. (B) Bar graphs represent the percentage of BrdU-positive cells in control (untreated), and cisplatin or carboplatin treated XP30R0 and TR30-2 cells. Each data point represents a mean of three experiments; error bars represent one standard deviation. Significant differences in the percentage of BrdU-positive XP30R0 and TR30-2 cells post-cisplatin-or carboplatin treatment, determined using Student t-test, are shown by * ($p < 0.05$) ** ($p < 0.005$).

Summary

Compared to untreated cells, the percentage of BrdU-positive pol η -deficient XP30R0 cells was reduced at 12 hours, while the percentage of TR30-2 cells was similar to control cells. Following treatment of M-phase cells with cisplatin and carboplatin, both XP30R0 and TR30-2 cells accumulated in S-phase at 24 and 36 hours post-treatment, consistent with strong arrest in S-phase.

3.9.3. Expression of cyclin B and cyclin E after treatment of M-phase XP30R0 and TR30-2 cells with cisplatin

To further characterise the effects of cisplatin on cell cycle progression, M-phase XP30R0 and TR30-2 cells were treated with cisplatin (1.66 μ M), and the levels of cyclin B and cyclin E were analysed by Western blotting at 12, 24 and 36 hours post-treatment. Cisplatin-treatment affected the levels of cyclin B and cyclin E in extracts of XP30R0 and TR30-2 cells, as determined by densitometric analysis of Western blots.

In control XP30R0 cells, cyclin B expression increased for up to 36 hours, as the cells progressed through S-phase and into G2/M-phase (Figure 3.9.3B, panel 1). Following treatment with cisplatin, cyclin B expression did not change between 24 and 36 hours post-treatment, as cells were arrested in S- and G2/M-phases (Figure 3.9.3B, panel 1). In control TR30-2 cells, cyclin B expression increased up to 24 hours, as the cells progressed through S-phase and into G2/M-phase (Figure 3.9.3B, panel 2). Following cisplatin treatment, there was little change in cyclin B expression compared to control cells (Figure 3.9.3B, panel 2).

In control XP30R0 cells, cyclin E expression decreased at 12 hours as cells progressed through S- and G2/M-phases, and increased at 24 and 36 hours consistent with cells progressing from G1-to S-phase (Figure 3.9.3B, panel 3). Cyclin E expression was lower at 24 and 36 hours compared to control cells, when cells were arrested at S- and G2/M-phases (Figure 3.9.3B, panel 3). In TR30-2 cells, cyclin E expression was generally higher than in XP30RO cells, and there was little change in the overall levels.

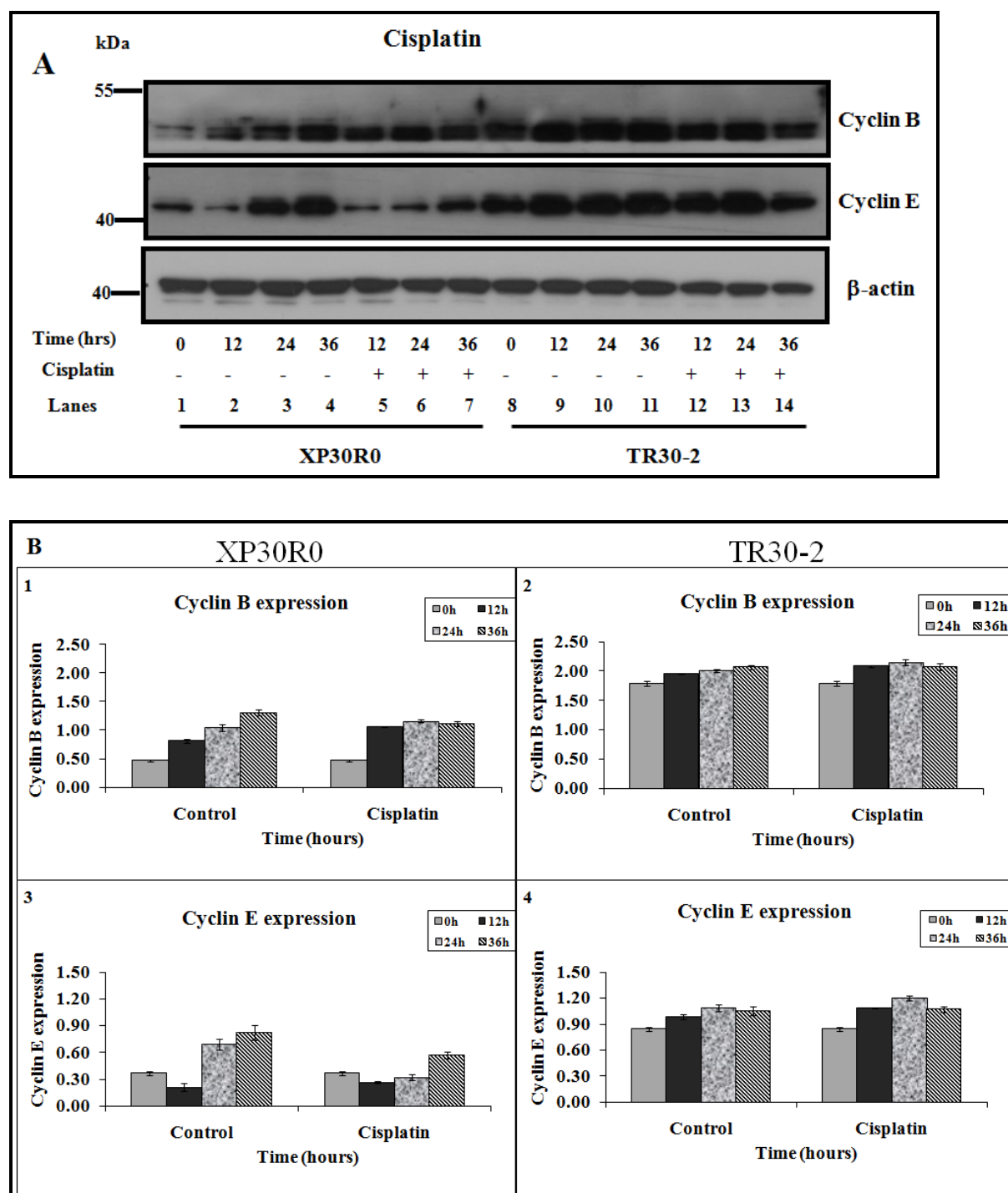


Figure 3.9.3. Effect of cisplatin on cyclin B and cyclin E expression. (A) M-phase XP30R0 and TR30-2 cells were treated with cisplatin (1.66 μ M) and harvested after 12, 24 and 36 hours. Cell extracts were analysed by SDS-PAGE and Western blotting. Panels 1, 2 and 3 show Western blots of cyclin B, cyclin E and actin respectively. Cyclin B and cyclin E expression was compared between controls and cisplatin-treated in both XP30R0 and TR30-2 cells. Western blots are representative of three experiments. (B) Graph, calculated using densitometry analysis, represents expression of cyclin B in XP30R0 and TR30-2 treated with cisplatin (panel 1 and 2) and cyclin E in XP30R0 and TR30-2 treated with cisplatin (panel 3 and 4) normalised to the respective actin levels in the sample. The values are an average of data from three

experiments and error bars represent one standard deviation. There was no statistical significance observed between control and cisplatin-treated cells.

3.9.4. Expression of cyclin B and cyclin E after treatment of M-phase XP30R0 and TR30-2 cells with carboplatin

XP30R0 and TR30-2 cells in M-phase were treated with carboplatin (50 μ M) and the levels of cyclins B and E were analysed by Western blotting at 0, 12, 24 and 36 hours post-treatment. Cisplatin-treatment affected the levels of cyclin B and cyclin E in extracts of XP30R0 and TR30-2 cells, as determined by densitometric analysis of Western blots.

In control XP30R0 cells, cyclin B expression increased up to 36 hours after mock-treatment, as the cells progressed through S-phase and into G2/M (Figure 3.9.4B, panel 1). Following treatment with carboplatin, cyclin B expression did not change at 24 and 36 hours post-treatment, as cells were arrested in S- and G2/M-phase (Figure 3.9.4B, panel 1). In control TR30-2 cells, cyclin B expression also increased at 12 hours as the cells progressed through S-phase and into G2/M (Figure 3.9.4B, panel 2). Following carboplatin treatment, cyclin B expression was lower at later times compared to control cells (Figure 3.9.4B, panel 2).

In control XP30R0 cells cyclin E expression was lower at 12 hours as cells progressed through the S- and G2/M-phases, and increased at 24 and 36 hours consistent with cells progressing from G1- to S-phase (Figure 3.9.4B, panel 3). However, following carboplatin treatment, cyclin E expression increased at 12 hours compared to control cells, consistent with delayed cell cycle progression (Figure 3.9.4B, panel 3). In TR30-2 cells, cyclin E expression increased at 24 and 36 hours in control cells. Following carboplatin treatment, cyclin E expression decreased at 24 and 36 hours compared to control consistent with cells being arrested in S-and G2/M-phases (Figure 3.9.4B, panel 4).

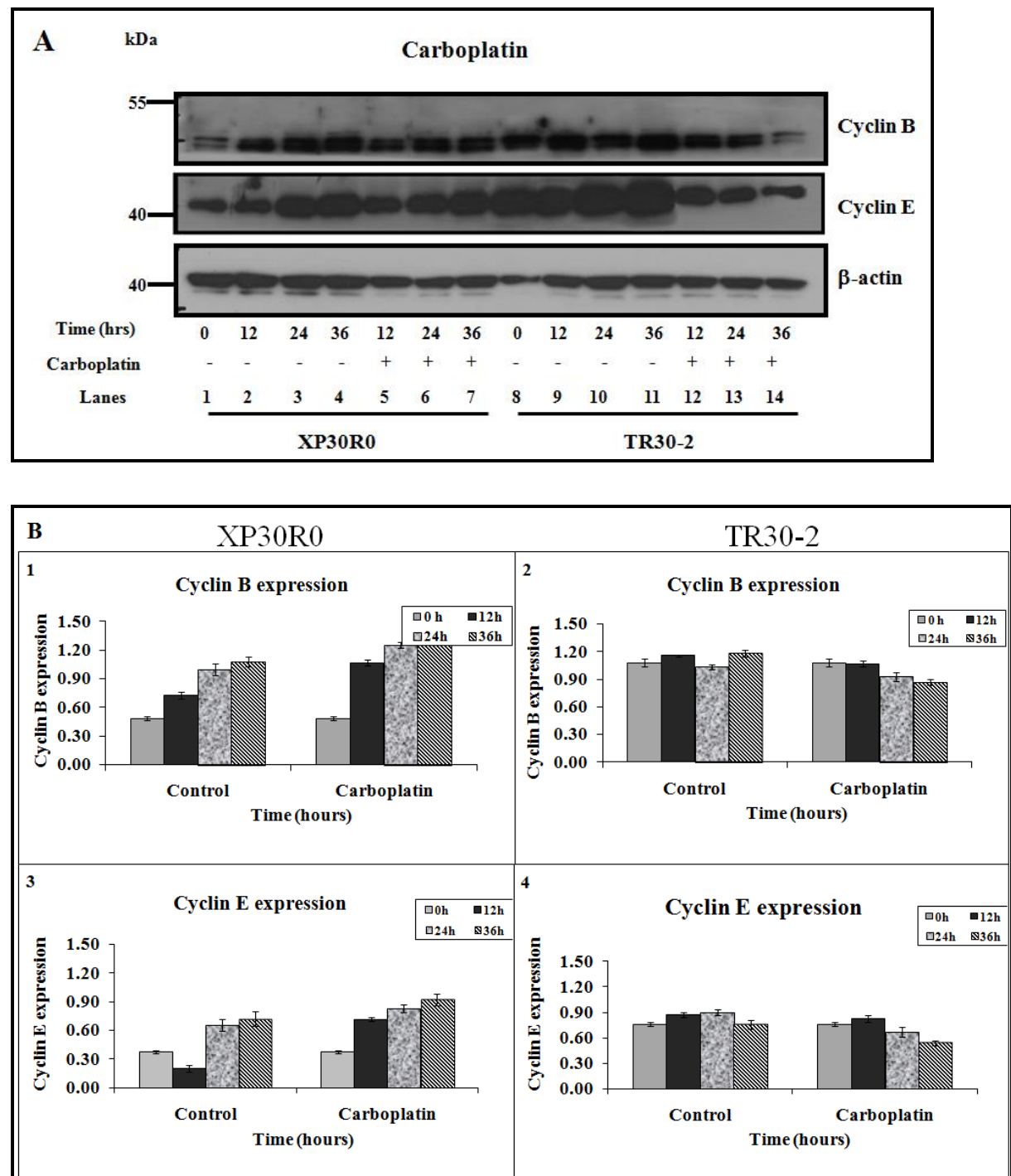


Figure 3.9.4. Effect of carboplatin on cyclin B and cyclin E levels. (A) M-phase XP30R0 and TR30-2 cells were treated with carboplatin (50 μ M) and harvested at 12, 24 and 36 hours. Cell extracts were prepared and analysed by SDS-PAGE and Western blotting. Panels 1, 2 and 3 show Western blots of cyclin B, cyclin E and actin respectively. Cyclin B and cyclin E expression was compared between control and carboplatin-treated in XP30R0 and TR30-2 cells. Western blots are representative of three experiments. (B) Graph, calculated using densitometry analysis, represents expression of cyclin B in XP30R0 and TR30-2 treated with carboplatin (panel 1 and 2) and cyclin E in XP30R0 and TR30-2 treated with carboplatin (panel 3 and 4) normalised to the respective actin levels in the sample. The values are an average of

data from three experiments and error bars represent one standard deviation. There was no statistical significance observed between control and carboplatin-treated cells.

3.10. Activation of DNA damage responses

3.10.1. H2AX phosphorylation in cisplatin- and carboplatin-treated M-phase XP30R0 cells

H2AX is phosphorylated by ATM at serine 139 generating γ H2AX at sites of DNA strand breaks (Kobayashi et al., 2009). To investigate H2AX phosphorylation in M-phase cells, pol η -deficient XP30R0 cells were treated with cisplatin (1.66 μ M) or carboplatin (50 μ M). Cells in M-phase were treated with drug, harvested after 12, 18, 24 and 36 hours, and analysed by SDS-PAGE and Western blotting. In control XP30R0 cells (Figure 3.10.1A and B, panel 1, lanes 1-5), no phosphorylation of H2AX on serine 139 was detected. Thus, nocodazole arrest and release did not generate significant DNA damage in these cells. In cisplatin-treated cells, phosphorylation of H2AX was strongly induced at 12 hours. H2AX phosphorylation increased with time up to 36 hours post-treatment (Figure 3.10.1A, panel 1, lanes 6-9). In case of carboplatin treatment, γ H2AX was also detectable at 12 hours post-treatment, and increased up to 36 hours post-treatment (Figure 3.10.1B, panel 1, lanes 6-9). Immunofluorescent studies were not carried out on M-phase cells because these cells failed to attach to the slides, an essential step to analyse these cells using immunofluorescence.

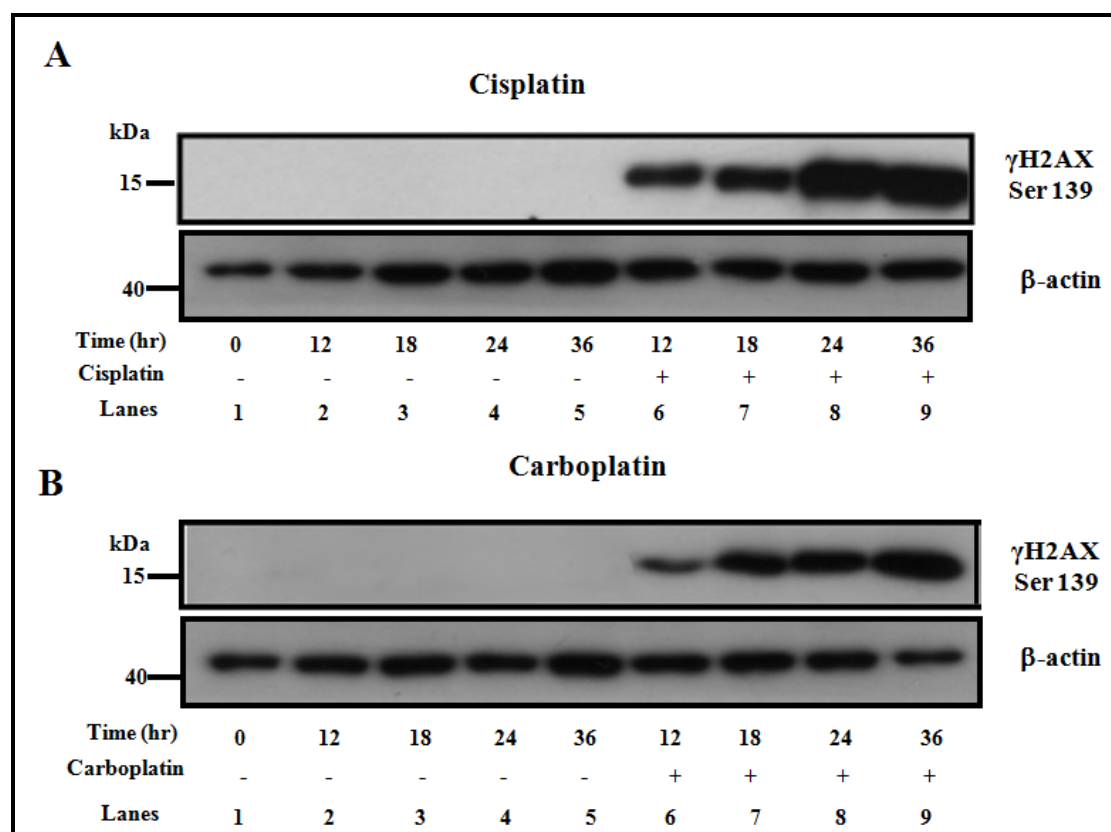


Figure 3.10.1 H2AX phosphorylation in cisplatin and carboplatin-treated M-phase XP30R0 cells. M-phase XP30R0 cells were treated with (A) cisplatin (1.66 μ M) or (B) carboplatin (50 μ M) and harvested at 12, 18, 24 and 36 hours. Cell extracts were prepared and analysed by SDS-PAGE and Western blotting. Panel 1 shows Western blot of H2AX phosphorylated at serine 139 using anti-H2AX phosphorylated at serine 139. Actin was used as a loading control. Western blots are representative of three experiments.

3.10.2. Phosphorylation of RPA2 on serine4/serine8 in cisplatin and carboplatin-treated M-phase XP30R0 and TR30-2 cells

To investigate the relationship between platinum-induced RPA2 phosphorylation and M-phase cells, XP30R0 and TR30-2 cells in M-phase were treated with cisplatin or carboplatin, harvested 12, 24 and 36 hours later. Cell extracts were prepared and analysed by SDS-PAGE and Western blotting. The mitotic form of RPA2 was detected in mitotic cells (Fig. 3.10.2A and B, lanes 1 and 8). RPA2 phosphorylated on serine4/serine8 in XP30R0 cells was strongly detected at 24 and 36 hours post-cisplatin and carboplatin-treatment, peaking at 24 hours following cisplatin treatment, and at 36 hours following carboplatin treatment (Figure 3.10.2A and B, panel 2, lanes

6 and 7). In TR30-2 cells, the extent of serine4/serine8 RPA2 phosphorylation was reduced compared to XP30R0 cells, but the timing of phosphorylation was identical (Figure 3.10.2A and B, panels 2, lanes 6, 7, 13 and 14). Thus, RPA2 phosphorylation again is a late event in response to cisplatin or carboplatin, when cells in mitosis were treated with drug. The timing of RPA2 phosphorylation corresponds to the time at which the majority of XP30R0 and TR30-2 cells are arrested in S-phase (Figure 3.9.1.1A and B). As noted, this may be consistent with a role for RPA phosphorylation in repair of double strand breaks occurring as a result of replication fork collapse (Cruet-Hennequart et al., 2006, Cruet-Hennequart et al., 2008, Kobayashi et al., 2009) in cells arrested in S-phase.

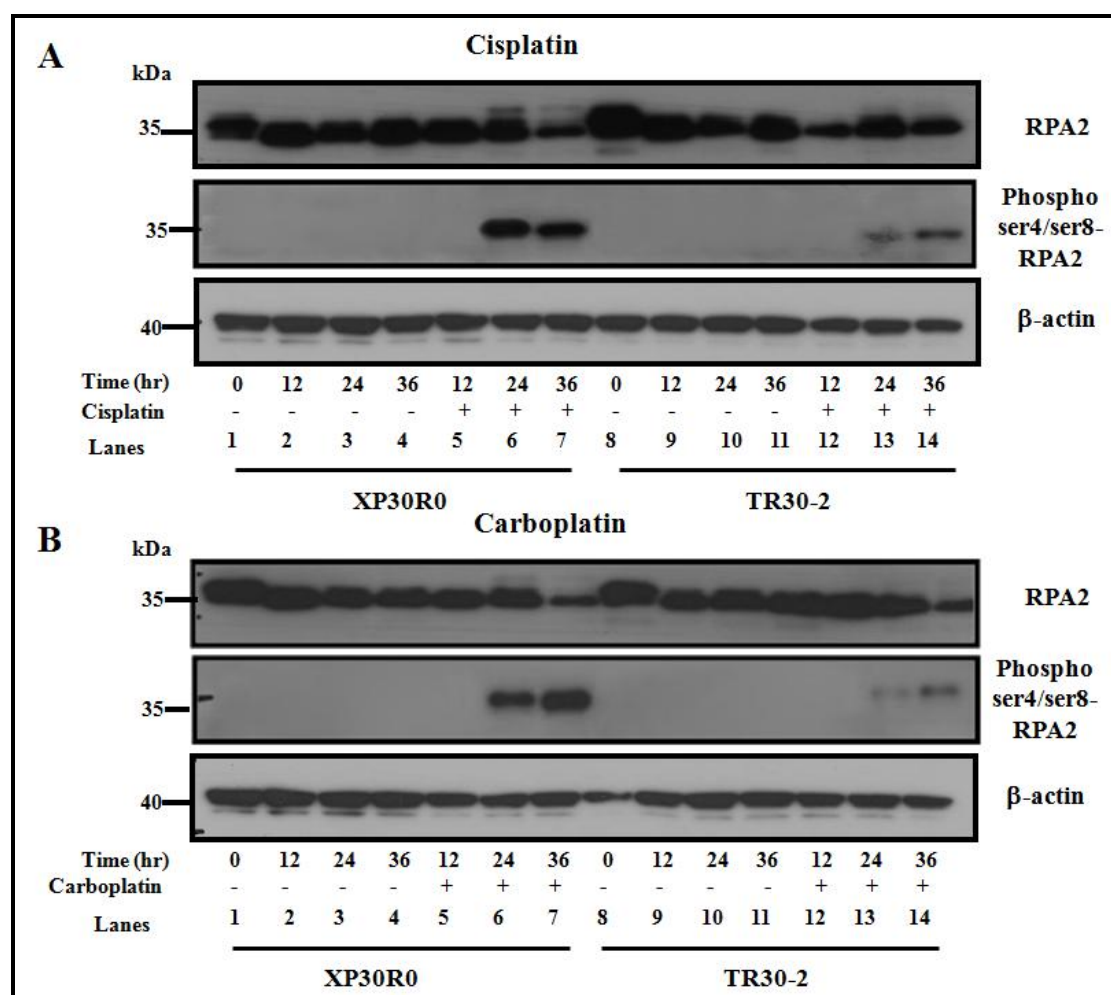


Figure 3.10.2. Time-course of RPA2 phosphorylation in M-phase treated XP30R0 and TR30-2 cells with cisplatin and carboplatin. XP30R0 and TR30-2 cells in M-phase were treated with (A) cisplatin (1.66 μ M) or (B) carboplatin (50 μ M) and harvested at 12, 24 and 36 hours. Cell extracts were prepared and analysed by SDS-PAGE and Western blotting. Panels 1, 2 and 3 show Western blots of RPA2; RPA2 phosphorylated on serine4/serine8 and actin using anti-RPA2, anti-RPA2

serine4/serine8 and anti- β -actin antibodies respectively. Western blots are representative of three experiments.

3.10.2.1. Effect of PIK kinase and CDK inhibitors on cisplatin- and carboplatin-induced RPA2 hyperphosphorylation in M-phase XP30R0 clls

To investigate the roles of DNA-PK, ATM and CDK in RPA2 phosphorylation, M-phase XP30R0 cells are co-treated with cisplatin or carboplatin and with either NU7441, a small molecule inhibitor of DNA-PK_{cs} or with KU55933, an inhibitor of ATM kinase (Veuger et al., 2003, Hickson et al., 2004, Cowell et al., 2005) or with roscovitine, an inhibitor of CDK1/2 (Anantha et al., 2007, Stephan et al., 2009) at M-phase. Cisplatin and carboplatin induced phosphorylation of RPA2 on serine4/serine8 (Figure 3.10.2.1A and B, panel 1, lane 3, 6 and 9) and (Figure 3.10.2.1A and B, panel 1, lane 2, 6 and 9). When cells were treated with cisplatin and NU7441 (Figure 3.10.2.1A and B, panel 1, lane 2) or carboplatin and NU7441 (Figure 3.10.2.1A and B, panel 1, lane 1) phosphorylation of RPA2 was reduced, consistent with data presented previously showing that NU7441 inhibited RPA phosphorylation on serine4/serine8 in G1- and S-phase cells, and with previous reports (Cruet-Hennequart et al., 2008).

There was no reduction in RPA2 phosphorylation on serine4/serine8 in cells treated with cisplatin or carboplatin and KU55933 (Figure 3.10.2.1A, panel 1, lane 5 and 6), demonstrating that ATM does not play a role in phosphorylation of RPA2 on serine4/serine8 (Cruet-Hennequart et al., 2008). Roscovitine inhibited cisplatin- and carboplatin-induced RPA2 phosphorylation (Figure 3.10.2.1A, panel 1, lane 8 and 9). The effect of roscovitine on RPA2 phosphorylation at serine4/serine8 was somewhat stronger in XP30R0 cells treated with carboplatin than those treated with cisplatin (Figure 3.10.2.1A and B, panel 1, lane 8 and 9). As noted previously, this may be consistent with a requirement for phosphorylation of RPA2 on serine 23 or serine 29 before the protein is phosphorylated on serine4/serine8 (Olson et al., 2006, Anantha et al., 2007).

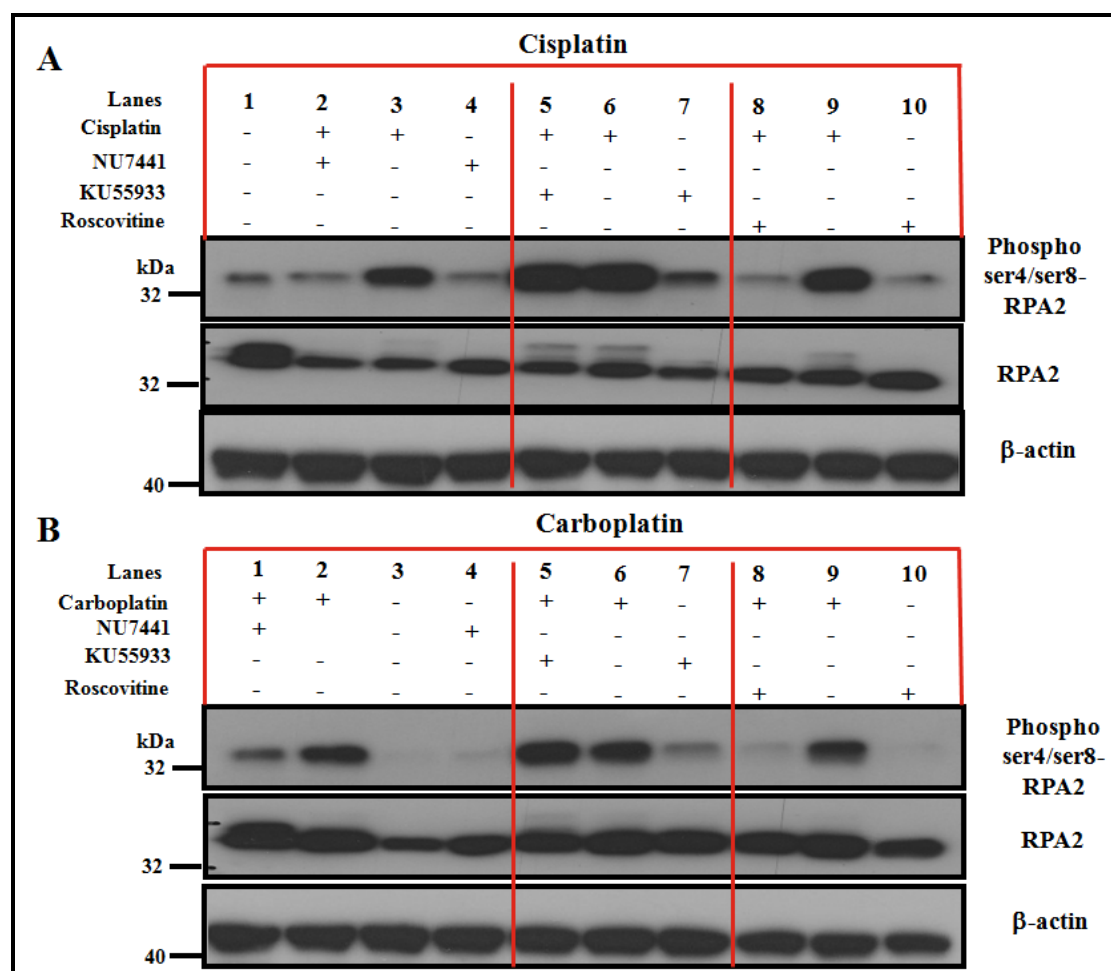


Figure 3.10.2.1. Effect of NU7441, KU55933 and roscovitine on cisplatin- or carboplatin-induced RPA2 phosphorylation in M-phase treated XP30R0 cells. Western blots of M-phase treated XP30R0 cells treated with (A) cisplatin (1.66 μ M) or (B) carboplatin (50 μ M) in the presence or absence of NU7441 (10 μ M) or KU55933 (10 μ M) or roscovitine (15 μ M) for 24 hours. Cell extracts were prepared and analysed by SDS-PAGE and Western blotting. Panels 1, 2 and 3 shows Western blots of RPA2 phosphorylated at serine4/ serine8, RPA2 and actin using anti-RPA2 ser 4/ser 8, anti-RPA2 and anti- β -actin antibodies respectively. Western blots are representative of three experiments.

3.10.3. The timing of cisplatin- and carboplatin-induced Chk1 and RPA2 phosphorylation in XP30R0 cells treated in M-phase

As noted above, in G1- and S-phase cells, Chk1 phosphorylation precedes RPA2 phosphorylation on serine 4/serine 8. The timing of Chk1 and RPA2 phosphorylation in M-phase XP30R0 cells treated with cisplatin (1.66 μ M) and carboplatin (50 μ M) was compared. Cells in M-phase were treated with drug, harvested after 12, 18, 24

and 36 hours, and analysed by SDS-PAGE and Western blotting. In control XP30RO cells (Figure 3.10.3A and B, panel 2, lanes 1-5) no phosphorylation of Chk1 was detectable (Figure 3.10.3A and B, panel 2, lane 3). In both cisplatin- and carboplatin-treated cells, phosphorylation of Chk1 was strongly detected 12 hours post-treatment, and the protein remained phosphorylated for up to 24 hours (Figure 3.10.3A and B, panel 2, lane 6, 7 and 8). At 36 hours following cisplatin and carboplatin treatment, Chk1 phosphorylation was reduced (Figure 3.10.3A and B, panel 2, lane 9). In control cells, slight phosphorylation of RPA2 at serine4/serine8 was detected at 24 hours (Figure 3.10.3A and B, panel 3, lanes 4). In cisplatin-treated cells, strong phosphorylation of RPA2 on serine4/serine8 was detectable 24 and 36 hours post-treatment (Figure 3.10.3A, panel 2, lanes 6-9). In carboplatin-treated cells phosphorylation of RPA2 at serine4/serine8 was also strongly detected from 24 to 36 hours post-treatment. (Figure 3.10.3B, panel 3, lanes 6-9). This data clearly shows that cisplatin and carboplatin-induced phosphorylation of Chk1 is an earlier event, while RPA2 phosphorylation on serine 4/serine 8 is a later event, in response to DNA damage in M-phase XP30RO cells.

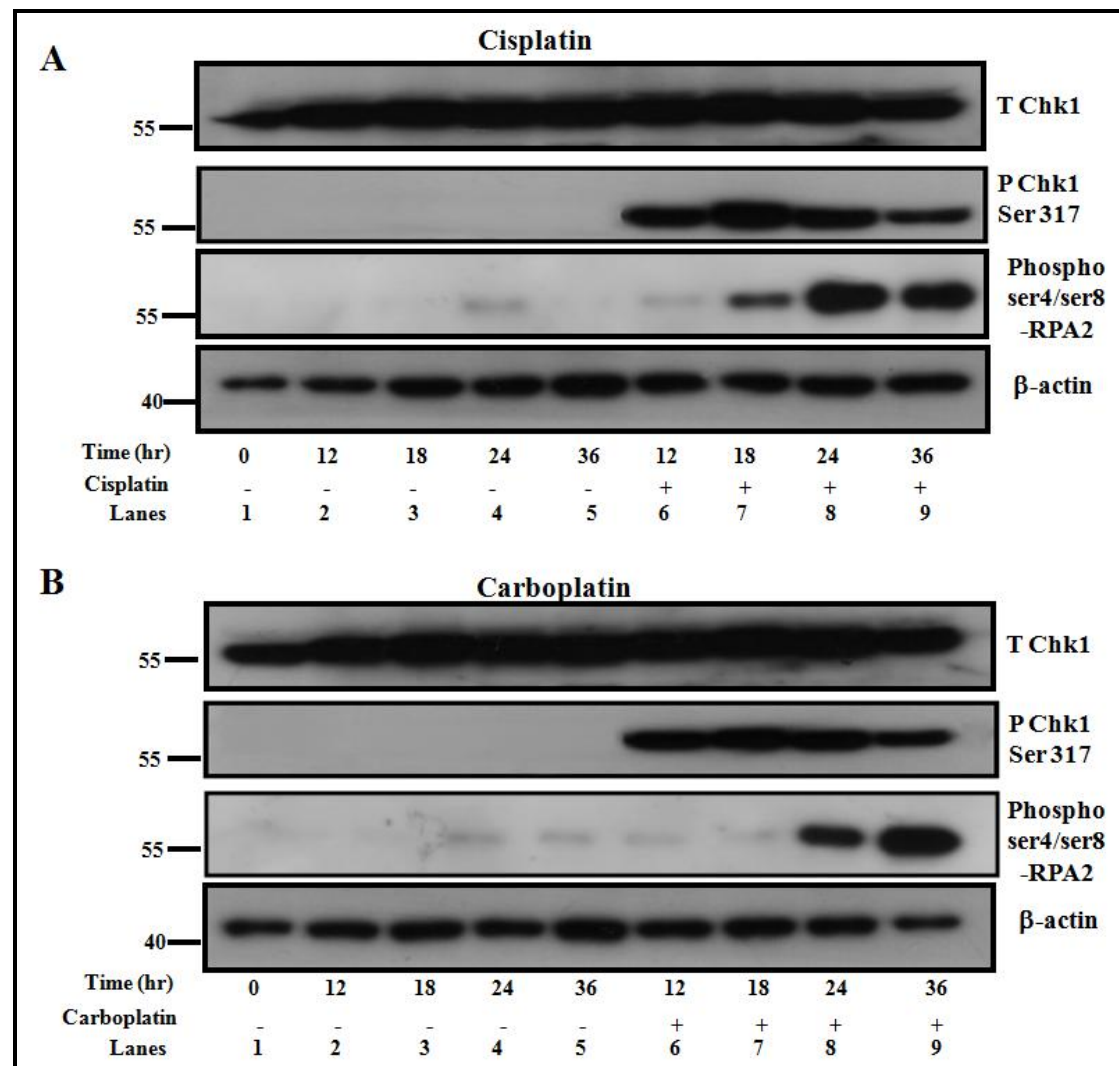


Figure 3.10.3. Chk1 and RPA2 phosphorylation in cisplatin- and carboplatin-treated M-phase XP30R0 cells. S-phase XP30R0 cells were treated with (A) cisplatin (1.66 μ M) or (B) carboplatin (50 μ M) and harvested at 12, 18, 24 and 36 hours. Cell extracts were prepared and analysed by SDS-PAGE and Western blotting. Panels 1, 2 and 3 show Western blots of Chk1 phosphorylated at serine 317, RPA2 phosphorylated at serine4/serine8 and β -actin respectively. Western blots are representative of three experiments.

Summary of effects of cisplatin and carboplatin on M-phase cells

Following treatment of XP30R0 cells in M-phase with cisplatin and carboplatin, there was evidence for a delay in cells exiting G1-phase. Both XP30R0 and TR30-2 cells were arrested in S-phase at 24 and 36 hours post-treatment. The expression of cyclin B and E was altered post treatment compared to the control cells in both XP30R0 and TR30-2 cells. The percentage of γ H2AX-positive cells was found to be similar in both

cisplatin-and carboplatin-treated cells. RPA2 phosphorylated on serine 4/ serine 8 was strongly induced in XP30R0 cells at 24 and 36 hours post-cisplatin and carboplatin treatment. In TR30-2 cells, this response occurred at identical times but was greatly reduced in intensity. Platinum-induced Chk1 phosphorylation on serine 317 occurred earlier than phosphorylation of RPA2 on serine4/serine8 following treatment of M-phase cells with cisplatin and carboplatin. DNA-PK and CDK1/2 were found to play a role in cisplatin and carboplatin-induced phosphorylation of RPA2 on serine4/serine8.

3.11. Comparison of the effects of cisplatin and carboplatin treatment in different cell cycle phases

The main aim of the present study was to investigate whether cell cycle stage at the time of treatment affected the response of pol η -deficient and expressing human cells to cisplatin and carboplatin. The cells were first synchronised by nocodazole to obtain populations enriched in mitotic cells. After nocodazole washout, cells were allowed to progress through the cell cycle, and harvested at 6 and 12 hours to obtain cells in G1- and S-phases, respectively (Section 3.5). Cells enriched in G1-, S- and M-phases were treated with cisplatin or carboplatin and analysed for cell viability, cell cycle progression and key DNA damage responses. Here the results described above are compared, to identify similarities and differences in the response to cells treated with cisplatin or carboplatin at different cell cycle phases.

3.11.1. Cell viability following treatment in different phases

Asynchronous pol η -deficient XP30R0 cells were more sensitive to cisplatin or carboplatin treatment than pol η -expressing TR30-2 cells. When cells were treated at specific cell cycle stages, S-phase cells were more sensitive to cisplatin or carboplatin, compared to cells in G1- and M-phase at the time of treatment.

3.11.2. Analysis of cell cycle progression among cells treated in different phases

Cell cycle progression was affected when XP30R0 and TR30-2 cells were treated at different phases with cisplatin and carboplatin, as determined using flow cytometry. When G1-phase pol η -deficient XP30R0 cells were treated with cisplatin, there was a slight delay in exiting G1-phase, followed by a strong S-phase arrest in later time points. Following carboplatin treatment, a strong S-phase arrest was detected at later time points. In TR30-2 cells expressing pol η , strong S-phase arrest was detected at later time points, 24 and 36 hours post-treatment.

When S-phase XP30R0 cells were treated with cisplatin, cells were arrested in S-phase. Following carboplatin treatment, cell cycle arrest at early times was less

pronounced than following cisplatin treatment, and there was evidence that cells were arrested in S-phase in the second round of replication. A similar observation was made in TR30-2 cells treated with either cisplatin or carboplatin.

When M-phase XP30R0 cells were treated with cisplatin or carboplatin, there was evidence for a delay in cells exiting G1-phase, followed by a strong S-phase arrest at later times. In TR30-2 cells, a strong S-phase arrest was detected at later times following drug treatment.

3.11.3. Analysis of key DNA damage responses in cells treated in different phases.

A number of cisplatin- and carboplatin-induced PIK kinase-mediated DNA damage responses were examined, including phosphorylation of H2AX, Chk1 and RPA2 phosphorylation.

H2AX phosphorylation on serine 139 was induced following cisplatin and carboplatin treatment of XP30R0 cells in G1-, S- and M-phases. Chk1 phosphorylation on serine 317 was also detected in both cisplatin- or carboplatin-treated XP30R0 cells in G1-, S- and M-phases treated cells. RPA2 phosphorylation on serine4/serine8 was induced by cisplatin and carboplatin, but this response was always a late event, irrespective of what phase the cells were in at the time of treatment. Thus, RPA2 phosphorylation on serine4/serine8 peaked between 24 and 36 hours post treatment. By comparing the timing of Chk1 phosphorylation and RPA2 phosphorylation, it was shown that Chk1 phosphorylation was an earlier event and the RPA2 phosphorylation was a late event in G1-, S- and M-phase cells treated with cisplatin or carboplatin. This is consistent with activation of the ATR-mediated S-phase checkpoint preceding induction of RPA phosphorylation.

Consistent with a role for replication-arrest induced strand breaks being required for RPA2 phosphorylation on serine4/serine8, this event usually occurred later than H2AX phosphorylation, a marker of strand breaks, and the intensity of RPA2 phosphorylation was enhanced in XP30RO cells lacking pol η , where replication arrest is enhanced (Cruet-Hennequart et al., 2008; 2009). NU7441 or roscovitine inhibited

RPA2 phosphorylation, independent of what cell cycle stage the cells were in at the time of cisplatin or carboplatin treatment.

Chapter 4: Discussion

A better understanding of the effects of platinum-based chemotherapeutic drugs, including cisplatin and carboplatin, on cell cycle progression and DNA damage responses is important to improve cancer treatment approaches. Cisplatin and carboplatin form DNA adducts which result in the blockage of replication fork progression, as replicative polymerases such as polymerase α , δ and ϵ cannot bypass the resulting structurally altered bases (Lehmann, 2002). Translesion synthesis polymerase including DNA polymerase η (pol η), have a more open active site to accommodate these DNA adducts, allowing replication to occur at sites of DNA damage (Biertumpfel et al., Alt et al., 2007). Pol η can bypass cisplatin-induced intrastrand crosslinks in DNA (Kartalou and Essigmann, 2001a, b, Chaney et al., 2005) and may also play a role in the bypass step during repair of interstrand crosslinks (Niedernhofer et al., 2004, Kawamoto et al., 2005, McIlwraith et al., 2005). These steps may decrease the cytotoxicity of platinum-based chemotherapeutic drugs (Kelland, 2007b). Thus, one of the approaches to increase the efficiency of platinum-based chemotherapeutic drugs may be through inhibition of pol η -mediated translesion synthesis. Previous studies have shown that pol η -deficient human cells are more sensitive to cisplatin than normal cells, and the increased sensitivity can be attributed to the lack of pol η (Bassett et al., 2004, Albertella et al., 2005b, Cruet-Hennequart et al., 2008, Cruet-Hennequart et al., 2009). To investigate the relationship between pol η and the response of human cells to platinum-induced DNA damage, the present study investigated the cell cycle dependence of cisplatin- and carboplatin-induced cytotoxicity and cell cycle arrest, in human pol η -deficient XP30RO cells and TR30-2 expressing pol η treated with drug at different cell cycle phases. To further characterise the effect of cisplatin and carboplatin exposure at different phases of the cell cycle, PIK kinase-activated DNA damage responses, including phosphorylation of Chk1, H2AX and RPA2, were characterised in the pol η -deficient cell line XP30RO.

To investigate the effect of treating cells in different phases of the cell cycle with platinum-based drugs, cells were initially enriched in mitosis using the mitotic inhibitor, nocodazole (Nusse and Egner, 1984, Kung et al., 1990, Stephan et al., 2009). Exposure to 0.1 μ M nocodazole strongly arrested both XP30RO and TR30-2 cells in mitosis, while resulting cell death was reduced compared to exposure to

higher doses of nocodazole. The yield of mitotic cells, collected using the shake-off method from nocodazole-arrested cells, was about 4.5-fold higher compared to the yield of mitotic cells collected by shake-off from an asynchronous population. Cell cycle progression was analysed to determine whether nocodazole affected subsequent progression of cells through the cell cycle. When compared with cells collected by shake-off from asynchronously growing cultures, it was found that cell cycle progression was not significantly different in the cells released from nocodazole arrest. Using flow cytometry, it was determined that when M-phase cells were reseeded after removing nocodazole, and harvested at 6 and 12 hours post-reseeding, cells were enriched in G1- and S-phase cells, respectively. While all cells had not exited mitosis six hours after re-seeding, this procedure generated enriched populations for further studies. Other synchronisation methods were not used in the present study, as it was found that XP30R0 cells could not be synchronised with double-thymidine block (data not shown), and that the large initial population of cells required to obtain synchronised cells using elutriation made this approach impractical, for the adherent cell lines used here.

Pol η -deficient XP30R0 fibroblasts are known to be more sensitive to UVC-induced DNA damage compared to normal fibroblasts (Yamada et al., 1997, Stary et al., 2003, Bassett et al., 2004). Pol η -deficient cells are more sensitive to cisplatin and related drugs compared to cells expressing pol η (Albertella et al., 2005a, Chen et al., 2006, Cruet-Hennequart et al., 2008). The toxicity of cisplatin and carboplatin towards XP30R0 and TR30-2 cells was determined using the XTT cell viability assay. Asynchronously growing pol η -deficient XP30R0 cells were more sensitive to cisplatin and carboplatin compared to TR30-2 cells that express pol η , consistent with previous reports. In addition to a role for pol η in cisplatin resistance, depletion of other polymerases, including REV1, REV3, or REV7 rendered HeLa cells hypersensitive to cisplatin-induced cytotoxicity (Hicks et al., 2010). In another study, in Fanc-G deficient mice (Krijger et al., 2010) were found to be highly sensitive to killing by cisplatin (Nojima et al., 2005). Other repair genes, such as ERCC1 also contribute to resistance of cells to cisplatin (Lee et al., 1993).

When cell viability was investigated in synchronised XP30R0 and TR30-2 cells treated with cisplatin or carboplatin in the G1-, S- or M-phases, cell cycle phase-dependence was observed, in particular in XP30R0 cells. Cells in S-phase were more sensitive to both cisplatin and carboplatin, compared to cells in G1- or M-phases at the time of treatment. The major difference observed was in S-phase cells, where there was an almost 3-fold reduction in viability in XP30R0 cells compared to TR30-2 cells. This indicates that pol η -mediated bypass of platinum-induced intrastrand crosslinks during replication in cells in S-phase may protect cells from the cytotoxic effects. In a study, by Mueller et al (2006), testicular germ cell tumour cells were synchronised by serum starvation, and treated with cisplatin in different phases. It was found that cells arrested in G2/M were most sensitive to cisplatin, as determined using flow cytometry, and PARP cleavage (Mueller et al., 2006). The present results identify a role for pol η in protecting cells in S-phase from cisplatin toxicity.

Pol η inserts the correct nucleotides opposite UV radiation-induced thymine-thymine dimers (Kannouche et al., 2004, Lehmann et al., 2007), and can also carry out bypass of cisplatin-induced guanine-guanine intrastrand crosslinks (Biertumpfel et al., Chaney et al., 2005, Alt et al., 2007). In the absence of pol η , increased cell cycle arrest is observed following cisplatin treatment (Cruet-Hennequart et al., 2008).

However, the effect of pol η expression on cell cycle progression has not been examined in synchronised cells. In the present study, XP30R0 and TR30-2 cells in different cell cycle phases were treated with cisplatin or carboplatin, and cell cycle progression was characterised. When G1-phase XP30R0 cells were treated with cisplatin or carboplatin, the percentage of G1-phase XP30R0 cells increased at 12 hours post-cisplatin or carboplatin. However, there was no statistically significant increase in TR30-2 G1-phase cells at 12 hours post-treatment. While this provides some evidence for cisplatin-induced G1 checkpoint activation particularly in XP30R0 cells, this effect was not as strong in pol η -expressing TR30-2 cells. The lack of functional p53 in SV40-transformed XP30R0 cells might contribute to the p53 independent G1 checkpoint response in these cells (Cleaver, 2000, Cleaver et al., 2002, Limoli et al., 2002, Cleaver, 2004).

The major effect of exposure of G1-phase cells to cisplatin or carboplatin was arrest of cell cycle progression in S-phase, indicating not all DNA damage was removed before the cells enter S-phase. The percentage of cells in S-phase increased at 24 and 36 hours post-treatment, indicating that XP30R0 cells have difficulty in progressing through S-phase. Reduced BrdU incorporation and increased cyclin B expression, 24 and 36 hours after drug treatment is consistent with cell cycle arrest in S- and G2-phases. This is consistent with previously published data on asynchronous XP30R0 cells treated with platinum-based drugs (Cruet-Hennequart et al., 2008, Cruet-Hennequart et al., 2009), or UVC radiation (Cruet-Hennequart et al., 2006). The percentage of cells in G1-phase in both XP30R0 and TR30-2 cells at 24 and 36 hours post-treatment was reduced, due to the failure of the cells to traverse the cell cycle and re-enter G1-phase.

When S-phase XP30R0 cells were treated with cisplatin, the percentage of cells in S-phase was arrested up to 36 hours post-treatment. At this time, the percentage of cells in G1 was low, while the percentage in G2+M remained high. This indicates a strong and prolonged S-phase arrest, with delayed progression through the cell cycle, suggesting that cells have not re-entered G1-phase by 36 hours post-cisplatin treatment. S-phase arrest was consistent with increased BrdU staining compared to untreated cells. Cyclin B levels in the cisplatin-treated XP30R0 cells remained the same. In carboplatin-treated cells, cell cycle progression was comparable to that of the controls, and was also less strongly inhibited in comparison to cisplatin-treated cells. However, the percentage of S-phase cells increased at 36 hours following carboplatin-treatment, consistent with an increased percentage of BrdU-positive cells at this time. This late arrest may indicate that cells arrest in S-phase during the second cell cycle. One possibility could be due to the slower formation of carboplatin-adducts than cisplatin-induced adducts (Knox et al., 1986), because carboplatin has a more stable leaving group than cisplatin (Harrap, 1985). Thus one interpretation could be that, while some DNA damage clearly has occurred as shown by activation of Chk1 phosphorylation, when cells in S-phase are treated with carboplatin, not enough adducts have formed in the DNA to strongly arrest replication before the cells exit S-phase. After the cells exit S-phase, increased numbers of carboplatin adducts are formed so that, when cells re-enter S-phase in the second round of replication cells are arrested in S-phase. This interpretation is supported by the study by Mojas *et al.*

(2007), in which mammalian MMR-proficient 293T L α ⁺ cells were treated with the methylating agent N-methyl-N'-nitro-N-nitrosoguanidine (MNNG). It was found that replication fork progression was unaffected in the first round of replication, but caused G2 arrest in the second round of replication (Mojas et al., 2007). To confirm that the timing of carboplatin adduct formation contributed to the effects observed in the present study, the level of carboplatin-adducts formed over time in DNA would need to be measured (Hah et al., 2006, Thomas et al., 2006).

In the case of S-phase TR30-2 cells treated with either cisplatin or carboplatin, no significant difference was observed between control and treated cells, except that there was an increase in the percentage of S-phase cells at 36 hours post-treatment. The percentage of BrdU-positive cells also increased at 36 hours post-treatment. Again, this suggests that arrest may occur in the second round of replication; however this was not investigated further. Cyclin B expression increased at 24 hours post-carboplatin treatment as the cells progressed through the cell cycle similar to control cells, whereas cyclin B decreased at 36 hours, consistent with arrest in S-phase at this time. The main difference between XP30R0 and TR30-2 cells treated in S-phase was that pol η -deficient cells accumulated in S-phase 12 and 24 hours after cisplatin treatment, while this did not occur in TR30-2 cells indicating a role for pol η in allowing replication of DNA with cisplatin-induced damage. In the case of carboplatin treatment, both XP30R0 and TR30-2 cells arrested in S-phase 36 hours post-treatment. This late arrest may be related to the level or type of adducts formed by carboplatin as outlined above.

When M-phase XP30R0 cells were treated with cisplatin and carboplatin, compared to control cells, the percentage of cells in G1-phase increased, while the percentage of S-phase cells decreased at 12 hours post treatment. This indicates a delay in cells exiting G1-phase, preventing the progression of cells into S-phase. Cyclin E expression was found to be decreased at 12 hours in particular in cisplatin-treated cells, and to a lesser extent in carboplatin-treated cells. This is consistent with reduced numbers of cells in early S-phase, possibly due to the delay in exiting G1. There was an increase in the percentage of S-phase cells at 24 and 36 hours post-cisplatin and carboplatin-treatment, indicating a strong S-phase arrest. This was consistent with the decreased BrdU incorporation post-cisplatin and carboplatin-treatment. Cyclin B

expression did not change in XP30R0 cells, 24 and 36 hours post-treatment with cisplatin and carboplatin, as cells were arrested in S-phase. In the case of TR30-2 cells treated with cisplatin or carboplatin, the percentage of cells in S-phase was increased at 12 hours post-treatment, compared to XP30R0 cells. The cells were arrested in S-phase consistent with reduced BrdU incorporation with statistically significant differences observed between the control cells and cisplatin-or carboplatin-treated cells.

As noted, the main difference between cell cycle progression following treatment of pol η -deficient XP30R0 cells and pol η -expressing TR30-2 cells treated with cisplatin and carboplatin in M-phase, was a decrease in the percentage of cells in S-phase at 12 hours in XP30R0 cells compared to TR30-2 cells. XP30R0 cells appear to exit G1 more slowly compared to TR30-2 cells. The basis of this effect has not been elucidated, but there is some evidence that pol η may have effects outside of S-phase.

For example, when *pol* η reconstituted XPV cells were treated with UV, REV1 and pol η foci were induced in both S-phase and G1-phase cells, suggesting that pol η may function both during and outside S-phase (Akagi et al., 2009). However, both XP30R0 and TR30-2 cells showed an increased percentage of cells in S-phase at 24 and 36 hours post-treatment, suggesting strong S-phase arrest independent of pol η , when cells exit G1-phase.

In the present study, both XP30R0 and TR30-2 cells were found to exit mitosis following cisplatin or carboplatin treatment. In contrast another study by Stephan et al (2009) showed that when mitotically-arrested HeLa cells were treated with IR, exit from mitosis was delayed (Stephan et al., 2009). Whether this reflects differences in the cell line, or in the type of damage remains to be determined.

Arrest of cells upon entry into S-phase was found to be a common outcome of exposure of cells to cisplatin. This is generally consistent with other reports. In a recent study (Ubezio et al., 2009) in which cells were synchronised using centrifugal elutriation, it was found that following treatment of cells at different phases of the cell cycle with 10 μ M cisplatin, cells in S- and G2-phases were arrested, consistent with the results from the present study. In asynchronously growing mouse leukaemia L1210/0 cells, cisplatin induced G2-phase arrest (Sorenson et al., 1990, Ohmori et al.,

1998). In xenografted head and neck carcinoma, accumulation of cells in S-phase and G2/M-phase was detected following cisplatin treatment (Jackel and Kopf-Maier, 1991). The present study provides evidence that the absence of pol η expression results in a reduced ability to overcome cisplatin-induced S-phase arrest, consistent with a role for pol η in translesion synthesis past cisplatin, carboplatin and oxaliplatin adducts (Albertella et al., 2005a).

Both cisplatin and carboplatin affected cyclin E and B expression. While changes in cyclin levels are likely to affect CDK activity, kinase activity would need to be directly analysed in cells treated with platinum-based drugs. Deregulation of cyclin E in an ovarian cancer cell line increased cyclin E-associated kinase activity, and sensitised tumour cells to cisplatin (Bedrosian et al., 2004). Increased cyclin E-associated kinase activity is an important predictive marker of the response of patients to platinum-based therapy. Cyclin E protein levels are a significant predictor for preventing recurrence of cancer (Bedrosian et al., 2007). Other cyclins, including cyclin D, may also play an important role in predicting cisplatin sensitivity in cancer treatment. For example, a study by Akervall et al (2004) showed that overexpression of cyclin D is associated with increased sensitivity to cisplatin in squamous cell carcinoma of the head and neck (Akervall et al., 2004).

Cisplatin- and carboplatin-induced DNA damage activates PIK kinases, resulting in phosphorylation of numerous PIK kinase substrates, including phosphorylation of the damage-response proteins Chk1, H2AX and RPA2 (Kastan and Lim, 2000, Abraham, 2001, Shiloh, 2006, Douglas et al., 2007, Cruet-Hennequart et al., 2009). To further characterise the effect of cisplatin and carboplatin treatment at different phases of the cell cycle in pol η -deficient cells, phosphorylation of Chk1, H2AX and RPA2 was investigated. In response to DNA damage, histone H2AX is phosphorylated by ATM at serine 139, generating γ H2AX (Rogakou et al., 1998), an early marker of DNA strand breaks. Although cisplatin does not cause double strand breaks directly, cisplatin induces H2AX phosphorylation in UV41 and irs3 cell lines (Olive and Banath, 2009). It is proposed that cisplatin-induced H2AX phosphorylation in S-phase cells results from replication fork arrest at adducts formed by cisplatin, resulting in fork collapse and double-strand break formation (Olive and Banath, 2009). Dephosphorylation of H2AX by the protein phosphatases PP4 and PP2A also

plays a role in the DNA damage response (Douglas et al., Chowdhury et al., 2008, Nakada et al., 2008). In the present study, phosphorylation of H2AX on ser 139 was detected in XP30RO cells treated with cisplatin and carboplatin in all phases of the cell cycle. Following treatment of G1-phase XP30RO cells, cisplatin-induced γ H2AX was detected at 24 and 36 hours post-treatment, consistent with the time cells were arrested in S-phase. Following carboplatin-treatment, strong γ H2AX was detected 36 hours. In S-phase XP30RO cells treated with cisplatin, strong γ H2AX formation was detected at 24 and 36 hours post-treatment, again consistent with cells being arrested in S-phase. In carboplatin-treated cells phosphorylation of H2AX was sustained until 36 hours. Following exposure of M-phase XP30RO cells to cisplatin or carboplatin, γ H2AX was detected at all time points examined. γ H2AX immunofluorescence confirmed the data obtained by Western blotting for γ H2AX, in that γ H2AX-positive cells were detected following treatment of G1- and S-phase XP30RO cells with cisplatin or carboplatin. The peak of γ H2AX staining was observed 24 hours following cisplatin treatment, but at 36 hours following carboplatin treatment. Whether the platinum-induced γ H2AX in XP30RO cells results from replication arrest at interstrand or intrastrand crosslinks, or from ICL repair remains to be determined. In one study, it was found that cisplatin-induced γ H2AX was replication-dependent and not repair-dependent, as cisplatin induced H2AX phosphorylation in the repair-deficient CHO cell line UV41 (Olive and Banath, 2009). H2AX phosphorylation is S-phase dependent, as when the replication fork encounters cisplatin-induced ICLs, strand breaks can result (Clingen et al., 2008). While ICLs are repaired during S-phase using a pathway requiring the ERCC1-XPF endonuclease followed by homologous recombination, γ H2AX can be generated even in ERCC1-XPF-defective CHO cells (Clingen et al., 2008).

Cisplatin-induced intrastrand crosslinks can also induce H2AX phosphorylation due to replication arrest, resulting in fork collapse and generation of DSBs (Kobayashi et al., 2009). Thus, γ H2AX acts as a marker for cisplatin-induced DNA damage (Clingen et al., 2008). In a study by Mogi et al (2007), γ H2AX foci were numerous and intense in XPV fibroblast cells lacking pol η , following psoralen-crosslink formation, suggesting that pol η normally plays an important role in reducing formation of γ H2AX (Mogi et al., 2008). In a study by Marti et al (2006), UV

radiation induced phosphorylation of H2AX in NER-deficient cells was found to occur in all phases of the cell cycle, but was highest in S-phase, and decreased in G1 phase cells (Marti et al., 2006). Formation of cisplatin-induced γ H2AX foci may also be a useful indicator of cisplatin-induced cell death (Olive and Banath, 2009).

Checkpoint kinase 1 (Chk1) is phosphorylated by ATR on serine 317 following exposure to both cisplatin and carboplatin (Zhao and Piwnica-Worms, 2001, Sorensen et al., 2005, Kulkarni and Das, 2008). Chk1 activity regulates replication arrest and entry into mitosis (Cimprich and Cortez, 2008). Since Chk1 is an ATR substrate, while RPA2 phosphorylation on serine 4/serine 8 is DNA-PK-dependent, the timing of these events gives an insight into the relationship between checkpoint activation and DNA strand break formation. To understand the relationship between the timing of phosphorylation of the PIKK substrates Chk1 and RPA2, following treatment of XP30R0 cells in different cell cycle phases with cisplatin or carboplatin, Chk1 phosphorylation on serine 317 and RPA2 phosphorylation on serine 4/serine 8 was investigated. In both cisplatin- and carboplatin-treated XP30R0 cells, Chk1 phosphorylation was an earlier event and was detected at 12 hours post-treatment. Activation of Chk1 was consistent with the onset of S-phase arrest, as determined by flow cytometry. In a study by Lewis et al (2009), following cisplatin treatment of GM847/kdATR and GK41 fibroblast cells, ATR-dependent S-phase arrest was induced, consistent with activation of an intra-S-phase checkpoint mediated by Chk1 (Lewis et al., 2009). In addition, Chk1 interacts with Rad51 and is phosphorylated in a Chk1-dependent manner thereby, plays an important role in homologous recombination repair in cells treated with hydroxyurea (Sorensen et al., 2005).

In contrast to Chk1 phosphorylation, in all cases RPA2 phosphorylation on serine 4/serine 8 was a later event, and was detected at 18 hours post-treatment. RPA is a trimeric single stranded DNA binding protein (Binz et al., 2004). RPA2, the 32kDa subunit of RPA, is phosphorylated at a number of sites in the N-terminal region in both a cell cycle-dependent and a DNA damage-dependent manner (Liu and Weaver, 1993, Carty et al., 1994, Niu et al., 1997, Oakley et al., 2001, Oakley et al., 2003, Olson et al., 2006, Anantha et al., 2008). RPA2 is phosphorylated at serine 33, threonine 21 and serine 4/serine 8 following DNA damage (Liu and Weaver, 1993, Carty et al., 1994, Oakley et al., 2003, Patrick et al., 2005, Olson et al., 2006, Anantha

et al., 2008). In the present study, phosphorylation of RPA2 at serine 4/serine 8 was investigated following treatment of XP30R0 and TR30-2 cells with cisplatin and carboplatin in the G1-, S- and M-phases of the cell cycle. When XP30R0 and TR30-2 cells were treated in different stages of the cell cycle, RPA2 phosphorylation was detected at 24 and 36 hours post-treatment. However, RPA2 phosphorylation was much more strongly induced in pol η -deficient XP30R0 cells compared to pol η -proficient TR30-2 and was the biggest different between XP30R0 and TR30-2 cells. The major difference between cisplatin- and carboplatin-induced RPA2 phosphorylation was that the peak of carboplatin-induced RPA2 phosphorylation in XP30R0 cells was detected later, at 36 hours post-treatment, than cisplatin-induced RPA2 phosphorylation, which peaked at 24 hours post-treatment. By comparing cell cycle progression of both XP30R0 and TR30-2 cells following treatment, the induction of RPA2 phosphorylation corresponded to when cells had accumulated in S-phase. The functional role of DNA damage-induced RPA2 phosphorylation on serine 4/serine 8 is not completely clear, but recent evidence indicates that it may play a role in regulating RPA function in homologous recombination (Shi et al., Sleeth et al., 2007, Sugiyama and Kantake, 2009). This would be consistent with the delayed onset of RPA2 serine 4/serine 8 phosphorylation, and it being associated with prolonged arrest in S-phase, which may generate strand breaks, a target for repair by HR (Cruet-Hennequart et al., 2009).

The results of immunofluorescence carried out to detect nuclear phosphorylated RPA2 staining, were consistent with the western blotting data. RPA2 phosphoserine 4/serine 8-positive cells following cisplatin or carboplatin treatment was detected at 24 and 36 hours post-treatment of G1- and S-phase XP30R0 cells, with increased phosphorylation at 24 hours post-cisplatin and stronger phosphorylation at 36 hours post-carboplatin treatment. Since Western blot analysis showed that phosphorylation of RPA2 on serine 4/serine 8 was weakly induced in TR30-2 cells treated with cisplatin or carboplatin, immunofluorescence assay was not performed in these cells. The delay in RPA2 phosphorylation following carboplatin treatment compared to cisplatin treatment could be due to differences in the rates of adduct formation or repair, affecting the extent of replication arrest in the cells (Kelland, 2007a).

ATR is activated following DNA damage such as replication arrest, while ATM and DNA-PK following DNA strand breaks (Durocher and Jackson, 2001, Abraham, 2004, Bakkenist and Kastan, 2004, Harper and Elledge, 2007, Brnzei and Foiani, 2008, Cimprich and Cortez, 2008). Cisplatin- and carboplatin-induced phosphorylation of RPA2 at serine 4/serine 8 requires DNA-PK (Cruet-Hennequart et al., 2008, Cruet-Hennequart et al., 2009). Although serine 4 and serine 8 are not located in the consensus S/TQ sites for phosphorylation by PIKKs (Zernik-Kobak et al., 1997), DNA-PK can phosphorylate serines and threonines that are located outside of PIKK consensus site in the DNA repair proteins, Artemis (Ma et al., 2005) and XRCC4 (Yu et al., 2003). DNA-PK may phosphorylate serine or threonine residues that are followed by a hydrophobic residue (Meek et al., 2004, Patrick et al., 2005). In the present study, small molecule inhibitors of ATM, DNA-PK and CDK1/2 were used to investigate the kinase dependence of RPA phosphorylation on serine 4/serine 8. The effects of the inhibitors on RPA2 serine 4/serine 8 phosphorylation were independent of which phase the cells were in at the time of treatment, supporting the conclusion that RPA2 phosphorylation occurs in cells arrested in S-phase. When XP30R0 cells were treated with cisplatin or carboplatin and co-treated with NU7441, a small molecule inhibitor of DNA-PK, RPA2 phosphorylation on serine 4/serine 8 significantly decreased. In contrast, co-treatment with the ATM inhibitor, KU55933, did not affect RPA2 phosphorylation on serine 4/serine 8, indicating that ATM does not play a role in RPA2 phosphorylation on serine 4/serine 8 (Cruet-Hennequart et al., 2008). Roscovitine, an inhibitor of CDK1/2, inhibited RPA2 phosphorylation on serine 4/serine 8 was also significantly decreased. RPA2 is phosphorylated by CDKs on serine 23 and serine 29 during the normal cell cycle. Serine 23 phosphorylation occurs in S-phase cells, while serine 29 phosphorylation occurs in M-phase (Oakley et al., 2003, Anantha et al., 2007, Stephan et al., 2009). Currently there is no evidence that CDKs directly phosphorylate RPA2 on serine 4/serine 8. However, this may be consistent with a requirement for phosphorylation of RPA2 on serine 23 or serine 29, before the protein can be phosphorylated on serine 4/serine 8 (Olson et al., 2006, Anantha et al., 2007).

Following treatment of cells in different phases of cell cycle, with cisplatin and carboplatin, cells in S-phase were more sensitive compared to other phases and S-phase arrest was seen in cells treated in different phases of the cell cycle. This showed that the maximum effect of cisplatin and carboplatin treatment was obtained in S-phase cells.

Chapter 5: Conclusions and future directions

In the present study, a number of DNA damage responses have been characterised following treatment of pol η -deficient and pol η -expressing cells in different phases of the cell cycle with cisplatin or carboplatin. The main effect of drug treatment was strong S-phase arrest, which could be sustained for up to 36 hours post-treatment in both pol η -deficient and pol η -expressing cells. Further investigation of cellular responses at times post-36 hours is required to determine whether cells undergo cell death or continue replication in the presence of damage. One method to study the effect of continued replication on genomic stability is by scoring cells for sister chromatid exchanges (SCEs) and other chromosomal aberrations (Korkola and Gray, 2010).

Following treatment with cisplatin and carboplatin, cell cycle progression is affected due to the formation of intrastrand and interstrand crosslinks in DNA. Comparison of the formation and repair of cisplatin- and carboplatin-induced adducts to oxaliplatin-induced adducts could also be useful, as oxaliplatin-induced adducts have a different structure. The measurement of the level of adducts formed post-treatment and the rate of adduct repair could provide an insight into the mode of action of these drugs in cells in each cell cycle phase. Intrastrand crosslinks can be measured using high performance liquid chromatography along with mass spectrometric detection methods (Harrington et al., 2010). Interstrand adducts can also be detected by single cell gel electrophoresis ('comet assay') method. This would provide a better understanding of the relationship between cisplatin and carboplatin-induced crosslink formation, cell cycle arrest and activation of the DNA damage response.

In the present study, cells in G1-, S- and M-phases of the cell cycle were treated with cisplatin and carboplatin. To extend this study, cells could also be enriched in G2-phase of the cell cycle using, for example, elutriation or longer release from nocodazole and then treated with cisplatin or carboplatin to understand the effects of platinum-based drugs on cell cycle progression following treatment of cells in G2 phase. Phosphorylation of various DNA damage response proteins including γ -H2AX, Chk1 and RPA2 could be studied using immunofluorescence analysis of G2- and M-phase cells.

In the present study, it was shown that phosphorylation of RPA2 on serine4/serine8 was greatly increased in pol η -deficient cells (XP30R0) compared to TR30-2 cells

expressing pol η . Although phosphorylation of RPA2 on serine4/ serine8 is associated with cisplatin or carboplatin treatment, the exact role of this phosphorylation event in the DNA damage response is still not fully understood. This could be further investigated by blocking damage-induced RPA2 phosphorylation by inhibiting the kinase responsible for phosphorylation, in this case the DNA-PK, by using a small molecule inhibitor (Leahy et al., 2004). Inhibition of the activity of phosphorylated RPA2, for example, in protein-protein interactions, is another possible approach. However, further investigation is required to identify inhibitors of phosphor RPA2 interactions. DNA damage-induced RPA2 phosphorylation on other sites such as serine 33 and threonine 21 also require further investigation. Since, RPA2 phosphorylation on serine4/serine8 was strongly and specifically induced by cisplatin and carboplatin treatment particularly in pol η -deficient cells, it might also be of interest to investigate whether this phosphorylation event would be a useful marker of the response to cisplatin in cells from cancer patients (Manthey et al., 2010).

The relevance of the present study to the treatment of cancer patients with platinum-based chemotherapeutic drugs such as cisplatin derives from the observation that treating cells at a specific phase of the cell cycle increases the toxicity of the drug. In particular, it was found that cells in S phase were more sensitive to cisplatin and carboplatin. One approach might be to use these drugs in combination with antimetabolites such as hydroxyurea, which arrests cells in S-phase. This could increase the toxicity of cisplatin and improve the efficacy of platinum-based chemotherapeutic drugs in the treatment of cancers. Another aspect is the identification of cellular pathways that could be targeted to increase the efficacy of platinum-based drugs. Following cisplatin and carboplatin treatment, a number of downstream proteins in the DNA damage response are activated through a signalling cascade to induce an appropriate cellular response. In the present study, pol η , a translesion synthesis polymerase which efficiently bypasses platinum-induced DNA adducts, was shown be important in determining the sensitivity of human cells to these drugs. Inhibiting pol η is one potential approach that might reduce the capacity of cells to tolerate platinum-induced DNA adducts. The ssDNA binding protein RPA was strongly phosphorylated on the RPA2 subunit in response to cisplatin and carboplatin. Thus, one of the approaches to improve the efficacy of platinum-based drugs could be by inhibiting the phosphorylation of RPA2, which could prevent

recruitment of repair proteins, possibly increasing the toxicity of these agents. Overall, the present work has identified key cellular pathways that could potentially be targeted in the future to improve the clinical efficacy of platinum-based drugs.

Chapter 6: Bibliography

1. Aabo, K., Adams, M., Adnitt, P., Alberts, D.S., Athanazziou, A., Barley, V., Bell, D.R., Bianchi, U., Bolis, G., Brady, M.F., *et al.* (1998). Chemotherapy in advanced ovarian cancer: four systematic meta-analyses of individual patient data from 37 randomized trials. Advanced Ovarian Cancer Trialists' Group. *Br J Cancer* 78, 1479-1487.
2. Abdulovic, A.L., and Jinks-Robertson, S. (2006). The in vivo characterization of translesion synthesis across UV-induced lesions in *Saccharomyces cerevisiae*: insights into Pol zeta- and Pol eta-dependent frameshift mutagenesis. *Genetics* 172, 1487-1498.
3. Abraham, R.T. (2001). Cell cycle checkpoint signaling through the ATM and ATR kinases. *Genes Dev* 15, 2177-2196.
4. Abraham, R.T. (2004). PI 3-kinase related kinases: 'big' players in stress-induced signaling pathways. *DNA Repair (Amst)* 3, 883-887.
5. Acharya, N., Haracska, L., Prakash, S., and Prakash, L. (2007). Complex formation of yeast Rev1 with DNA polymerase eta. *Mol Cell Biol* 27, 8401-8408.
6. Adams, M.M., and Carpenter, P.B. (2006). Tying the loose ends together in DNA double strand break repair with 53BP1. *Cell Div* 1, 19.
7. Akagi, J., Masutani, C., Kataoka, Y., Kan, T., Ohashi, E., Mori, T., Ohmori, H., and Hanaoka, F. (2009). Interaction with DNA polymerase eta is required for nuclear accumulation of REV1 and suppression of spontaneous mutations in human cells. *DNA Repair (Amst)* 8, 585-599.
8. Akervall, J., Kurnit, D.M., Adams, M., Zhu, S., Fisher, S.G., Bradford, C.R., and Carey, T.E. (2004). Overexpression of cyclin D1 correlates with sensitivity to cisplatin in squamous cell carcinoma cell lines of the head and neck. *Acta Otolaryngol* 124, 851-857.
9. Albertella, M.R., Green, C.M., Lehmann, A.R., and O'Connor, M.J. (2005a). A role for polymerase eta in the cellular tolerance to cisplatin-induced damage. *Cancer Res* 65, 9799-9806.
10. Albertella, M.R., Lau, A., and O'Connor, M.J. (2005b). The overexpression of specialized DNA polymerases in cancer. *DNA Repair (Amst)* 4, 583-593.
11. Allalunis-Turner, M.J., Barron, G.M., Day, R.S., 3rd, Dobler, K.D., and Mirzayans, R. (1993). Isolation of two cell lines from a human malignant glioma specimen differing in sensitivity to radiation and chemotherapeutic drugs. *Radiat Res* 134, 349-354.
12. Allen, C., Ashley, A.K., Hromas, R., and Nickoloff, J.A. (2011). More forks on the road to replication stress recovery. *J Mol Cell Biol* 3, 4-12.
13. Alt, A., Lammens, K., Chiocchini, C., Lammens, A., Pieck, J.C., Kuch, D., Hopfner, K.P., and Carell, T. (2007). Bypass of DNA lesions generated during anticancer treatment with cisplatin by DNA polymerase eta. *Science* 318, 967-970.
14. Aly, A., and Ganesan, S. (2011). BRCA1, PARP, and 53BP1: conditional synthetic lethality and synthetic viability. *J Mol Cell Biol* 3, 66-74.
15. Anantha, R.W., Sokolova, E., and Borowiec, J.A. (2008). RPA phosphorylation facilitates mitotic exit in response to mitotic DNA damage. *Proc Natl Acad Sci U S A* 105, 12903-12908.
16. Anantha, R.W., Vassin, V.M., and Borowiec, J.A. (2007). Sequential and synergistic modification of human RPA stimulates chromosomal DNA repair. *J Biol Chem* 282, 35910-35923.

17. Anciano Granadillo, V.J., Earley, J.N., Shuck, S.C., Georgiadis, M.M., Fitch, R.W., and Turchi, J.J. (2010). Targeting the OB-Folds of Replication Protein A with Small Molecules. *J Nucleic Acids* 2010, 304035.
18. Aprelikova, O., Xiong, Y., and Liu, E.T. (1995). Both p16 and p21 families of cyclin-dependent kinase (CDK) inhibitors block the phosphorylation of cyclin-dependent kinases by the CDK-activating kinase. *J Biol Chem* 270, 18195-18197.
19. Ardizzoni, A., Boni, L., Tiseo, M., Fossella, F.V., Schiller, J.H., Paesmans, M., Radosavljevic, D., Paccagnella, A., Zatloukal, P., Mazzanti, P., *et al.* (2007). Cisplatin- versus carboplatin-based chemotherapy in first-line treatment of advanced non-small-cell lung cancer: an individual patient data meta-analysis. *J Natl Cancer Inst* 99, 847-857.
20. Arioka, H., Nishio, K., Ishida, T., Fukumoto, H., Fukuoka, K., Nomoto, T., Kurokawa, H., Yokote, H., Abe, S., and Saijo, N. (1999). Enhancement of cisplatin sensitivity in high mobility group 2 cDNA-transfected human lung cancer cells. *Jpn J Cancer Res* 90, 108-115.
21. Arora, S., Kothandapani, A., Tillison, K., Kalman-Maltese, V., and Patrick, S.M. (2010). Downregulation of XPF-ERCC1 enhances cisplatin efficacy in cancer cells. *DNA Repair (Amst)* 9, 745-753.
22. Artandi, S.E., and DePinho, R.A. (2010). Telomeres and telomerase in cancer. *Carcinogenesis* 31, 9-18.
23. Arunkumar, A.I., Stauffer, M.E., Bochkareva, E., Bochkarev, A., and Chazin, W.J. (2003). Independent and coordinated functions of replication protein A tandem high affinity single-stranded DNA binding domains. *J Biol Chem* 278, 41077-41082.
24. Ashworth, A. (2008). A synthetic lethal therapeutic approach: poly(ADP) ribose polymerase inhibitors for the treatment of cancers deficient in DNA double-strand break repair. *J Clin Oncol* 26, 3785-3790.
25. Auclair, Y., Rouget, R., Belisle, J.M., Costantino, S., and Drobetsky, E.A. (2010). Requirement for functional DNA polymerase eta in genome-wide repair of UV-induced DNA damage during S phase. *DNA Repair (Amst)* 9, 754-764.
26. Audeh, M.W., Carmichael, J., Penson, R.T., Friedlander, M., Powell, B., Bell-McGuinn, K.M., Scott, C., Weitzel, J.N., Oaknin, A., Loman, N., *et al.* (2010). Oral poly(ADP-ribose) polymerase inhibitor olaparib in patients with BRCA1 or BRCA2 mutations and recurrent ovarian cancer: a proof-of-concept trial. *Lancet* 376, 245-251.
27. Bakkenist, C.J., and Kastan, M.B. (2003). DNA damage activates ATM through intermolecular autophosphorylation and dimer dissociation. *Nature* 421, 499-506.
28. Bakkenist, C.J., and Kastan, M.B. (2004). Initiating cellular stress responses. *Cell* 118, 9-17.
29. Ball, H.L., Ehrhardt, M.R., Mordes, D.A., Glick, G.G., Chazin, W.J., and Cortez, D. (2007). Function of a conserved checkpoint recruitment domain in ATRIP proteins. *Mol Cell Biol* 27, 3367-3377.
30. Ball, H.L., Myers, J.S., and Cortez, D. (2005). ATRIP binding to replication protein A-single-stranded DNA promotes ATR-ATRIP localization but is dispensable for Chk1 phosphorylation. *Mol Biol Cell* 16, 2372-2381.
31. Balsamo, A., Mancini, F., Milanese, C., Orlandini, E., Ortore, G., Pinza, M., Rapposelli, S., and Rossello, A. (2003). Synthesis and prostaglandin synthase

- inhibitory activity of new aromatic O-alkyloxime ethers substituted with methylsulfonamido or methylsulfonyl groups on their aliphatic portion. *Farmaco* 58, 707-714.
32. Banath, J.P., and Olive, P.L. (2003). Expression of phosphorylated histone H2AX as a surrogate of cell killing by drugs that create DNA double-strand breaks. *Cancer Res* 63, 4347-4350.
33. Banath, J.P., Wallace, S.S., Thompson, J., and Olive, P.L. (1999). Radiation-induced DNA base damage detected in individual aerobic and hypoxic cells with endonuclease III and formamidopyrimidine-glycosylase. *Radiat Res* 151, 550-558.
34. Bao, S., Tibbetts, R.S., Brumbaugh, K.M., Fang, Y., Richardson, D.A., Ali, A., Chen, S.M., Abraham, R.T., and Wang, X.F. (2001). ATR/ATM-mediated phosphorylation of human Rad17 is required for genotoxic stress responses. *Nature* 411, 969-974.
35. Bartek, J., Falck, J., and Lukas, J. (2001). CHK2 kinase--a busy messenger. *Nat Rev Mol Cell Biol* 2, 877-886.
36. Bartek, J., Lukas, C., and Lukas, J. (2004). Checking on DNA damage in S phase. *Nat Rev Mol Cell Biol* 5, 792-804.
37. Bartek, J., and Lukas, J. (2001). Mammalian G1- and S-phase checkpoints in response to DNA damage. *Curr Opin Cell Biol* 13, 738-747.
38. Bassett, E., King, N.M., Bryant, M.F., Hector, S., Pendyala, L., Chaney, S.G., and Cordeiro-Stone, M. (2004). The role of DNA polymerase eta in translesion synthesis past platinum-DNA adducts in human fibroblasts. *Cancer Res* 64, 6469-6475.
39. Bassett, E., Vaisman, A., Tropea, K.A., McCall, C.M., Masutani, C., Hanaoka, F., and Chaney, S.G. (2002). Frameshifts and deletions during in vitro translesion synthesis past Pt-DNA adducts by DNA polymerases beta and eta. *DNA Repair (Amst)* 1, 1003-1016.
40. Basu, A., and Krishnamurthy, S. Cellular responses to Cisplatin-induced DNA damage. *J Nucleic Acids* 2010.
41. Bedrosian, I., Lee, C., Tucker, S.L., Palla, S.L., Lu, K., and Keyomarsi, K. (2007). Cyclin E-associated kinase activity predicts response to platinum-based chemotherapy. *Clin Cancer Res* 13, 4800-4806.
42. Bedrosian, I., Lu, K.H., Verschraegen, C., and Keyomarsi, K. (2004). Cyclin E deregulation alters the biologic properties of ovarian cancer cells. *Oncogene* 23, 2648-2657.
43. Ben-Yehoyada, M., Wang, L.C., Kozekov, I.D., Rizzo, C.J., Gottesman, M.E., and Gautier, J. (2009). Checkpoint signaling from a single DNA interstrand crosslink. *Mol Cell* 35, 704-715.
44. Berardini, M., Foster, P.L., and Loechler, E.L. (1999). DNA polymerase II (polB) is involved in a new DNA repair pathway for DNA interstrand cross-links in *Escherichia coli*. *J Bacteriol* 181, 2878-2882.
45. Berdasco, M., and Esteller, M. (2010). Aberrant epigenetic landscape in cancer: how cellular identity goes awry. *Dev Cell* 19, 698-711.
46. Bermudez, V.P., Lindsey-Boltz, L.A., Cesare, A.J., Maniwa, Y., Griffith, J.D., Hurwitz, J., and Sancar, A. (2003). Loading of the human 9-1-1 checkpoint complex onto DNA by the checkpoint clamp loader hRad17-replication factor C complex in vitro. *Proc Natl Acad Sci U S A* 100, 1633-1638.

47. Bernstein, C., Bernstein, H., Payne, C.M., and Garewal, H. (2002). DNA repair/pro-apoptotic dual-role proteins in five major DNA repair pathways: fail-safe protection against carcinogenesis. *Mutat Res* 511, 145-178.
48. Besaratinia, A., Synold, T.W., Xi, B., and Pfeifer, G.P. (2004). G-to-T transversions and small tandem base deletions are the hallmark of mutations induced by ultraviolet a radiation in mammalian cells. *Biochemistry* 43, 8169-8177.
49. Bessho, T., Mu, D., and Sancar, A. (1997). Initiation of DNA interstrand cross-link repair in humans: the nucleotide excision repair system makes dual incisions 5' to the cross-linked base and removes a 22- to 28-nucleotide-long damage-free strand. *Mol Cell Biol* 17, 6822-6830.
50. Betous, R., Rey, L., Wang, G., Pillaire, M.J., Puget, N., Selves, J., Biard, D.S., Shin-ya, K., Vasquez, K.M., Cazaux, C., *et al.* (2009). Role of TLS DNA polymerases eta and kappa in processing naturally occurring structured DNA in human cells. *Mol Carcinog* 48, 369-378.
51. Bhana, S., Hewer, A., Phillips, D.H., and Lloyd, D.R. (2008). p53-dependent global nucleotide excision repair of cisplatin-induced intrastrand cross links in human cells. *Mutagenesis* 23, 131-136.
52. Bharti, A., Kraeft, S.K., Gounder, M., Pandey, P., Jin, S., Yuan, Z.M., Lees-Miller, S.P., Weichselbaum, R., Weaver, D., Chen, L.B., *et al.* (1998). Inactivation of DNA-dependent protein kinase by protein kinase Cdelta: implications for apoptosis. *Mol Cell Biol* 18, 6719-6728.
53. Bhattacharyya, A., Ear, U.S., Koller, B.H., Weichselbaum, R.R., and Bishop, D.K. (2000). The breast cancer susceptibility gene BRCA1 is required for subnuclear assembly of Rad51 and survival following treatment with the DNA cross-linking agent cisplatin. *J Biol Chem* 275, 23899-23903.
54. Bhattacharyya, D., Ramachandran, S., Sharma, S., Pathmasiri, W., King, C.L., Baskerville-Abraham, I., Boysen, G., Swenberg, J.A., Campbell, S.L., Dokholyan, N.V., *et al.* (2011). Flanking bases influence the nature of DNA distortion by platinum 1,2-intrastrand (GG) cross-links. *PLoS One* 6, e23582.
55. Bianco, P.R., Tracy, R.B., and Kowalczykowski, S.C. (1998). DNA strand exchange proteins: a biochemical and physical comparison. *Front Biosci* 3, D570-603.
56. Bienko, M., Green, C.M., Crosetto, N., Rudolf, F., Zapart, G., Coull, B., Kannouche, P., Wider, G., Peter, M., Lehmann, A.R., *et al.* (2005). Ubiquitin-binding domains in Y-family polymerases regulate translesion synthesis. *Science* 310, 1821-1824.
57. Biertumpfel, C., Zhao, Y., Kondo, Y., Ramon-Maiques, S., Gregory, M., Lee, J.Y., Masutani, C., Lehmann, A.R., Hanaoka, F., and Yang, W. Structure and mechanism of human DNA polymerase eta. *Nature* 465, 1044-1048.
58. Biertumpfel, C., Zhao, Y., Kondo, Y., Ramon-Maiques, S., Gregory, M., Lee, J.Y., Masutani, C., Lehmann, A.R., Hanaoka, F., and Yang, W. (2010). Structure and mechanism of human DNA polymerase eta. *Nature* 465, 1044-1048.
59. Bingham, J.P., Hartley, J.A., Souhami, R.L., and Grimaldi, K.A. (1996). Strand-specific measurement of cisplatin-induced DNA damage and repair using quantitative PCR. *Nucleic Acids Res* 24, 987-989.
60. Binz, S.K., Sheehan, A.M., and Wold, M.S. (2004). Replication protein A phosphorylation and the cellular response to DNA damage. *DNA Repair (Amst)* 3, 1015-1024.

61. Blackburn, E. (1999). The telomere and telomerase: how Do they interact? *Mt Sinai J Med* 66, 292-300.
62. Blommaert, F.A., and Saris, C.P. (1995). Detection of platinum-DNA adducts by 32P-postlabelling. *Nucleic Acids Res* 23, 1300-1306.
63. Blommaert, F.A., van Dijk-Knijnenburg, H.C., Dijt, F.J., den Engelse, L., Baan, R.A., Berends, F., and Fichtinger-Schepman, A.M. (1995). Formation of DNA adducts by the anticancer drug carboplatin: different nucleotide sequence preferences in vitro and in cells. *Biochemistry* 34, 8474-8480.
64. Bochkarev, A., and Bochkareva, E. (2004). From RPA to BRCA2: lessons from single-stranded DNA binding by the OB-fold. *Curr Opin Struct Biol* 14, 36-42.
65. Bochkareva, E., Frappier, L., Edwards, A.M., and Bochkarev, A. (1998). The RPA32 subunit of human replication protein A contains a single-stranded DNA-binding domain. *J Biol Chem* 273, 3932-3936.
66. Bochkareva, E., Korolev, S., Lees-Miller, S.P., and Bochkarev, A. (2002). Structure of the RPA trimerization core and its role in the multistep DNA-binding mechanism of RPA. *EMBO J* 21, 1855-1863.
67. Bohgaki, T., Bohgaki, M., and Hakem, R. (2010). DNA double-strand break signaling and human disorders. *Genome Integr* 1, 15.
68. Bonilla, C.Y., Melo, J.A., and Toczyski, D.P. (2008). Colocalization of sensors is sufficient to activate the DNA damage checkpoint in the absence of damage. *Mol Cell* 30, 267-276.
69. Bonner, W.M., Mannironi, C., Orr, A., Pilch, D.R., and Hatch, C.L. (1993). Histone H2A.X gene transcription is regulated differently than transcription of other replication-linked histone genes. *Mol Cell Biol* 13, 984-992.
70. Boone, J.M. (2009). Dose spread functions in computed tomography: a Monte Carlo study. *Med Phys* 36, 4547-4554.
71. Bootsma, D., and Hoeijmakers, J.H. (1991). The genetic basis of xeroderma pigmentosum. *Ann Genet* 34, 143-150.
72. Bosotti, R., Isacchi, A., and Sonnhammer, E.L. (2000). FAT: a novel domain in PIK-related kinases. *Trends Biochem Sci* 25, 225-227.
73. Bostock, C.J., Prescott, D.M., and Kirkpatrick, J.B. (1971). An evaluation of the double thymidine block for synchronizing mammalian cells at the G1-S border. *Exp Cell Res* 68, 163-168.
74. Boubnov, N.V., and Weaver, D.T. (1995). scid cells are deficient in Ku and replication protein A phosphorylation by the DNA-dependent protein kinase. *Mol Cell Biol* 15, 5700-5706.
75. Boulton, S., Kyle, S., and Durkacz, B.W. (2000). Mechanisms of enhancement of cytotoxicity in etoposide and ionising radiation-treated cells by the protein kinase inhibitor wortmannin. *Eur J Cancer* 36, 535-541.
76. Boutros, R., Dozier, C., and Ducommun, B. (2006). The when and wheres of CDC25 phosphatases. *Curr Opin Cell Biol* 18, 185-191.
77. Brnzei, D., and Foiani, M. (2008). Regulation of DNA repair throughout the cell cycle. *Nat Rev Mol Cell Biol* 9, 297-308.
78. Braun, K.A., Lao, Y., He, Z., Ingles, C.J., and Wold, M.S. (1997). Role of protein-protein interactions in the function of replication protein A (RPA): RPA modulates the activity of DNA polymerase alpha by multiple mechanisms. *Biochemistry* 36, 8443-8454.

79. Brewerton, S.C., Dore, A.S., Drake, A.C., Leuther, K.K., and Blundell, T.L. (2004). Structural analysis of DNA-PKcs: modelling of the repeat units and insights into the detailed molecular architecture. *J Struct Biol* 145, 295-306.
80. Broughton, B.C., Cordonnier, A., Kleijer, W.J., Jaspers, N.G., Fawcett, H., Raams, A., Garritsen, V.H., Stry, A., Avril, M.F., Boudsocq, F., *et al.* (2002). Molecular analysis of mutations in DNA polymerase eta in xeroderma pigmentosum-variant patients. *Proc Natl Acad Sci U S A* 99, 815-820.
81. Brush, G.S., Clifford, D.M., Marinco, S.M., and Bartrand, A.J. (2001). Replication protein A is sequentially phosphorylated during meiosis. *Nucleic Acids Res* 29, 4808-4817.
82. Budd, M.E., and Campbell, J.L. (2009). Interplay of Mre11 nuclease with Dna2 plus Sgs1 in Rad51-dependent recombinational repair. *PLoS One* 4, e4267.
83. Bugreev, D.V., Rossi, M.J., and Mazin, A.V. (2011). Cooperation of RAD51 and RAD54 in regression of a model replication fork. *Nucleic Acids Res* 39, 2153-2164.
84. Burger, H., Loos, W.J., Eechoute, K., Verweij, J., Mathijssen, R.H., and Wiemer, E.A. (2011). Drug transporters of platinum-based anticancer agents and their clinical significance. *Drug Resist Updat* 14, 22-34.
85. Burgess, A., Vigneron, S., Brioude, E., Labbe, J.C., Lorca, T., and Castro, A. (2010). Loss of human Greatwall results in G2 arrest and multiple mitotic defects due to deregulation of the cyclin B-Cdc2/PP2A balance. *Proc Natl Acad Sci U S A* 107, 12564-12569.
86. Burma, S., Chen, B.P., Murphy, M., Kurimasa, A., and Chen, D.J. (2001). ATM phosphorylates histone H2AX in response to DNA double-strand breaks. *J Biol Chem* 276, 42462-42467.
87. Burma, S., and Chen, D.J. (2004). Role of DNA-PK in the cellular response to DNA double-strand breaks. *DNA Repair (Amst)* 3, 909-918.
88. Burtelow, M.A., Roos-Mattjus, P.M., Rauen, M., Babendure, J.R., and Karnitz, L.M. (2001). Reconstitution and molecular analysis of the hRad9-hHus1-hRad1 (9-1-1) DNA damage responsive checkpoint complex. *J Biol Chem* 276, 25903-25909.
89. Buscemi, G., Perego, P., Carenini, N., Nakanishi, M., Chessa, L., Chen, J., Khanna, K., and Delia, D. (2004). Activation of ATM and Chk2 kinases in relation to the amount of DNA strand breaks. *Oncogene* 23, 7691-7700.
90. Byfield, J.E., and Calabro-Jones, P.M. (1981). Carrier-dependent and carrier-independent transport of anti-cancer alkylating agents. *Nature* 294, 281-283.
91. Calvert, A.H., Harland, S.J., Newell, D.R., Siddik, Z.H., Jones, A.C., McElwain, T.J., Raju, S., Wiltshaw, E., Smith, I.E., Baker, J.M., *et al.* (1982). Early clinical studies with cis-diammine-1,1-cyclobutane dicarboxylate platinum II. *Cancer Chemother Pharmacol* 9, 140-147.
92. Carty, M.P., Zernik-Kobak, M., McGrath, S., and Dixon, K. (1994). UV light-induced DNA synthesis arrest in HeLa cells is associated with changes in phosphorylation of human single-stranded DNA-binding protein. *EMBO J* 13, 2114-2123.
93. Castedo, M., Perfettini, J.L., Roumier, T., Yakushijin, K., Horne, D., Medema, R., and Kroemer, G. (2004). The cell cycle checkpoint kinase Chk2 is a negative regulator of mitotic catastrophe. *Oncogene* 23, 4353-4361.
94. Celeste, A., Fernandez-Capetillo, O., Kruhlak, M.J., Pilch, D.R., Staudt, D.W., Lee, A., Bonner, R.F., Bonner, W.M., and Nussenzweig, A. (2003). Histone

- H2AX phosphorylation is dispensable for the initial recognition of DNA breaks. *Nat Cell Biol* 5, 675-679.
95. Celli, C.M., and Jaiswal, A.K. (2003). Role of GRP58 in mitomycin C-induced DNA cross-linking. *Cancer Res* 63, 6016-6025.
96. Chailleux, C., Tyteca, S., Papin, C., Boudsocq, F., Puget, N., Courilleau, C., Grigoriev, M., Canitrot, Y., and Trouche, D. (2010). Physical interaction between the histone acetyl transferase Tip60 and the DNA double-strand breaks sensor MRN complex. *Biochem J* 426, 365-371.
97. Chan, D.W., Chen, B.P., Prithivirajasingh, S., Kurimasa, A., Story, M.D., Qin, J., and Chen, D.J. (2002). Autophosphorylation of the DNA-dependent protein kinase catalytic subunit is required for rejoining of DNA double-strand breaks. *Genes Dev* 16, 2333-2338.
98. Chaney, S.G., Campbell, S.L., Bassett, E., and Wu, Y. (2005). Recognition and processing of cisplatin- and oxaliplatin-DNA adducts. *Crit Rev Oncol Hematol* 53, 3-11.
99. Chapman, J.R., and Jackson, S.P. (2008). Phospho-dependent interactions between NBS1 and MDC1 mediate chromatin retention of the MRN complex at sites of DNA damage. *EMBO Rep* 9, 795-801.
100. Chehab, N.H., Malikzay, A., Appel, M., and Halazonetis, T.D. (2000). Chk2/hCds1 functions as a DNA damage checkpoint in G(1) by stabilizing p53. *Genes Dev* 14, 278-288.
101. Chen, B.P., Chan, D.W., Kobayashi, J., Burma, S., Asaithamby, A., Morotomi-Yano, K., Botvinick, E., Qin, J., and Chen, D.J. (2005). Cell cycle dependence of DNA-dependent protein kinase phosphorylation in response to DNA double strand breaks. *J Biol Chem* 280, 14709-14715.
102. Chen, M.J., Lin, Y.T., Lieberman, H.B., Chen, G., and Lee, E.Y. (2001). ATM-dependent phosphorylation of human Rad9 is required for ionizing radiation-induced checkpoint activation. *J Biol Chem* 276, 16580-16586.
103. Chen, Y.W., Cleaver, J.E., Hanaoka, F., Chang, C.F., and Chou, K.M. (2006). A novel role of DNA polymerase eta in modulating cellular sensitivity to chemotherapeutic agents. *Mol Cancer Res* 4, 257-265.
104. Chijiwa, S., Masutani, C., Hanaoka, F., Iwai, S., and Kuraoka, I. (2010). Polymerization by DNA polymerase eta is blocked by cis-diamminedichloroplatinum(II) 1,3-d(GpTpG) cross-link: implications for cytotoxic effects in nucleotide excision repair-negative tumor cells. *Carcinogenesis* 31, 388-393.
105. Choi, J.H., Lindsey-Boltz, L.A., Kemp, M., Mason, A.C., Wold, M.S., and Sancar, A. (2010a). Reconstitution of RPA-covered single-stranded DNA-activated ATR-Chk1 signaling. *Proc Natl Acad Sci U S A* 107, 13660-13665.
106. Choi, J.Y., Lim, S., Kim, E.J., Jo, A., and Guengerich, F.P. (2010b). Translesion synthesis across abasic lesions by human B-family and Y-family DNA polymerases alpha, delta, eta, iota, kappa, and REV1. *J Mol Biol* 404, 34-44.
107. Chowdhury, D., Xu, X., Zhong, X., Ahmed, F., Zhong, J., Liao, J., Dykxhoorn, D.M., Weinstock, D.M., Pfeifer, G.P., and Lieberman, J. (2008). A PP4-phosphatase complex dephosphorylates gamma-H2AX generated during DNA replication. *Mol Cell* 31, 33-46.
108. Ciarimboli, G., Deuster, D., Knief, A., Sperling, M., Holtkamp, M., Edemir, B., Pavenstadt, H., Lanvers-Kaminsky, C., am Zehnhoff-Dinnesen, A., Schinkel, A.H., *et al.* (2010). Organic cation transporter 2 mediates cisplatin-

- induced oto- and nephrotoxicity and is a target for protective interventions. *Am J Pathol* 176, 1169-1180.
109. Ciccia, A., and Elledge, S.J. (2010). The DNA damage response: making it safe to play with knives. *Mol Cell* 40, 179-204.
110. Cimini, D., Fioravanti, D., Salmon, E.D., and Degrassi, F. (2002). Merotelic kinetochore orientation versus chromosome mono-orientation in the origin of lagging chromosomes in human primary cells. *J Cell Sci* 115, 507-515.
111. Cimini, D., Moree, B., Canman, J.C., and Salmon, E.D. (2003). Merotelic kinetochore orientation occurs frequently during early mitosis in mammalian tissue cells and error correction is achieved by two different mechanisms. *J Cell Sci* 116, 4213-4225.
112. Cimprich, K.A., and Cortez, D. (2008). ATR: an essential regulator of genome integrity. *Nat Rev Mol Cell Biol* 9, 616-627.
113. Ciosk, R., Zachariae, W., Michaelis, C., Shevchenko, A., Mann, M., and Nasmyth, K. (1998). An ESP1/PDS1 complex regulates loss of sister chromatid cohesion at the metaphase to anaphase transition in yeast. *Cell* 93, 1067-1076.
114. Ciullo, M., Debily, M.A., Rozier, L., Autiero, M., Billault, A., Mayau, V., El Marhomy, S., Guardiola, J., Bernheim, A., Coullin, P., *et al.* (2002). Initiation of the breakage-fusion-bridge mechanism through common fragile site activation in human breast cancer cells: the model of PIP gene duplication from a break at FRA7L. *Hum Mol Genet* 11, 2887-2894.
115. Cleaver, J.E. (2000). Common pathways for ultraviolet skin carcinogenesis in the repair and replication defective groups of xeroderma pigmentosum. *J Dermatol Sci* 23, 1-11.
116. Cleaver, J.E. (2004). Defective repair replication of DNA in xeroderma pigmentosum. 1968. *DNA Repair (Amst)* 3, 183-187.
117. Cleaver, J.E., Bartholomew, J., Char, D., Crowley, E., Feeney, L., and Limoli, C.L. (2002). Polymerase eta and p53 jointly regulate cell survival, apoptosis and Mre11 recombination during S phase checkpoint arrest after UV irradiation. *DNA Repair (Amst)* 1, 41-57.
118. Cleaver, J.E., and Revet, I. (2008). Clinical implications of the basic defects in Cockayne syndrome and xeroderma pigmentosum and the DNA lesions responsible for cancer, neurodegeneration and aging. *Mech Ageing Dev* 129, 492-497.
119. Cliby, W.A., Roberts, C.J., Cimprich, K.A., Stringer, C.M., Lamb, J.R., Schreiber, S.L., and Friend, S.H. (1998). Overexpression of a kinase-inactive ATR protein causes sensitivity to DNA-damaging agents and defects in cell cycle checkpoints. *EMBO J* 17, 159-169.
120. Clingen, P.H., Wu, J.Y., Miller, J., Mistry, N., Chin, F., Wynne, P., Prise, K.M., and Hartley, J.A. (2008). Histone H2AX phosphorylation as a molecular pharmacological marker for DNA interstrand crosslink cancer chemotherapy. *Biochem Pharmacol* 76, 19-27.
121. Collis, S.J., DeWeese, T.L., Jeggo, P.A., and Parker, A.R. (2005). The life and death of DNA-PK. *Oncogene* 24, 949-961.
122. Cook, P.J., Ju, B.G., Telese, F., Wang, X., Glass, C.K., and Rosenfeld, M.G. (2009). Tyrosine dephosphorylation of H2AX modulates apoptosis and survival decisions. *Nature* 458, 591-596.

123. Cordonnier, A.M., and Fuchs, R.P. (1999). Replication of damaged DNA: molecular defect in xeroderma pigmentosum variant cells. *Mutat Res* 435, 111-119.
124. Cortez, D. (2003). Caffeine inhibits checkpoint responses without inhibiting the ataxia-telangiectasia-mutated (ATM) and ATM- and Rad3-related (ATR) protein kinases. *J Biol Chem* 278, 37139-37145.
125. Cortez, D., Guntuku, S., Qin, J., and Elledge, S.J. (2001). ATR and ATRIP: partners in checkpoint signaling. *Science* 294, 1713-1716.
126. Coste, F., Malinge, J.M., Serre, L., Shepard, W., Roth, M., Leng, M., and Zelwer, C. (1999). Crystal structure of a double-stranded DNA containing a cisplatin interstrand cross-link at 1.63 Å resolution: hydration at the platinated site. *Nucleic Acids Res* 27, 1837-1846.
127. Couve, S., Mace-Aime, G., Rosselli, F., and Saparbaev, M.K. (2009). The human oxidative DNA glycosylase NEIL1 excises psoralen-induced interstrand DNA cross-links in a three-stranded DNA structure. *J Biol Chem* 284, 11963-11970.
128. Cowell, I.G., Durkacz, B.W., and Tilby, M.J. (2005). Sensitization of breast carcinoma cells to ionizing radiation by small molecule inhibitors of DNA-dependent protein kinase and ataxia telangiectasia mutated. *Biochem Pharmacol* 71, 13-20.
129. Cox, M.M., Goodman, M.F., Kreuzer, K.N., Sherratt, D.J., Sandler, S.J., and Marians, K.J. (2000). The importance of repairing stalled replication forks. *Nature* 404, 37-41.
130. Cruet-Hennequart, S., Coyne, S., Glynn, M.T., Oakley, G.G., and Carty, M.P. (2006). UV-induced RPA phosphorylation is increased in the absence of DNA polymerase eta and requires DNA-PK. *DNA Repair (Amst)* 5, 491-504.
131. Cruet-Hennequart, S., Glynn, M.T., Murillo, L.S., Coyne, S., and Carty, M.P. (2008). Enhanced DNA-PK-mediated RPA2 hyperphosphorylation in DNA polymerase eta-deficient human cells treated with cisplatin and oxaliplatin. *DNA Repair (Amst)* 7, 582-596.
132. Cruet-Hennequart, S., Villalan, S., Kaczmarczyk, A., O'Meara, E., Sokol, A.M., and Carty, M.P. (2009). Characterization of the effects of cisplatin and carboplatin on cell cycle progression and DNA damage response activation in DNA polymerase eta-deficient human cells. *Cell Cycle* 8, 3039-3050.
133. Crul, M., van Waardenburg, R.C., Bocxe, S., van Eijndhoven, M.A., Pluim, D., Beijnen, J.H., and Schellens, J.H. (2003). DNA repair mechanisms involved in gemcitabine cytotoxicity and in the interaction between gemcitabine and cisplatin. *Biochem Pharmacol* 65, 275-282.
134. Cui, X., Yu, Y., Gupta, S., Cho, Y.M., Lees-Miller, S.P., and Meek, K. (2005). Autophosphorylation of DNA-dependent protein kinase regulates DNA end processing and may also alter double-strand break repair pathway choice. *Mol Cell Biol* 25, 10842-10852.
135. Cybulski, K.E., and Howlett, N.G. (2011). FANCP/SLX4: a Swiss army knife of DNA interstrand crosslink repair. *Cell Cycle* 10, 1757-1763.
136. Dai, Y., and Grant, S. (2010). New insights into checkpoint kinase 1 in the DNA damage response signaling network. *Clin Cancer Res* 16, 376-383.
137. Dammermann, A., Desai, A., and Oegema, K. (2003). The minus end in sight. *Curr Biol* 13, R614-624.

138. Davis, P.K., Ho, A., and Dowdy, S.F. (2001). Biological methods for cell-cycle synchronization of mammalian cells. *Biotechniques* 30, 1322-1326, 1328, 1330-1321.
139. de Boer, J., and Hoeijmakers, J.H. (2000). Nucleotide excision repair and human syndromes. *Carcinogenesis* 21, 453-460.
140. De Bont, R., and van Larebeke, N. (2004). Endogenous DNA damage in humans: a review of quantitative data. *Mutagenesis* 19, 169-185.
141. De Brabander, M., De May, J., Joniau, M., and Geuens, G. (1977). Ultrastructural immunocytochemical distribution of tubulin in cultured cells treated with microtubule inhibitors. *Cell Biol Int Rep* 1, 177-183.
142. de la Casa-Esperon, E., and Sapienza, C. (2003). Natural selection and the evolution of genome imprinting. *Annu Rev Genet* 37, 349-370.
143. de Toledo, S.M., Azzam, E.I., Dahlberg, W.K., Gooding, T.B., and Little, J.B. (2000). ATM complexes with HDM2 and promotes its rapid phosphorylation in a p53-independent manner in normal and tumor human cells exposed to ionizing radiation. *Oncogene* 19, 6185-6193.
144. De Vlaminck, I., Vidic, I., van Loenhout, M.T., Kanaar, R., Lebbink, J.H., and Dekker, C. (2010). Torsional regulation of hRPA-induced unwinding of double-stranded DNA. *Nucleic Acids Res* 38, 4133-4142.
145. de Winter, J.P., and Joenje, H. (2009). The genetic and molecular basis of Fanconi anemia. *Mutat Res* 668, 11-19.
146. Deckbar, D., Birraux, J., Krempler, A., Tchouandong, L., Beucher, A., Walker, S., Stiff, T., Jeggo, P., and Lobrich, M. (2007). Chromosome breakage after G2 checkpoint release. *J Cell Biol* 176, 749-755.
147. DeFazio, L.G., Stansel, R.M., Griffith, J.D., and Chu, G. (2002). Synapsis of DNA ends by DNA-dependent protein kinase. *EMBO J* 21, 3192-3200.
148. Delacote, F., and Lopez, B.S. (2008). Importance of the cell cycle phase for the choice of the appropriate DSB repair pathway, for genome stability maintenance: the trans-S double-strand break repair model. *Cell Cycle* 7, 33-38.
149. Delbos, F., Aoufouchi, S., Faili, A., Weill, J.C., and Reynaud, C.A. (2007). DNA polymerase eta is the sole contributor of A/T modifications during immunoglobulin gene hypermutation in the mouse. *J Exp Med* 204, 17-23.
150. Delbos, F., De Smet, A., Faili, A., Aoufouchi, S., Weill, J.C., and Reynaud, C.A. (2005). Contribution of DNA polymerase eta to immunoglobulin gene hypermutation in the mouse. *J Exp Med* 201, 1191-1196.
151. Deng, J., Harding, H.P., Raught, B., Gingras, A.C., Berlanga, J.J., Scheuner, D., Kaufman, R.J., Ron, D., and Sonenberg, N. (2002). Activation of GCN2 in UV-irradiated cells inhibits translation. *Curr Biol* 12, 1279-1286.
152. Denissenko, M.F., Pao, A., Tang, M., and Pfeifer, G.P. (1996). Preferential formation of benzo[a]pyrene adducts at lung cancer mutational hotspots in P53. *Science* 274, 430-432.
153. Detres, Y., Armstrong, R.A., and Connelly, X.M. (2001). Ultraviolet-induced responses in two species of climax tropical marine macrophytes. *J Photochem Photobiol B* 62, 55-66.
154. Diamant, N., Hendel, A., Vered, I., Carell, T., Reissner, T., de Wind, N., Geacinov, N., and Livneh, Z. (2011). DNA damage bypass operates in the S and G2 phases of the cell cycle and exhibits differential mutagenicity. *Nucleic Acids Res*.

155. DiTullio, R.A., Jr., Mochan, T.A., Venere, M., Bartkova, J., Sehested, M., Bartek, J., and Halazonetis, T.D. (2002). 53BP1 functions in an ATM-dependent checkpoint pathway that is constitutively activated in human cancer. *Nat Cell Biol* 4, 998-1002.
156. Dobbs, T.A., Tainer, J.A., and Lees-Miller, S.P. (2010). A structural model for regulation of NHEJ by DNA-PKcs autophosphorylation. *DNA Repair (Amst)* 9, 1307-1314.
157. Doles, J., Oliver, T.G., Cameron, E.R., Hsu, G., Jacks, T., Walker, G.C., and Hemann, M.T. (2010). Suppression of Rev3, the catalytic subunit of Pol{zeta}, sensitizes drug-resistant lung tumors to chemotherapy. *Proc Natl Acad Sci U S A* 107, 20786-20791.
158. Donahue, B.A., Augot, M., Bellon, S.F., Treiber, D.K., Toney, J.H., Lippard, S.J., and Essigmann, J.M. (1990). Characterization of a DNA damage-recognition protein from mammalian cells that binds specifically to intrastrand d(GpG) and d(ApG) DNA adducts of the anticancer drug cisplatin. *Biochemistry* 29, 5872-5880.
159. Douglas, P., Cui, X., Block, W.D., Yu, Y., Gupta, S., Ding, Q., Ye, R., Morrice, N., Lees-Miller, S.P., and Meek, K. (2007). The DNA-dependent protein kinase catalytic subunit is phosphorylated in vivo on threonine 3950, a highly conserved amino acid in the protein kinase domain. *Mol Cell Biol* 27, 1581-1591.
160. Douglas, P., Moorhead, G., Xu, X., and Lees-Miller, S. Choreographing the DNA damage response: PP6 joins the dance. *Cell Cycle* 9, 1221-1222.
161. Douglas, P., Moorhead, G.B., Ye, R., and Lees-Miller, S.P. (2001). Protein phosphatases regulate DNA-dependent protein kinase activity. *J Biol Chem* 276, 18992-18998.
162. Downey, M., and Durocher, D. (2006). gammaH2AX as a checkpoint maintenance signal. *Cell Cycle* 5, 1376-1381.
163. Durocher, D., and Jackson, S.P. (2001). DNA-PK, ATM and ATR as sensors of DNA damage: variations on a theme? *Curr Opin Cell Biol* 13, 225-231.
164. Dutta, A., and Stillman, B. (1992a). cdc2 family kinases phosphorylate a human cell DNA replication factor, RPA, and activate DNA replication. *EMBO J* 11, 2189-2199.
165. Dutta, A., and Stillman, B. (1992b). cdc2 family kinases phosphorylate a human cell DNA replication factor, RPA, and activate DNA replication. *Embo J* 11, 2189-2199.
166. Eastman, A., and Barry, M.A. (1987). Interaction of trans-diamminedichloroplatinum(II) with DNA: formation of monofunctional adducts and their reaction with glutathione. *Biochemistry* 26, 3303-3307.
167. Eckardt, A., Sinikovic, B., Hofele, C., Bremer, M., and Reuter, C. (2007). Preoperative paclitaxel/carboplatin radiochemotherapy for stage III/IV resectable oral and oropharyngeal cancer: seven-year follow-up of a phase II trial. *Oncology* 73, 198-203.
168. Edwards, B.K., Ward, E., Kohler, B.A., Ehemann, C., Zauber, A.G., Anderson, R.N., Jemal, A., Schymura, M.J., Lansdorp-Vogelaar, I., Seeff, L.C., *et al.* (2010). Annual report to the nation on the status of cancer, 1975-2006, featuring colorectal cancer trends and impact of interventions (risk factors, screening, and treatment) to reduce future rates. *Cancer* 116, 544-573.

169. Eid, W., Steger, M., El-Shemerly, M., Ferretti, L.P., Pena-Diaz, J., Konig, C., Valtorta, E., Sartori, A.A., and Ferrari, S. (2010). DNA end resection by CtIP and exonuclease 1 prevents genomic instability. *EMBO Rep* 11, 962-968.
170. Elledge, S.J. (1996). Cell cycle checkpoints: preventing an identity crisis. *Science* 274, 1664-1672.
171. Epe, B. (2002). Role of endogenous oxidative DNA damage in carcinogenesis: what can we learn from repair-deficient mice? *Biol Chem* 383, 467-475.
172. Faili, A., Aoufouchi, S., Weller, S., Vuillier, F., Sary, A., Sarasin, A., Reynaud, C.A., and Weill, J.C. (2004). DNA polymerase eta is involved in hypermutation occurring during immunoglobulin class switch recombination. *J Exp Med* 199, 265-270.
173. Falck, J., Coates, J., and Jackson, S.P. (2005). Conserved modes of recruitment of ATM, ATR and DNA-PKcs to sites of DNA damage. *Nature* 434, 605-611.
174. Falck, J., Mailand, N., Syljuasen, R.G., Bartek, J., and Lukas, J. (2001). The ATM-Chk2-Cdc25A checkpoint pathway guards against radioresistant DNA synthesis. *Nature* 410, 842-847.
175. Falck, J., Petrini, J.H., Williams, B.R., Lukas, J., and Bartek, J. (2002). The DNA damage-dependent intra-S phase checkpoint is regulated by parallel pathways. *Nat Genet* 30, 290-294.
176. Falik-Zaccai, T.C., Keren, Z., and Slor, H. (2009). The versatile DNA nucleotide excision repair (NER) and its medical significance. *Pediatr Endocrinol Rev* 7, 117-122.
177. Fanning, E., Klimovich, V., and Nager, A.R. (2006). A dynamic model for replication protein A (RPA) function in DNA processing pathways. *Nucleic Acids Res* 34, 4126-4137.
178. Fastrup, H., Bekker-Jensen, S., Bartek, J., Lukas, J., and Mailand, N. (2009). USP7 counteracts SCFbetaTrCP- but not APCdh1-mediated proteolysis of Claspin. *J Cell Biol* 184, 13-19.
179. Fichtinger-Schepman, A.M., van der Veer, J.L., den Hartog, J.H., Lohman, P.H., and Reedijk, J. (1985). Adducts of the antitumor drug cis-diamminedichloroplatinum(II) with DNA: formation, identification, and quantitation. *Biochemistry* 24, 707-713.
180. Filipski, K.K., Loos, W.J., Verweij, J., and Sparreboom, A. (2008). Interaction of Cisplatin with the human organic cation transporter 2. *Clin Cancer Res* 14, 3875-3880.
181. Fink, D., Aebi, S., and Howell, S.B. (1998). The role of DNA mismatch repair in drug resistance. *Clin Cancer Res* 4, 1-6.
182. Fischer, U., Hemmer, D., Heckel, D., Michel, A., Feiden, W., Steudel, W.I., Hulsebos, T., and Meese, E. (2001). KUB3 amplification and overexpression in human gliomas. *Glia* 36, 1-10.
183. Fischhaber, P.L., Gerlach, V.L., Feaver, W.J., Hatahet, Z., Wallace, S.S., and Friedberg, E.C. (2002). Human DNA polymerase kappa bypasses and extends beyond thymine glycols during translesion synthesis in vitro, preferentially incorporating correct nucleotides. *J Biol Chem* 277, 37604-37611.
184. Fong, P.C., Boss, D.S., Yap, T.A., Tutt, A., Wu, P., Mergui-Roelvink, M., Mortimer, P., Swaisland, H., Lau, A., O'Connor, M.J., *et al.* (2009). Inhibition of poly(ADP-ribose) polymerase in tumors from BRCA mutation carriers. *N Engl J Med* 361, 123-134.

185. Fong, P.C., Yap, T.A., Boss, D.S., Carden, C.P., Mergui-Roelvink, M., Gourley, C., De Greve, J., Lubinski, J., Shanley, S., Messiou, C., *et al.* (2010). Poly(ADP)-ribose polymerase inhibition: frequent durable responses in BRCA carrier ovarian cancer correlating with platinum-free interval. *J Clin Oncol* 28, 2512-2519.
186. Foster, D.A., Yellen, P., Xu, L., and Saqcena, M. (2010). Regulation of G1 Cell Cycle Progression: Distinguishing the Restriction Point from a Nutrient-Sensing Cell Growth Checkpoint(s). *Genes Cancer* 1, 1124-1131.
187. Fourier, L., Brooks, P., and Malinge, J.M. (2003). Binding discrimination of MutS to a set of lesions and compound lesions (base damage and mismatch) reveals its potential role as a cisplatin-damaged DNA sensing protein. *J Biol Chem* 278, 21267-21275.
188. Fried, L.M., Koumenis, C., Peterson, S.R., Green, S.L., van Zijl, P., Allalunis-Turner, J., Chen, D.J., Fishel, R., Giaccia, A.J., Brown, J.M., *et al.* (1996). The DNA damage response in DNA-dependent protein kinase-deficient SCID mouse cells: replication protein A hyperphosphorylation and p53 induction. *Proc Natl Acad Sci U S A* 93, 13825-13830.
189. Friedberg, E.C. (2001). How nucleotide excision repair protects against cancer. *Nat Rev Cancer* 1, 22-33.
190. Friedberg, E.C., Lehmann, A.R., and Fuchs, R.P. (2005). Trading places: how do DNA polymerases switch during translesion DNA synthesis? *Mol Cell* 18, 499-505.
191. Fukagawa, T. (2004). Centromere DNA, proteins and kinetochore assembly in vertebrate cells. *Chromosome Res* 12, 557-567.
192. Furuta, B., Harada, A., Kobayashi, Y., Takeuchi, K., Kobayashi, T., and Umeda, M. (2002). Identification and functional characterization of nadrin variants, a novel family of GTPase activating protein for rho GTPases. *J Neurochem* 82, 1018-1028.
193. Furuya, K., Poitelea, M., Guo, L., Caspari, T., and Carr, A.M. (2004). Chk1 activation requires Rad9 S/TQ-site phosphorylation to promote association with C-terminal BRCT domains of Rad4TOPBP1. *Genes Dev* 18, 1154-1164.
194. Futcher, B. (1999). Cell cycle synchronization. *Methods Cell Sci* 21, 79-86.
195. Galaris, D., and Evangelou, A. (2002). The role of oxidative stress in mechanisms of metal-induced carcinogenesis. *Crit Rev Oncol Hematol* 42, 93-103.
196. Gan, G.N., Wittschieben, J.P., Wittschieben, B.O., and Wood, R.D. (2008). DNA polymerase zeta (pol zeta) in higher eukaryotes. *Cell Res* 18, 174-183.
197. Gao, D., Inuzuka, H., Korenjak, M., Tseng, A., Wu, T., Wan, L., Kirschner, M., Dyson, N., and Wei, W. (2009). Cdh1 regulates cell cycle through modulating the claspin/Chk1 and the Rb/E2F1 pathways. *Mol Biol Cell* 20, 3305-3316.
198. Gao, Y., Chaudhuri, J., Zhu, C., Davidson, L., Weaver, D.T., and Alt, F.W. (1998). A targeted DNA-PKcs-null mutation reveals DNA-PK-independent functions for KU in V(D)J recombination. *Immunity* 9, 367-376.
199. Garcia-Muse, T., and Boulton, S.J. (2005). Distinct modes of ATR activation after replication stress and DNA double-strand breaks in *Caenorhabditis elegans*. *EMBO J* 24, 4345-4355.
200. Gari, K., Decaillet, C., Stasiak, A.Z., Stasiak, A., and Constantinou, A. (2008). The Fanconi anemia protein FANCM can promote branch migration of Holliday junctions and replication forks. *Mol Cell* 29, 141-148.

201. Gatei, M., Sloper, K., Sorensen, C., Syljuasen, R., Falck, J., Hobson, K., Savage, K., Lukas, J., Zhou, B.B., Bartek, J., *et al.* (2003). Ataxia-telangiectasia-mutated (ATM) and NBS1-dependent phosphorylation of Chk1 on Ser-317 in response to ionizing radiation. *J Biol Chem* 278, 14806-14811.
202. Gelhaus, S.L., Harvey, R.G., Penning, T.M., and Blair, I.A. (2011). Regulation of benzo[a]pyrene-mediated DNA- and glutathione-adduct formation by 2,3,7,8-tetrachlorodibenzo-p-dioxin in human lung cells. *Chem Res Toxicol* 24, 89-98.
203. Geng, Y., Eaton, E.N., Picon, M., Roberts, J.M., Lundberg, A.S., Gifford, A., Sardet, C., and Weinberg, R.A. (1996). Regulation of cyclin E transcription by E2Fs and retinoblastoma protein. *Oncogene* 12, 1173-1180.
204. Gening, L.V. (2011). DNA polymerase iota of mammals as a participant in translesion synthesis of DNA. *Biochemistry (Mosc)* 76, 61-68.
205. Gibbs, P.E., McDonald, J., Woodgate, R., and Lawrence, C.W. (2005). The relative roles in vivo of *Saccharomyces cerevisiae* Pol eta, Pol zeta, Rev1 protein and Pol32 in the bypass and mutation induction of an abasic site, T-T (6-4) photoadduct and T-T cis-syn cyclobutane dimer. *Genetics* 169, 575-582.
206. Gillet, S., Decottignies, P., Chardonnet, S., and Le Marechal, P. (2006). Cadmium response and redoxin targets in *Chlamydomonas reinhardtii*: a proteomic approach. *Photosynth Res* 89, 201-211.
207. Goldberg, M., Stucki, M., Falck, J., D'Amours, D., Rahman, D., Pappin, D., Bartek, J., and Jackson, S.P. (2003). MDC1 is required for the intra-S-phase DNA damage checkpoint. *Nature* 421, 952-956.
208. Gomes, X.V., and Wold, M.S. (1995). Structural analysis of human replication protein A. Mapping functional domains of the 70-kDa subunit. *J Biol Chem* 270, 4534-4543.
209. Goodarzi, A.A., Yu, Y., Riballo, E., Douglas, P., Walker, S.A., Ye, R., Harer, C., Marchetti, C., Morrice, N., Jeggo, P.A., *et al.* (2006). DNA-PK autophosphorylation facilitates Artemis endonuclease activity. *EMBO J* 25, 3880-3889.
210. Goodman, M.F. (2002). Error-prone repair DNA polymerases in prokaryotes and eukaryotes. *Annu Rev Biochem* 71, 17-50.
211. Goodship, J., Gill, H., Carter, J., Jackson, A., Splitt, M., and Wright, M. (2000). Autozygosity mapping of a seckel syndrome locus to chromosome 3q22. 1-q24. *Am J Hum Genet* 67, 498-503.
212. Gorboulev, V., Ulzheimer, J.C., Akhoundova, A., Ulzheimer-Teuber, I., Karbach, U., Quester, S., Baumann, C., Lang, F., Busch, A.E., and Koepsell, H. (1997). Cloning and characterization of two human polyspecific organic cation transporters. *DNA Cell Biol* 16, 871-881.
213. Goto, S., Kamada, K., Soh, Y., Ihara, Y., and Kondo, T. (2002). Significance of nuclear glutathione S-transferase pi in resistance to anti-cancer drugs. *Jpn J Cancer Res* 93, 1047-1056.
214. Goudelock, D.M., Jiang, K., Pereira, E., Russell, B., and Sanchez, Y. (2003). Regulatory interactions between the checkpoint kinase Chk1 and the proteins of the DNA-dependent protein kinase complex. *J Biol Chem* 278, 29940-29947.
215. Greenberg, R.A., Sobhian, B., Pathania, S., Cantor, S.B., Nakatani, Y., and Livingston, D.M. (2006). Multifactorial contributions to an acute DNA damage response by BRCA1/BARD1-containing complexes. *Genes Dev* 20, 34-46.

216. Grimme, J.M., Honda, M., Wright, R., Okuno, Y., Rothenberg, E., Mazin, A.V., Ha, T., and Spies, M. (2010). Human Rad52 binds and wraps single-stranded DNA and mediates annealing via two hRad52-ssDNA complexes. *Nucleic Acids Res* 38, 2917-2930.
217. Gronbaek, K., Worm, J., Ralfkiaer, E., Ahrenkiel, V., Hokland, P., and Guldberg, P. (2002). ATM mutations are associated with inactivation of the ARF-TP53 tumor suppressor pathway in diffuse large B-cell lymphoma. *Blood* 100, 1430-1437.
218. Grudzinski, J.J., Tome, W., Weichert, J.P., and Jeraj, R. (2010). The biological effectiveness of targeted radionuclide therapy based on a whole-body pharmacokinetic model. *Phys Med Biol* 55, 5723-5734.
219. Gu, F., You, C., Liu, J., Chen, A., Yu, Y., Wang, X., Wan, D., Gu, J., Yuan, H., Li, Y., *et al.* (2007). Cloning, expression and characterization of human tissue-specific DNA polymerase lambda2. *Sci China C Life Sci* 50, 457-465.
220. Guo, C., Fischhaber, P.L., Luk-Paszyc, M.J., Masuda, Y., Zhou, J., Kamiya, K., Kisker, C., and Friedberg, E.C. (2003). Mouse Rev1 protein interacts with multiple DNA polymerases involved in translesion DNA synthesis. *EMBO J* 22, 6621-6630.
221. Guo, C., Sonoda, E., Tang, T.S., Parker, J.L., Bielen, A.B., Takeda, S., Ulrich, H.D., and Friedberg, E.C. (2006a). REV1 protein interacts with PCNA: significance of the REV1 BRCT domain in vitro and in vivo. *Mol Cell* 23, 265-271.
222. Guo, C., Tang, T.S., Bienko, M., Parker, J.L., Bielen, A.B., Sonoda, E., Takeda, S., Ulrich, H.D., Dikic, I., and Friedberg, E.C. (2006b). Ubiquitin-binding motifs in REV1 protein are required for its role in the tolerance of DNA damage. *Mol Cell Biol* 26, 8892-8900.
223. Hader, D.P., and Sinha, R.P. (2005). Solar ultraviolet radiation-induced DNA damage in aquatic organisms: potential environmental impact. *Mutat Res* 571, 221-233.
224. Hah, S.S., Stivers, K.M., de Vere White, R.W., and Henderson, P.T. (2006). Kinetics of carboplatin-DNA binding in genomic DNA and bladder cancer cells as determined by accelerator mass spectrometry. *Chem Res Toxicol* 19, 622-626.
225. Halicka, H.D., Huang, X., Traganos, F., King, M.A., Dai, W., and Darzynkiewicz, Z. (2005). Histone H2AX phosphorylation after cell irradiation with UV-B: relationship to cell cycle phase and induction of apoptosis. *Cell Cycle* 4, 339-345.
226. Hamada, J., Nakata, D., Nakae, D., Kobayashi, Y., Akai, H., Konishi, Y., Okada, F., Shibata, T., Hosokawa, M., and Moriuchi, T. (2001). Increased oxidative DNA damage in mammary tumor cells by continuous epidermal growth factor stimulation. *J Natl Cancer Inst* 93, 214-219.
227. Hammarsten, O., DeFazio, L.G., and Chu, G. (2000). Activation of DNA-dependent protein kinase by single-stranded DNA ends. *J Biol Chem* 275, 1541-1550.
228. Hammond, E.M., Green, S.L., and Giaccia, A.J. (2003). Comparison of hypoxia-induced replication arrest with hydroxyurea and aphidicolin-induced arrest. *Mutat Res* 532, 205-213.
229. Hanada, K., Budzowska, M., Davies, S.L., van Drunen, E., Onizawa, H., Beverloo, H.B., Maas, A., Essers, J., Hickson, I.D., and Kanaar, R. (2007).

- The structure-specific endonuclease Mus81 contributes to replication restart by generating double-strand DNA breaks. *Nat Struct Mol Biol* 14, 1096-1104.
230. Hanahan, D., and Weinberg, R.A. Hallmarks of cancer: the next generation. *Cell* 144, 646-674.
231. Hanahan, D., and Weinberg, R.A. (2000). The hallmarks of cancer. *Cell* 100, 57-70.
232. Hanawalt, P.C. (2002). Subpathways of nucleotide excision repair and their regulation. *Oncogene* 21, 8949-8956.
233. Haracska, L., Acharya, N., Unk, I., Johnson, R.E., Hurwitz, J., Prakash, L., and Prakash, S. (2005). A single domain in human DNA polymerase ι mediates interaction with PCNA: implications for translesion DNA synthesis. *Mol Cell Biol* 25, 1183-1190.
234. Haracska, L., Kondratick, C.M., Unk, I., Prakash, S., and Prakash, L. (2001a). Interaction with PCNA is essential for yeast DNA polymerase ϵ function. *Mol Cell* 8, 407-415.
235. Haracska, L., Unk, I., Johnson, R.E., Johansson, E., Burgers, P.M., Prakash, S., and Prakash, L. (2001b). Roles of yeast DNA polymerases δ and ζ and of Rev1 in the bypass of abasic sites. *Genes Dev* 15, 945-954.
236. Hardcastle, I.R., Cockcroft, X., Curtin, N.J., El-Murr, M.D., Leahy, J.J., Stockley, M., Golding, B.T., Rigoreau, L., Richardson, C., Smith, G.C., *et al.* (2005). Discovery of potent chromen-4-one inhibitors of the DNA-dependent protein kinase (DNA-PK) using a small-molecule library approach. *J Med Chem* 48, 7829-7846.
237. Haring, S.J., Mason, A.C., Binz, S.K., and Wold, M.S. (2008). Cellular functions of human RPA1. Multiple roles of domains in replication, repair, and checkpoints. *J Biol Chem* 283, 19095-19111.
238. Harrington, C.F., Le Pla, R.C., Jones, G.D., Thomas, A.L., and Farmer, P.B. (2010). Determination of cisplatin 1,2-intrastrand guanine-guanine DNA adducts in human leukocytes by high-performance liquid chromatography coupled to inductively coupled plasma mass spectrometry. *Chem Res Toxicol* 23, 1313-1321.
239. Harley, C.B., Futcher, A.B., and Greider, C.W. (1990). Telomeres shorten during ageing of human fibroblasts. *Nature* 345, 458-460.
240. Harper, J.V. (2005). Synchronization of cell populations in G1/S and G2/M phases of the cell cycle. *Methods Mol Biol* 296, 157-166.
241. Harper, J.W., Adami, G.R., Wei, N., Keyomarsi, K., and Elledge, S.J. (1993). The p21 Cdk-interacting protein Cip1 is a potent inhibitor of G1 cyclin-dependent kinases. *Cell* 75, 805-816.
242. Harper, J.W., and Elledge, S.J. (2007). The DNA damage response: ten years after. *Mol Cell* 28, 739-745.
243. Harrap, K.R. (1985). Preclinical studies identifying carboplatin as a viable cisplatin alternative. *Cancer Treat Rev* 12 Suppl A, 21-33.
244. Hartwell, L.H., and Weinert, T.A. (1989). Checkpoints: controls that ensure the order of cell cycle events. *Science* 246, 629-634.
245. Hayflick, L., and Moorhead, P.S. (1961). The serial cultivation of human diploid cell strains. *Exp Cell Res* 25, 585-621.
246. He, G., Kuang, J., Khokhar, A.R., and Siddik, Z.H. (2011). The impact of S- and G2-checkpoint response on the fidelity of G1-arrest by cisplatin and its comparison to a non-cross-resistant platinum(IV) analog. *Gynecol Oncol* 122, 402-409.

247. He, S., Cook, B.L., Deverman, B.E., Weihe, U., Zhang, F., Prachand, V., Zheng, J., and Weintraub, S.J. (2000). E2F is required to prevent inappropriate S-phase entry of mammalian cells. *Mol Cell Biol* 20, 363-371.
248. Helin, K., Harlow, E., and Fattaey, A. (1993). Inhibition of E2F-1 transactivation by direct binding of the retinoblastoma protein. *Mol Cell Biol* 13, 6501-6508.
249. Helt, C.E., Wang, W., Keng, P.C., and Bambara, R.A. (2005). Evidence that DNA damage detection machinery participates in DNA repair. *Cell Cycle* 4, 529-532.
250. Herrick, J., and Bensimon, A. (2009). Introduction to molecular combing: genomics, DNA replication, and cancer. *Methods Mol Biol* 521, 71-101.
251. Hershko, A., and Ciechanover, A. (1998). The ubiquitin system. *Annu Rev Biochem* 67, 425-479.
252. Hewish, M., Lord, C.J., Martin, S.A., Cunningham, D., and Ashworth, A. (2010). Mismatch repair deficient colorectal cancer in the era of personalized treatment. *Nat Rev Clin Oncol* 7, 197-208.
253. Hicks, J.K., Chute, C.L., Paulsen, M.T., Ragland, R.L., Howlett, N.G., Gueranger, Q., Glover, T.W., and Canman, C.E. (2010). Differential roles for DNA polymerases eta, zeta, and REV1 in lesion bypass of intrastrand versus interstrand DNA cross-links. *Mol Cell Biol* 30, 1217-1230.
254. Hickson, I., Zhao, Y., Richardson, C.J., Green, S.J., Martin, N.M., Orr, A.I., Reaper, P.M., Jackson, S.P., Curtin, N.J., and Smith, G.C. (2004). Identification and characterization of a novel and specific inhibitor of the ataxia-telangiectasia mutated kinase ATM. *Cancer Res* 64, 9152-9159.
255. Higby, D.J., Wallace, H.J., Jr., Albert, D., and Holland, J.F. (1974). Diamminodichloroplatinum in the chemotherapy of testicular tumors. *J Urol* 112, 100-104.
256. Hirai, H., Roussel, M.F., Kato, J.Y., Ashmun, R.A., and Sherr, C.J. (1995). Novel INK4 proteins, p19 and p18, are specific inhibitors of the cyclin D-dependent kinases CDK4 and CDK6. *Mol Cell Biol* 15, 2672-2681.
257. Hirao, A., Cheung, A., Duncan, G., Girard, P.M., Elia, A.J., Wakeham, A., Okada, H., Sarkissian, T., Wong, J.A., Sakai, T., *et al.* (2002). Chk2 is a tumor suppressor that regulates apoptosis in both an ataxia telangiectasia mutated (ATM)-dependent and an ATM-independent manner. *Mol Cell Biol* 22, 6521-6532.
258. Hirao, A., Kong, Y.Y., Matsuoka, S., Wakeham, A., Ruland, J., Yoshida, H., Liu, D., Elledge, S.J., and Mak, T.W. (2000). DNA damage-induced activation of p53 by the checkpoint kinase Chk2. *Science* 287, 1824-1827.
259. Hishiki, A., Hashimoto, H., Hanafusa, T., Kamei, K., Ohashi, E., Shimizu, T., Ohmori, H., and Sato, M. (2009). Structural basis for novel interactions between human translesion synthesis polymerases and proliferating cell nuclear antigen. *J Biol Chem* 284, 10552-10560.
260. Hiyama, H., Iavarone, A., LaBaer, J., and Reeves, S.A. (1997). Regulated ectopic expression of cyclin D1 induces transcriptional activation of the cdk inhibitor p21 gene without altering cell cycle progression. *Oncogene* 14, 2533-2542.
261. Hoege, C., Pfander, B., Moldovan, G.L., Pyrowolakis, G., and Jentsch, S. (2002). RAD6-dependent DNA repair is linked to modification of PCNA by ubiquitin and SUMO. *Nature* 419, 135-141.

262. Hoeijmakers, J.H. (2001a). DNA repair mechanisms. *Maturitas* 38, 17-22; discussion 22-13.
263. Hoeijmakers, J.H. (2001b). Genome maintenance mechanisms for preventing cancer. *Nature* 411, 366-374.
264. Hoeijmakers, J.H. (2007). Genome maintenance mechanisms are critical for preventing cancer as well as other aging-associated diseases. *Mech Ageing Dev* 128, 460-462.
265. Hoeijmakers, J.H. (2009). DNA damage, aging, and cancer. *N Engl J Med* 361, 1475-1485.
266. Hoffmann, I., Draetta, G., and Karsenti, E. (1994). Activation of the phosphatase activity of human cdc25A by a cdk2-cyclin E dependent phosphorylation at the G1/S transition. *EMBO J* 13, 4302-4310.
267. Holzer, A.K., Manorek, G.H., and Howell, S.B. (2006). Contribution of the major copper influx transporter CTR1 to the cellular accumulation of cisplatin, carboplatin, and oxaliplatin. *Mol Pharmacol* 70, 1390-1394.
268. Hongo, A., Seki, S., Akiyama, K., and Kudo, T. (1994). A comparison of in vitro platinum-DNA adduct formation between carboplatin and cisplatin. *Int J Biochem* 26, 1009-1016.
269. Hopfner, K.P., Craig, L., Moncalian, G., Zinkel, R.A., Usui, T., Owen, B.A., Karcher, A., Henderson, B., Bodmer, J.L., McMurray, C.T., *et al.* (2002a). The Rad50 zinc-hook is a structure joining Mre11 complexes in DNA recombination and repair. *Nature* 418, 562-566.
270. Hopfner, K.P., Putnam, C.D., and Tainer, J.A. (2002b). DNA double-strand break repair from head to tail. *Curr Opin Struct Biol* 12, 115-122.
271. Howard, J., and Hyman, A.A. (2003). Dynamics and mechanics of the microtubule plus end. *Nature* 422, 753-758.
272. Huang, T.T., Nijman, S.M., Mirchandani, K.D., Galardy, P.J., Cohn, M.A., Haas, W., Gygi, S.P., Ploegh, H.L., Bernards, R., and D'Andrea, A.D. (2006). Regulation of monoubiquitinated PCNA by DUB autocleavage. *Nat Cell Biol* 8, 339-347.
273. Huang, X., Okafuji, M., Traganos, F., Luther, E., Holden, E., and Darzynkiewicz, Z. (2004). Assessment of histone H2AX phosphorylation induced by DNA topoisomerase I and II inhibitors topotecan and mitoxantrone and by the DNA cross-linking agent cisplatin. *Cytometry A* 58, 99-110.
274. Huang, X.X., Bernerd, F., and Halliday, G.M. (2009). Ultraviolet A within sunlight induces mutations in the epidermal basal layer of engineered human skin. *Am J Pathol* 174, 1534-1543.
275. Hunt, T. (1991). Cyclins and their partners: from a simple idea to complicated reality. *Semin Cell Biol* 2, 213-222.
276. Hurov, K.E., Cotta-Ramusino, C., and Elledge, S.J. (2010). A genetic screen identifies the Triple T complex required for DNA damage signaling and ATM and ATR stability. *Genes Dev* 24, 1939-1950.
277. Hyatt, G.A., and Beebe, D.C. (1992). Use of a double-label method to detect rapid changes in the rate of cell proliferation. *J Histochem Cytochem* 40, 619-627.
278. Iftode, C., Daniely, Y., and Borowiec, J.A. (1999). Replication protein A (RPA): the eukaryotic SSB. *Crit Rev Biochem Mol Biol* 34, 141-180.
279. Ikari, A., Nagatani, Y., Tsukimoto, M., Harada, H., Miwa, M., and Takagi, K. (2005). Sodium-dependent glucose transporter reduces peroxynitrite and cell

- p injury caused by cisplatin in renal tubular epithelial cells.
- Biochim Biophys Acta*
- 1717, 109-117.
280. Ikura, T., Tashiro, S., Kakino, A., Shima, H., Jacob, N., Amunugama, R., Yoder, K., Izumi, S., Kuraoka, I., Tanaka, K., *et al.* (2007). DNA damage-dependent acetylation and ubiquitination of H2AX enhances chromatin dynamics. *Mol Cell Biol* 27, 7028-7040.
 281. Inui, H., Oh, K.S., Nadem, C., Ueda, T., Khan, S.G., Metin, A., Gozukara, E., Emmert, S., Slor, H., Busch, D.B., *et al.* (2008). Xeroderma pigmentosum-variant patients from America, Europe, and Asia. *J Invest Dermatol* 128, 2055-2068.
 282. Ishida, S., Lee, J., Thiele, D.J., and Herskowitz, I. (2002). Uptake of the anticancer drug cisplatin mediated by the copper transporter Ctr1 in yeast and mammals. *Proc Natl Acad Sci U S A* 99, 14298-14302.
 283. Itakura, E., Umeda, K., Sekoguchi, E., Takata, H., Ohsumi, M., and Matsuura, A. (2004). ATR-dependent phosphorylation of ATRIP in response to genotoxic stress. *Biochem Biophys Res Commun* 323, 1197-1202.
 284. Ivanov, V.I., and Minchenkova, L.E. (1994). [The A-form of DNA: in search of the biological role]. *Mol Biol (Mosk)* 28, 1258-1271.
 285. Izzard, R.A., Jackson, S.P., and Smith, G.C. (1999). Competitive and noncompetitive inhibition of the DNA-dependent protein kinase. *Cancer Res* 59, 2581-2586.
 286. Jackel, M., and Kopf-Maier, P. (1991). Influence of cisplatin on cell-cycle progression in xenografted human head and neck carcinomas. *Cancer Chemother Pharmacol* 27, 464-471.
 287. Jackiewicz, Z., Zubik-Kowal, B., and Basse, B. (2009). Finite-difference and pseudo-spectral methods for the numerical simulations of in vitro human tumor cell population kinetics. *Math Biosci Eng* 6, 561-572.
 288. Jackson, D., Dhar, K., Wahl, J.K., Wold, M.S., and Borgstahl, G.E. (2002). Analysis of the human replication protein A:Rad52 complex: evidence for crosstalk between RPA32, RPA70, Rad52 and DNA. *J Mol Biol* 321, 133-148.
 289. Jamieson, E.R., and Lippard, S.J. (1999). Structure, Recognition, and Processing of Cisplatin-DNA Adducts. *Chem Rev* 99, 2467-2498.
 290. Jazayeri, A., Falck, J., Lukas, C., Bartek, J., Smith, G.C., Lukas, J., and Jackson, S.P. (2006). ATM- and cell cycle-dependent regulation of ATR in response to DNA double-strand breaks. *Nat Cell Biol* 8, 37-45.
 291. Jemal, A., Center, M.M., DeSantis, C., and Ward, E.M. (2010). Global patterns of cancer incidence and mortality rates and trends. *Cancer Epidemiol Biomarkers Prev* 19, 1893-1907.
 292. Jemal, A., Siegel, R., Ward, E., Hao, Y., Xu, J., Murray, T., and Thun, M.J. (2008). Cancer statistics, 2008. *CA Cancer J Clin* 58, 71-96.
 293. Jiang, X.R., Jimenez, G., Chang, E., Frolkis, M., Kusler, B., Sage, M., Beeche, M., Bodnar, A.G., Wahl, G.M., Tlsty, T.D., *et al.* (1999). Telomerase expression in human somatic cells does not induce changes associated with a transformed phenotype. *Nat Genet* 21, 111-114.
 294. Jiricny, J. (2000). Mismatch repair: the praying hands of fidelity. *Curr Biol* 10, R788-790.
 295. Jiricny, J. (2006). The multifaceted mismatch-repair system. *Nat Rev Mol Cell Biol* 7, 335-346.

296. Joensuu, H. (2008). Systemic chemotherapy for cancer: from weapon to treatment. *Lancet Oncol* 9, 304.
297. Johnson, R.E., Haracska, L., Prakash, S., and Prakash, L. (2001). Role of DNA polymerase zeta in the bypass of a (6-4) TT photoproduct. *Mol Cell Biol* 21, 3558-3563.
298. Johnson, R.E., Kondratieck, C.M., Prakash, S., and Prakash, L. (1999). hRAD30 mutations in the variant form of xeroderma pigmentosum. *Science* 285, 263-265.
299. Johnson, R.E., Washington, M.T., Haracska, L., Prakash, S., and Prakash, L. (2000). Eukaryotic polymerases iota and zeta act sequentially to bypass DNA lesions. *Nature* 406, 1015-1019.
300. Jordan, M.A., Thrower, D., and Wilson, L. (1992). Effects of vinblastine, podophyllotoxin and nocodazole on mitotic spindles. Implications for the role of microtubule dynamics in mitosis. *J Cell Sci* 102 (Pt 3), 401-416.
301. Jordan, P., and Carmo-Fonseca, M. (2000). Molecular mechanisms involved in cisplatin cytotoxicity. *Cell Mol Life Sci* 57, 1229-1235.
302. Kaelin, W.G. (2005). The von Hippel-Lindau tumor suppressor protein: roles in cancer and oxygen sensing. *Cold Spring Harb Symp Quant Biol* 70, 159-166.
303. Kanaar, R., and Wyman, C. (2008). DNA repair by the MRN complex: break it to make it. *Cell* 135, 14-16.
304. Kannouche, P., Fernandez de Henestrosa, A.R., Coull, B., Vidal, A.E., Gray, C., Zicha, D., Woodgate, R., and Lehmann, A.R. (2002). Localization of DNA polymerases eta and iota to the replication machinery is tightly co-ordinated in human cells. *EMBO J* 21, 6246-6256.
305. Kannouche, P., Fernandez de Henestrosa, A.R., Coull, B., Vidal, A.E., Gray, C., Zicha, D., Woodgate, R., and Lehmann, A.R. (2003). Localization of DNA polymerases eta and iota to the replication machinery is tightly co-ordinated in human cells. *EMBO J* 22, 1223-1233.
306. Kannouche, P., and Sary, A. (2003). Xeroderma pigmentosum variant and error-prone DNA polymerases. *Biochimie* 85, 1123-1132.
307. Kannouche, P.L., and Lehmann, A.R. (2004). Ubiquitination of PCNA and the polymerase switch in human cells. *Cell Cycle* 3, 1011-1013.
308. Kannouche, P.L., Wing, J., and Lehmann, A.R. (2004). Interaction of human DNA polymerase eta with monoubiquitinated PCNA: a possible mechanism for the polymerase switch in response to DNA damage. *Mol Cell* 14, 491-500.
309. Kappes, U.P., Luo, D., Potter, M., Schulmeister, K., and Runger, T.M. (2006). Short- and long-wave UV light (UVB and UVA) induce similar mutations in human skin cells. *J Invest Dermatol* 126, 667-675.
310. Karlsson-Rosenthal, C., and Millar, J.B. (2006). Cdc25: mechanisms of checkpoint inhibition and recovery. *Trends Cell Biol* 16, 285-292.
311. Kartalou, M., and Essigmann, J.M. (2001a). Mechanisms of resistance to cisplatin. *Mutat Res* 478, 23-43.
312. Kartalou, M., and Essigmann, J.M. (2001b). Recognition of cisplatin adducts by cellular proteins. *Mutat Res* 478, 1-21.
313. Kasparkova, J., Mackay, F.S., Brabec, V., and Sadler, P.J. (2003). Formation of platinated GG cross-links on DNA by photoactivation of a platinum(IV) azide complex. *J Biol Inorg Chem* 8, 741-745.

314. Kasparkova, J., Marini, V., Bursova, V., and Brabec, V. (2008). Biophysical studies on the stability of DNA intrastrand cross-links of transplatin. *Biophys J* 95, 4361-4371.
315. Kass, E.M., Ahn, J., Tanaka, T., Freed-Pastor, W.A., Keezer, S., and Prives, C. (2007). Stability of checkpoint kinase 2 is regulated via phosphorylation at serine 456. *J Biol Chem* 282, 30311-30321.
316. Kastan, M.B., and Bartek, J. (2004). Cell-cycle checkpoints and cancer. *Nature* 432, 316-323.
317. Kastan, M.B., and Lim, D.S. (2000). The many substrates and functions of ATM. *Nat Rev Mol Cell Biol* 1, 179-186.
318. Katano, K., Safaei, R., Samimi, G., Holzer, A., Rochdi, M., and Howell, S.B. (2003). The copper export pump ATP7B modulates the cellular pharmacology of carboplatin in ovarian carcinoma cells. *Mol Pharmacol* 64, 466-473.
319. Kawamoto, T., Araki, K., Sonoda, E., Yamashita, Y.M., Harada, K., Kikuchi, K., Masutani, C., Hanaoka, F., Nozaki, K., Hashimoto, N., *et al.* (2005). Dual roles for DNA polymerase eta in homologous DNA recombination and translesion DNA synthesis. *Mol Cell* 20, 793-799.
320. Kelland, L. (2007a). Broadening the clinical use of platinum drug-based chemotherapy with new analogues. Satraplatin and picoplatin. *Expert Opin Investig Drugs* 16, 1009-1021.
321. Kelland, L. (2007b). The resurgence of platinum-based cancer chemotherapy. *Nat Rev Cancer* 7, 573-584.
322. Kemp, M.G., Mason, A.C., Carreira, A., Reardon, J.T., Haring, S.J., Borgstahl, G.E., Kowalczykowski, S.C., Sancar, A., and Wold, M.S. (2010). An alternative form of replication protein A expressed in normal human tissues supports DNA repair. *J Biol Chem* 285, 4788-4797.
323. Kenny, M.K., Schlegel, U., Furneaux, H., and Hurwitz, J. (1990). The role of human single-stranded DNA binding protein and its individual subunits in simian virus 40 DNA replication. *J Biol Chem* 265, 7693-7700.
324. Kerzendorfer, C., and O'Driscoll, M. (2009). Human DNA damage response and repair deficiency syndromes: linking genomic instability and cell cycle checkpoint proficiency. *DNA Repair (Amst)* 8, 1139-1152.
325. Keshav, K.F., Chen, C., and Dutta, A. (1995). Rpa4, a homolog of the 34-kilodalton subunit of the replication protein A complex. *Mol Cell Biol* 15, 3119-3128.
326. Keys, H.M., Bundy, B.N., Stehman, F.B., Muderspach, L.I., Chafe, W.E., Suggs, C.L., 3rd, Walker, J.L., and Gersell, D. (1999). Cisplatin, radiation, and adjuvant hysterectomy compared with radiation and adjuvant hysterectomy for bulky stage IB cervical carcinoma. *N Engl J Med* 340, 1154-1161.
327. Kim, J.E., Minter-Dykhouse, K., and Chen, J. (2006). Signaling networks controlled by the MRN complex and MDC1 during early DNA damage responses. *Mol Carcinog* 45, 403-408.
328. Kim, S.M., Kumagai, A., Lee, J., and Dunphy, W.G. (2005). Phosphorylation of Chk1 by ATM- and Rad3-related (ATR) in *Xenopus* egg extracts requires binding of ATRIP to ATR but not the stable DNA-binding or coiled-coil domains of ATRIP. *J Biol Chem* 280, 38355-38364.
329. Kim, S.T., Lim, D.S., Canman, C.E., and Kastan, M.B. (1999). Substrate specificities and identification of putative substrates of ATM kinase family members. *J Biol Chem* 274, 37538-37543.

330. Kim, S.T., Xu, B., and Kastan, M.B. (2002). Involvement of the cohesin protein, Smc1, in Atm-dependent and independent responses to DNA damage. *Genes Dev* 16, 560-570.
331. Kirschner, K., and Melton, D.W. (2010). Multiple roles of the ERCC1-XPF endonuclease in DNA repair and resistance to anticancer drugs. *Anticancer Res* 30, 3223-3232.
332. Kitagawa, R., Bakkenist, C.J., McKinnon, P.J., and Kastan, M.B. (2004). Phosphorylation of SMC1 is a critical downstream event in the ATM-NBS1-BRCA1 pathway. *Genes Dev* 18, 1423-1438.
333. Klein, S., Zenvirth, D., Dror, V., Barton, A.B., Kaback, D.B., and Simchen, G. (1996). Patterns of meiotic double-strand breakage on native and artificial yeast chromosomes. *Chromosoma* 105, 276-284.
334. Knipscheer, P., Raschle, M., Smogorzewska, A., Enoiu, M., Ho, T.V., Schärer, O.D., Elledge, S.J., and Walter, J.C. (2009). The Fanconi anemia pathway promotes replication-dependent DNA interstrand cross-link repair. *Science* 326, 1698-1701.
335. Knox, R.J., Friedlos, F., Lydall, D.A., and Roberts, J.J. (1986). Mechanism of cytotoxicity of anticancer platinum drugs: evidence that cis-diamminedichloroplatinum(II) and cis-diammine-(1,1-cyclobutanedicarboxylato)platinum(II) differ only in the kinetics of their interaction with DNA. *Cancer Res* 46, 1972-1979.
336. Kobayashi, J., Tauchi, H., Chen, B., Burma, S., Tashiro, S., Matsuura, S., Tanimoto, K., Chen, D.J., and Komatsu, K. (2009). Histone H2AX participates the DNA damage-induced ATM activation through interaction with NBS1. *Biochem Biophys Res Commun* 380, 752-757.
337. Koberle, B., Tomicic, M.T., Usanova, S., and Kaina, B. (2010). Cisplatin resistance: preclinical findings and clinical implications. *Biochim Biophys Acta* 1806, 172-182.
338. Koepsell, H., and Endou, H. (2004). The SLC22 drug transporter family. *Pflugers Arch* 447, 666-676.
339. Kolas, N.K., Chapman, J.R., Nakada, S., Ylanko, J., Chahwan, R., Sweeney, F.D., Panier, S., Mendez, M., Wildenhain, J., Thomson, T.M., *et al.* (2007). Orchestration of the DNA-damage response by the RNF8 ubiquitin ligase. *Science* 318, 1637-1640.
340. Kolodner, R.D., and Marsischky, G.T. (1999). Eukaryotic DNA mismatch repair. *Curr Opin Genet Dev* 9, 89-96.
341. Komander, D., Clague, M.J., and Urbe, S. (2009). Breaking the chains: structure and function of the deubiquitinases. *Nat Rev Mol Cell Biol* 10, 550-563.
342. Koprinarova, M., Markovska, P., Iliev, I., Anachkova, B., and Russev, G. (2010). Sodium butyrate enhances the cytotoxic effect of cisplatin by abrogating the cisplatin imposed cell cycle arrest. *BMC Mol Biol* 11, 49.
343. Korkola, J., and Gray, J.W. (2010). Breast cancer genomes--form and function. *Curr Opin Genet Dev* 20, 4-14.
344. Koshiyama, M., Kinezaki, M., Uchida, T., and Sumitomo, M. (2005). Chemosensitivity testing of a novel platinum analog, nedaplatin (254-S), in human gynecological carcinomas: a comparison with cisplatin. *Anticancer Res* 25, 4499-4502.

345. Kozlov, S., Gueven, N., Keating, K., Ramsay, J., and Lavin, M.F. (2003). ATP activates ataxia-telangiectasia mutated (ATM) in vitro. Importance of autophosphorylation. *J Biol Chem* 278, 9309-9317.
346. Kozlov, S.V., Graham, M.E., Peng, C., Chen, P., Robinson, P.J., and Lavin, M.F. (2006). Involvement of novel autophosphorylation sites in ATM activation. *EMBO J* 25, 3504-3514.
347. Krasikova, Y.S., Rechkunova, N.I., Maltseva, E.A., Petruseva, I.O., and Lavrik, O.I. (2010). Localization of xeroderma pigmentosum group A protein and replication protein A on damaged DNA in nucleotide excision repair. *Nucleic Acids Res* 38, 8083-8094.
348. Kraus, E., Leung, W.Y., and Haber, J.E. (2001). Break-induced replication: a review and an example in budding yeast. *Proc Natl Acad Sci U S A* 98, 8255-8262.
349. Krijger, P.H., Wit, N., van den Berk, P.C., and Jacobs, H. The Fanconi anemia core complex is dispensable during somatic hypermutation and class switch recombination. *PLoS One* 5, e15236.
350. Krogh, B.O., and Symington, L.S. (2004). Recombination proteins in yeast. *Annu Rev Genet* 38, 233-271.
351. Krokan, H., Wist, E., and Prydz, H. (1977). DNA replication intermediates in whole HeLa cells and isolated nuclei. *Biochim Biophys Acta* 475, 553-561.
352. Krylov, D.M., Nasmyth, K., and Koonin, E.V. (2003). Evolution of eukaryotic cell cycle regulation: stepwise addition of regulatory kinases and late advent of the CDKs. *Curr Biol* 13, 173-177.
353. Kubbies, M., Goller, B., Schetters, B., Bartosek, I., and Albert, W. (1991). Glutathione restores normal cell activation and cell cycle progression in cis-platinum treated human lymphocytes. *Br J Cancer* 64, 843-849.
354. Kues, W.A., Anger, M., Carnwath, J.W., Paul, D., Motlik, J., and Niemann, H. (2000). Cell cycle synchronization of porcine fetal fibroblasts: effects of serum deprivation and reversible cell cycle inhibitors. *Biol Reprod* 62, 412-419.
355. Kulkarni, A., and Das, K.C. (2008). Differential roles of ATR and ATM in p53, Chk1, and histone H2AX phosphorylation in response to hyperoxia: ATR-dependent ATM activation. *Am J Physiol Lung Cell Mol Physiol* 294, L998-L1006.
356. Kung, A.L., Sherwood, S.W., and Schimke, R.T. (1990). Cell line-specific differences in the control of cell cycle progression in the absence of mitosis. *Proc Natl Acad Sci U S A* 87, 9553-9557.
357. Kweekel, D.M., Gelderblom, H., and Guchelaar, H.J. (2005). Pharmacology of oxaliplatin and the use of pharmacogenomics to individualize therapy. *Cancer Treat Rev* 31, 90-105.
358. Laemmli, U.K. (1970). Cleavage of structural proteins during the assembly of the head of bacteriophage T4. *Nature* 227, 680-685.
359. Lam, M.H., Liu, Q., Elledge, S.J., and Rosen, J.M. (2004). Chk1 is haploinsufficient for multiple functions critical to tumor suppression. *Cancer Cell* 6, 45-59.
360. Lan, L., Hayashi, T., Rabeya, R.M., Nakajima, S., Kanno, S., Takao, M., Matsunaga, T., Yoshino, M., Ichikawa, M., Riele, H., *et al.* (2004). Functional and physical interactions between ERCC1 and MSH2 complexes for resistance to cis-diamminedichloroplatinum(II) in mammalian cells. *DNA Repair (Amst)* 3, 135-143.

361. Landwehr, R., Bogdanova, N.V., Antonenkova, N., Meyer, A., Bremer, M., Park-Simon, T.W., Hillemanns, P., Karstens, J.H., Schindler, D., and Dork, T. (2011). Mutation analysis of the SLX4/FANCP gene in hereditary breast cancer. *Breast Cancer Res Treat*.
362. Lao, Y., Gomes, X.V., Ren, Y., Taylor, J.S., and Wold, M.S. (2000). Replication protein A interactions with DNA. III. Molecular basis of recognition of damaged DNA. *Biochemistry* 39, 850-859.
363. Lapenna, S., and Giordano, A. (2009). Cell cycle kinases as therapeutic targets for cancer. *Nat Rev Drug Discov* 8, 547-566.
364. Lavin, M.F. (2007). ATM and the Mre11 complex combine to recognize and signal DNA double-strand breaks. *Oncogene* 26, 7749-7758.
365. Lavin, M.F. (2008). Ataxia-telangiectasia: from a rare disorder to a paradigm for cell signalling and cancer. *Nat Rev Mol Cell Biol* 9, 759-769.
366. Lavin, M.F., and Shiloh, Y. (1997). The genetic defect in ataxia-telangiectasia. *Annu Rev Immunol* 15, 177-202.
367. Leahy, J.J., Golding, B.T., Griffin, R.J., Hardcastle, I.R., Richardson, C., Rigoreau, L., and Smith, G.C. (2004). Identification of a highly potent and selective DNA-dependent protein kinase (DNA-PK) inhibitor (NU7441) by screening of chromenone libraries. *Bioorg Med Chem Lett* 14, 6083-6087.
368. Lee, D.H., Pan, Y., Kanner, S., Sung, P., Borowiec, J.A., and Chowdhury, D. (2010). A PP4 phosphatase complex dephosphorylates RPA2 to facilitate DNA repair via homologous recombination. *Nat Struct Mol Biol* 17, 365-372.
369. Lee, J.H., Park, C.J., Shin, J.S., Ikegami, T., Akutsu, H., and Choi, B.S. (2004). NMR structure of the DNA decamer duplex containing double T*G mismatches of cis-syn cyclobutane pyrimidine dimer: implications for DNA damage recognition by the XPC-hHR23B complex. *Nucleic Acids Res* 32, 2474-2481.
370. Lee, K.B., Parker, R.J., Bohr, V., Cornelison, T., and Reed, E. (1993). Cisplatin sensitivity/resistance in UV repair-deficient Chinese hamster ovary cells of complementation groups 1 and 3. *Carcinogenesis* 14, 2177-2180.
371. Lee, S.I., Brown, M.K., and Eastman, A. (1999). Comparison of the efficacy of 7-hydroxystaurosporine (UCN-01) and other staurosporine analogs to abrogate cisplatin-induced cell cycle arrest in human breast cancer cell lines. *Biochem Pharmacol* 58, 1713-1721.
372. Lees-Miller, S.P., Sakaguchi, K., Ullrich, S.J., Appella, E., and Anderson, C.W. (1992). Human DNA-activated protein kinase phosphorylates serines 15 and 37 in the amino-terminal transactivation domain of human p53. *Mol Cell Biol* 12, 5041-5049.
373. Lees, E. (1995). Cyclin dependent kinase regulation. *Curr Opin Cell Biol* 7, 773-780.
374. Lehmann, A.R. (2002). Replication of damaged DNA in mammalian cells: new solutions to an old problem. *Mutat Res* 509, 23-34.
375. Lehmann, A.R. (2005). Replication of damaged DNA by translesion synthesis in human cells. *FEBS Lett* 579, 873-876.
376. Lehmann, A.R., Kirk-Bell, S., Arlett, C.F., Paterson, M.C., Lohman, P.H., de Weerd-Kastelein, E.A., and Bootsma, D. (1975). Xeroderma pigmentosum cells with normal levels of excision repair have a defect in DNA synthesis after UV-irradiation. *Proc Natl Acad Sci U S A* 72, 219-223.

377. Lehmann, A.R., Niimi, A., Ogi, T., Brown, S., Sabbioneda, S., Wing, J.F., Kannouche, P.L., and Green, C.M. (2007). Translesion synthesis: Y-family polymerases and the polymerase switch. *DNA Repair (Amst)* 6, 891-899.
378. Lempiainen, H., and Halazonetis, T.D. (2009). Emerging common themes in regulation of PIKKs and PI3Ks. *EMBO J* 28, 3067-3073.
379. Lenne-Samuel, N., Janel-Bintz, R., Kolbanovskiy, A., Geacintov, N.E., and Fuchs, R.P. (2000). The processing of a Benzo(a)pyrene adduct into a frameshift or a base substitution mutation requires a different set of genes in *Escherichia coli*. *Mol Microbiol* 38, 299-307.
380. Levine, R.L., Miller, H., Grollman, A., Ohashi, E., Ohmori, H., Masutani, C., Hanaoka, F., and Moriya, M. (2001). Translesion DNA synthesis catalyzed by human pol eta and pol kappa across 1,N6-ethenodeoxyadenosine. *J Biol Chem* 276, 18717-18721.
381. Lewis, K.A., Lilly, K.K., Reynolds, E.A., Sullivan, W.P., Kaufmann, S.H., and Cliby, W.A. (2009). Ataxia telangiectasia and rad3-related kinase contributes to cell cycle arrest and survival after cisplatin but not oxaliplatin. *Mol Cancer Ther* 8, 855-863.
382. Lieber, M.R. (2010). The mechanism of double-strand DNA break repair by the nonhomologous DNA end-joining pathway. *Annu Rev Biochem* 79, 181-211.
383. Limbo, O., Chahwan, C., Yamada, Y., de Bruin, R.A., Wittenberg, C., and Russell, P. (2007). Ctp1 is a cell-cycle-regulated protein that functions with Mre11 complex to control double-strand break repair by homologous recombination. *Mol Cell* 28, 134-146.
384. Limoli, C.L., Giedzinski, E., Bonner, W.M., and Cleaver, J.E. (2002). UV-induced replication arrest in the xeroderma pigmentosum variant leads to DNA double-strand breaks, gamma -H2AX formation, and Mre11 relocalization. *Proc Natl Acad Sci U S A* 99, 233-238.
385. Lincz, L.F. (1998). Deciphering the apoptotic pathway: all roads lead to death. *Immunol Cell Biol* 76, 1-19.
386. Lindqvist, A., Kallstrom, H., Lundgren, A., Barsoum, E., and Rosenthal, C.K. (2005). Cdc25B cooperates with Cdc25A to induce mitosis but has a unique role in activating cyclin B1-Cdk1 at the centrosome. *J Cell Biol* 171, 35-45.
387. Lisby, M., Antunez de Mayolo, A., Mortensen, U.H., and Rothstein, R. (2003a). Cell cycle-regulated centers of DNA double-strand break repair. *Cell Cycle* 2, 479-483.
388. Lisby, M., Barlow, J.H., Burgess, R.C., and Rothstein, R. (2004). Choreography of the DNA damage response: spatiotemporal relationships among checkpoint and repair proteins. *Cell* 118, 699-713.
389. Lisby, M., Mortensen, U.H., and Rothstein, R. (2003b). Colocalization of multiple DNA double-strand breaks at a single Rad52 repair centre. *Nat Cell Biol* 5, 572-577.
390. Lisby, M., and Rothstein, R. (2004). DNA repair: keeping it together. *Curr Biol* 14, R994-996.
391. Lisby, M., and Rothstein, R. (2005). Localization of checkpoint and repair proteins in eukaryotes. *Biochimie* 87, 579-589.
392. Liu, V.F., and Weaver, D.T. (1993). The ionizing radiation-induced replication protein A phosphorylation response differs between ataxia telangiectasia and normal human cells. *Mol Cell Biol* 13, 7222-7231.

393. Liu, Y., Pilankatta, R., Hatori, Y., Lewis, D., and Inesi, G. (2010). Comparative features of copper ATPases ATP7A and ATP7B heterologously expressed in COS-1 cells. *Biochemistry* 49, 10006-10012.
394. Livneh, Z. (2001). DNA damage control by novel DNA polymerases: translesion replication and mutagenesis. *J Biol Chem* 276, 25639-25642.
395. Livneh, Z. (2006). Keeping mammalian mutation load in check: regulation of the activity of error-prone DNA polymerases by p53 and p21. *Cell Cycle* 5, 1918-1922.
396. Livneh, Z., Ziv, O., and Shachar, S. (2010). Multiple two-polymerase mechanisms in mammalian translesion DNA synthesis. *Cell Cycle* 9, 729-735.
397. Llorca, O., Rivera-Calzada, A., Grantham, J., and Willison, K.R. (2003). Electron microscopy and 3D reconstructions reveal that human ATM kinase uses an arm-like domain to clamp around double-stranded DNA. *Oncogene* 22, 3867-3874.
398. Lobachev, K., Vitriol, E., Stemple, J., Resnick, M.A., and Bloom, K. (2004). Chromosome fragmentation after induction of a double-strand break is an active process prevented by the RMX repair complex. *Curr Biol* 14, 2107-2112.
399. Loehrer, P.J., and Einhorn, L.H. (1984). Drugs five years later. Cisplatin. *Ann Intern Med* 100, 704-713.
400. Loffler, H., Rebacz, B., Ho, A.D., Lukas, J., Bartek, J., and Kramer, A. (2006). Chk1-dependent regulation of Cdc25B functions to coordinate mitotic events. *Cell Cycle* 5, 2543-2547.
401. Longhese, M.P., Neecke, H., Paciotti, V., Lucchini, G., and Plevani, P. (1996). The 70 kDa subunit of replication protein A is required for the G1/S and intra-S DNA damage checkpoints in budding yeast. *Nucleic Acids Res* 24, 3533-3537.
402. Longo, N.S., and Lipsky, P.E. (2006). Why do B cells mutate their immunoglobulin receptors? *Trends Immunol* 27, 374-380.
403. Lord, C.J., Garrett, M.D., and Ashworth, A. (2006). Targeting the double-strand DNA break repair pathway as a therapeutic strategy. *Clin Cancer Res* 12, 4463-4468.
404. Losiewicz, M.D., Carlson, B.A., Kaur, G., Sausville, E.A., and Worland, P.J. (1994). Potent inhibition of CDC2 kinase activity by the flavonoid L86-8275. *Biochem Biophys Res Commun* 201, 589-595.
405. Lou, Z., Chen, B.P., Asaithamby, A., Minter-Dykhouse, K., Chen, D.J., and Chen, J. (2004). MDC1 regulates DNA-PK autophosphorylation in response to DNA damage. *J Biol Chem* 279, 46359-46362.
406. Lou, Z., Chini, C.C., Minter-Dykhouse, K., and Chen, J. (2003). Mediator of DNA damage checkpoint protein 1 regulates BRCA1 localization and phosphorylation in DNA damage checkpoint control. *J Biol Chem* 278, 13599-13602.
407. Lovly, C.M., Yan, L., Ryan, C.E., Takada, S., and Piwnica-Worms, H. (2008). Regulation of Chk2 ubiquitination and signaling through autophosphorylation of serine 379. *Mol Cell Biol* 28, 5874-5885.
408. Luciani, M.G., Oehlmann, M., and Blow, J.J. (2004). Characterization of a novel ATR-dependent, Chk1-independent, intra-S-phase checkpoint that suppresses initiation of replication in *Xenopus*. *J Cell Sci* 117, 6019-6030.
409. Ludlow, J.W. (1993). Interactions between SV40 large-tumor antigen and the growth suppressor proteins pRB and p53. *FASEB J* 7, 866-871.

410. Ludlow, J.W., Glendening, C.L., Livingston, D.M., and DeCarprio, J.A. (1993). Specific enzymatic dephosphorylation of the retinoblastoma protein. *Mol Cell Biol* 13, 367-372.
411. Lukas, C., Falck, J., Bartkova, J., Bartek, J., and Lukas, J. (2003). Distinct spatiotemporal dynamics of mammalian checkpoint regulators induced by DNA damage. *Nat Cell Biol* 5, 255-260.
412. Lukas, C., Melander, F., Stucki, M., Falck, J., Bekker-Jensen, S., Goldberg, M., Lerenthal, Y., Jackson, S.P., Bartek, J., and Lukas, J. (2004). Mdc1 couples DNA double-strand break recognition by Nbs1 with its H2AX-dependent chromatin retention. *EMBO J* 23, 2674-2683.
413. Luo, R.X., Postigo, A.A., and Dean, D.C. (1998). Rb interacts with histone deacetylase to repress transcription. *Cell* 92, 463-473.
414. Ma, Y., and Lieber, M.R. (2002). Binding of inositol hexakisphosphate (IP6) to Ku but not to DNA-PKcs. *J Biol Chem* 277, 10756-10759.
415. Ma, Y., Pannicke, U., Lu, H., Niewolik, D., Schwarz, K., and Lieber, M.R. (2005a). The DNA-dependent protein kinase catalytic subunit phosphorylation sites in human Artemis. *J Biol Chem* 280, 33839-33846.
416. Ma, Y., Schwarz, K., and Lieber, M.R. (2005b). The Artemis:DNA-PKcs endonuclease cleaves DNA loops, flaps, and gaps. *DNA Repair (Amst)* 4, 845-851.
417. Mahadevaiah, S.K., Turner, J.M., Baudat, F., Rogakou, E.P., de Boer, P., Blanco-Rodriguez, J., Jasin, M., Keeney, S., Bonner, W.M., and Burgoyne, P.S. (2001). Recombinational DNA double-strand breaks in mice precede synapsis. *Nat Genet* 27, 271-276.
418. Mahmoudi, M., Mercer, J., and Bennett, M. (2006). DNA damage and repair in atherosclerosis. *Cardiovasc Res* 71, 259-268.
419. Maiato, H., Sampaio, P., and Sunkel, C.E. (2004). Microtubule-associated proteins and their essential roles during mitosis. *Int Rev Cytol* 241, 53-153.
420. Mailand, N., Falck, J., Lukas, C., Syljuasen, R.G., Welcker, M., Bartek, J., and Lukas, J. (2000). Rapid destruction of human Cdc25A in response to DNA damage. *Science* 288, 1425-1429.
421. Maitra, A., Roberts, H., Weinberg, A.G., and Geradts, J. (2001). Loss of p16(INK4a) expression correlates with decreased survival in pediatric osteosarcomas. *Int J Cancer* 95, 34-38.
422. Malinge, J.M., Giraud-Panis, M.J., and Leng, M. (1999). Interstrand cross-links of cisplatin induce striking distortions in DNA. *J Inorg Biochem* 77, 23-29.
423. Malumbres, M., and Barbacid, M. (2005). Mammalian cyclin-dependent kinases. *Trends Biochem Sci* 30, 630-641.
424. Malumbres, M., and Barbacid, M. (2009). Cell cycle, CDKs and cancer: a changing paradigm. *Nat Rev Cancer* 9, 153-166.
425. Manthey, K.C., Glanzer, J.G., Dimitrova, D.D and Oakley, G.G. (2010). Hyperphosphorylation of replication protein A in cisplatin-resistant and -sensitive head and neck squamous cell carcinoma cell lines. *Head Neck*, 32, 636-645.
426. Maraia, R.J. (1991). The subset of mouse B1 (Alu-equivalent) sequences expressed as small processed cytoplasmic transcripts. *Nucleic Acids Res* 19, 5695-5702.
427. Marti, T.M., Hefner, E., Feeney, L., Natale, V., and Cleaver, J.E. (2006). H2AX phosphorylation within the G1 phase after UV irradiation depends on

- nucleotide excision repair and not DNA double-strand breaks. *Proc Natl Acad Sci U S A* *103*, 9891-9896.
428. Martomo, S.A., Yang, W.W., Vaisman, A., Maas, A., Yokoi, M., Hoeijmakers, J.H., Hanaoka, F., Woodgate, R., and Gearhart, P.J. (2006). Normal hypermutation in antibody genes from congenic mice defective for DNA polymerase η . *DNA Repair (Amst)* *5*, 392-398.
429. Martomo, S.A., Yang, W.W., Wersto, R.P., Ohkumo, T., Kondo, Y., Yokoi, M., Masutani, C., Hanaoka, F., and Gearhart, P.J. (2005). Different mutation signatures in DNA polymerase η - and MSH6-deficient mice suggest separate roles in antibody diversification. *Proc Natl Acad Sci U S A* *102*, 8656-8661.
430. Maser, R.S., Monsen, K.J., Nelms, B.E., and Petrini, J.H. (1997). hMre11 and hRad50 nuclear foci are induced during the normal cellular response to DNA double-strand breaks. *Mol Cell Biol* *17*, 6087-6096.
431. Mason, A.C., Roy, R., Simmons, D.T., and Wold, M.S. (2010). Functions of alternative replication protein A in initiation and elongation. *Biochemistry* *49*, 5919-5928.
432. Masutani, C., Araki, M., Yamada, A., Kusumoto, R., Nogimori, T., Maekawa, T., Iwai, S., and Hanaoka, F. (1999). Xeroderma pigmentosum variant (XP-V) correcting protein from HeLa cells has a thymine dimer bypass DNA polymerase activity. *EMBO J* *18*, 3491-3501.
433. Masutani, C., Kusumoto, R., Iwai, S., and Hanaoka, F. (2000). Mechanisms of accurate translesion synthesis by human DNA polymerase η . *EMBO J* *19*, 3100-3109.
434. Matsumoto, Y., Umeda, N., Suzuki, N., Sakai, K., and Hirano, K. (1999). A gel-electrophoretic analysis for improved sensitivity and specificity of DNA-dependent protein kinase activity. *J Radiat Res (Tokyo)* *40*, 183-196.
435. Matsuoka, S., Ballif, B.A., Smogorzewska, A., McDonald, E.R., 3rd, Hurov, K.E., Luo, J., Bakalarski, C.E., Zhao, Z., Solimini, N., Lerenthal, Y., *et al.* (2007). ATM and ATR substrate analysis reveals extensive protein networks responsive to DNA damage. *Science* *316*, 1160-1166.
436. Matsuoka, S., Rotman, G., Ogawa, A., Shiloh, Y., Tamai, K., and Elledge, S.J. (2000). Ataxia telangiectasia-mutated phosphorylates Chk2 in vivo and in vitro. *Proc Natl Acad Sci U S A* *97*, 10389-10394.
437. McClue, S.J., Blake, D., Clarke, R., Cowan, A., Cummings, L., Fischer, P.M., MacKenzie, M., Melville, J., Stewart, K., Wang, S., *et al.* (2002). In vitro and in vivo antitumor properties of the cyclin dependent kinase inhibitor CYC202 (R-roscovitine). *Int J Cancer* *102*, 463-468.
438. McCulloch, S.D., Kokoska, R.J., and Kunkel, T.A. (2004). Efficiency, fidelity and enzymatic switching during translesion DNA synthesis. *Cell Cycle* *3*, 580-583.
439. McCulloch, S.D., and Kunkel, T.A. (2008). The fidelity of DNA synthesis by eukaryotic replicative and translesion synthesis polymerases. *Cell Res* *18*, 148-161.
440. McDonald, J.P., Frank, E.G., Plosky, B.S., Rogozin, I.B., Masutani, C., Hanaoka, F., Woodgate, R., and Gearhart, P.J. (2003). 129-derived strains of mice are deficient in DNA polymerase η and have normal immunoglobulin hypermutation. *J Exp Med* *198*, 635-643.
441. McDonald, J.P., Tissier, A., Frank, E.G., Iwai, S., Hanaoka, F., and Woodgate, R. (2001). DNA polymerase η and related rad30-like enzymes. *Philos Trans R Soc Lond B Biol Sci* *356*, 53-60.

442. McEachern, M.J., and Haber, J.E. (2006). Break-induced replication and recombinational telomere elongation in yeast. *Annu Rev Biochem* 75, 111-135.
443. McEachern, M.J., Krauskopf, A., and Blackburn, E.H. (2000). Telomeres and their control. *Annu Rev Genet* 34, 331-358.
444. McIlwraith, M.J., Vaisman, A., Liu, Y., Fanning, E., Woodgate, R., and West, S.C. (2005). Human DNA polymerase η promotes DNA synthesis from strand invasion intermediates of homologous recombination. *Mol Cell* 20, 783-792.
445. McKee, A.H., and Kleckner, N. (1997). Mutations in *Saccharomyces cerevisiae* that block meiotic prophase chromosome metabolism and confer cell cycle arrest at pachytene identify two new meiosis-specific genes SAE1 and SAE3. *Genetics* 146, 817-834.
446. McSherry, T.D., and Mueller, P.R. (2004). *Xenopus* Cds1 is regulated by DNA-dependent protein kinase and ATR during the cell cycle checkpoint response to double-stranded DNA ends. *Mol Cell Biol* 24, 9968-9985.
447. Medeiros, L.R., Rosa, D.D., Bozzetti, M.C., Fachel, J.M., Furness, S., Garry, R., Rosa, M.I., and Stein, A.T. (2009). Laparoscopy versus laparotomy for benign ovarian tumour. *Cochrane Database Syst Rev*, CD004751.
448. Meek, K., Gupta, S., Ramsden, D.A., and Lees-Miller, S.P. (2004). The DNA-dependent protein kinase: the director at the end. *Immunol Rev* 200, 132-141.
449. Meijer, L., Borgne, A., Mulner, O., Chong, J.P., Blow, J.J., Inagaki, N., Inagaki, M., Delcros, J.G., and Moulinoux, J.P. (1997). Biochemical and cellular effects of roscovitine, a potent and selective inhibitor of the cyclin-dependent kinases cdc2, cdk2 and cdk5. *Eur J Biochem* 243, 527-536.
450. Melo, J., and Toczyski, D. (2002). A unified view of the DNA-damage checkpoint. *Curr Opin Cell Biol* 14, 237-245.
451. Menoyo, A., Alazzouzi, H., Espin, E., Armengol, M., Yamamoto, H., and Schwartz, S., Jr. (2001). Somatic mutations in the DNA damage-response genes ATR and CHK1 in sporadic stomach tumors with microsatellite instability. *Cancer Res* 61, 7727-7730.
452. Merrill, G.F. (1998). Cell synchronization. *Methods Cell Biol* 57, 229-249.
453. Mihara, K., Cao, X.R., Yen, A., Chandler, S., Driscoll, B., Murphree, A.L., T'Ang, A., and Fung, Y.K. (1989). Cell cycle-dependent regulation of phosphorylation of the human retinoblastoma gene product. *Science* 246, 1300-1303.
454. Mimitou, E.P., and Symington, L.S. (2008). Sae2, Exo1 and Sgs1 collaborate in DNA double-strand break processing. *Nature* 455, 770-774.
455. Mirkin, S.M. (2008). Discovery of alternative DNA structures: a heroic decade (1979-1989). *Front Biosci* 13, 1064-1071.
456. Mizutani, A., Okada, T., Shibutani, S., Sonoda, E., Hocheegger, H., Nishigori, C., Miyachi, Y., Takeda, S., and Yamazoe, M. (2004). Extensive chromosomal breaks are induced by tamoxifen and estrogen in DNA repair-deficient cells. *Cancer Res* 64, 3144-3147.
457. Mochan, T.A., Venere, M., DiTullio, R.A., Jr., and Halazonetis, T.D. (2003). 53BP1 and NBS1 function in parallel interacting pathways activating ataxia-telangiectasia mutated (ATM) in response to DNA damage. *Cancer Res* 63, 8586-8591.

458. Mochida, S., Esashi, F., Aono, N., Tamai, K., O'Connell, M.J., and Yanagida, M. (2004). Regulation of checkpoint kinases through dynamic interaction with Crb2. *EMBO J* 23, 418-428.
459. Mogi, S., Butcher, C.E., and Oh, D.H. (2008). DNA polymerase eta reduces the gamma-H2AX response to psoralen interstrand crosslinks in human cells. *Exp Cell Res* 314, 887-895.
460. Mojas, N., Lopes, M., and Jiricny, J. (2007). Mismatch repair-dependent processing of methylation damage gives rise to persistent single-stranded gaps in newly replicated DNA. *Genes Dev* 21, 3342-3355.
461. Moldovan, G.L., and D'Andrea, A.D. (2009). FANCD2 hurdles the DNA interstrand crosslink. *Cell* 139, 1222-1224.
462. Moldovan, G.L., Pfander, B., and Jentsch, S. (2007). PCNA, the maestro of the replication fork. *Cell* 129, 665-679.
463. More, S.S., Akil, O., Ianculescu, A.G., Geier, E.G., Lustig, L.R., and Giacomini, K.M. (2010). Role of the copper transporter, CTR1, in platinum-induced ototoxicity. *J Neurosci* 30, 9500-9509.
464. Moreau, J.L., Marques, F., Barakat, A., Schatt, P., Lozano, J.C., Peaucellier, G., Picard, A., and Genevieve, A.M. (1998). Cdk2 activity is dispensable for the onset of DNA replication during the first mitotic cycles of the sea urchin early embryo. *Dev Biol* 200, 182-197.
465. Morris, M.J., and Bosl, G.J. (1999). High-dose chemotherapy as primary treatment for poor-risk germ-cell tumors: the Memorial Sloan-Kettering experience (1988-1999). *Int J Cancer* 83, 834-838.
466. Motoyama, N., and Naka, K. (2004). DNA damage tumor suppressor genes and genomic instability. *Curr Opin Genet Dev* 14, 11-16.
467. Mueller, S., Schittenhelm, M., Honecker, F., Malenke, E., Lauber, K., Wesselborg, S., Hartmann, J.T., Bokemeyer, C., and Mayer, F. (2006). Cell-cycle progression and response of germ cell tumors to cisplatin in vitro. *Int J Oncol* 29, 471-479.
468. Mukherjee, B., Kessinger, C., Kobayashi, J., Chen, B.P., Chen, D.J., Chatterjee, A., and Burma, S. (2006). DNA-PK phosphorylates histone H2AX during apoptotic DNA fragmentation in mammalian cells. *DNA Repair (Amst)* 5, 575-590.
469. Mukhopadhyay, U., Thurston, J., Whitmire, K.H., Siddik, Z.H., and Khokhar, A.R. (2003). Preparation, characterization, and antitumor activity of new cisplatin analogues with 1-methyl-4-(methylamino)piperidine: crystal structure of [PtII(1-methyl-4-(methylamino) piperidine)(oxalate)]. *J Inorg Biochem* 94, 179-185.
470. Mullen, J.R., Kaliraman, V., Ibrahim, S.S., and Brill, S.J. (2001). Requirement for three novel protein complexes in the absence of the Sgs1 DNA helicase in *Saccharomyces cerevisiae*. *Genetics* 157, 103-118.
471. Muniandy, P.A., Liu, J., Majumdar, A., Liu, S.T., and Seidman, M.M. (2010). DNA interstrand crosslink repair in mammalian cells: step by step. *Crit Rev Biochem Mol Biol* 45, 23-49.
472. Muniandy, P.A., Thapa, D., Thazhathveetil, A.K., Liu, S.T., and Seidman, M.M. (2009). Repair of laser-localized DNA interstrand cross-links in G1 phase mammalian cells. *J Biol Chem* 284, 27908-27917.
473. Murakami-Sekimata, A., Huang, D., Piening, B.D., Bangur, C., and Paulovich, A.G. (2010). The *Saccharomyces cerevisiae* RAD9, RAD17 and RAD24

- genes are required for suppression of mutagenic post-replicative repair during chronic DNA damage. *DNA Repair (Amst)* 9, 824-834.
474. Murakumo, Y., Ogura, Y., Ishii, H., Numata, S., Ichihara, M., Croce, C.M., Fishel, R., and Takahashi, M. (2001). Interactions in the error-prone postreplication repair proteins hREV1, hREV3, and hREV7. *J Biol Chem* 276, 35644-35651.
 475. Murray, D., and Meyn, R.E. (1986). Cell cycle-dependent cytotoxicity of alkylating agents: determination of nitrogen mustard-induced DNA cross-links and their repair in Chinese hamster ovary cells synchronized by centrifugal elutriation. *Cancer Res* 46, 2324-2329.
 476. Musacchio, A., and Salmon, E.D. (2007). The spindle-assembly checkpoint in space and time. *Nat Rev Mol Cell Biol* 8, 379-393.
 477. Mutomba, M.C., and Wang, C.C. (1996). Effects of aphidicolin and hydroxyurea on the cell cycle and differentiation of *Trypanosoma brucei* bloodstream forms. *Mol Biochem Parasitol* 80, 89-102.
 478. Naim, V., and Rosselli, F. (2009). The FANC pathway and mitosis: a replication legacy. *Cell Cycle* 8, 2907-2911.
 479. Nakada, S., Chen, G.I., Gingras, A.C., and Durocher, D. (2008). PP4 is a gamma H2AX phosphatase required for recovery from the DNA damage checkpoint. *EMBO Rep* 9, 1019-1026.
 480. Nakajima, S., Lan, L., Kanno, S., Takao, M., Yamamoto, K., Eker, A.P., and Yasui, A. (2004). UV light-induced DNA damage and tolerance for the survival of nucleotide excision repair-deficient human cells. *J Biol Chem* 279, 46674-46677.
 481. Nakanishi, M., Shimada, M., and Niida, H. (2006). Genetic instability in cancer cells by impaired cell cycle checkpoints. *Cancer Sci* 97, 984-989.
 482. Nakayama, K., Miyazaki, K., Kanzaki, A., Fukumoto, M., and Takebayashi, Y. (2001). Expression and cisplatin sensitivity of copper-transporting P-type adenosine triphosphatase (ATP7B) in human solid carcinoma cell lines. *Oncol Rep* 8, 1285-1287.
 483. Namiki, Y., and Zou, L. (2006). ATRIP associates with replication protein A-coated ssDNA through multiple interactions. *Proc Natl Acad Sci U S A* 103, 580-585.
 484. Nasmyth, K., and Haering, C.H. (2005). The structure and function of SMC and kleisin complexes. *Annu Rev Biochem* 74, 595-648.
 485. Neal, J.A., Fletcher, K.L., McCormick, J.J., and Maher, V.M. (2010). The role of hRev7, the accessory subunit of hPolzeta, in translesion synthesis past DNA damage induced by benzo[a]pyrene diol epoxide (BPDE). *BMC Cell Biol* 11, 97.
 486. Negayama, K., Terada, S., and Kawanishi, K. (1992). [Clinical significance of anti-*Helicobacter pylori* antibody in the diagnosis of *Helicobacter pylori* infection in chronic gastritis]. *Kansenshogaku Zasshi* 66, 1597-1598.
 487. Negrini, S., Gorgoulis, V.G., and Halazonetis, T.D. (2010). Genomic instability--an evolving hallmark of cancer. *Nat Rev Mol Cell Biol* 11, 220-228.
 488. Nelson, J.R., Lawrence, C.W., and Hinkle, D.C. (1996). Deoxycytidyl transferase activity of yeast REV1 protein. *Nature* 382, 729-731.
 489. Neumann, T., Kirschstein, S.O., Camacho Gomez, J.A., Kittler, L., and Unger, E. (2001). Determination of the net exchange rate of tubulin dimer in steady-

- state microtubules by fluorescence correlation spectroscopy. *Biol Chem* 382, 387-391.
490. Nghiem, P., Park, P.K., Kim Ys, Y.S., Desai, B.N., and Schreiber, S.L. (2002). ATR is not required for p53 activation but synergizes with p53 in the replication checkpoint. *J Biol Chem* 277, 4428-4434.
491. Nguyen, D.X., Bos, P.D., and Massague, J. (2009). Metastasis: from dissemination to organ-specific colonization. *Nat Rev Cancer* 9, 274-284.
492. Niedernhofer, L.J., Odijk, H., Budzowska, M., van Drunen, E., Maas, A., Theil, A.F., de Wit, J., Jaspers, N.G., Beverloo, H.B., Hoeijmakers, J.H., *et al.* (2004). The structure-specific endonuclease Ercc1-Xpf is required to resolve DNA interstrand cross-link-induced double-strand breaks. *Mol Cell Biol* 24, 5776-5787.
493. Niedzwiedz, W., Mosedale, G., Johnson, M., Ong, C.Y., Pace, P., and Patel, K.J. (2004). The Fanconi anaemia gene FANCC promotes homologous recombination and error-prone DNA repair. *Mol Cell* 15, 607-620.
494. Niida, H., and Nakanishi, M. (2006). DNA damage checkpoints in mammals. *Mutagenesis* 21, 3-9.
495. Niida, H., Tsuge, S., Katsuno, Y., Konishi, A., Takeda, N., and Nakanishi, M. (2005). Depletion of Chk1 leads to premature activation of Cdc2-cyclin B and mitotic catastrophe. *J Biol Chem* 280, 39246-39252.
496. Nikiforov, Y.E., Nikiforova, M., and Fagin, J.A. (1998). Prevalence of minisatellite and microsatellite instability in radiation-induced post-Chernobyl pediatric thyroid carcinomas. *Oncogene* 17, 1983-1988.
497. Niu, H., Erdjument-Bromage, H., Pan, Z.Q., Lee, S.H., Tempst, P., and Hurwitz, J. (1997). Mapping of amino acid residues in the p34 subunit of human single-stranded DNA-binding protein phosphorylated by DNA-dependent protein kinase and Cdc2 kinase in vitro. *J Biol Chem* 272, 12634-12641.
498. Nojima, K., Hochegger, H., Saberi, A., Fukushima, T., Kikuchi, K., Yoshimura, M., Orelli, B.J., Bishop, D.K., Hirano, S., Ohzeki, M., *et al.* (2005). Multiple repair pathways mediate tolerance to chemotherapeutic cross-linking agents in vertebrate cells. *Cancer Res* 65, 11704-11711.
499. Nordberg, J., and Arner, E.S. (2001). Reactive oxygen species, antioxidants, and the mammalian thioredoxin system. *Free Radic Biol Med* 31, 1287-1312.
500. Nuss, J.E., Patrick, S.M., Oakley, G.G., Alter, G.M., Robison, J.G., Dixon, K., and Turchi, J.J. (2005). DNA damage induced hyperphosphorylation of replication protein A. 1. Identification of novel sites of phosphorylation in response to DNA damage. *Biochemistry* 44, 8428-8437.
501. Nussbaumer, S., Fleury-Souverain, S., Schappler, J., Rudaz, S., Veuthey, J.L., and Bonnabry, P. (2011). Quality control of pharmaceutical formulations containing cisplatin, carboplatin, and oxaliplatin by micellar and microemulsion electrokinetic chromatography (MEKC, MEEKC). *J Pharm Biomed Anal* 55, 253-258.
502. Nusse, M., and Egner, H.J. (1984). Can nocodazole, an inhibitor of microtubule formation, be used to synchronize mammalian cells? Accumulation of cells in mitosis studied by two parametric flow cytometry using acridine orange and by DNA distribution analysis. *Cell Tissue Kinet* 17, 13-23.
503. O'Brien, J., Renwick, A.G., Constable, A., Dybing, E., Muller, D.J., Schlatter, J., Slob, W., Tueting, W., van Benthem, J., Williams, G.M., *et al.* (2006).

- Approaches to the risk assessment of genotoxic carcinogens in food: a critical appraisal. *Food Chem Toxicol* 44, 1613-1635.
504. O'Driscoll, M. (2009). Mouse models for ATR deficiency. *DNA Repair (Amst)* 8, 1333-1337.
505. O'Neill, T., Dwyer, A.J., Ziv, Y., Chan, D.W., Lees-Miller, S.P., Abraham, R.H., Lai, J.H., Hill, D., Shiloh, Y., Cantley, L.C., *et al.* (2000). Utilization of oriented peptide libraries to identify substrate motifs selected by ATM. *J Biol Chem* 275, 22719-22727.
506. O'Neill, T., Giarratani, L., Chen, P., Iyer, L., Lee, C.H., Bobiak, M., Kanai, F., Zhou, B.B., Chung, J.H., and Rathbun, G.A. (2002). Determination of substrate motifs for human Chk1 and hCds1/Chk2 by the oriented peptide library approach. *J Biol Chem* 277, 16102-16115.
507. Oakley, G.G., Loberg, L.I., Yao, J., Risinger, M.A., Yunker, R.L., Zernik-Kobak, M., Khanna, K.K., Lavin, M.F., Carty, M.P., and Dixon, K. (2001). UV-induced hyperphosphorylation of replication protein a depends on DNA replication and expression of ATM protein. *Mol Biol Cell* 12, 1199-1213.
508. Oakley, G.G., Patrick, S.M., Yao, J., Carty, M.P., Turchi, J.J., and Dixon, K. (2003). RPA phosphorylation in mitosis alters DNA binding and protein-protein interactions. *Biochemistry* 42, 3255-3264.
509. Ogi, T., Shinkai, Y., Tanaka, K., and Ohmori, H. (2002). Polkappa protects mammalian cells against the lethal and mutagenic effects of benzo[a]pyrene. *Proc Natl Acad Sci U S A* 99, 15548-15553.
510. Ohashi, E., Bebenek, K., Matsuda, T., Feaver, W.J., Gerlach, V.L., Friedberg, E.C., Ohmori, H., and Kunkel, T.A. (2000). Fidelity and processivity of DNA synthesis by DNA polymerase kappa, the product of the human DINB1 gene. *J Biol Chem* 275, 39678-39684.
511. Ohashi, E., Murakumo, Y., Kanjo, N., Akagi, J., Masutani, C., Hanaoka, F., and Ohmori, H. (2004). Interaction of hREV1 with three human Y-family DNA polymerases. *Genes Cells* 9, 523-531.
512. Ohmori, H., Friedberg, E.C., Fuchs, R.P., Goodman, M.F., Hanaoka, F., Hinkle, D., Kunkel, T.A., Lawrence, C.W., Livneh, Z., Nohmi, T., *et al.* (2001). The Y-family of DNA polymerases. *Mol Cell* 8, 7-8.
513. Ohmori, T., Yang, J.L., Price, J.O., and Arteaga, C.L. (1998). Blockade of tumor cell transforming growth factor-betas enhances cell cycle progression and sensitizes human breast carcinoma cells to cytotoxic chemotherapy. *Exp Cell Res* 245, 350-359.
514. Ohnishi, T., Mori, E., and Takahashi, A. (2009). DNA double-strand breaks: their production, recognition, and repair in eukaryotes. *Mutat Res* 669, 8-12.
515. Olive, P.L., and Banath, J.P. (2009). Kinetics of H2AX phosphorylation after exposure to cisplatin. *Cytometry B Clin Cytom* 76, 79-90.
516. Oliver, A.W., Knapp, S., and Pearl, L.H. (2007). Activation segment exchange: a common mechanism of kinase autophosphorylation? *Trends Biochem Sci* 32, 351-356.
517. Olson, E., Nievera, C.J., Klimovich, V., Fanning, E., and Wu, X. (2006). RPA2 is a direct downstream target for ATR to regulate the S-phase checkpoint. *J Biol Chem* 281, 39517-39533.
518. Orelli, B., McClendon, T.B., Tsodikov, O.V., Ellenberger, T., Niedernhofer, L.J., and Scharer, O.D. (2010). The XPA-binding domain of ERCC1 is required for nucleotide excision repair but not other DNA repair pathways. *J Biol Chem* 285, 3705-3712.

519. Pagano, M., Durst, M., Joswig, S., Draetta, G., and Jansen-Durr, P. (1992). Binding of the human E2F transcription factor to the retinoblastoma protein but not to cyclin A is abolished in HPV-16-immortalized cells. *Oncogene* 7, 1681-1686.
520. Panacheva, L.A., Shpagina, L.A., Musatova, A.S., Liulina, N.V., and Zakrevskaia, A.E. (2005). [Genesis under occupational exposure to toxic and radiation hazards]. *Med Tr Prom Ekol*, 21-24.
521. Park, E.J., Chan, D.W., Park, J.H., Oettinger, M.A., and Kwon, J. (2003). DNA-PK is activated by nucleosomes and phosphorylates H2AX within the nucleosomes in an acetylation-dependent manner. *Nucleic Acids Res* 31, 6819-6827.
522. Patrick, S.M., Oakley, G.G., Dixon, K., and Turchi, J.J. (2005). DNA damage induced hyperphosphorylation of replication protein A. 2. Characterization of DNA binding activity, protein interactions, and activity in DNA replication and repair. *Biochemistry* 44, 8438-8448.
523. Patrick, S.M., and Turchi, J.J. (1999). Replication protein A (RPA) binding to duplex cisplatin-damaged DNA is mediated through the generation of single-stranded DNA. *J Biol Chem* 274, 14972-14978.
524. Pedram, A., Razandi, M., Evinger, A.J., Lee, E., and Levin, E.R. (2009). Estrogen inhibits ATR signaling to cell cycle checkpoints and DNA repair. *Mol Biol Cell* 20, 3374-3389.
525. Pegg, A.E., Kanugula, S., Edara, S., Pauly, G.T., Moschel, R.C., and Goodtzova, K. (1998). Reaction of O6-benzylguanine-resistant mutants of human O6-alkylguanine-DNA alkyltransferase with O6-benzylguanine in oligodeoxyribonucleotides. *J Biol Chem* 273, 10863-10867.
526. Pellegrini, L., Yu, D.S., Lo, T., Anand, S., Lee, M., Blundell, T.L., and Venkitaraman, A.R. (2002). Insights into DNA recombination from the structure of a RAD51-BRCA2 complex. *Nature* 420, 287-293.
527. Pestryakov, P.E., Khlimankov, D.Y., Bochkareva, E., Bochkarev, A., and Lavrik, O.I. (2004). Human replication protein A (RPA) binds a primer-template junction in the absence of its major ssDNA-binding domains. *Nucleic Acids Res* 32, 1894-1903.
528. Pestryakov, P.E., Weisshart, K., Schlott, B., Khodyreva, S.N., Kremmer, E., Grosse, F., Lavrik, O.I., and Nasheuer, H.P. (2003). Human replication protein A. The C-terminal RPA70 and the central RPA32 domains are involved in the interactions with the 3'-end of a primer-template DNA. *J Biol Chem* 278, 17515-17524.
529. Petersen, S., Casellas, R., Reina-San-Martin, B., Chen, H.T., Difilippantonio, M.J., Wilson, P.C., Hanitsch, L., Celeste, A., Muramatsu, M., Pilch, D.R., *et al.* (2001). AID is required to initiate Nbs1/gamma-H2AX focus formation and mutations at sites of class switching. *Nature* 414, 660-665.
530. Pfeifer, G.P., Denissenko, M.F., Olivier, M., Tretyakova, N., Hecht, S.S., and Hainaut, P. (2002). Tobacco smoke carcinogens, DNA damage and p53 mutations in smoking-associated cancers. *Oncogene* 21, 7435-7451.
531. Phillips, L.G., and Sale, J.E. (2010). The Werner's Syndrome protein collaborates with REV1 to promote replication fork progression on damaged DNA. *DNA Repair (Amst)* 9, 1064-1072.
532. Pilch, D.R., Sedelnikova, O.A., Redon, C., Celeste, A., Nussenzweig, A., and Bonner, W.M. (2003). Characteristics of gamma-H2AX foci at DNA double-strand breaks sites. *Biochem Cell Biol* 81, 123-129.

533. Pillaire, M.J., Hoffmann, J.S., Defais, M., and Villani, G. (1995). Replication of DNA containing cisplatin lesions and its mutagenic consequences. *Biochimie* 77, 803-807.
534. Plosky, B.S., Vidal, A.E., Fernandez de Henestrosa, A.R., McLenigan, M.P., McDonald, J.P., Mead, S., and Woodgate, R. (2006). Controlling the subcellular localization of DNA polymerases iota and eta via interactions with ubiquitin. *EMBO J* 25, 2847-2855.
535. Plosky, B.S., and Woodgate, R. (2004). Switching from high-fidelity replicases to low-fidelity lesion-bypass polymerases. *Curr Opin Genet Dev* 14, 113-119.
536. Pondaven, P., Meijer, L., and Beach, D. (1990). Activation of M-phase-specific histone H1 kinase by modification of the phosphorylation of its p34cdc2 and cyclin components. *Genes Dev* 4, 9-17.
537. Prakash, S., Johnson, R.E., and Prakash, L. (2005). Eukaryotic translesion synthesis DNA polymerases: specificity of structure and function. *Annu Rev Biochem* 74, 317-353.
538. Qin, L.F., and Ng, I.O. (2002). Induction of apoptosis by cisplatin and its effect on cell cycle-related proteins and cell cycle changes in hepatoma cells. *Cancer Lett* 175, 27-38.
539. Rabik, C.A., and Dolan, M.E. (2007). Molecular mechanisms of resistance and toxicity associated with platinating agents. *Cancer Treat Rev* 33, 9-23.
540. Raghavan, D. (2003). Chemotherapy and cystectomy for invasive transitional cell carcinoma of bladder. *Urol Oncol* 21, 468-474.
541. Rajeswaran, A., Trojan, A., Burnand, B., and Giannelli, M. (2008). Efficacy and side effects of cisplatin- and carboplatin-based doublet chemotherapeutic regimens versus non-platinum-based doublet chemotherapeutic regimens as first line treatment of metastatic non-small cell lung carcinoma: a systematic review of randomized controlled trials. *Lung Cancer* 59, 1-11.
542. Raschle, M., Van Komen, S., Chi, P., Ellenberger, T., and Sung, P. (2004). Multiple interactions with the Rad51 recombinase govern the homologous recombination function of Rad54. *J Biol Chem* 279, 51973-51980.
543. Rauen, M., Burtelow, M.A., Dufault, V.M., and Karnitz, L.M. (2000). The human checkpoint protein hRad17 interacts with the PCNA-like proteins hRad1, hHus1, and hRad9. *J Biol Chem* 275, 29767-29771.
544. Redon, C., Pilch, D., Rogakou, E., Sedelnikova, O., Newrock, K., and Bonner, W. (2002). Histone H2A variants H2AX and H2AZ. *Curr Opin Genet Dev* 12, 162-169.
545. Reed, S.I. (1996). Cyclin E: in mid-cycle. *Biochim Biophys Acta* 1287, 151-153.
546. Reeves, R., and Adair, J.E. (2005). Role of high mobility group (HMG) chromatin proteins in DNA repair. *DNA Repair (Amst)* 4, 926-938.
547. Rey, L., Sidorova, J.M., Puget, N., Boudsocq, F., Biard, D.S., Monnat, R.J., Jr., Cazaux, C., and Hoffmann, J.S. (2009). Human DNA polymerase eta is required for common fragile site stability during unperturbed DNA replication. *Mol Cell Biol* 29, 3344-3354.
548. Reyes-Turcu, F.E., and Wilkinson, K.D. (2009). Polyubiquitin binding and disassembly by deubiquitinating enzymes. *Chem Rev* 109, 1495-1508.
549. Riedl, T., Hanaoka, F., and Egly, J.M. (2003). The comings and goings of nucleotide excision repair factors on damaged DNA. *EMBO J* 22, 5293-5303.

- 550. Riethman, H.C., Moyzis, R.K., Meyne, J., Burke, D.T., and Olson, M.V. (1989). Cloning human telomeric DNA fragments into *Saccharomyces cerevisiae* using a yeast-artificial-chromosome vector. *Proc Natl Acad Sci U S A* 86, 6240-6244.
- 551. Robinson, H.M., Black, E.J., Brown, R., and Gillespie, D.A. (2007). DNA mismatch repair and Chk1-dependent centrosome amplification in response to DNA alkylation damage. *Cell Cycle* 6, 982-992.
- 552. Rochette, P.J., Therrien, J.P., Drouin, R., Perdiz, D., Bastien, N., Drobetsky, E.A., and Sage, E. (2003). UVA-induced cyclobutane pyrimidine dimers form predominantly at thymine-thymine dipyrimidines and correlate with the mutation spectrum in rodent cells. *Nucleic Acids Res* 31, 2786-2794.
- 553. Rogakou, E.P., Nieves-Neira, W., Boon, C., Pommier, Y., and Bonner, W.M. (2000). Initiation of DNA fragmentation during apoptosis induces phosphorylation of H2AX histone at serine 139. *J Biol Chem* 275, 9390-9395.
- 554. Rogakou, E.P., Pilch, D.R., Orr, A.H., Ivanova, V.S., and Bonner, W.M. (1998). DNA double-stranded breaks induce histone H2AX phosphorylation on serine 139. *J Biol Chem* 273, 5858-5868.
- 555. Rojas, A., Figueroa, H., and Morales, E. (2010). Fueling inflammation at tumor microenvironment: the role of multiligand/RAGE axis. *Carcinogenesis* 31, 334-341.
- 556. Roos-Mattjus, P., Hopkins, K.M., Oestreich, A.J., Vroman, B.T., Johnson, K.L., Naylor, S., Lieberman, H.B., and Karnitz, L.M. (2003). Phosphorylation of human Rad9 is required for genotoxin-activated checkpoint signaling. *J Biol Chem* 278, 24428-24437.
- 557. Rosenberg, B., VanCamp, L., Trosko, J.E., and Mansour, V.H. (1969). Platinum compounds: a new class of potent antitumour agents. *Nature* 222, 385-386.
- 558. Rosenzweig, K.E., Youmell, M.B., Palayoor, S.T., and Price, B.D. (1997). Radiosensitization of human tumor cells by the phosphatidylinositol3-kinase inhibitors wortmannin and LY294002 correlates with inhibition of DNA-dependent protein kinase and prolonged G2-M delay. *Clin Cancer Res* 3, 1149-1156.
- 559. Rothkamm, K., Balroop, S., Shekhdar, J., Fernie, P., and Goh, V. (2007). Leukocyte DNA damage after multi-detector row CT: a quantitative biomarker of low-level radiation exposure. *Radiology* 242, 244-251.
- 560. Rybak, L.P., and Whitworth, C.A. (2005). Ototoxicity: therapeutic opportunities. *Drug Discov Today* 10, 1313-1321.
- 561. Safaei, R., Katano, K., Samimi, G., Naerdemann, W., Stevenson, J.L., Rochdi, M., and Howell, S.B. (2004). Cross-resistance to cisplatin in cells with acquired resistance to copper. *Cancer Chemother Pharmacol* 53, 239-246.
- 562. Sakaue-Sawano, A., Kobayashi, T., Ohtawa, K., and Miyawaki, A. (2011). Drug-induced cell cycle modulation leading to cell-cycle arrest, nuclear mis-segregation, or endoreplication. *BMC Cell Biol* 12, 2.
- 563. Salas, T.R., Petruseva, I., Lavrik, O., and Saintome, C. (2009). Evidence for direct contact between the RPA3 subunit of the human replication protein A and single-stranded DNA. *Nucleic Acids Res* 37, 38-46.
- 564. Samimi, G., Safaei, R., Katano, K., Holzer, A.K., Rochdi, M., Tomioka, M., Goodman, M., and Howell, S.B. (2004). Increased expression of the copper efflux transporter ATP7A mediates resistance to cisplatin, carboplatin, and oxaliplatin in ovarian cancer cells. *Clin Cancer Res* 10, 4661-4669.

565. Sand-Dejmek, J., Adelmant, G., Sobhian, B., Calkins, A.S., Marto, J., Iglehart, D.J., and Lazaro, J.B. (2011). Concordant and opposite roles of DNA-PK and the "facilitator of chromatin transcription" (FACT) in DNA repair, apoptosis and necrosis after cisplatin. *Mol Cancer* 10, 74.
566. Saris, C.P., van de Vaart, P.J., Rietbroek, R.C., and Blommaert, F.A. (1996). In vitro formation of DNA adducts by cisplatin, lobaplatin and oxaliplatin in calf thymus DNA in solution and in cultured human cells. *Carcinogenesis* 17, 2763-2769.
567. Sartori, A.A., Lukas, C., Coates, J., Mistrik, M., Fu, S., Bartek, J., Baer, R., Lukas, J., and Jackson, S.P. (2007). Human CtIP promotes DNA end resection. *Nature* 450, 509-514.
568. Savell, J., Rao, S., Pledger, W.J., and Wharton, W. (2001). Permanent growth arrest in irradiated human fibroblasts. *Radiat Res* 155, 554-563.
569. Savitsky, K., Bar-Shira, A., Gilad, S., Rotman, G., Ziv, Y., Vanagaite, L., Tagle, D.A., Smith, S., Uziel, T., Sfez, S., *et al.* (1995a). A single ataxia telangiectasia gene with a product similar to PI-3 kinase. *Science* 268, 1749-1753.
570. Savitsky, K., Sfez, S., Tagle, D.A., Ziv, Y., Sartiel, A., Collins, F.S., Shiloh, Y., and Rotman, G. (1995b). The complete sequence of the coding region of the ATM gene reveals similarity to cell cycle regulators in different species. *Hum Mol Genet* 4, 2025-2032.
571. Scheeff, E.D., Briggs, J.M., and Howell, S.B. (1999). Molecular modeling of the intrastrand guanine-guanine DNA adducts produced by cisplatin and oxaliplatin. *Mol Pharmacol* 56, 633-643.
572. Schiebel, E. (2000). gamma-tubulin complexes: binding to the centrosome, regulation and microtubule nucleation. *Curr Opin Cell Biol* 12, 113-118.
573. Scorsetti, M., Alongi, F., Castiglioni, S., Clivio, A., Fogliata, A., Lobefalo, F., Mancosu, P., Navarria, P., Palumbo, V., Pellegrini, C., *et al.* (2011). Feasibility and early clinical assessment of flattening filter free (FFF) based stereotactic body radiotherapy (SBRT) treatments. *Radiat Oncol* 6, 113.
574. Screpanti, E., Santaguida, S., Nguyen, T., Silvestri, R., Gussio, R., Musacchio, A., Hamel, E., and De Wulf, P. (2010). A screen for kinetochore-microtubule interaction inhibitors identifies novel antitubulin compounds. *PLoS One* 5, e11603.
575. Sedelnikova, O.A., Rogakou, E.P., Panyutin, I.G., and Bonner, W.M. (2002). Quantitative detection of (125)IdU-induced DNA double-strand breaks with gamma-H2AX antibody. *Radiat Res* 158, 486-492.
576. Sedletska, Y., Fourrier, L., and Malinge, J.M. (2007). Modulation of MutS ATP-dependent functional activities by DNA containing a cisplatin compound lesion (base damage and mismatch). *J Mol Biol* 369, 27-40.
577. Sedletska, Y., Giraud-Panis, M.J., and Malinge, J.M. (2005). Cisplatin is a DNA-damaging antitumour compound triggering multifactorial biochemical responses in cancer cells: importance of apoptotic pathways. *Curr Med Chem Anticancer Agents* 5, 251-265.
578. Segurado, M., and Tercero, J.A. (2009). The S-phase checkpoint: targeting the replication fork. *Biol Cell* 101, 617-627.
579. Shachar, S., Ziv, O., Avkin, S., Adar, S., Wittschieben, J., Reissner, T., Chaney, S., Friedberg, E.C., Wang, Z., Carell, T., *et al.* (2009). Two-polymerase mechanisms dictate error-free and error-prone translesion DNA synthesis in mammals. *EMBO J* 28, 383-393.

- 580. Sharan, S.K., Morimatsu, M., Albrecht, U., Lim, D.S., Regel, E., Dinh, C., Sands, A., Eichele, G., Hasty, P., and Bradley, A. (1997). Embryonic lethality and radiation hypersensitivity mediated by Rad51 in mice lacking Brca2. *Nature* 386, 804-810.
- 581. Sharma, R., Graham, J., Blagden, S., and Gabra, H. (2011). Sustained platelet-sparing effect of weekly low dose paclitaxel allows effective, tolerable delivery of extended dose dense weekly carboplatin in platinum resistant/refractory epithelial ovarian cancer. *BMC Cancer* 11, 289.
- 582. Sharma, R.I., and Smith, T.A. (2008). Colorectal tumor cells treated with 5-FU, oxaliplatin, irinotecan, and cetuximab exhibit changes in 18F-FDG incorporation corresponding to hexokinase activity and glucose transport. *J Nucl Med* 49, 1386-1394.
- 583. Sheaff, R.J., Groudine, M., Gordon, M., Roberts, J.M., and Clurman, B.E. (1997). Cyclin E-CDK2 is a regulator of p27Kip1. *Genes Dev* 11, 1464-1478.
- 584. Shen, X., Jun, S., O'Neal, L.E., Sonoda, E., Bemark, M., Sale, J.E., and Li, L. (2006). REV3 and REV1 play major roles in recombination-independent repair of DNA interstrand cross-links mediated by monoubiquitinated proliferating cell nuclear antigen (PCNA). *J Biol Chem* 281, 13869-13872.
- 585. Shen, Y., Betzendahl, I., Sun, F., Tinneberg, H.R., and Eichenlaub-Ritter, U. (2005). Non-invasive method to assess genotoxicity of nocodazole interfering with spindle formation in mammalian oocytes. *Reprod Toxicol* 19, 459-471.
- 586. Sherr, C.J. (1994). G1 phase progression: cycling on cue. *Cell* 79, 551-555.
- 587. Shi, W., Feng, Z., Zhang, J., Gonzalez-Suarez, I., Vanderwaal, R.P., Wu, X., Powell, S.N., Roti Roti, J.L., and Gonzalo, S. The role of RPA2 phosphorylation in homologous recombination in response to replication arrest. *Carcinogenesis* 31, 994-1002.
- 588. Shiloh, Y. (2001). ATM (ataxia telangiectasia mutated): expanding roles in the DNA damage response and cellular homeostasis. *Biochem Soc Trans* 29, 661-666.
- 589. Shiloh, Y. (2003). ATM and related protein kinases: safeguarding genome integrity. *Nat Rev Cancer* 3, 155-168.
- 590. Shiloh, Y. (2006). The ATM-mediated DNA-damage response: taking shape. *Trends Biochem Sci* 31, 402-410.
- 591. Shiloh, Y., and Rotman, G. (1996). Ataxia-telangiectasia and the ATM gene: linking neurodegeneration, immunodeficiency, and cancer to cell cycle checkpoints. *J Clin Immunol* 16, 254-260.
- 592. Shinohara, A., and Ogawa, T. (1998). Stimulation by Rad52 of yeast Rad51-mediated recombination. *Nature* 391, 404-407.
- 593. Shiomi, Y., Shinozaki, A., Nakada, D., Sugimoto, K., Usukura, J., Obuse, C., and Tsurimoto, T. (2002). Clamp and clamp loader structures of the human checkpoint protein complexes, Rad9-1-1 and Rad17-RFC. *Genes Cells* 7, 861-868.
- 594. Shirazi, F.H., Molepo, J.M., Stewart, D.J., Ng, C.E., Raaphorst, G.P., and Goel, R. (1996). Cytotoxicity, accumulation, and efflux of cisplatin and its metabolites in human ovarian carcinoma cells. *Toxicol Appl Pharmacol* 140, 211-218.
- 595. Sibanda, B.L., Chirgadze, D.Y., and Blundell, T.L. (2010). Crystal structure of DNA-PKcs reveals a large open-ring cradle comprised of HEAT repeats. *Nature* 463, 118-121.

596. Siddik, Z.H. (2003). Cisplatin: mode of cytotoxic action and molecular basis of resistance. *Oncogene* 22, 7265-7279.
597. Silvian, L.F., Toth, E.A., Pham, P., Goodman, M.F., and Ellenberger, T. (2001). Crystal structure of a DinB family error-prone DNA polymerase from *Sulfolobus solfataricus*. *Nat Struct Biol* 8, 984-989.
598. Sinha, R.P., and Hader, D.P. (2002). UV-induced DNA damage and repair: a review. *Photochem Photobiol Sci* 1, 225-236.
599. Skirnisdottir, I., Lindborg, K., and Sorbe, B. (2007). Adjuvant chemotherapy with carboplatin and taxane compared with single drug carboplatin in early stage epithelial ovarian carcinoma. *Oncol Rep* 18, 1249-1256.
600. Sleeth, K.M., Sorensen, C.S., Issaeva, N., Dziegielewska, J., Bartek, J., and Helleday, T. (2007). RPA mediates recombination repair during replication stress and is displaced from DNA by checkpoint signalling in human cells. *J Mol Biol* 373, 38-47.
601. Smeaton, M.B., Hlavin, E.M., Noronha, A.M., Murphy, S.P., Wilds, C.J., and Miller, P.S. (2009). Effect of cross-link structure on DNA interstrand cross-link repair synthesis. *Chem Res Toxicol* 22, 1285-1297.
602. Smits, V.A., and Medema, R.H. (2001). Checking out the G(2)/M transition. *Biochim Biophys Acta* 1519, 1-12.
603. Smogorzewska, A., Matsuoka, S., Vinciguerra, P., McDonald, E.R., 3rd, Hurov, K.E., Luo, J., Ballif, B.A., Gygi, S.P., Hofmann, K., D'Andrea, A.D., *et al.* (2007). Identification of the FANCI protein, a monoubiquitinated FANCD2 paralog required for DNA repair. *Cell* 129, 289-301.
604. So, S., Davis, A.J., and Chen, D.J. (2009). Autophosphorylation at serine 1981 stabilizes ATM at DNA damage sites. *J Cell Biol* 187, 977-990.
605. Sobhian, B., Shao, G., Lilli, D.R., Culhane, A.C., Moreau, L.A., Xia, B., Livingston, D.M., and Greenberg, R.A. (2007). RAP80 targets BRCA1 to specific ubiquitin structures at DNA damage sites. *Science* 316, 1198-1202.
606. Song, I.S., Savaraj, N., Siddik, Z.H., Liu, P., Wei, Y., Wu, C.J., and Kuo, M.T. (2004). Role of human copper transporter Ctr1 in the transport of platinum-based antitumor agents in cisplatin-sensitive and cisplatin-resistant cells. *Mol Cancer Ther* 3, 1543-1549.
607. Sonoda, E., Okada, T., Zhao, G.Y., Tateishi, S., Araki, K., Yamaizumi, M., Yagi, T., Verkaik, N.S., van Gent, D.C., Takata, M., *et al.* (2003). Multiple roles of Rev3, the catalytic subunit of polzeta in maintaining genome stability in vertebrates. *EMBO J* 22, 3188-3197.
608. Sorensen, C.S., Hansen, L.T., Dziegielewska, J., Syljuasen, R.G., Lundin, C., Bartek, J., and Helleday, T. (2005). The cell-cycle checkpoint kinase Chk1 is required for mammalian homologous recombination repair. *Nat Cell Biol* 7, 195-201.
609. Sorenson, C.M., Barry, M.A., and Eastman, A. (1990). Analysis of events associated with cell cycle arrest at G2 phase and cell death induced by cisplatin. *J Natl Cancer Inst* 82, 749-755.
610. Sorenson, C.M., and Eastman, A. (1988). Mechanism of cis-diamminedichloroplatinum(II)-induced cytotoxicity: role of G2 arrest and DNA double-strand breaks. *Cancer Res* 48, 4484-4488.
611. Soria, G., Belluscio, L., van Cappellen, W.A., Kanaar, R., Essers, J., and Gottifredi, V. (2009). DNA damage induced Pol eta recruitment takes place independently of the cell cycle phase. *Cell Cycle* 8, 3340-3348.

612. Soucek, T., Pusch, O., Hengstschlager-Ottanad, E., Adams, P.D., and Hengstschlager, M. (1997). Deregulated expression of E2F-1 induces cyclin A- and E-associated kinase activities independently from cell cycle position. *Oncogene* 14, 2251-2257.
613. Spagnolo, L., Rivera-Calzada, A., Pearl, L.H., and Llorca, O. (2006). Three-dimensional structure of the human DNA-PKcs/Ku70/Ku80 complex assembled on DNA and its implications for DNA DSB repair. *Mol Cell* 22, 511-519.
614. St Onge, R.P., Udell, C.M., Casselman, R., and Davey, S. (1999). The human G2 checkpoint control protein hRAD9 is a nuclear phosphoprotein that forms complexes with hRAD1 and hHUS1. *Mol Biol Cell* 10, 1985-1995.
615. Stallons, L.J., and McGregor, W.G. (2010). Translesion synthesis polymerases in the prevention and promotion of carcinogenesis. *J Nucleic Acids* 2010.
616. Stary, A., Kannouche, P., Lehmann, A.R., and Sarasin, A. (2003). Role of DNA polymerase eta in the UV mutation spectrum in human cells. *J Biol Chem* 278, 18767-18775.
617. Stehlikova, K., Kostrhunova, H., Kasparkova, J., and Brabec, V. (2002). DNA bending and unwinding due to the major 1,2-GG intrastrand cross-link formed by antitumor cis-diamminedichloroplatinum(II) are flanking-base independent. *Nucleic Acids Res* 30, 2894-2898.
618. Stelter, P., and Ulrich, H.D. (2003). Control of spontaneous and damage-induced mutagenesis by SUMO and ubiquitin conjugation. *Nature* 425, 188-191.
619. Stephan, H., Concannon, C., Kremmer, E., Carty, M.P., and Nasheuer, H.P. (2009). Ionizing radiation-dependent and independent phosphorylation of the 32-kDa subunit of replication protein A during mitosis. *Nucleic Acids Res* 37, 6028-6041.
620. Stiff, T., Walker, S.A., Cersaletti, K., Goodarzi, A.A., Petermann, E., Concannon, P., O'Driscoll, M., and Jeggo, P.A. (2006). ATR-dependent phosphorylation and activation of ATM in response to UV treatment or replication fork stalling. *EMBO J* 25, 5775-5782.
621. Stracker, T.H., Couto, S.S., Cordon-Cardo, C., Matos, T., and Petrini, J.H. (2008). Chk2 suppresses the oncogenic potential of DNA replication-associated DNA damage. *Mol Cell* 31, 21-32.
622. Stracker, T.H., Theunissen, J.W., Morales, M., and Petrini, J.H. (2004). The Mre11 complex and the metabolism of chromosome breaks: the importance of communicating and holding things together. *DNA Repair (Amst)* 3, 845-854.
623. Strigini, P., Carobbi, S., Sansone, R., Lombardo, C., and Santi, L. (1991). Molecular epidemiology of cancer in immune deficiency. *Cancer Detect Prev* 15, 115-126.
624. Strumberg, D., Pilon, A.A., Smith, M., Hickey, R., Malkas, L., and Pommier, Y. (2000). Conversion of topoisomerase I cleavage complexes on the leading strand of ribosomal DNA into 5'-phosphorylated DNA double-strand breaks by replication runoff. *Mol Cell Biol* 20, 3977-3987.
625. Stucki, M., Clapperton, J.A., Mohammad, D., Yaffe, M.B., Smerdon, S.J., and Jackson, S.P. (2005). MDC1 directly binds phosphorylated histone H2AX to regulate cellular responses to DNA double-strand breaks. *Cell* 123, 1213-1226.

626. Sugiyama, T., and Kantake, N. (2009). Dynamic regulatory interactions of rad51, rad52, and replication protein-a in recombination intermediates. *J Mol Biol* 390, 45-55.
627. Sullivan, M., and Morgan, D.O. (2007). Finishing mitosis, one step at a time. *Nat Rev Mol Cell Biol* 8, 894-903.
628. Sullivan, S.T., Ciccarese, A., Fanizzi, F.P., and Marzilli, L.G. (2001a). Cisplatin-DNA cross-link retro models with a chirality-neutral carrier ligand: evidence for the importance of "second-sphere communication". *Inorg Chem* 40, 455-462.
629. Sullivan, S.T., Ciccarese, A., Fanizzi, F.P., and Marzilli, L.G. (2001b). A rare example of three abundant conformers in one retro model of the cisplatin-DNA d(GpG) intrastrand cross link. Unambiguous evidence that guanine O6 to carrier amine ligand hydrogen bonding is not important. possible effect of the Lippard base pair step adjacent to the lesion on carrier ligand hydrogen bonding in DNA adducts. *J Am Chem Soc* 123, 9345-9355.
630. Sung, K.E., and Burns, M.A. (2006). Optimization of dielectrophoretic DNA stretching in microfabricated devices. *Anal Chem* 78, 2939-2947.
631. Sutton, M.D. (2010). Coordinating DNA polymerase traffic during high and low fidelity synthesis. *Biochim Biophys Acta* 1804, 1167-1179.
632. Suzuki, N., Ohashi, E., Kolbanovskiy, A., Geacintov, N.E., Grollman, A.P., Ohmori, H., and Shibutani, S. (2002). Translesion synthesis by human DNA polymerase kappa on a DNA template containing a single stereoisomer of dG-(+)- or dG-(-)-anti-N(2)-BPDE (7,8-dihydroxy-anti-9,10-epoxy-7,8,9,10-tetrahydrobenzo[a]pyrene). *Biochemistry* 41, 6100-6106.
633. Svetlova, M., Solovjeva, L., Pleskach, N., Yartseva, N., Yakovleva, T., Tomilin, N., and Hanawalt, P. (2002). Clustered sites of DNA repair synthesis during early nucleotide excision repair in ultraviolet light-irradiated quiescent human fibroblasts. *Exp Cell Res* 276, 284-295.
634. Sy, S.M., Huen, M.S., and Chen, J. (2009). MRG15 is a novel PALB2-interacting factor involved in homologous recombination. *J Biol Chem* 284, 21127-21131.
635. Szymkowski, D.E., Yarema, K., Essigmann, J.M., Lippard, S.J., and Wood, R.D. (1992). An intrastrand d(GpG) platinum crosslink in duplex M13 DNA is refractory to repair by human cell extracts. *Proc Natl Acad Sci U S A* 89, 10772-10776.
636. Takahashi, A., and Ohnishi, T. (2005). Does gammaH2AX foci formation depend on the presence of DNA double strand breaks? *Cancer Lett* 229, 171-179.
637. Takahashi, T.S., Yiu, P., Chou, M.F., Gygi, S., and Walter, J.C. (2004). Recruitment of Xenopus Scc2 and cohesin to chromatin requires the pre-replication complex. *Nat Cell Biol* 6, 991-996.
638. Takai, H., Naka, K., Okada, Y., Watanabe, M., Harada, N., Saito, S., Anderson, C.W., Appella, E., Nakanishi, M., Suzuki, H., *et al.* (2002). Chk2-deficient mice exhibit radioresistance and defective p53-mediated transcription. *EMBO J* 21, 5195-5205.
639. Takata, M., Sasaki, M.S., Sonoda, E., Morrison, C., Hashimoto, M., Utsumi, H., Yamaguchi-Iwai, Y., Shinohara, A., and Takeda, S. (1998). Homologous recombination and non-homologous end-joining pathways of DNA double-strand break repair have overlapping roles in the maintenance of chromosomal integrity in vertebrate cells. *EMBO J* 17, 5497-5508.

640. Takedachi, A., Saijo, M., and Tanaka, K. (2010). DDB2 complex-mediated ubiquitylation around DNA damage is oppositely regulated by XPC and Ku and contributes to the recruitment of XPA. *Mol Cell Biol* 30, 2708-2723.
641. Talluri, S., Isaac, C.E., Ahmad, M., Henley, S.A., Francis, S.M., Martens, A.L., Bremner, R., and Dick, F.A. (2010). A G1 checkpoint mediated by the retinoblastoma protein that is dispensable in terminal differentiation but essential for senescence. *Mol Cell Biol* 30, 948-960.
642. Tanioka, M., Masaki, T., Ono, R., Nagano, T., Otsoshi-Honda, E., Matsumura, Y., Takigawa, M., Inui, H., Miyachi, Y., Moriwaki, S., *et al.* (2007). Molecular analysis of DNA polymerase eta gene in Japanese patients diagnosed as xeroderma pigmentosum variant type. *J Invest Dermatol* 127, 1745-1751.
643. Taya, Y. (1997). RB kinases and RB-binding proteins: new points of view. *Trends Biochem Sci* 22, 14-17.
644. Taylor, W.R., and Stark, G.R. (2001). Regulation of the G2/M transition by p53. *Oncogene* 20, 1803-1815.
645. Terada, Y., Tatsuka, M., Jinno, S., and Okayama, H. (1995). Requirement for tyrosine phosphorylation of Cdk4 in G1 arrest induced by ultraviolet irradiation. *Nature* 376, 358-362.
646. Terz, J.J., Lawrence, W., Jr., and Cox, B. (1977). Analysis of the cycling and noncycling cell population of human solid tumors. *Cancer* 40, 1462-1470.
647. Thakur, M., Wernick, M., Collins, C., Limoli, C.L., Crowley, E., and Cleaver, J.E. (2001). DNA polymerase eta undergoes alternative splicing, protects against UV sensitivity and apoptosis, and suppresses Mre11-dependent recombination. *Genes Chromosomes Cancer* 32, 222-235.
648. Thomas, J.O., and Travers, A.A. (2001). HMG1 and 2, and related 'architectural' DNA-binding proteins. *Trends Biochem Sci* 26, 167-174.
649. Thomas, J.P., Lautermann, J., Liedert, B., Seiler, F., and Thomale, J. (2006). High accumulation of platinum-DNA adducts in strial marginal cells of the cochlea is an early event in cisplatin but not carboplatin ototoxicity. *Mol Pharmacol* 70, 23-29.
650. Thompson, L.H., and Hinz, J.M. (2009). Cellular and molecular consequences of defective Fanconi anemia proteins in replication-coupled DNA repair: mechanistic insights. *Mutat Res* 668, 54-72.
651. Tiainen, M., Pajalunga, D., Ferrantelli, F., Soddu, S., Salvatori, G., Sacchi, A., and Crescenzi, M. (1996). Terminally differentiated skeletal myotubes are not confined to G0 but can enter G1 upon growth factor stimulation. *Cell Growth Differ* 7, 1039-1050.
652. Tibbetts, R.S., Cortez, D., Brumbaugh, K.M., Scully, R., Livingston, D., Elledge, S.J., and Abraham, R.T. (2000). Functional interactions between BRCA1 and the checkpoint kinase ATR during genotoxic stress. *Genes Dev* 14, 2989-3002.
653. Timofeev, O., Cizmecioglu, O., Settele, F., Kempf, T., and Hoffmann, I. (2010). Cdc25 phosphatases are required for timely assembly of CDK1-cyclin B at the G2/M transition. *J Biol Chem* 285, 16978-16990.
654. Tissier, A., Kannouche, P., Reck, M.P., Lehmann, A.R., Fuchs, R.P., and Cordonnier, A. (2004). Co-localization in replication foci and interaction of human Y-family members, DNA polymerase pol eta and REV1 protein. *DNA Repair (Amst)* 3, 1503-1514.

655. Tissier, M., Delamotte, B., and Mouhanna, D. (2000). Frustrated heisenberg magnets: A nonperturbative approach. *Phys Rev Lett* 84, 5208-5211.
656. Tobey, R.A., Oishi, N., and Crissman, H.A. (1990). Cell cycle synchronization: reversible induction of G2 synchrony in cultured rodent and human diploid fibroblasts. *Proc Natl Acad Sci U S A* 87, 5104-5108.
657. Todd, R.C., and Lippard, S.J. (2009). Inhibition of transcription by platinum antitumor compounds. *Metallomics* 1, 280-291.
658. Tomita, M. (2010). Involvement of DNA-PK and ATM in radiation- and heat-induced DNA damage recognition and apoptotic cell death. *J Radiat Res (Tokyo)* 51, 493-501.
659. Tomkiel, J.E., Alansari, H., Tang, N., Virgin, J.B., Yang, X., VandeVord, P., Karvonen, R.L., Granda, J.L., Kraut, M.J., Ensley, J.F., *et al.* (2002). Autoimmunity to the M(r) 32,000 subunit of replication protein A in breast cancer. *Clin Cancer Res* 8, 752-758.
660. Topping, R.P., Wilkinson, J.C., and Scarpinato, K.D. (2009). Mismatch repair protein deficiency compromises cisplatin-induced apoptotic signaling. *J Biol Chem* 284, 14029-14039.
661. Toueille, M., El-Andaloussi, N., Frouin, I., Freire, R., Funk, D., Shevelev, I., Friedrich-Heineken, E., Villani, G., Hottiger, M.O., and Hubscher, U. (2004). The human Rad9/Rad1/Hus1 damage sensor clamp interacts with DNA polymerase beta and increases its DNA substrate utilisation efficiency: implications for DNA repair. *Nucleic Acids Res* 32, 3316-3324.
662. Traganos, F. (2004). Mechanism of antitumor drug action assessed by cytometry. *Methods Cell Biol* 75, 257-305.
663. Trincao, J., Johnson, R.E., Escalante, C.R., Prakash, S., Prakash, L., and Aggarwal, A.K. (2001). Structure of the catalytic core of *S. cerevisiae* DNA polymerase eta: implications for translesion DNA synthesis. *Mol Cell* 8, 417-426.
664. Trujillo, K.M., Yuan, S.S., Lee, E.Y., and Sung, P. (1998). Nuclease activities in a complex of human recombination and DNA repair factors Rad50, Mre11, and p95. *J Biol Chem* 273, 21447-21450.
665. Tutt, A., Robson, M., Garber, J.E., Domchek, S.M., Audeh, M.W., Weitzel, J.N., Friedlander, M., Arun, B., Loman, N., Schmutzler, R.K., *et al.* (2010). Oral poly(ADP-ribose) polymerase inhibitor olaparib in patients with BRCA1 or BRCA2 mutations and advanced breast cancer: a proof-of-concept trial. *Lancet* 376, 235-244.
666. Ubezio, P., Lupi, M., Branduardi, D., Cappella, P., Cavallini, E., Colombo, V., Matera, G., Natoli, C., Tomasoni, D., and D'Incalci, M. (2009). Quantitative assessment of the complex dynamics of G1, S, and G2-M checkpoint activities. *Cancer Res* 69, 5234-5240.
667. Umbricht, C.B., Erdile, L.F., Jabs, E.W., and Kelly, T.J. (1993). Cloning, overexpression, and genomic mapping of the 14-kDa subunit of human replication protein A. *J Biol Chem* 268, 6131-6138.
668. Umez, K., Sugawara, N., Chen, C., Haber, J.E., and Kolodner, R.D. (1998). Genetic analysis of yeast RPA1 reveals its multiple functions in DNA metabolism. *Genetics* 148, 989-1005.
669. Usanova, S., Piee-Staffa, A., Sied, U., Thomale, J., Schneider, A., Kaina, B., and Koberle, B. (2010). Cisplatin sensitivity of testis tumour cells is due to deficiency in interstrand-crosslink repair and low ERCC1-XPF expression. *Mol Cancer* 9, 248.

670. Vaisman, A., and Chaney, S.G. (2000). The efficiency and fidelity of translesion synthesis past cisplatin and oxaliplatin GpG adducts by human DNA polymerase beta. *J Biol Chem* 275, 13017-13025.
671. Vaisman, A., Lehmann, A.R., and Woodgate, R. (2004). DNA polymerases eta and iota. *Adv Protein Chem* 69, 205-228.
672. Vaisman, A., Masutani, C., Hanaoka, F., and Chaney, S.G. (2000). Efficient translesion replication past oxaliplatin and cisplatin GpG adducts by human DNA polymerase eta. *Biochemistry* 39, 4575-4580.
673. van der Vijgh, W.J. (1991). Clinical pharmacokinetics of carboplatin. *Clin Pharmacokinet* 21, 242-261.
674. van Kranen, H.J., and de Gruijl, F.R. (1999). Mutations in cancer genes of UV-induced skin tumors of hairless mice. *J Epidemiol* 9, S58-65.
675. Van, P.L., Yim, K.W., Jin, D.Y., Dapolito, G., Kurimasa, A., and Jeang, K.T. (2001). Genetic evidence of a role for ATM in functional interaction between human T-cell leukemia virus type 1 Tax and p53. *J Virol* 75, 396-407.
676. Van Sloun, P.P., Varlet, I., Sonneveld, E., Boei, J.J., Romeijn, R.J., Eeken, J.C., and De Wind, N. (2002). Involvement of mouse Rev3 in tolerance of endogenous and exogenous DNA damage. *Mol Cell Biol* 22, 2159-2169.
677. van Steeg, H., and Kraemer, K.H. (1999). Xeroderma pigmentosum and the role of UV-induced DNA damage in skin cancer. *Mol Med Today* 5, 86-94.
678. Vassin, V.M., Wold, M.S., and Borowiec, J.A. (2004). Replication protein A (RPA) phosphorylation prevents RPA association with replication centers. *Mol Cell Biol* 24, 1930-1943.
679. Vaughan, S., and Dawe, H.R. (2011). Common themes in centriole and centrosome movements. *Trends Cell Biol* 21, 57-66.
680. Vermeulen, K., Van Bockstaele, D.R., and Berneman, Z.N. (2003). The cell cycle: a review of regulation, deregulation and therapeutic targets in cancer. *Cell Prolif* 36, 131-149.
681. Vesterdal, A. (1991). [Attractive theories]. *Sygeplejersken* 91, 14.
682. Veuger, S.J., Curtin, N.J., Richardson, C.J., Smith, G.C., and Durkacz, B.W. (2003). Radiosensitization and DNA repair inhibition by the combined use of novel inhibitors of DNA-dependent protein kinase and poly(ADP-ribose) polymerase-1. *Cancer Res* 63, 6008-6015.
683. Vidal, A.E., Kannouche, P., Podust, V.N., Yang, W., Lehmann, A.R., and Woodgate, R. (2004). Proliferating cell nuclear antigen-dependent coordination of the biological functions of human DNA polymerase iota. *J Biol Chem* 279, 48360-48368.
684. Vilenchik, M.M., and Knudson, A.G. (2003). Endogenous DNA double-strand breaks: production, fidelity of repair, and induction of cancer. *Proc Natl Acad Sci U S A* 100, 12871-12876.
685. Volpe, J.P., and Cleaver, J.E. (1995). Xeroderma pigmentosum variant cells are resistant to immortalization. *Mutat Res* 337, 111-117.
686. Wagner, J.M., and Karnitz, L.M. (2009). Cisplatin-induced DNA damage activates replication checkpoint signaling components that differentially affect tumor cell survival. *Mol Pharmacol* 76, 208-214.
687. Walker, J.R., Corpina, R.A., and Goldberg, J. (2001). Structure of the Ku heterodimer bound to DNA and its implications for double-strand break repair. *Nature* 412, 607-614.
688. Walther, A.P., Bjerke, M.P., and Wold, M.S. (1999). A novel assay for examining the molecular reactions at the eukaryotic replication fork: activities

- of replication protein A required during elongation. *Nucleic Acids Res* 27, 656-664.
689. Wang, B., and Elledge, S.J. (2007). Ubc13/Rnf8 ubiquitin ligases control foci formation of the Rap80/Abraxas/Brca1/Brcc36 complex in response to DNA damage. *Proc Natl Acad Sci U S A* 104, 20759-20763.
690. Wang, B., Matsuoka, S., Ballif, B.A., Zhang, D., Smogorzewska, A., Gygi, S.P., and Elledge, S.J. (2007a). Abraxas and RAP80 form a BRCA1 protein complex required for the DNA damage response. *Science* 316, 1194-1198.
691. Wang, D., and Lippard, S.J. (2005). Cellular processing of platinum anticancer drugs. *Nat Rev Drug Discov* 4, 307-320.
692. Wang, J., Biedermann, K.A., and Brown, J.M. (1992). Repair of DNA and chromosome breaks in cells exposed to SR 4233 under hypoxia or to ionizing radiation. *Cancer Res* 52, 4473-4477.
693. Wang, X., Peterson, C.A., Zheng, H., Nairn, R.S., Legerski, R.J., and Li, L. (2001). Involvement of nucleotide excision repair in a recombination-independent and error-prone pathway of DNA interstrand cross-link repair. *Mol Cell Biol* 21, 713-720.
694. Wang, X., Swain, J.E., Bollen, M., Liu, X.T., Ohl, D.A., and Smith, G.D. (2004). Endogenous regulators of protein phosphatase-1 during mouse oocyte development and meiosis. *Reproduction* 128, 493-502.
695. Wang, Y., Woodgate, R., McManus, T.P., Mead, S., McCormick, J.J., and Maher, V.M. (2007b). Evidence that in xeroderma pigmentosum variant cells, which lack DNA polymerase eta, DNA polymerase iota causes the very high frequency and unique spectrum of UV-induced mutations. *Cancer Res* 67, 3018-3026.
696. Ward, I., and Chen, J. (2004). Early events in the DNA damage response. *Curr Top Dev Biol* 63, 1-35.
697. Watanabe, K., Tateishi, S., Kawasuji, M., Tsurimoto, T., Inoue, H., and Yamaizumi, M. (2004). Rad18 guides poleta to replication stalling sites through physical interaction and PCNA monoubiquitination. *EMBO J* 23, 3886-3896.
698. Welsh, C., Day, R., McGurk, C., Masters, J.R., Wood, R.D., and Koberle, B. (2004). Reduced levels of XPA, ERCC1 and XPF DNA repair proteins in testis tumor cell lines. *Int J Cancer* 110, 352-361.
699. Wesoly, J., Agarwal, S., Sigurdsson, S., Bussen, W., Van Komen, S., Qin, J., van Steeg, H., van Benthem, J., Wassenaar, E., Baarends, W.M., *et al.* (2006). Differential contributions of mammalian Rad54 paralogs to recombination, DNA damage repair, and meiosis. *Mol Cell Biol* 26, 976-989.
700. Williams, C.J., Grandal, I., Vesprini, D.J., Wojtyra, U., Danska, J.S., and Guidos, C.J. (2001). Irradiation promotes V(D)J joining and RAG-dependent neoplastic transformation in SCID T-cell precursors. *Mol Cell Biol* 21, 400-413.
701. Williams, R.S., Dodson, G.E., Limbo, O., Yamada, Y., Williams, J.S., Guenther, G., Classen, S., Glover, J.N., Iwasaki, H., Russell, P., *et al.* (2009). Nbs1 flexibly tethers Ctp1 and Mre11-Rad50 to coordinate DNA double-strand break processing and repair. *Cell* 139, 87-99.
702. Willmore, E., de Caux, S., Sunter, N.J., Tilby, M.J., Jackson, G.H., Austin, C.A., and Durkacz, B.W. (2004). A novel DNA-dependent protein kinase inhibitor, NU7026, potentiates the cytotoxicity of topoisomerase II poisons used in the treatment of leukemia. *Blood* 103, 4659-4665.

703. Wilsker, D., and Bunz, F. (2007). Loss of ataxia telangiectasia mutated- and Rad3-related function potentiates the effects of chemotherapeutic drugs on cancer cell survival. *Mol Cancer Ther* 6, 1406-1413.
704. Wobbe, C.R., Weissbach, L., Borowiec, J.A., Dean, F.B., Murakami, Y., Bullock, P., and Hurwitz, J. (1987). Replication of simian virus 40 origin-containing DNA in vitro with purified proteins. *Proc Natl Acad Sci U S A* 84, 1834-1838.
705. Wold, M.S. (1997). Replication protein A: a heterotrimeric, single-stranded DNA-binding protein required for eukaryotic DNA metabolism. *Annu Rev Biochem* 66, 61-92.
706. Wolff, J., Knipping, L., and Sackett, D.L. (1996). Charge-shielding and the "paradoxical" stimulation of tubulin polymerization by guanidine hydrochloride. *Biochemistry* 35, 5910-5920.
707. Wong, A.K., Pero, R., Ormonde, P.A., Tavtigian, S.V., and Bartel, P.L. (1997). RAD51 interacts with the evolutionarily conserved BRC motifs in the human breast cancer susceptibility gene *brca2*. *J Biol Chem* 272, 31941-31944.
708. Wong, J.M., Ionescu, D., and Ingles, C.J. (2003). Interaction between BRCA2 and replication protein A is compromised by a cancer-predisposing mutation in BRCA2. *Oncogene* 22, 28-33.
709. Woynarowski, J.M., Faivre, S., Herzig, M.C., Arnett, B., Chapman, W.G., Trevino, A.V., Raymond, E., Chaney, S.G., Vaisman, A., Varchenko, M., *et al.* (2000). Oxaliplatin-induced damage of cellular DNA. *Mol Pharmacol* 58, 920-927.
710. Wozniak, K., and Blasiak, J. (2002). Recognition and repair of DNA-cisplatin adducts. *Acta Biochim Pol* 49, 583-596.
711. Wu, F., Lin, X., Okuda, T., and Howell, S.B. (2004a). DNA polymerase zeta regulates cisplatin cytotoxicity, mutagenicity, and the rate of development of cisplatin resistance. *Cancer Res* 64, 8029-8035.
712. Wu, H.I., Brown, J.A., Dorie, M.J., Lazzeroni, L., and Brown, J.M. (2004b). Genome-wide identification of genes conferring resistance to the anticancer agents cisplatin, oxaliplatin, and mitomycin C. *Cancer Res* 64, 3940-3948.
713. Wu, L., and Hickson, I.D. (2006). DNA helicases required for homologous recombination and repair of damaged replication forks. *Annu Rev Genet* 40, 279-306.
714. Wu, L., Luo, K., Lou, Z., and Chen, J. (2008). MDC1 regulates intra-S-phase checkpoint by targeting NBS1 to DNA double-strand breaks. *Proc Natl Acad Sci U S A* 105, 11200-11205.
715. Wu, X., Takenaka, K., Sonoda, E., Hochegeger, H., Kawanishi, S., Kawamoto, T., Takeda, S., and Yamazoe, M. (2006a). Critical roles for polymerase zeta in cellular tolerance to nitric oxide-induced DNA damage. *Cancer Res* 66, 748-754.
716. Wu, X., Yang, Z., Liu, Y., and Zou, Y. (2005). Preferential localization of hyperphosphorylated replication protein A to double-strand break repair and checkpoint complexes upon DNA damage. *Biochem J* 391, 473-480.
717. Wu, Y., Sugiyama, T., and Kowalczykowski, S.C. (2006b). DNA annealing mediated by Rad52 and Rad59 proteins. *J Biol Chem* 281, 15441-15449.
718. Wyka, I.M., Dhar, K., Binz, S.K., and Wold, M.S. (2003). Replication protein A interactions with DNA: differential binding of the core domains and analysis of the DNA interaction surface. *Biochemistry* 42, 12909-12918.

719. Xu, X., Aprelikova, O., Moens, P., Deng, C.X., and Furth, P.A. (2003). Impaired meiotic DNA-damage repair and lack of crossing-over during spermatogenesis in BRCA1 full-length isoform deficient mice. *Development* 130, 2001-2012.
720. Xu, Z.Y., Loignon, M., Han, F.Y., Panasci, L., and Aloyz, R. (2005). Xrcc3 induces cisplatin resistance by stimulation of Rad51-related recombinational repair, S-phase checkpoint activation, and reduced apoptosis. *J Pharmacol Exp Ther* 314, 495-505.
721. Yager, J.D., and Liehr, J.G. (1996). Molecular mechanisms of estrogen carcinogenesis. *Annu Rev Pharmacol Toxicol* 36, 203-232.
722. Yajima, H., Lee, K.J., and Chen, B.P. (2006). ATR-dependent phosphorylation of DNA-dependent protein kinase catalytic subunit in response to UV-induced replication stress. *Mol Cell Biol* 26, 7520-7528.
723. Yamada, M., O'Regan, E., Brown, R., and Karran, P. (1997). Selective recognition of a cisplatin-DNA adduct by human mismatch repair proteins. *Nucleic Acids Res* 25, 491-496.
724. Yamamoto, K., Hirano, S., Ishiai, M., Morishima, K., Kitao, H., Namikoshi, K., Kimura, M., Matsushita, N., Arakawa, H., Buerstedde, J.M., *et al.* (2005). Fanconi anemia protein FANCD2 promotes immunoglobulin gene conversion and DNA repair through a mechanism related to homologous recombination. *Mol Cell Biol* 25, 34-43.
725. Yang, J., Yu, Y., Hamrick, H.E., and Duerksen-Hughes, P.J. (2003). ATM, ATR and DNA-PK: initiators of the cellular genotoxic stress responses. *Carcinogenesis* 24, 1571-1580.
726. Yao, J., Dixon, K., and Carty, M.P. (2001). A single (6-4) photoproduct inhibits plasmid DNA replication in xeroderma pigmentosum variant cell extracts. *Environ Mol Mutagen* 38, 19-29.
727. Yilmaz, S., Sancar, A., and Kemp, M.G. (2011). Multiple ATR-Chk1 pathway proteins preferentially associate with checkpoint-inducing DNA substrates. *PLoS One* 6, e22986.
728. Yoon, J.H., Prakash, L., and Prakash, S. (2009). Highly error-free role of DNA polymerase eta in the replicative bypass of UV-induced pyrimidine dimers in mouse and human cells. *Proc Natl Acad Sci U S A* 106, 18219-18224.
729. You, Z., Chahwan, C., Bailis, J., Hunter, T., and Russell, P. (2005). ATM activation and its recruitment to damaged DNA require binding to the C terminus of Nbs1. *Mol Cell Biol* 25, 5363-5379.
730. Yu, Y., Wang, W., Ding, Q., Ye, R., Chen, D., Merkle, D., Schriemer, D., Meek, K., and Lees-Miller, S.P. (2003). DNA-PK phosphorylation sites in XRCC4 are not required for survival after radiation or for V(D)J recombination. *DNA Repair (Amst)* 2, 1239-1252.
731. Yuzhakov, A., Kelman, Z., and O'Donnell, M. (1999). Trading places on DNA--a three-point switch underlies primer handoff from primase to the replicative DNA polymerase. *Cell* 96, 153-163.
732. Zamble, D.B., and Lippard, S.J. (1995). Cisplatin and DNA repair in cancer chemotherapy. *Trends Biochem Sci* 20, 435-439.
733. Zamble, D.B., Mu, D., Reardon, J.T., Sancar, A., and Lippard, S.J. (1996). Repair of cisplatin--DNA adducts by the mammalian excision nuclease. *Biochemistry* 35, 10004-10013.

734. Zeng, X., Negrete, G.A., Kasmer, C., Yang, W.W., and Gearhart, P.J. (2004). Absence of DNA polymerase eta reveals targeting of C mutations on the nontranscribed strand in immunoglobulin switch regions. *J Exp Med* 199, 917-924.
735. Zeng, X., Winter, D.B., Kasmer, C., Kraemer, K.H., Lehmann, A.R., and Gearhart, P.J. (2001). DNA polymerase eta is an A-T mutator in somatic hypermutation of immunoglobulin variable genes. *Nat Immunol* 2, 537-541.
736. Zernik-Kobak, M., Vasunia, K., Connelly, M., Anderson, C.W., and Dixon, K. (1997). Sites of UV-induced phosphorylation of the p34 subunit of replication protein A from HeLa cells. *J Biol Chem* 272, 23896-23904.
737. Zhang, H.S., Gavin, M., Dahiya, A., Postigo, A.A., Ma, D., Luo, R.X., Harbour, J.W., and Dean, D.C. (2000a). Exit from G1 and S phase of the cell cycle is regulated by repressor complexes containing HDAC-Rb-hSWI/SNF and Rb-hSWI/SNF. *Cell* 101, 79-89.
738. Zhang, X., Rosenstein, B.S., Wang, Y., Lebwohl, M., and Wei, H. (1997). Identification of possible reactive oxygen species involved in ultraviolet radiation-induced oxidative DNA damage. *Free Radic Biol Med* 23, 980-985.
739. Zhang, X.P., Galkin, V.E., Yu, X., Egelman, E.H., and Heyer, W.D. (2009). Loop 2 in *Saccharomyces cerevisiae* Rad51 protein regulates filament formation and ATPase activity. *Nucleic Acids Res* 37, 158-171.
740. Zhang, Y., and Xiong, Y. (2001). A p53 amino-terminal nuclear export signal inhibited by DNA damage-induced phosphorylation. *Science* 292, 1910-1915.
741. Zhang, Y., Yuan, F., Wu, X., Wang, M., Rechkoblit, O., Taylor, J.S., Geacintov, N.E., and Wang, Z. (2000b). Error-free and error-prone lesion bypass by human DNA polymerase kappa in vitro. *Nucleic Acids Res* 28, 4138-4146.
742. Zhao, H., and Piwnica-Worms, H. (2001). ATR-mediated checkpoint pathways regulate phosphorylation and activation of human Chk1. *Mol Cell Biol* 21, 4129-4139.
743. Zhao, H., Watkins, J.L., and Piwnica-Worms, H. (2002). Disruption of the checkpoint kinase 1/cell division cycle 25A pathway abrogates ionizing radiation-induced S and G2 checkpoints. *Proc Natl Acad Sci U S A* 99, 14795-14800.
744. Zhao, Y., Thomas, H.D., Batey, M.A., Cowell, I.G., Richardson, C.J., Griffin, R.J., Calvert, A.H., Newell, D.R., Smith, G.C., and Curtin, N.J. (2006). Preclinical evaluation of a potent novel DNA-dependent protein kinase inhibitor NU7441. *Cancer Res* 66, 5354-5362.
745. Zheng, H., Wang, X., Legerski, R.J., Glazer, P.M., and Li, L. (2006). Repair of DNA interstrand cross-links: interactions between homology-dependent and homology-independent pathways. *DNA Repair (Amst)* 5, 566-574.
746. Zheng, Z., Park, J.Y., Guillemette, C., Schantz, S.P., and Lazarus, P. (2001). Tobacco carcinogen-detoxifying enzyme UGT1A7 and its association with orolaryngeal cancer risk. *J Natl Cancer Inst* 93, 1411-1418.
747. Zhou, B.B., and Elledge, S.J. (2000). The DNA damage response: putting checkpoints in perspective. *Nature* 408, 433-439.
748. Zhu, Z., Chung, W.H., Shim, E.Y., Lee, S.E., and Ira, G. (2008). Sgs1 helicase and two nucleases Dna2 and Exo1 resect DNA double-strand break ends. *Cell* 134, 981-994.
749. Zou, L., and Elledge, S.J. (2003). Sensing DNA damage through ATRIP recognition of RPA-ssDNA complexes. *Science* 300, 1542-1548.